General Disclaimer

One or more of the Following Statements may affect this Document

- This document has been reproduced from the best copy furnished by the organizational source. It is being released in the interest of making available as much information as possible.

- This document may contain data, which exceeds the sheet parameters. It was furnished in this condition by the organizational source and is the best copy available.

- This document may contain tone-on-tone or color graphs, charts and/or pictures, which have been reproduced in black and white.

- This document is paginated as submitted by the original source.

- Portions of this document are not fully legible due to the historical nature of some of the material. However, it is the best reproduction available from the original submission.

NASA TM X- 63527

A STUDY FROM KINEMATICS - THE PROBLEMS OF INTERCEPT AND PURSUIT

JAMES B. EADES
GEORGE H. WYATT

MARCH 1969

GSFC ———— GODDARD SPACE FLIGHT CENTER ————
GREENBELT, MARYLAND

A STUDY FROM KINEMATICS – THE PROBLEMS OF INTERCEPT AND PURSUIT

by

James B. Eades, Jr.[*]
Special Projects Branch

and

George H. Wyatt
Mathematics and Computing Branch

ABSTRACT

This investigation is primarily concerned with the planar problems of intercept and pursuit as seen from both the mathematical and physical points of view. Specific applications are not the major intent here, yet the ideas of reality are a strong undercurrent retained in these developments. Several specific problem studies are undertaken, for illustrative purposes; and, ample graphical results are included in order to present a clearer picture of the happenings which occur during each of the maneuvers. In addition to describing the typical and specific trajectories, information is included which pertains to the time of flight, range and range-rate histories, as well as the acceleration levels to be experienced by the maneuvering vehicles. Categorically, the cases studied here include the simple linear intercept problem, the pursuit of a vehicle moving along a straight line path and a case wherein the target flies a circular trajectory.

[*]NAS-NASA Resident Research Associate, on leave from the Virginia Polytechnic Institute, Blacksburg, Virginia.

TABLE OF CONTENTS

TABLE OF CONTENTS (Continued)

LIST CF ILLUSTRATIONS

viii

A STUDY FROM KINEMATICS – THE PROBLEMS OF INTERCEPT AND PURSUIT

I. INTRODUCTION

The problems of intercept and pursuit have been subjects of interest to mathematicians and to engineers and scientists for a very long period in time. The mathematician has been concerned, principally, with the problem's solution, especially since analytic studies may be achieved when suitable simplifying assumptions are introduced. On the other hand, the engineers and physicists most likely have been concerned with the applications aspects of these problems. In this regard one might visualize, as applications, the study of one tactical vehicle intent upon colliding with – on intercepting – another vehicle at some position in (mathematical or physical) space. In theory, then, it would be reasonable to conclude that these studies might apply to a missile intercepting a moving air-craft as a target; the track of a torpedo as it seeks to intercept its target; the flight of one space vehicle in pursuit of another; or, as is frequently mentioned in mathematical studies, the "hound and hare" problem.

In this investigation no particular application is inferred, even though any of the above, and/or other, example cases may come to mind. Throughout the development undertaken in this study the thread of reality, and application, has been retained and held in the investigator's mind. The assumptions which have been employed herein were those necessary to produce the results which are included. Basically, these simplifications were no more or less restrictive than necessary, in any particular phase of the developments, in order to produce the results acquired in each and every instance. Wherever possible the mathematics were related to the physics; and, the discussions have tended to indicate this by suggesting applications and/or physical reality in most every instance.

From the observations made here it would appear that even though the basic ideas are well known, this work will enhance the general knowledge of these modes for maneuvering. The including of range-rate and acceleration information should point to the nature of the physically realistic constraints which could exist for intercept and pursuit operations. Hopefully, those practical minded persons who work in design and analysis may find, here, facts which are useful, or methods which can be applied to their needs.

As a summary, the contents of this paper include a study of the planar inter-cept and pursuit situations – as kinematic investigations – with examples intro-duced to direct attention to the several aspects of these problems. Also,

graphical results are included to clarify the mathematical and physical inter-pretations which can be given to the various case studies. Under these categories one will find the simple intercept case, and variations of it, as well as the planar pursuit problem with one analytical and one computer developed solution. In the first case, the pursuit of a target moving in a straight line is introduced for in-vestigation; while in the second case the problem considered is that of a target moving along a fixed circular path. For both of these studies ample graphic results are presented to clarify the contents and to stimulate the interested reader.

II. THE PROBLEMS OF INTERCEPT AND PURSUIT

In a classical sense the problem of Intercept is concerned with the finding of a point in space where two bodies will collide as a result of their traveling along predetermined paths of motion. The Pursuit problem, on the other hand, is concerned with the finding of a flight path which allows a chase (or pursuing) vehicle to overtake and collide with a target particle which may be traveling along an unknown, a priori, path. In the case of a pursuit, the interceptor flies along a trajectory so that it always "looks" at its target; and contrary to this, for a simple intercept the "chase" vehicle flies along a precalculated path which "directs" it to that point in space where the collision is to occur. One obvious disadvantage of this simple maneuver is that the paths (thus the collision point) must be predetermined; and therefore, these are based on a known (or assumed) initial state of motion for the target. Hence any variation in the direction and/or speed of the target will cause the intended collision point to be incorrectly located, and collision will not occur.

As a variation of the simple intercept case, one might consider the "lead in intercept" situation, whereby (say) some change in the interceptor's speed along its path would produce an "earlier" collision. In this case, an "altered" collision position would exist, and would be found to lie between the initial point and the "simple" collision point.

The several situations noted above are illustrated in the sketches shown below. For the intercept problem to be studied herein, the target is presumed to fly along a known, predetermined straight-line path; and, generally, it will do this at a fixed speed. The pursuit maneuver which will be investigated is a planar case with the vehicles assumed to be in flight at fixed speeds; however, the pursuit's track is not known or calculated as a priori information.
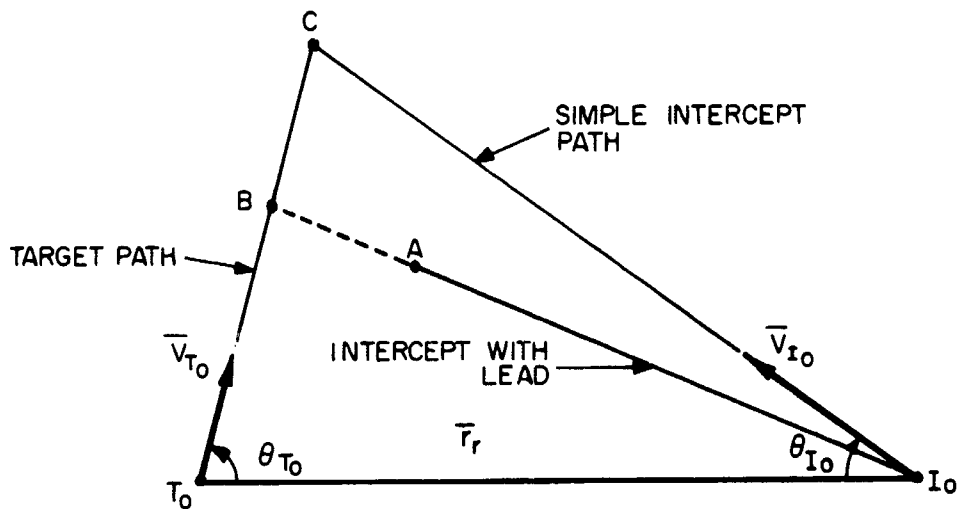
Sketch II.1. Illustrating the INTERCEPT Case (T and I denote the Target and Interceptor positions at $t = 0$); C designates the COLLISION Point, occuring at $t = t_i$). The angles θ_{i_0} denote the inclination of the respective velocity vectors relative to the range vector $\bar{r}_r$.

Point A, on the lead Intercept Path, suggest a position where V_I is increased so that an *earlier intercept* would occur (at B).
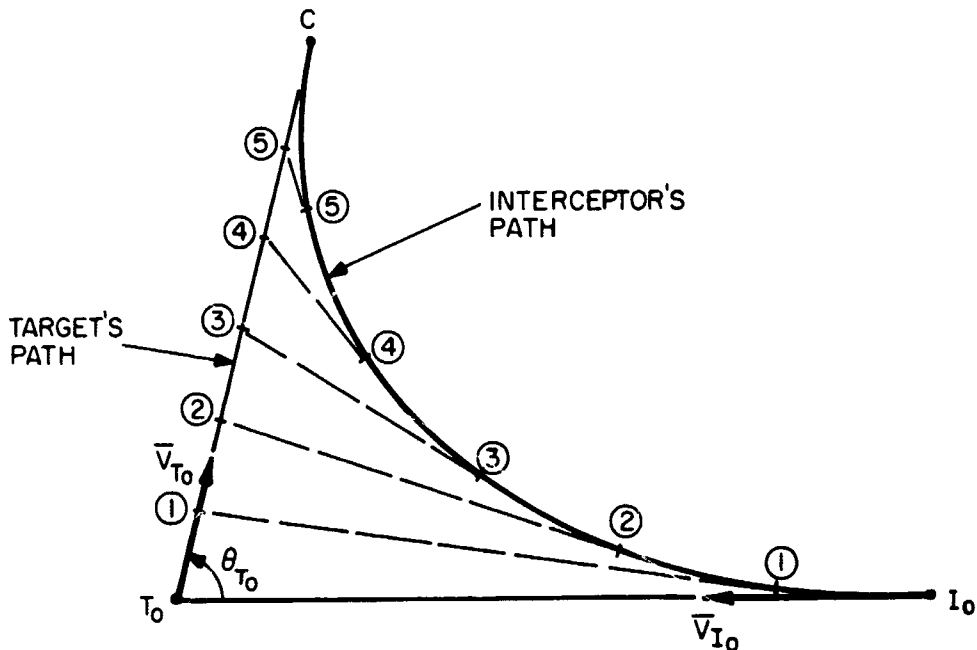
Sketch II.2. Illustrating *Pursuit.* Here the interceptor has its velocity vector always pointing to the instantaneous position of the target (T). Once more collision occurs at "C". Since I "looks" at T continually, the path of motion is a curvilinear track — in contrast to the linear path described for the simple intercept case. Note that in the terminal phase of this maneuver the interceptor is "chasing" the target (from dead astern).

3

III. THE INTERCEPT MANEUVER

III.1. General Considerations

This problem, like that of Pursuit, is principally one of kinematics; that is the track flown by the interceptor (or pursuit vehicle) is dependent only on the relative positions of these two vehicles, and their speeds.

To illustrate the nature of the general governing equation for the intercept case consider the diagram, shown below, depicting conditions as they exist at some general, intermediate time, t ($t_0 \leq t \leq t_i$). The horizon serves as a reference direction to aid in "locating" the relative displacement vector (or range vector) $\bar{r}_r$; and in describing the inclination of the velocity vectors $\bar{V}_j$ ($j = I, T$). For the notation employed here the angles Φ_j serve to describe the velocity inclination with respect to $\bar{r}_r$ while the θ_j (and $\dot{\theta}$) locate the range vector ($\bar{r}_r$), and the velocity vectors ($\bar{V}_T$, $\bar{V}_r$), relative to the horizon.
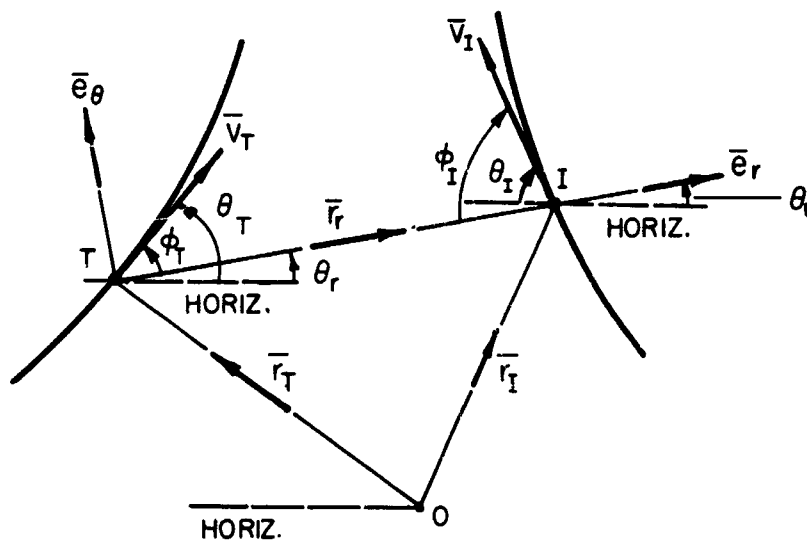
Sketch III.1. Illustrating a *general* intercept situation. T and I designate Target and Interceptor, respectively; O is an inertial origin; $\bar{r}_T$ and $\bar{r}_I$ locate the vehicles wrt O; and, $\bar{r}_r$ is the relative position (range) vector. The angles Φ_j locate the vectors $\bar{V}_j$ relative to $\bar{r}_r$, while the θ_j locate the $\bar{V}_j$ relative to the horizon; θ_r describes the inclination of $\bar{r}_r$ wrt the horizon.

From the sketch (preceding page) one can see that, vectorially,

$$\overline{r}_r = \overline{r}_I - \overline{r}_T \tag{III.1}$$

thus the <u>range rate</u>, or the relative velocity vector, is

$$\overline{V}_r \triangleq \frac{d\overline{r}_r}{dt} \equiv \frac{d}{dt}(\overline{r}_I - \overline{r}_T)$$

which is equivalent to writing

$$\overline{V}_r = \overline{V}_I - \overline{V}_T. \tag{III.2}$$

With $\overline{V}_r$ described (kinematically), through $\overline{r}_r$, then it follows that in reference to a (moving) coordinate frame attached to T (target) one can write, also,

$$\overline{V}_r \triangleq \frac{d(\overline{r}_r)}{dt} = \overline{e}_r \frac{dr_r}{dt} + r_r \frac{d\overline{e}_r}{dt}. \tag{III.3}$$

since $\overline{r}_r \triangleq r_r \overline{e}_r$.

Here dr_r/dt is called the <u>range rate</u>, with r_r being the linear range; while the quantity $d\overline{e}_r/dt$ arises as a consequence of the "rotation" given to the position vector, $\overline{r}_r$.

Recalling that from kinematics

$$\frac{d\overline{e}_r}{dt} = \overline{\omega} \times \overline{e}_r,$$

where $\overline{\omega}$ is the angular velocity vector for the moving unit triad ($\overline{e}_r$, $\overline{e}_\theta$, $\overline{e}_z$), then if the motions are planar (i.e., T and I occupy the same plane) it should be evident that $\overline{\omega} \equiv \dot{\theta}_r \overline{e}_z$, hence

$$\frac{d\overline{e}_r}{dt} = \overline{\omega} \times \overline{e}_r = \dot{\theta}_r (\overline{e}_z \times \overline{e}_r) = \dot{\theta}_r \overline{e}_\theta .$$

Thus, from Eq. (III.3) one sees that

$$\overline{V}_r = \dot{r}_r \overline{e}_r + r_r \dot{\theta}_r \overline{e}_\theta , \qquad (III.4)$$

inferring that the relative velocity ($\overline{V}_r$) is composed of a radial (or range rate) component plus a transverse part which is orthogonal to the range vector ($\overline{r}_r$).

Making use of Eqs. (III.2) and (III.4) it is apparent that the inertial and relative speed components may be related in the following fashion:

Since

$$\overline{V}_r = \overline{V}_I - \overline{V}_T ,$$

and

$$\overline{V}_r = \dot{r}_r \overline{e}_r + r_r \dot{\theta}_r \overline{e}_\theta ,$$

then

$$\dot{r}_r \equiv \overline{V}_r \cdot \overline{e}_r = \overline{V}_I \cdot \overline{e}_r - \overline{V}_T \cdot \overline{e}_r$$

$$= V_I \cos (\pi - \phi_I) - V_T \cos (\phi_T)$$

$$= V_I \cos [\pi - (\theta_I + \theta_r)] - V_T \cos [\theta_T - \theta_r] ,$$

or

$$\dot{r}_r = - [V_I \cos \phi_I + V_T \cos \phi_T] = - [V_I \cos (\theta_I + \theta_r) + V_T \cos (\theta_T - \theta_r)] .$$
$$(III.5)$$

Likewise, it follows that

$$r_r \dot{\theta}_r \overset{\Delta}{=} \overline{V}_r \cdot \overline{e}_\theta = \overline{V}_I \cdot \overline{e}_\theta - \overline{V}_T \cdot \overline{e}_\theta ,$$

6

leading to

$$r_r \dot{\theta}_r = V_I \sin \phi_I - V_T \sin \phi_T = V_I \sin (\theta_I + \theta_r) - V_T \sin (\theta_T - \theta_r) \qquad \text{(III.6)}$$

wherein the angles θ_j, may be regarded as "inertial" position indicators, while the ϕ_j serve as relative position angles.

III.2. The Simple Intercept Problem

The case to be considered here is a restricted version of the more general situation noted in the preceding paragraphs. Here it will be assumed that:

(1) The target flies a straight line path at a fixed speed (thus, $V_T \equiv V_{T_0} = $ constant).

(2) The problem is planar throughout (that is, $\bar{e}_r$, $\bar{e}_\theta$ define the directions for all in-plane components, and $\bar{e}_z$ is normal to the plane of motion).

(3) One can neglect any influence from winds, atmospherics, etc. (thus the problem reduces to a kinematic discussion).

(4) The interceptor has a fixed speed (V_I = constant), and will fly along a line path (hence $\bar{V}_I$ is a constant).

Since both vehicles move over fixed distances in the same time interval (flying at fixed speeds) then it follows that

$$\phi_T = \phi_{T_0} \quad \text{and} \quad \phi_I = \phi_{I_0} \quad \text{(constants)};$$

and, likewise

$$\theta_I = \theta_{I_0}, \text{ as well as, } \theta_T = \theta_{T_0};$$

in addition, $\dot{\theta}_r = 0$. Now, with θ_r being an arbitrary angle let this be set at $\theta_r = 0$; thus the sketch (on following page) geometrically describes the problem under discussion.
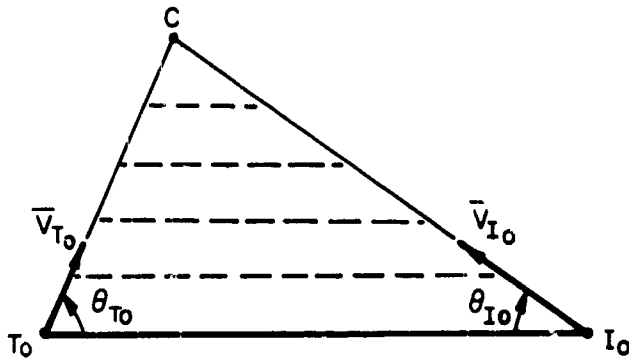
With both vehicles flying at fixed speeds, it is prudent to define a speed ratio,

$$\not{k} \overset{\Delta}{=} \frac{V_I}{V_T} \equiv \frac{V_{I_0}}{V_{T_0}}. \tag{III.7}$$

Specializing Eqs. (III.5) and (III.6) for the present case it follows that

$$\dot{r}_r = - (V_I \cos \phi_I + V_T \cos \phi_T) = - [V_I \cos (\theta_I) + V_T \cos (\theta_T)],$$

and, since there is no transverse speed apparent to this problem,

$$0 = V_I \sin \phi_I - V_T \sin \phi_T = V_I \sin \theta_I - V_T \sin \theta_T;$$

or

$$\dot{r}_r = - V_T [\not{k} \cos \theta_I + \cos \theta_T],$$

and

$$\frac{V_I}{V_T} \overset{\Delta}{=} \not{k} = \frac{\sin \theta_T}{\sin \theta_I}; \tag{III.8}$$

8

thus

$$\dot{r}_r = - V_T \; [\sqrt{k^2 - \sin^2 \theta_T} + \cos \theta_T] \, . \tag{III.9}$$

Equation (III.9) defines the range rate in terms of the known (a priori) constants describing the path flown by the Target Vehicle.

In order to describe the range (r_r) one could integrate Eq. (III.9) from an initial state (r_{r_0}, t = 0) to (say) a general condition (r_r, t) obtaining, as a result,

$$r_r = r_{r_0} - V_T \; [\sqrt{k^2 - \sin^2 \theta_T} + \cos \theta_T] \, t \, . \tag{III.10}$$

At the collision point $r_r = 0$ and $t = t_i$; thus one finds from the expression above that

$$r_{r_0} = V_T \; [\sqrt{k^2 - \sin^2 \theta_T} + \cos \theta_T] \, t_i$$

leading to a time to intercept relation given by

$$t_i = \frac{r_{r_0}}{V_T \; [\sqrt{k^2 - \sin^2 \theta_T} + \cos \theta_T]} \tag{III.11}$$

A graph of Eq. (III.11) has been prepared to illustrate the influence of θ_T (or θ_{T_0}) and k on the time-to-intercept. (See Figure III.1). For this represen-tation the time is presented as the non-dimensional factor, $t_i V_T / r_{r_0}$; this was done to remove the influence of any specific flight condition(s). The variation with θ_T, as shown here, includes all cases from the head-on intercept ($\theta_T = 0$), up to and including the pure chase intercept ($\theta_T = \pi$).

From this figure one can see that k plays only a minor role, in the intercept, so long as θ_T is no larger than (say) $\pi/3$. Above $\pi/2$ the value of k becomes a much more dominant factor. As one might expect the smaller the value of k the longer the time to intercept, as the maneuver approaches the pure chase

9
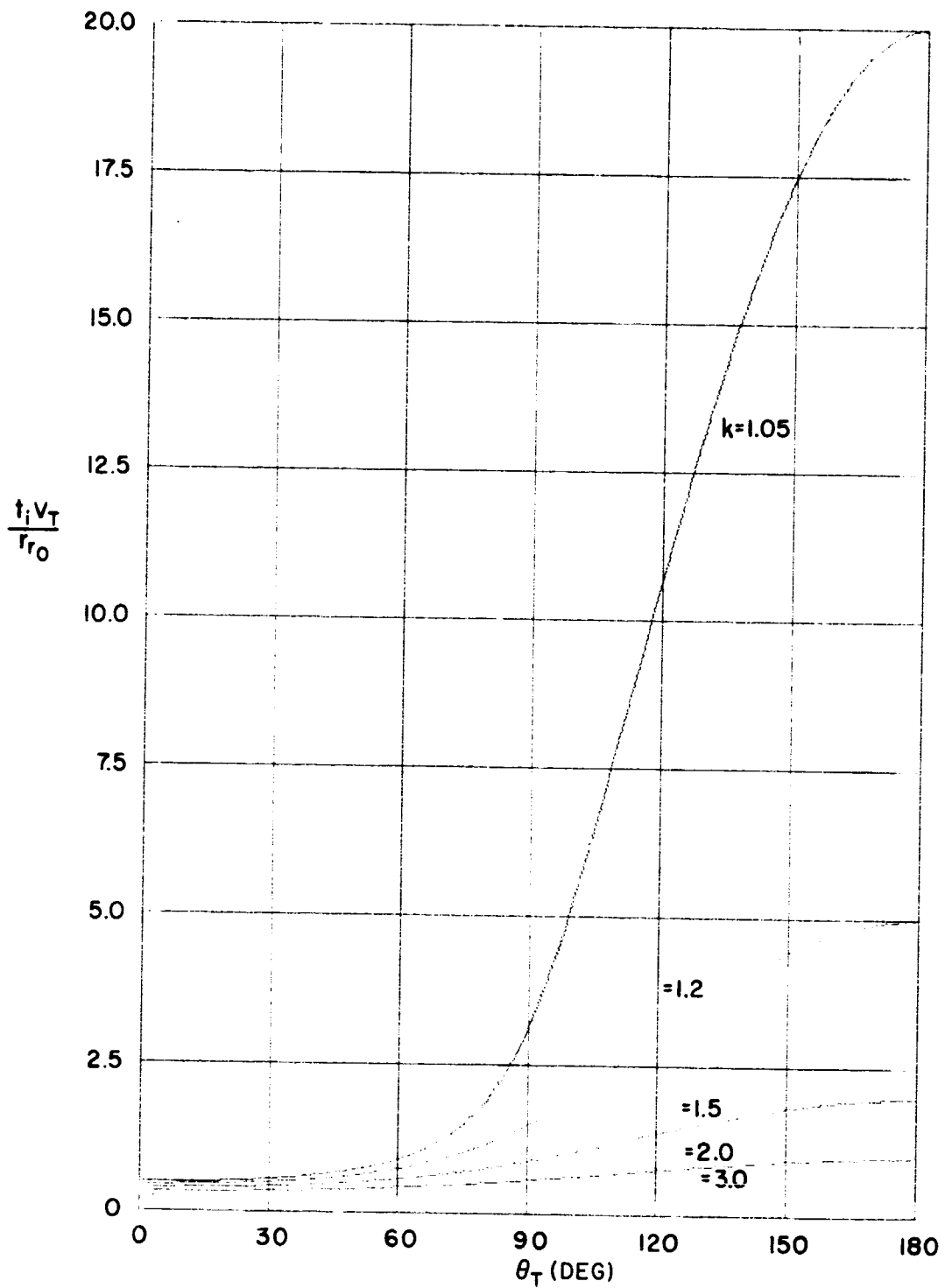
Fig. III.1. Dimensionless time to intercept, as a function of θ_T (the inclination angle for the target).

configuration. Contrary to this, as k increases (say to a value of 3), the time to intercept becomes almost insensitive to θ_T; that is, the relative (direction) orientation of the two vehicles is a fact of diminishing influence.

Combining Eqs. (III.10) and (III.11) one notes that the range-time expression can be given simply as

$$r_r = r_{r_0} \left(1 - \frac{t}{t_i} \right) \qquad \text{(III.12a)}$$

while the range rate-time relationship is simply

$$\dot{r}_r = - \frac{r_{r_0}}{t_i}, \qquad \text{(III.12b)}$$

suggesting the constancy of this quantity for any particular problem.

III.3. An Example

Recalling that $k = \sin\phi_T / \sin\phi_I$ (here), or $k \equiv \sin\theta_T / \sin\theta_I$, then there are certain conditions whereby two possible intercepts might occur for the same value of k (note that $k > 1.0$ applies, however). To illustrate this situation, one such possible set of cases is examined below.
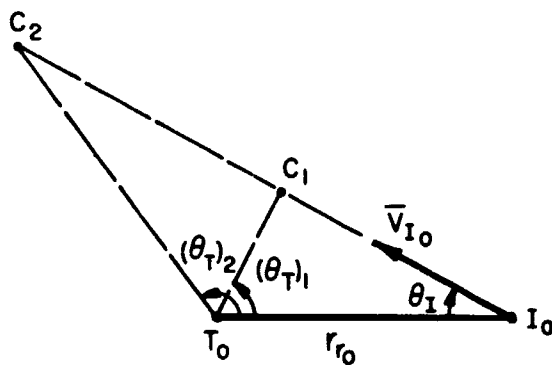
Sketch III.3. Illustrating this example and showing the influence of θ_T on the intercept.

Let the two cases be designated as $(\ )_1$, $(\ )_2$; then, for

$$\theta_I = 30°, \quad \text{and} \quad (\theta_T)_1 = 60°;$$

$$\theta_I = 30°, \quad \text{and} \quad (\theta_T)_2 = 120°;$$

it follows that

$$(k)_1 \overset{\Delta}{=} \left(\frac{V_I}{V_T}\right)_1 = \frac{(\sin \theta_T)_1}{\sin \theta_I} = \frac{\sin(60°)}{\sin(30°)} \equiv \sqrt{3},$$

and

$$(k)_2 = \frac{(\sin \theta_T)_2}{\sin \theta_I} = \frac{\sin(120°)}{\sin 30°} \equiv \sqrt{3},$$

illustrating the consistency of k here. Now, from Eq. (III.11)

$$\left(\frac{V_T t_i}{r_{r0}}\right)_1 = \frac{1}{\sqrt{k_1^2 - (\sin^2 \theta_T)_I} + (\cos \theta_T)_I} \equiv \frac{2}{3 + \sqrt{3}},$$

and

$$\left(\frac{V_T t_i}{r_{r0}}\right)_2 = \frac{1}{\sqrt{k_2^2 - (\sin^2 \theta_T)_2} + (\cos \theta_T)_2} \equiv 1,$$

so that for fixed values of V_T and r_{r0} one sees that the flight time to C_2 is longer than the time needed to reach the collision point C_1 (as should be expected, in agreement with the sketch on preceding page!).

III.4. The Intercept With Lead

By incorporating an added speed increment, or allowing a segment of the intercept path to be flown at an increased speed, then the collision occurs earlier (in time), and after the target vehicle has flown a shorter distance (see the sketch below). Normally, without the speed change intercept would occur at C; however when the path length segment (A to B) is flown at an increased speed (say V_{II}) then intercept will occur at point B.
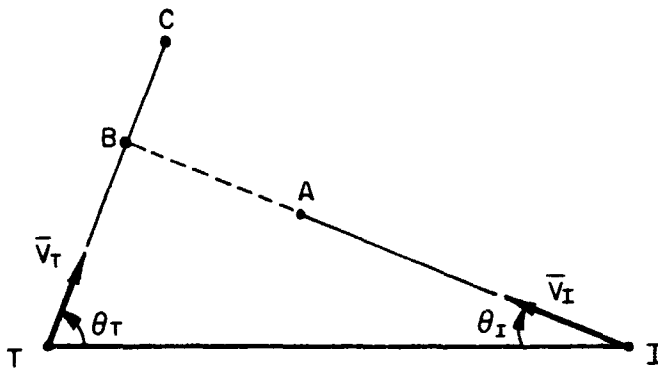
Sketch III.4. Illustrating "intercept with lead", due to a change in V_I.

A simple method for describing this case would be to define a second value for V_I (say, V_I') which includes the temporal influence of V_{II}. That is, write this new interceptor speed as

$$V_I' = \frac{V_I t_A + V_{II} t_B}{t_A + t_B} , \qquad \text{(III.13)}$$

where t_A and t_B are the times needed to reach pt. A and pt. B (along path segments $\widehat{IA}$ and $\widehat{AB}$), respectively. Then, using V_I' in place of V_I (described earlier) the same mathematical expressions apply (approximately) for the range, range-rate and time of flight.

III.5. Geometric Descriptions

It has been indicated that the simple Intercept Problem can be described solely in terms of the speeds (or V_T and k), the initial range (r_{r_0}) and the time to intercept (t_i). Also it has been noted that in some instances the problem may

have two possible solutions (exclusive of the time to intercept), provided $\hbar > 1.0$. In order to gain a clearer understanding of these situations a geometric description of the problem is presented below.

The sketch shown here describes the problem, generally, and indicates the relevant parameters entering into this discussion. In order to best present this case a set of (planar) space oriented axes are selected and utilized to locate the two maneuvering particles. Once again the assumptions of the Simple Intercept Problem are presumed to hold. Arbitrarily, the origin for the inertial coordinates is chosen to coincide with the target (T) at initial time (t = 0).
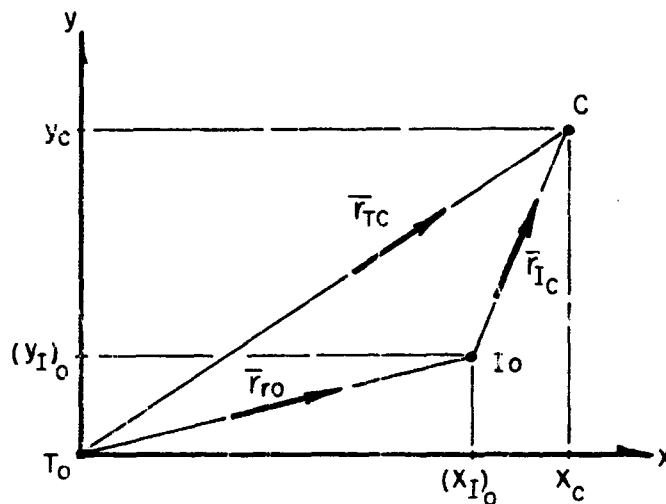
Sketch III.5. To illustrate the Intercept Problem. The axes (x, y) are inertially defined and have their origin at T_0 (position of T at t = 0).

From the sketch, one notes that

$$\bar{r}_r = \bar{r}_{T_c} - \bar{r}_{I_c},$$

where $\bar{r}_{T_c}$ and $\bar{r}_{I_c}$ locate the collision point wrt the target (T) and the Interceptor (I).

14

In terms of the coordinates (x, y) write

$$\bar{r}_{r_0} \triangleq x_{IO}\, \bar{e}_x + y_{IO}\, \bar{e}_y,$$

$$\bar{r}_{T_c} \triangleq x_c\, \bar{e}_x + y_c\, \bar{e}_y,$$

and, hence,

$$\bar{r}_{IC} \triangleq (x_c - x_{IO})\, \bar{e}_x + (y_c - y_{IO})\, \bar{e}_y. \qquad (\text{III.14})$$

Recognizing that while flying at their prescribed fixed speeds (V_j) the vehicles do cover distances proportional to their speed (in a given time), then

$$\hbar \triangleq \frac{V_I}{V_T} \equiv \frac{r_{I_c}}{r_{T_c}},$$

or

$$\hbar^2\, r_{T_c}^{\ 2} = r_{I_c}^{\ 2},$$

which expands to

$$\hbar^2\, (x_c^2 + y_c^2) = [(x_c - x_{IO})^2 + (y_c - y_{IO})^2],$$

and leads directly to

$$(\hbar^2 - 1)\, (x_c^2 + y_c^2) = (x_{IO}^2 + y_{IO}^2) - 2[x_c\, x_{IO} + y_c\, y_{IO}]. \qquad (\text{III.15})$$

Suppose that the loci for all possible intercept (or collision) points define a circle. To describe such a figure, which would have "C" as a point on the circumference, one could write

$$(x_c - \xi_c)^2 + (y_c - \eta_c)^2 = R_0^2,$$

where the coordinates (ξ_c, η_c) locate the center of the circle of loci, and R_0 is its radius. Next, rearranging Eq. (III.15), and accounting for the description of r_{r_0}, it can be shown that

$$\left(x_c^2 + 2\,\frac{x_{IO}}{\hbar^2 - 1}\,x_c\right) + \left(y_c^2 + 2\,\frac{y_{IO}}{\hbar^2 - 1}\,y_c\right) = \frac{r_{r_0}^2}{\hbar^2 - 1} \; ;$$

so that completing the square (here) leads directly to

$$\left(x_c - \frac{x_{IO}}{1 - \hbar^2}\right)^2 + \left(y_c - \frac{y_{IO}}{1 - \hbar^2}\right)^2 = \frac{\hbar^2}{(1 - \hbar^2)^2}\,r_{r_0}^2 \qquad (III.16)$$

(for $\hbar^2 < 1.0$).

This expression describes the circle with its center located at (ξ_c, η_c); one whose radius (R_0) is noted to be

$$R_0 = \frac{\hbar\, r_{r_0}}{(1 - \hbar^2)} .$$

Here the coordinates of the center are recognized to be,

$$\xi_c = \frac{x_{IO}}{1 - \hbar^2}, \qquad (III.17a)$$

and

$$\eta_c = \frac{y_{IO}}{1 - \hbar^2}, \quad \text{for } (\hbar^2 < 1.0). \qquad (III.17b)$$

16

Remembering that $k \triangleq V_I/V_T$, then the more interesting cases would be those which have $k^2 > 1.0$. For this requirement it can be proven that the loci of collision points describe a circle with center and radius defined by

$$\xi_c = -\frac{x_{IO}}{k^2 - 1},$$

$$\eta_c = -\frac{y_{IO}}{k^2 - 1},$$

and

$$R_0 = \frac{k\, r_0}{k^2 - 1}, \qquad\qquad\qquad\qquad (III.18)$$

respectively (for $k > 1.0$).

III.6. A Limit Case for the Geometry

A cursory study of the results given by Eqs. (III.17) and (III.18) w'll acquaint the reader with the fact that as $k \to 1.0$ the central points recede (to large distances) from the origin; and, that the radii increase without limit. This would indicate that the loci of collision points degenerate from a circle to a straight line (and, in particular, this line bisects the distance between I and T). Naturally these loci are equidistant from I and T (since $k = 1.0$), hence the line of permissible intercept positions is orthogonal to $\overline{r}_{r_0}$.

III.7. Geometry of the Intercept

As an aid to understanding the graphics associated with this maneuver the figures shown below have been prepared using Eqs. (III.17) and (III.18). Generally, the contours for the intercept loci are circles, each corresponding to a fixed value of k; these are all centered along extensions of r_{r_0}, but are not concentric in their construction. Also, as the value of k decreases (from unity) the size of the circles decrease; and, as k increases in value (from unity) the size again decreases. The limit case ($k = 1$) is depicted as a straight line, bisecting the length TI ($= r_{r_0}$) and constructed perpendicular to it.

In a like manner it is easy to ascertain that the circles reduce to a point as
$k \to \infty$ and as $k \to 0$. A general composite diagram is shown in the (unscaled)
sketch below; more correct representations are included as Figures III.2 and III.3.
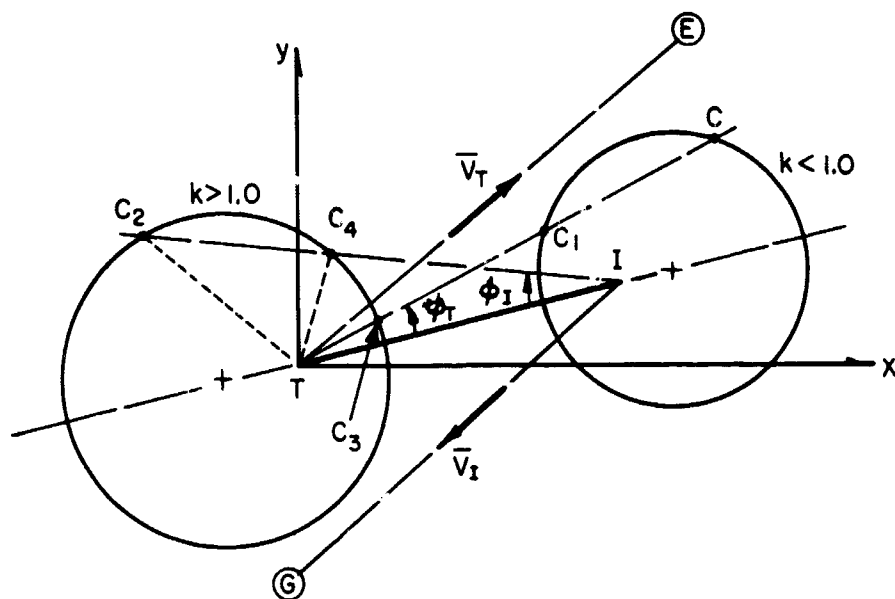
Sketch III.6. Depicting the geometry for the simple intercept maneuver. The
angles ϕ_T and ϕ_I are possible inclinations indicative of an intercept — T_0 and I_0
indicate the original positions of the Target and Interceptor (at $t = 0$). The
length $(TI)_0 \equiv r_{r_0}$ (initial range).

The sketch, above, indicates both the possible and impossible conditions
for an intercept based on a set of known Initial Conditions. Two cases ($k < 1.0$
and $k > 1.0$) are considered. First, for the case when $k < 1.0$, one notes that if
the target flies along the path inclined at ϕ_T (relative to the line TI) it is possible
for the interceptor to collide with the Target at two admissible points (C and C_1).
It should be evident that the intercept at C_1 occurs in lesser time than that
happening at point C; also the path direction for each of these intercepts is
different.

When the Target (T) flies along the line T Ⓔ (at the velocity $\overline{V}_T$) it is im-
possible for I to collide with T (for the value of $k(<1.0)$ used in constructing
the circle shown). The reason for such stems from the fact that this circle
represents all possible loci for a collision when the vehicles have the given
speed ratio (k) noted. Hence when the flight path (of T) does not touch the circle,
at least, no collision can occur.

18

Next, suppose that $k > 1.0$ (as shown). In this case, for a same prescribed value of ϕ_T, there is only one possible intercept to be made by I – this could occur at C_3 (as noted). And, to the contrary, if the interceptor flies along the line inclined at ϕ_I, relative to TI, it could intercept – and collide – with T at either of the points C_2 and/or C_4 (on the circle for $k > 1.0$). Necessarily, as in the previous case, when the interceptor flies along the line I Ⓖ, and the speed ratio is k (as noted above), no collision can occur since that line from I does not touch the circle of intercept points.

Incidentally, the maximum (minimum) inclinations of the paths from T and I are those which begin at T and I, respectively, and are just tangent to the intercept circles – for these k values considered. It can be shown that these limit cases occur for $|\phi_T|$ and/or $|\phi_I|$ equal to $\pi/2$. That is, the target and/or interceptor must fly from their initial positions orthogonal to the initial range vector ($\bar{r}_{r_0}$).

A pair of accurately scaled figures are included below to enhance the i˙ ˙rative geometry of this intercept problem (see Figs. III.2, III.3). Several circles, for different values of $k \gtrless 1.0$, are indicated on these plots. In addition to the circles, the location of their centers and a typical pair of possible intercept positions (C and C') are shown. Also, the loci for all $k = 1.0$ intercepts are included on these graphs; this locus is the straight line appearing on both figures.

IV. THE PURSUIT PROBLEM

IV.1. General Considerations

The second type of collision example to be studied here is that one classed as the pursuit problem. This differs from the Simple Intercept situation in that now the path for the interceptor is a continually varying curve in space. A basic premise in this study is the idea that the interceptor always "looks" at the Target, hence the velocity vector ($\bar{V}_I$) is continually pointing at the Target vehicle (s e the sketch on following page).

In concurrence with the previous investigation it will be assumed that the speed of each vehicle is a constant, thus their speed ratio is (again) the constant

$$k \triangleq \frac{V_I}{V_T}. \qquad \text{(IV.1)}$$

19
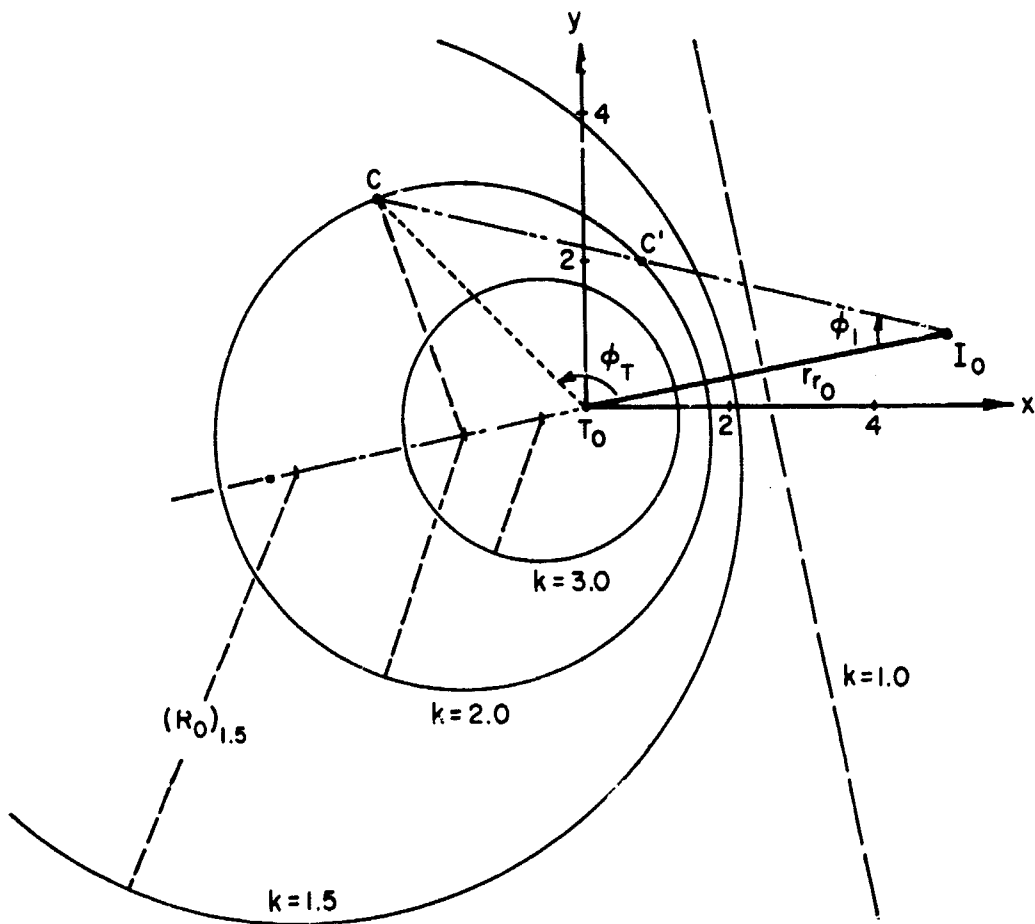
Fig. III.2. Geometry of the Planar Intercept Problem for $k \geqslant 1.0$. Shown are several circles of positions where intercept can occur, each for a given value of k. Note that I can intercept T at two possible positions (C, C') for the case illustrated.
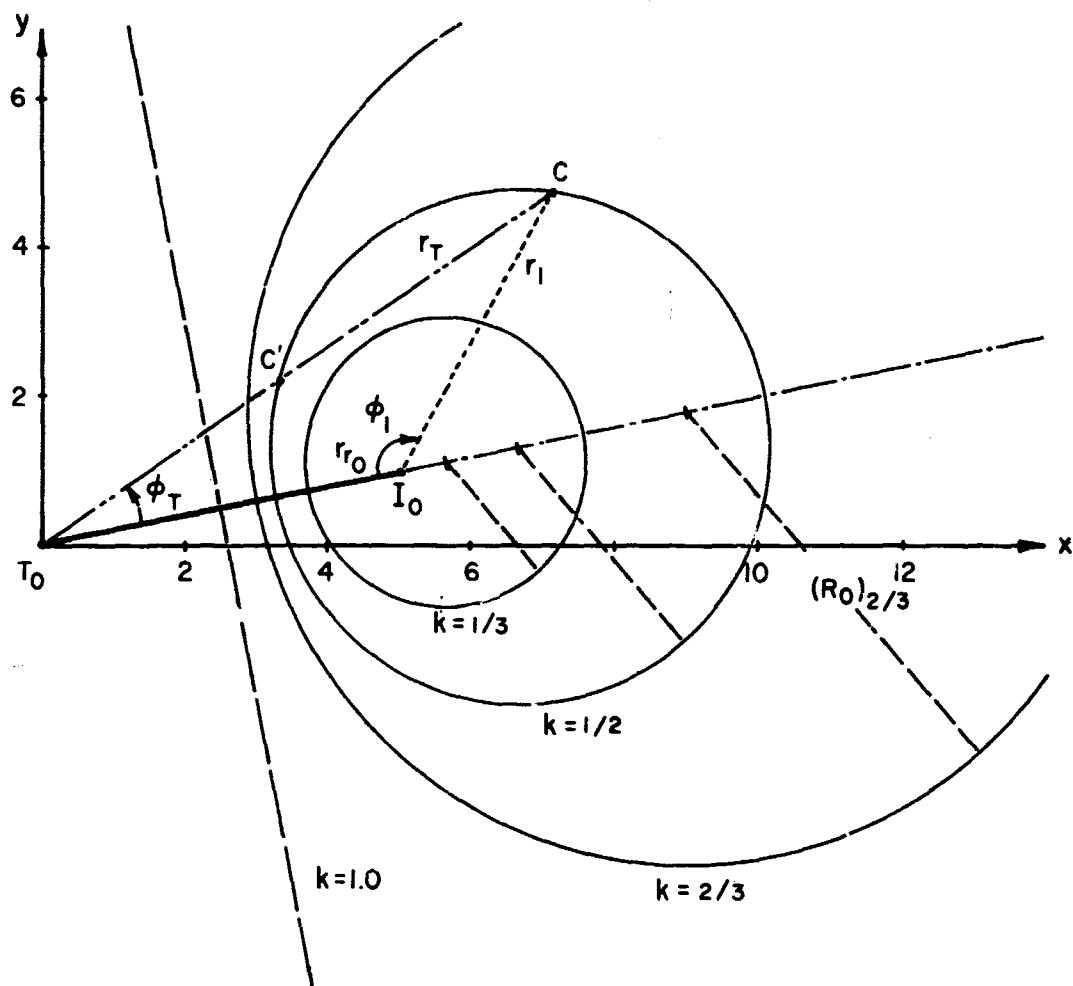
Fig. III.3. Geometry of the Intercept Problem for $k \leqslant 1.0$. The circles of intercept loci, their centers and relative sizes are indicated here. Note that two intercept points (C, C′) exist for a given value of Φ_T (or θ_T) and k.

21

In addition, it is presumed that the flight path of the target is known, a priori, and that the interceptor's path is to be determined.

In the initial phases of this investigation cartesian coordinates will be employed. It has been decided that a general origin will be selected, but not necessarily coincident with either vehicle; and that the quantities which refer to each vehicle will have an appropriate subscript affixed to them.
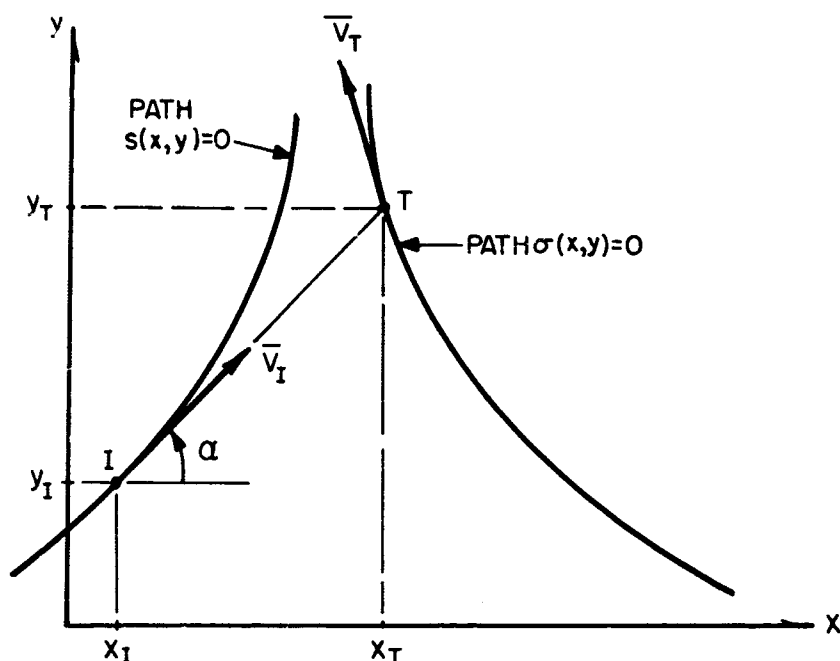
Sketch IV.1. Depicting the Pursuit Problem.

Note that $\bar{V}_I$ always points toward "T", and that Cartesian Coordinates are used for convenience. The subscripts are to describe the appropriate vehicle (I, T).

The paths $\sigma(x, y)$ and $s(x, y)$ will describe the track of the target and interceptor, respectively. The angle α indicates the inclination of $\bar{V}_I$ wrt the x-axis.

Since the speed of each vehicle is fixed, and in a constant ratio (see Eq. (IV.1)), then it follows that

$$\frac{ds}{dt} = \frac{d\sigma}{dt} \, k \, .$$

(IV.2)

Also, with $\overline{V}_I$ directed toward T, at all times, and being tangent to $\sigma(x, y)$, then

$$\frac{dy_I}{dx_I} = \tan \alpha = \frac{y_T - y_I}{x_T - x_I}. \qquad (IV.3)$$

In agreement with Eq. (IV.2) it follows that

$$(ds)^2 = k^2 (d\sigma)^2$$

or

$$k^2 [(dx_T)^2 + (dy_T)^2] = (dx_I)^2 + (dy_I)^2;$$

which is equivalent to

$$k^2 \left[\left(\frac{dx_T}{dx_I}\right)^2 + \left(\frac{dy_T}{dx_I}\right)^2 \right] = 1 + \left(\frac{dy_I}{dx_I}\right)^2 \qquad (IV.4)$$

This last expression connects the two paths of motion (s and σ) through their derivatives. The quantities on the left side of Eq. (IV.4) are obtained from the specification of the path (σ) for T. With these terms evaluated, then – in principle – an integration could be performed to give a description of the interceptor's flight path, s(x, y)!

Assuming that the Target's path is known, and can be written as (say) $\sigma(x, y) = 0$, then the problem reduces to that of obtaining a path for the interceptor, (say) s(x, y) = 0!

In order to describe this desired trajectory one could make use of Eq. (IV.4), obtaining the required derivatives from:

(1) the known path, $\sigma(x, y) = 0$;

and,

(2) the inclination expression for the line of sight, Eq. (IV.3).

That is, making use of:

(1)
$$\frac{d}{dx_I} (\sigma(x, y)) = 0;$$

and,

(2)
$$\frac{d}{dx_I} \left[\frac{dy_I}{dx_I} \right] = \frac{d}{dx_I} \left(\frac{y_T - y_I}{x_T - x_I} \right)$$

or from (1),

$$0 = \frac{\partial \sigma}{\partial x_T} \frac{dx_T}{dx_I} + \frac{\partial \sigma}{\partial y_T} \frac{dy_T}{dx_I} ; \qquad \text{(IV.5)}$$

and, replacing (2) with

$$\frac{d}{dx_I} \left[\frac{dy_I}{dx_I} (x_T - x_I) \right] = \frac{d}{dx_I} (y_T - y_I),$$

obtaining

$$\frac{dy_T}{dx_I} \quad \frac{dy_I}{dx_I} \frac{dx_T}{dx_I} + \frac{d^2y_I}{dx_I^2} (x_T - x_I), \qquad \text{(IV.6a)}$$

which can be alternately expressed as

$$\frac{dy_T}{dx_I} = \frac{dx_T}{dx_I} \left(\frac{y_T - y_I}{x_T - x_I} \right) + \frac{d^2y_I}{dx_I^2} (x_T - x_I). \qquad \text{(IV.6b)}$$

24

In theory, then, the interceptor's path can be acquired by incorporating Eqs. (IV.5), (IV.6) into Eq. (IV.4) and integrating; knowing, of course, the path $\sigma(x, y) = 0$.

IV.2. An Example:

As an example of this formulation the following case will be studied. For simplicity the orientation of the axes (x, y) have been described in a manner which should allow the presentation to be as uncomplicated as is feasible.

The problem situation, presented here, shows the Target (T) moving along a straight line path $(x_T = a)$, beginning at the initial point

$$(y_T)_0 = b; \quad (x_T)_0 = a. \tag{IV.7}$$

The interceptor is initially placed at the origin, thus

$$(x_I)_0 = (y_I)_0 = 0;$$

and its <u>initial</u> line-of-sight will be described as,

$$\left(\frac{dy_I}{dx_I}\right)_0 = \frac{(y_T - y_I)_0}{(x_T - x_I)_0} = \frac{b}{a}; \tag{IV.8*}$$

or, as an equivalent statement,

$$\tan \alpha_0 = \frac{b}{a}.$$

---

*As an alternate description for the line-of-sight $(\angle LOS)_T$, measured wrt $\overline{V}_{T_0}$, one could write $\angle(LOS)_{T_0} = (3\pi/2) - \alpha_0$, initially; or $\angle(LOS)_T = (3\pi/2) - \alpha$, generally.
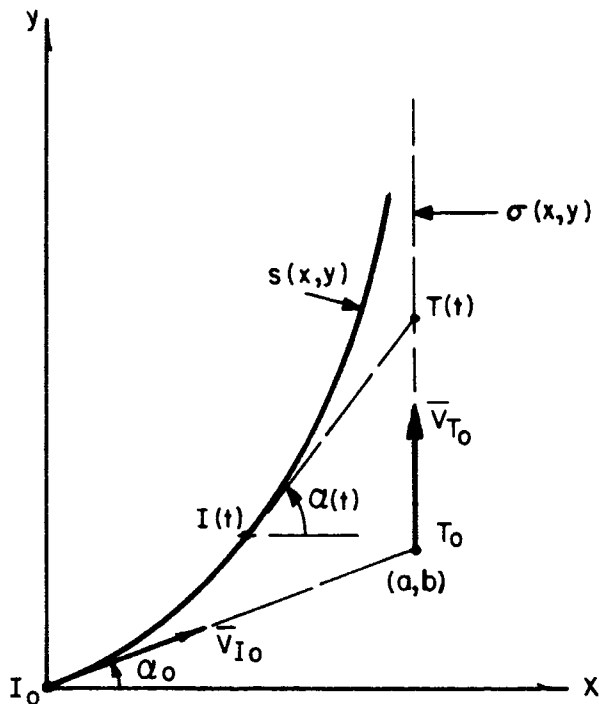
Sketch IV.2. Describing a pursuit problem wherein the target (T) flies a straight line path, and the interceptor (I) moves in the manner whereby it is always directed at the Target.

As illustrated on the sketch, the target moves along the linear path

$$\sigma(x,\ y) \equiv x_T - a = 0, \tag{IV.9}$$

at its constant velocity

$$\overline{V}_T = constant;$$

while the interceptor pursues the target along its trajectory $s(x,\ y)$, at a fixed speed but with its velocity vector always in the direction of the line of sight (i.e. at angle a). Note that

$$a = a(t)$$

$$\overline{V}_I = \overline{V}_I(t), \quad but \quad V_I = constant,$$

26

Solution:

Since $\sigma(x, y) = 0$ is as described in Eq. (IV.9), then it follows that

$$\frac{dx_T}{dx_I} = 0,$$

and consequently Eq. (IV.4) reduces to

$$\frac{dy_T}{dx_I} = \frac{d^2y_I}{dx_I^2} (x_T - x_I) = \left[\frac{d}{dx_I} \left(\frac{dy_I}{dx_I} \right) \right] (a - x_I). \qquad \text{(IV.10)}$$

Next, defining

$$p_I \stackrel{\Delta}{=} \frac{dy_I}{dx_I}, \quad \text{and} \quad p' \stackrel{\Delta}{=} \frac{d}{dx_I} (p_I),$$

then Eq. (IV.10) is compactly written as

$$\frac{dy_T}{dx_I} = (a - x_I) p'_I. \qquad \text{(IV.11)}$$

Now, from Eq. (IV.4) one notes that

$$k^2 \left[\left(\frac{dx_T}{dx_I} \right)^{2 \ 0} + \left(\frac{dy_T}{dx_I} \right)^2 \right] = 1 + p_I^2,$$

27

or

$$\frac{dy_T}{dx_I} = \frac{\sqrt{1 + p_I^2}}{k}.$$ (IV.12)

having chosen the positive radical. On combining Eqs. (IV.11) and (IV.12), then

$$p_I' = \frac{\sqrt{1 + p_I^2}}{k(a - x_I)},$$ (IV.13)

which is a differential equation describing the slope of the line of sight.

This last expression is separable, and consequently has — as a first integral — the solution form

$$\ln (p_I + \sqrt{1 + p_I^2}) = \ln (\mathcal{C}(a - x_I)^{-1/k})$$ (IV.14)

where $\mathcal{C}$ is a constant of integration. Obviously an alternate form of this resultant is

$$p_I = \frac{1}{2} \left[\mathcal{C} (a - x_I)^{-1/k} - \frac{(a - x_I)^{1/k}}{\mathcal{C}} \right]$$ (IV.15)

The quantity p_I measures the instantaneous slope of the path to the collision point; thus a second integration for a description of the trajectory is immediately available.

To facilitate manipulations here it is suggested that a transformation of the independent variable should be introduced. In this regard define

28

$$z \overset{\Delta}{=} a - x_I, \quad \text{hence} \quad dz = - dx_I;$$

then Eq. (IV.15) is rewritten and separated into

$$y_I = \frac{1}{2\mathcal{C}} \int z^{1/k} \, dz - \frac{\mathcal{C}}{2} \int z^{-1/k} \, dz,$$

which can be shown to yield

$$y_I = \mathcal{C}_1 + \frac{k}{2(k^2 - 1)} \left[\frac{(k-1)}{\mathcal{C}} z^{\frac{k+1}{k}} - \mathcal{C}(k+1) z^{\frac{k-1}{k}} \right], \quad \text{(IV.16)}$$

wherein $\mathcal{C}_1$ is an integration constant.

The two integration constants may be defined from the initial values: e.g., if

$$\left(\frac{dy_I}{dx_I} \right)_0 \overset{\Delta}{=} (p_I)_0 = \frac{b}{a} \, (\equiv \tan \alpha_0),$$

and

$$(x_I)_0 = (y_I)_0 = 0; \quad \text{or}, \quad z_0 = a \colon$$

then, as a consequence of these conditions, the final form of the expressions for p_I and y_I may be written as:

$$p_I = \frac{1}{2} \left[\frac{\dfrac{b}{a} + \sqrt{\dfrac{b^2}{a^2} + 1}}{\left(1 - \dfrac{x_I}{a}\right)^{1/k}} - \frac{\left(1 - \dfrac{x_I}{a}\right)^{1/k}}{\dfrac{b}{a} + \sqrt{\dfrac{b^2}{a^2} + 1}} \right], \quad \text{(IV.17)}$$

29

and

$$y_I = \frac{k\,a}{2(k^2 - 1)} \left\{ (k + 1)\left(\frac{b}{a} + \sqrt{\frac{b^2}{a^2} + 1}\right)\left[1 - \left(1 - \frac{x_I}{a}\right)^{\frac{k-1}{k}}\right]\right.$$

$$\left. - \frac{(k - 1)}{\frac{b}{a} + \sqrt{\frac{b^2}{a^2} + 1}}\left[1 - \left(1 - \frac{x_I}{a}\right)^{\frac{k+1}{k}}\right]\right\}, \qquad \text{(IV.18)}$$

since

$$\frac{C}{a^{1/k}} = \frac{b}{a} + \sqrt{\frac{b^2}{a^2} + 1} \quad (\equiv \tan \alpha_0 + \sec \alpha_0). \qquad \text{(IV.19)}$$

Equations (IV.17) and (IV.18) describe the angle α ($p_I = \tan \alpha$) and the trajectory for the interceptor ($y_I = y_I$ (x_I)), respectively. In these two expressions the independent variable (to manipulate) is the coordinate x_I, which has a range of values given by

$$0 \leq \frac{x_I}{a} \leq 1.0,$$

(see Sketch IV.2).

An examination of equation (IV.17) will demonstrate that p_I can be varied from $\tan \alpha_0$ to very large values (indicating $\alpha \rightarrow \pi/2$), when pursuit occurs.

As a means of illustrating the geometry of the trajectories obtained for this example; and to indicate the influence of k, and the initial launch orientation (α_0) on the problem, Figs. IV.1 have been prepared.

30
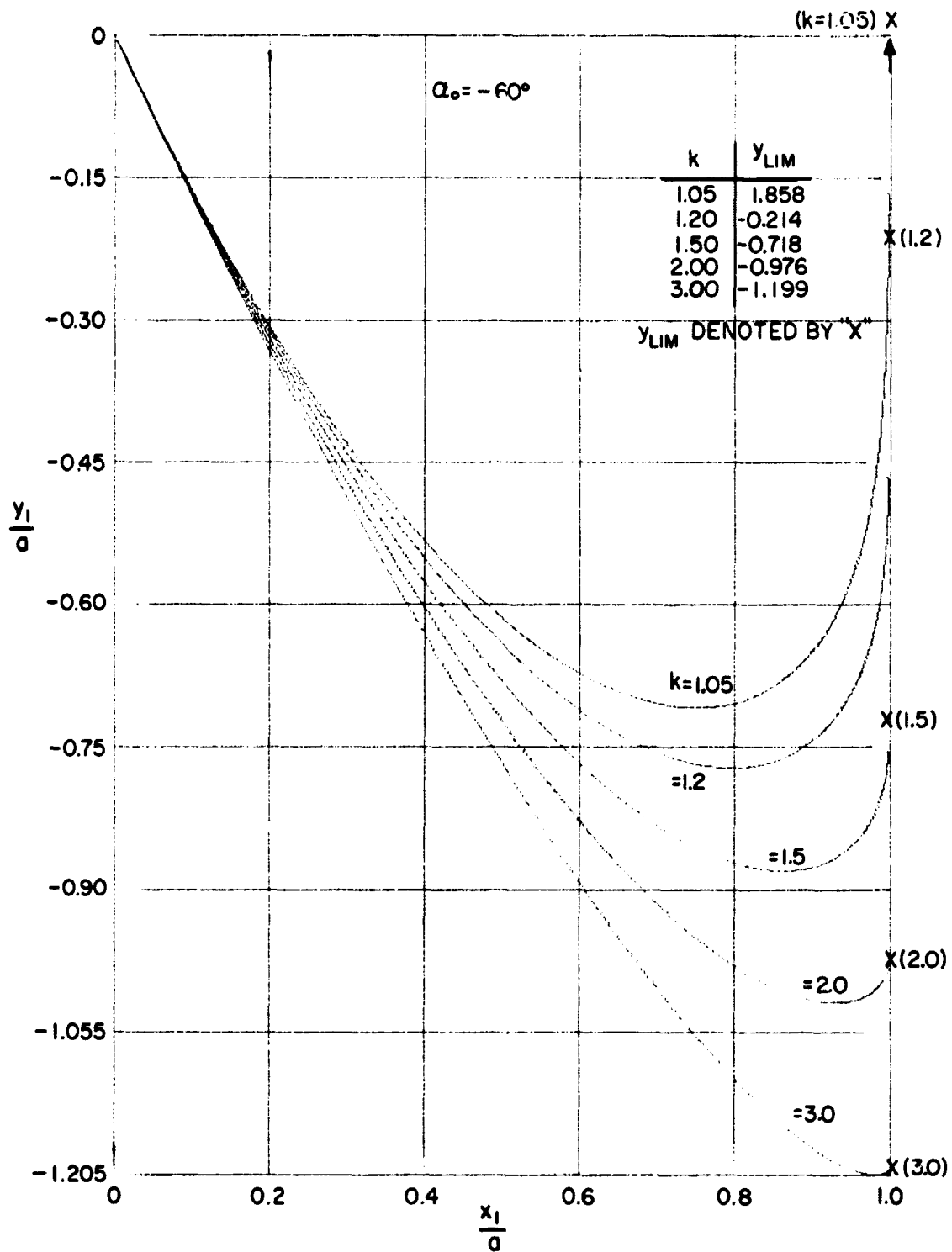
Fig. IV.1(a). Plot of the dimensionless pursuit trajectory, showing the influence of k for $\alpha_0 = -60°$. The values of y_{lim}/a are noted here to indicate the full extent of the motion.

31

(k=1.05)x

x(1.2)

$\alpha_o = -30°$

k	y_{LIM}
1.05	5.619
1.20	1.26
1.50	0.346
2.0	$\simeq 0$
3.0	−0.2165

y_{LIM} DENOTED BY "x"

1.25

1.06

0.87

0.675

$\dfrac{y_{I}}{a}$

0.48

0.29

x(1.5)

0.097

k=1.05

=1.2

=1.5

x(2.0)

-0.096

=2.0

x(3.0)

=3.0

-0.29

0   0.2   0.4   0.6   0.8   1.0

$\dfrac{x_{I}}{a}$
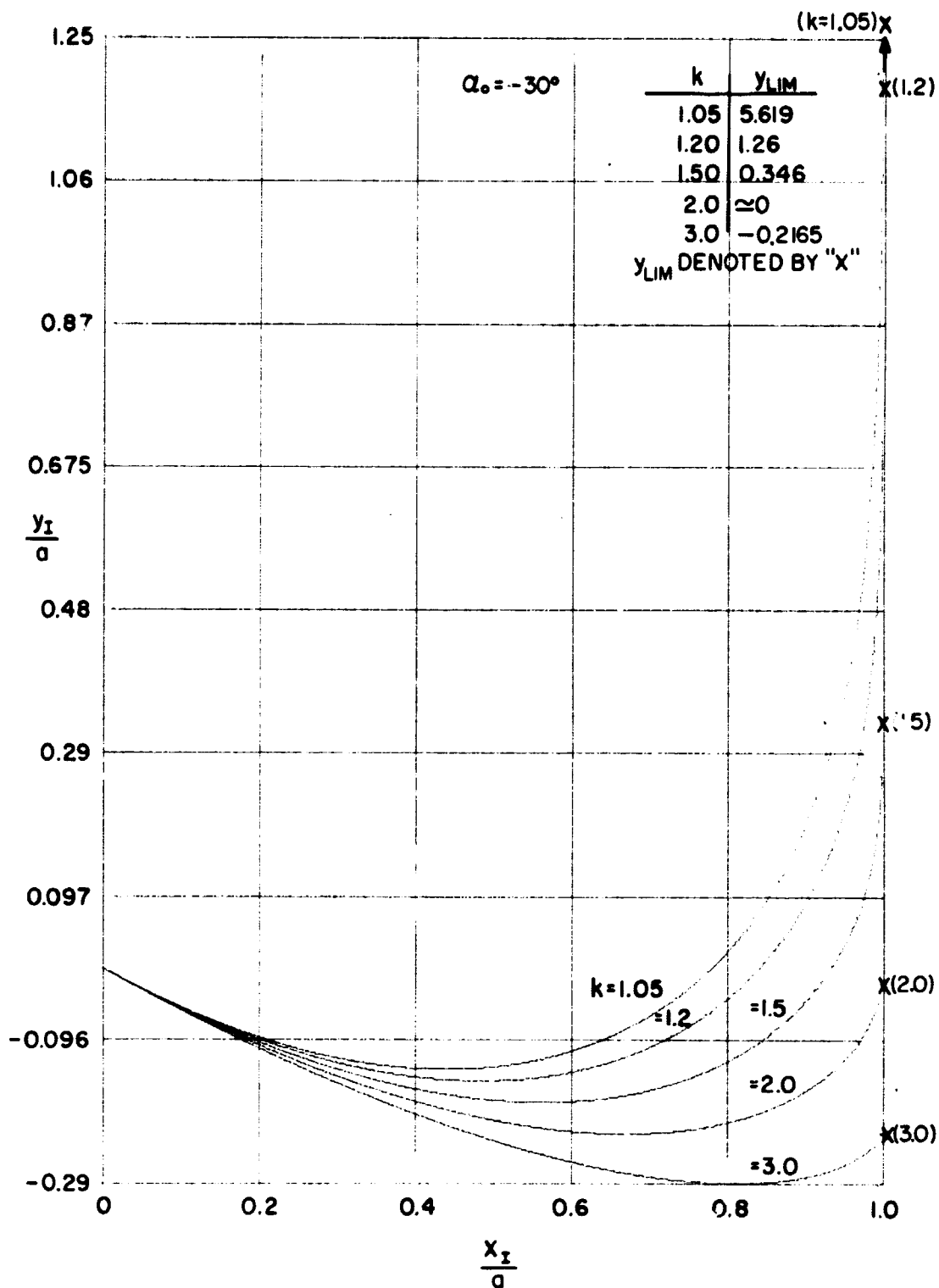
Fig. IV.1(b). Plot of the dimensionless pursuit trajectory, showing the influence of k for $\alpha_0 = -30°$. The values of y_{lim}/a are noted here to indicate the full extent of the motion.

(k 1.05) X
X(1.20)

2.68

α=0°

k	y_{LIM}
1.05	10.24
1.20	2.73
1.50	1.20
2.0	0.67
3.0	0.38

y_{LIM} DENOTED BY "X"

2.35

2.01

1.68

$\dfrac{y_I}{a}$

1.34

1.00

X(1.50)

1.67

X(2.0)

k=1.05

=1.2 ⟶ =1.5   =2.0   X(3.0)

=3.0

1.34

0

O   0.2   0.4   0.6   0.8   1.0

$\dfrac{x_I}{a}$
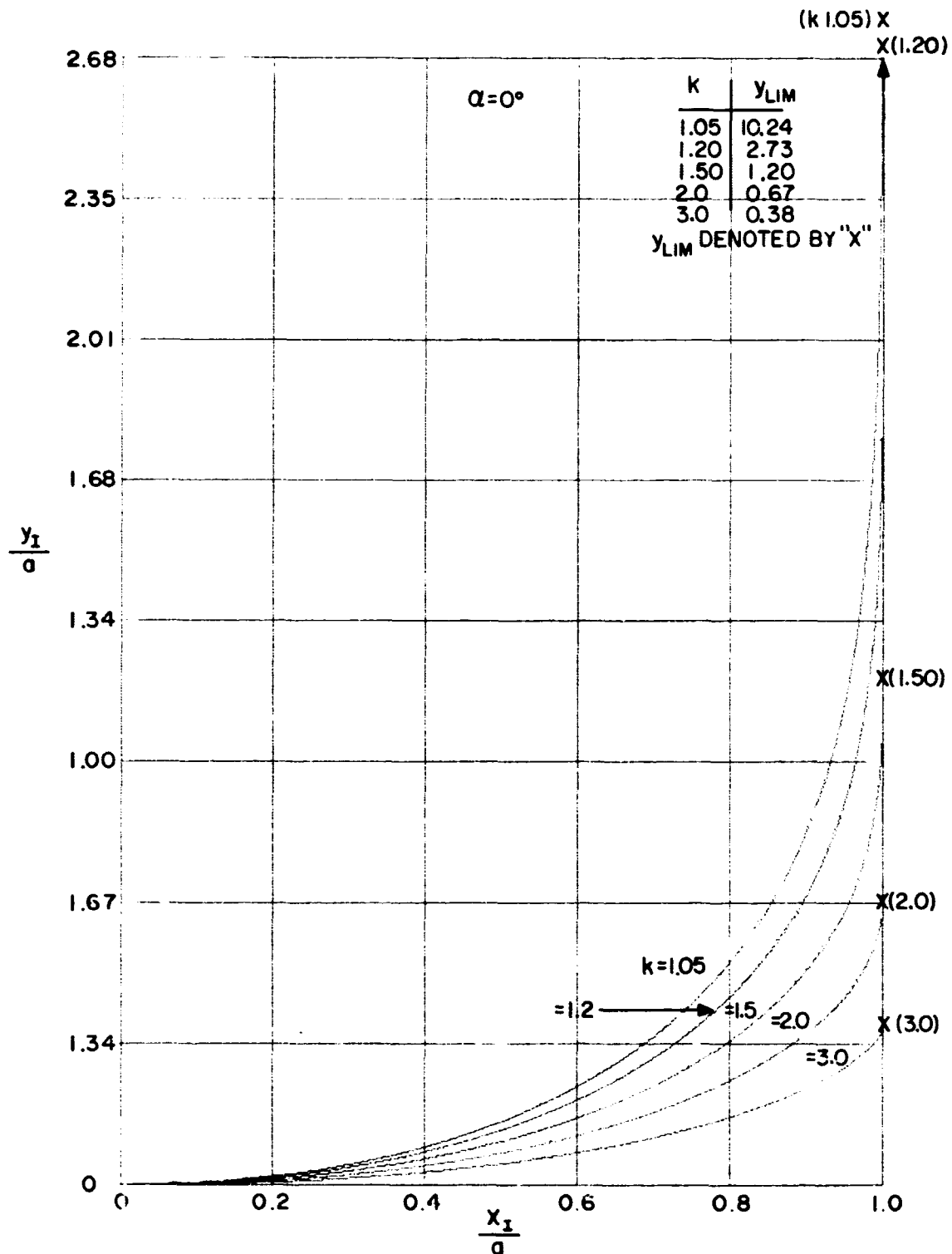
Fig. IV.1(c). Plot of the dimensionless pursuit trajectory, showing the influence of k for
$a_0 = 0°$. The values of y_{iim}/a are noted here to indicate the full extent of the motion.

33
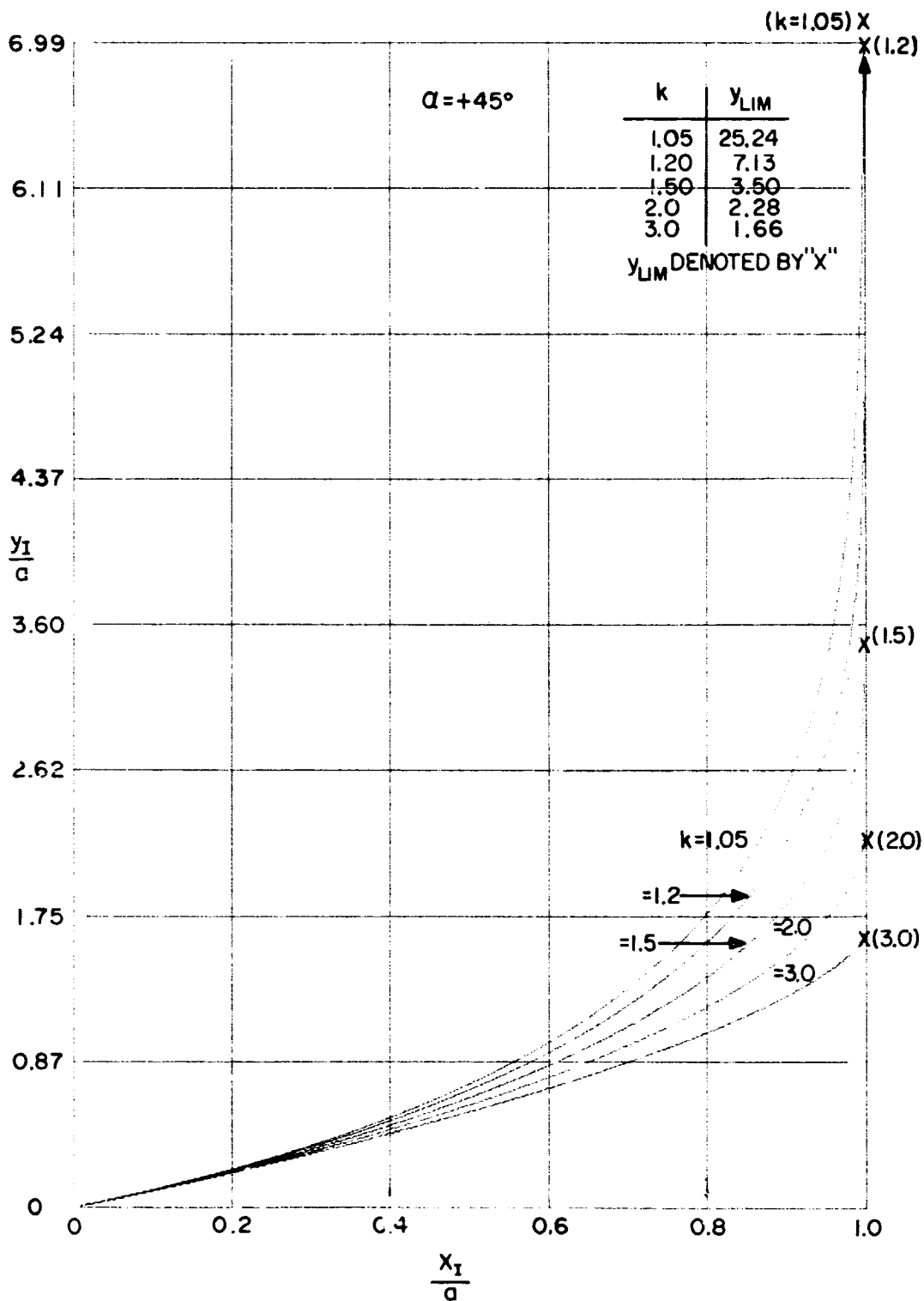
Fig. IV.1(d). Plot of the dimensionless pursuit trajectory, showing the influence of k for $a_0 = 45°$. The values of y_{lim}/a are noted here to indicate the full extent of the motion.
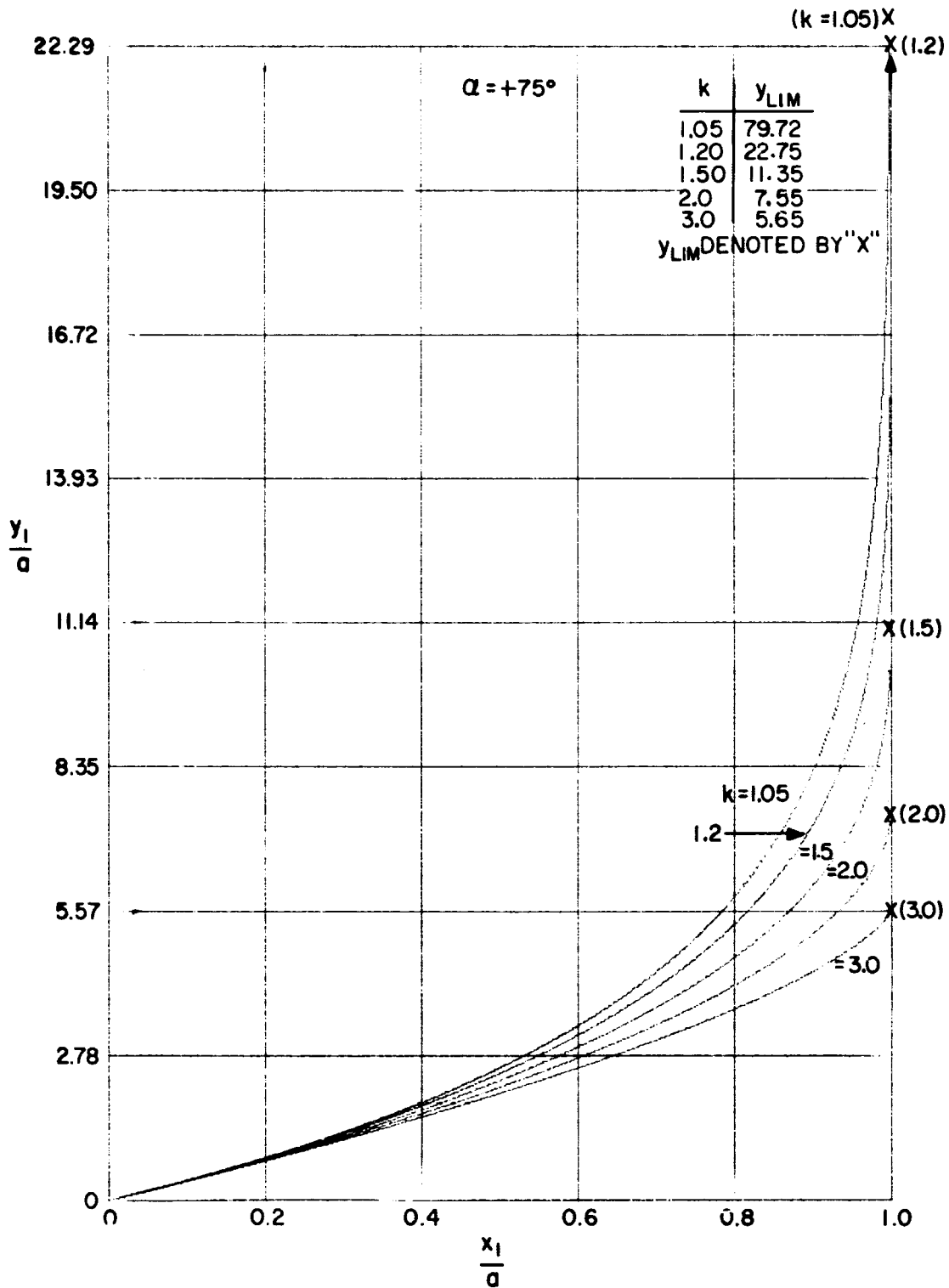
Fig. IV.1(e). Plot of the dimensionless pursuit trajectory, showing the influence of k for $a_0 = 75°$. The values of y_{lim}/a are noted here to indicate the full extent of the motion.

35

In agreement with the choice of coordinates used here, each trajectory will begin at the origin (0); and, by the philosophy of the pursuit maneuver, each will terminate with the interceptor approaching from dead astern of the target.

These figures are indicative of the fact that regardless of the initial orientation, the trajectory having the largest k value is that one which reaches the target the quickest, flies the shortest path and has the least path curvature, initially. It is also apparent that all of these paths have their largest curvature near the terminal phase of the motion; and, that this increases with k.

For convenience of representation the flight paths have been nondimensionalized by division with the distance, a; and are presented a hey would be traced on the plane of motion. Since each figure is for a different value of α_0 (from $-60°$ to $+75°$), and each trajectory will terminate at a different final displacement (y_{1im}) – dependent on the value of k – these final ordinates are indicated, but not to proper scale in each instance.

A study of these several plots should acquaint the reader with the influence of these various factors. The values, y_{1im}, are obtained from Eq. (IV.20), found in the next section; note that $y_{1im} \triangleq f(\alpha_0, k)$.

In order to clarify the physical picture of the initial orientation, one should recognize that when $\alpha_0 = -\pi/2$ the interceptor is positioned "dead ahead" of the target; at $\alpha_0 = +\pi/2$ the interceptor is "dead astern;" and, at $\alpha_0 = 0$ the interceptor is located at the "nine o'clock" position relative to the target.

IV.3. Limits for the Maneuver

It should be recalled that the initial value for y_I is, $y_I = 0$; while the upper (limit) for y_I must be obtained from Eq. (IV.18). In this regard one should recognize that $y_{I_{lim}} \triangleq y_I$ evaluated at $x_I/a = 1.0$; or, that

$$y_{I_{lim}} \triangleq \lim_{x_I \to a} y_I = \frac{k\,a}{2(k^2 - 1)} \left[(k + 1)\frac{C}{a^{1/k}} - \frac{(k - 1)}{C/a^{1/k}} \right]$$

36

which is the same as

$$y_{I_{lim}} = \frac{k\,a}{(k^2 - 1)} \left[\frac{1}{\tan \alpha_0 + \sec \alpha_0} + (k + 1) \tan \alpha_0 \right] \qquad \text{(IV.20)}$$

taking account of Eq. (IV.19).

IV.4. Flight Time

At the limit of y_I the Interceptor should have successfully collided with the Target. During the time lapse needed for this maneuver, the Target vehicle has flown from $y_T = b$ to $y_T = y_{I_{lim}}$ — and has done so at the <u>constant</u> speed V_T. Taking these facts into account, it is possible to determine the <u>time required</u> for this flight operation, as

$$t_m = \frac{\Delta \sigma}{V_T} \equiv \frac{y_{I_{lim}} - b}{V_T} \, , \qquad \text{(IV.21)}$$

where $y_{I_{lim}}$ is from Eq. (IV.20). Making the appropriate substitutions and manipulations, accounting for Eq. (IV.19), it is found that Eq. (IV.21) can be recast as

$$t_m = \frac{k\,a}{V_T\,(k^2 - 1)} \left[\frac{1}{\tan \alpha_0 + \sec \alpha_0} + \frac{k + 1}{k} \tan \alpha_0 \right] . \qquad \text{(IV.22)}$$

Having described the time to complete the pursuit operation, a plot of this expression (presented as the dimensionless parameter, $t_m V_T/a$) is included here with this time expressed as a function of α_0 (see Fig. IV.2). Because of the apparent singularities noted in Eq. (IV.22) values for the time have not been computed for $\alpha_0 = \pm \pi/2$ and $k = 1.0$. For the situations depicted on the figures, limits have been set at $k > 1.0$ and $|\alpha_0| \leq 80$ degrees.
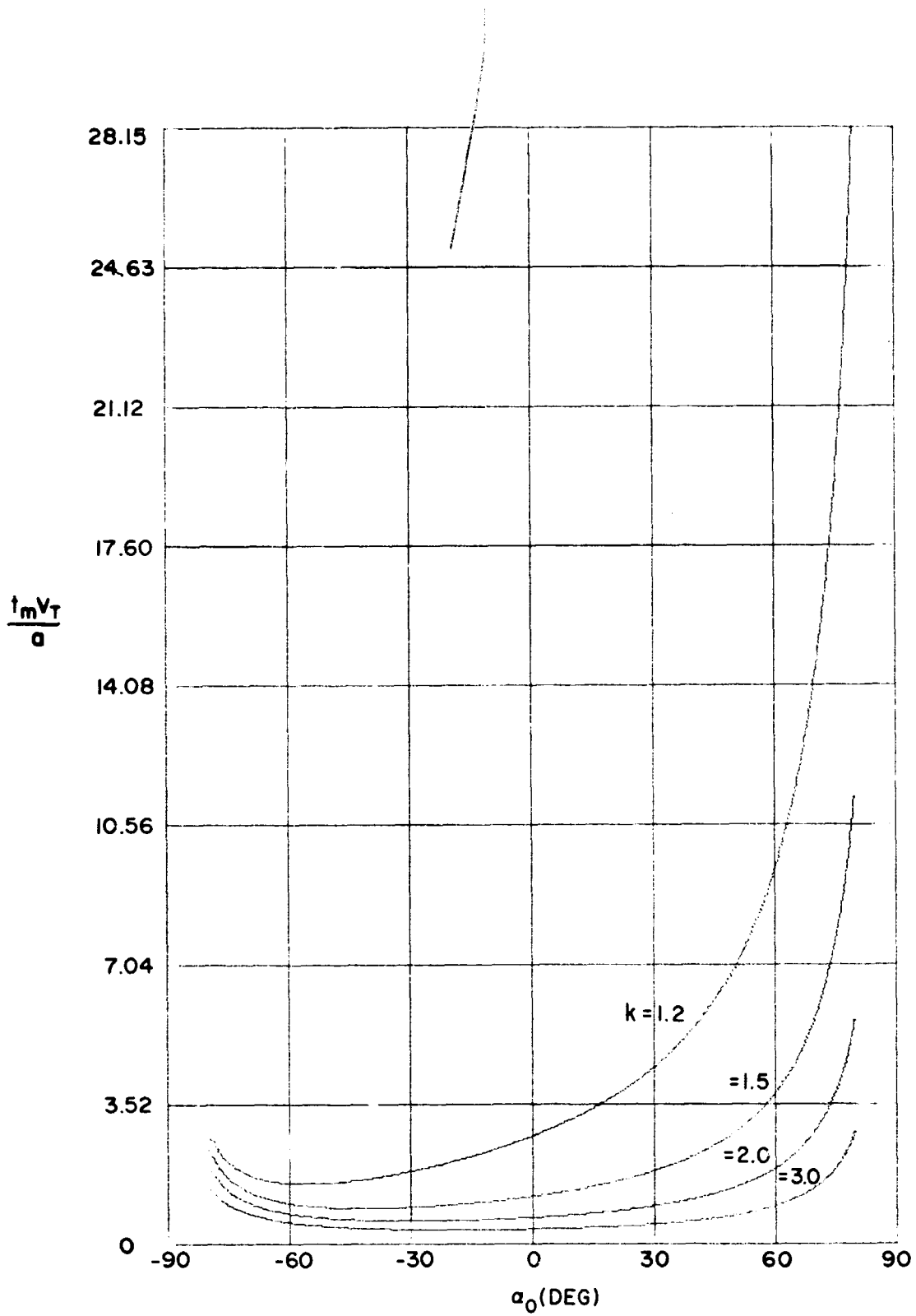
Fig. IV.2. Dimensionless time to complete the pursuit maneuver, as a function of initial orientation (a_0), for several values of k.
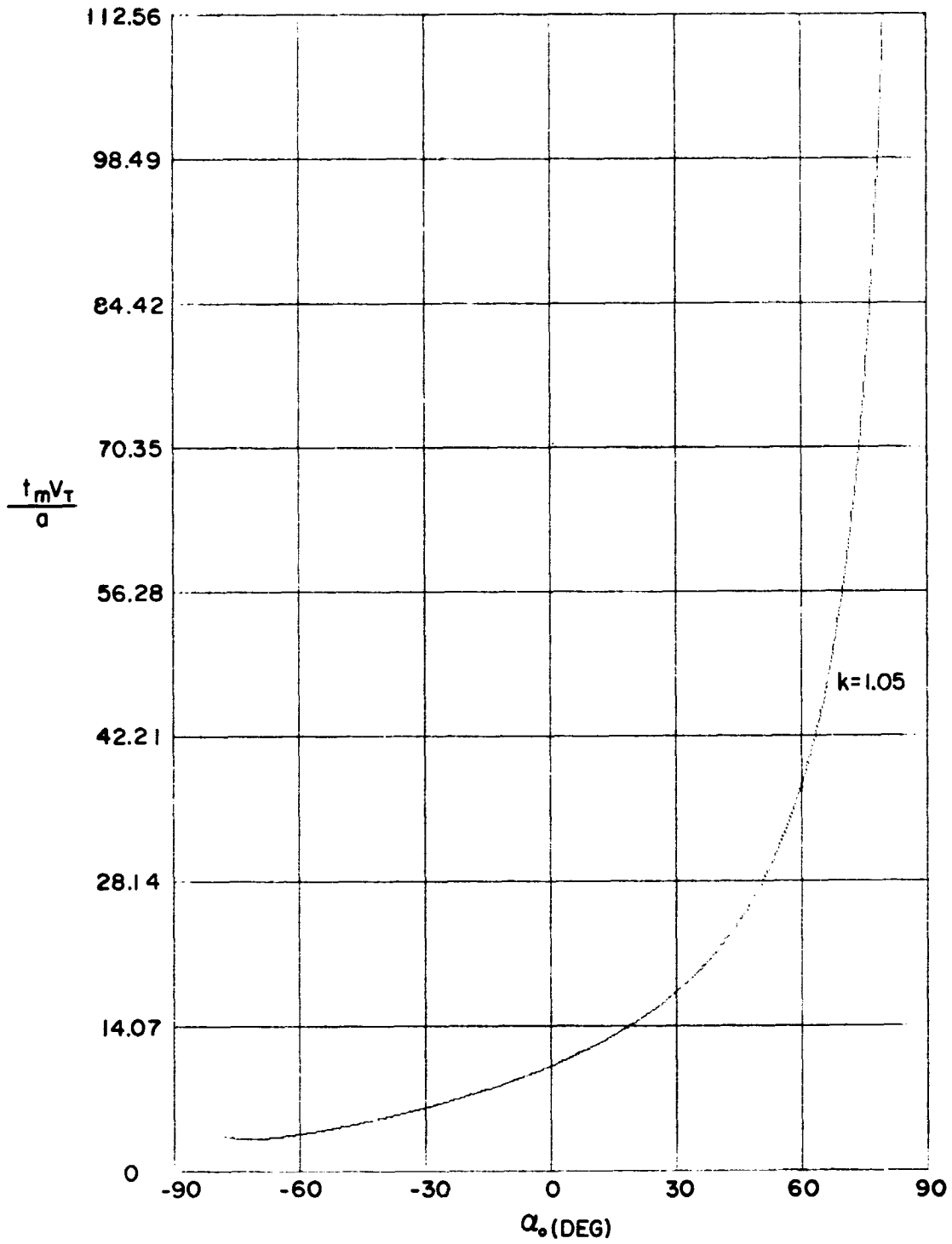
Fig. IV.2. (Continued). The dimensionless time for the pursuit maneuver, as a function of initial positioning (a_0) when $k = 1.05$.

From an inspection of this figure it is evident that over the general range of $|\alpha_0| \leq 60°$, and at large values of k, the time to intercept is not largely influenced by α_0. However as $|\alpha_0|$ increases the time required is increased and appears to grow rapidly as $|\alpha_0| \to \pi/2$. Also, it is seen that the least time requirement is experienced for some α_0 less than $0°$, and for "moderate" k values. It would seem that as k increases the least time occurs nearer to $\alpha_0 = 0°$ and that this requirement remains relatively fixed over a larger range of α_0. As a surmise to the physical situation, which occurs here, one might suggest that as α_0 approaches $-\pi/2$ the interceptor must be expending time in turning about to attain the final "chase" attitude. Evidentally the better maneuver to be undertaken in this instance would be an "intercept" rather than a "pursuit."

For the case of $\alpha_0 \to + \pi/2$, the interceptor must fly a pure chase path; it is evident from the figure that such an operation is as time consuming (or more so) as the turn-around operation required for $\alpha_0 \to -\pi/2$.

IV.5 The "Range" Between Vehicles

The distance (r_r) between the vehicles is usually referred to as the "range." Actually this is the relative separation distance between vehicles, and is a length which should be continually decreasing if the maneuver is being conducted in a satisfactory manner.
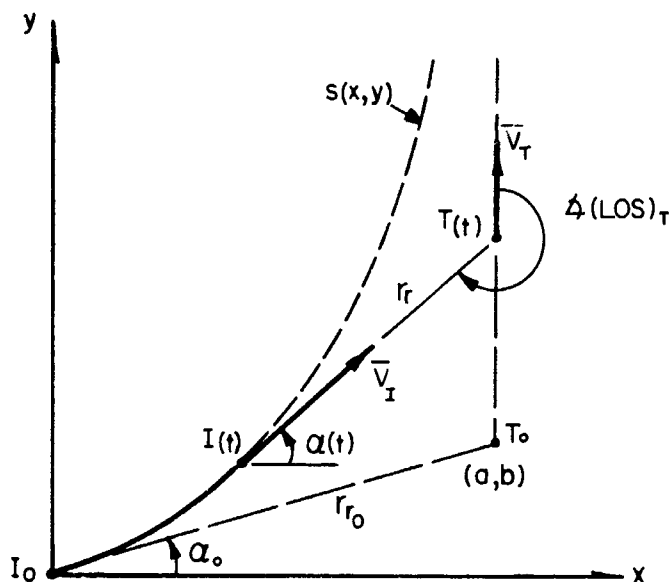
Sketch IV.3. Illustrating the "range" between vehicles; the initial value, r_{r_0}, is the length from I_0 to T_0. A subsequent range value, r_r, is the line length from $I(t)$ to $T(t)$. Also shown are the respective angles of inclination, for the LOS, α_0 and $\alpha(t)$.

40

The initial separation (r_{r_0}) is easily described (see the sketch on preceding page) as

$$r_{r_0} = \sqrt{(y_T - y_I)_0^2 + (x_T - x_I)_0^2} = a \sqrt{(b/a)^2 + 1} \equiv a \sqrt{(p_I)_0^2 + 1},$$

or, in terms of α_0,

$$r_{r_0} = a \sec \alpha_0, \qquad\qquad\qquad (IV.23)$$

since $(p_I)_0 \equiv \tan \alpha_0$ (see Eq. (IV.8)).

Similarly the range (r_r), at any instant during the operation, can be ascertained in a similar manner. That is, one notes that, in general,

$$r_r = \sqrt{(y_T - y_I)^2 + (a - x_I)^2};$$

however, from the figure it is seen that

$$(y_T - y_I) = p_I (a - x_I),$$

thus

$$r_r = a \left(1 - \frac{x_I}{a}\right) \sqrt{1 + p_I^2}, \qquad\qquad (IV.24a)$$

wherein $p_I = p_I (x_I/a)$ as indicated by Eq. (IV.17). An alternate form for Eq. (IV.24a) is easily shown to be

$$r_r = r_{r_0} \left(1 - \frac{x_I}{a}\right) \frac{\sec \alpha}{\sec \alpha_0} \qquad\qquad (IV.24b)$$

Using either of Eqs. (IV.24) it is possible to establish the distance between the vehicles (the "range") during this flight operation. The controlling variable in these calculations would be the quantity x_I/a which has the range in values, $0 \leq x_I/a \leq 1.0$.

IV.6. Distance Flown During Intercept

Equations (IV.21) and (IV.22) define and describe the time lapse which occurs during the maneuver of pursuit and collision, per se. As noted in the first of these expressions, the distance which the target vehicle flies, in time t_m, is $\Delta \sigma$; however, as seen in Eq. (IV.20) this quantity is dependent on α_0 (through $y_{I_{lim}}$). That is,

$$\Delta \sigma = V_T \, t_m = \frac{k \, a}{k^2 - 1} \left[\frac{1}{\tan \alpha_0 + \sec \alpha_0} + \frac{k + 1}{k} \tan \alpha_0 \right] ,$$

or

$$\Delta \sigma = r_0 \left[\frac{k + \sin \alpha_0}{k^2 - 1} \right] , \qquad\qquad (IV.25)$$

accounting for Eq. (IV.23).

The following figure (Fig. IV.3) plots Eq. (IV.25) for the range in values of α_0,

$$-\frac{\pi}{2} \leq \alpha_0 \leq +\frac{\pi}{2} ,$$

and for several values of k (from slightly greater than 1.0 through 2.5). As noted on the graph the "head-on" case ($\alpha_0 = - \pi/2$) shows a rather small dependence on k, as should be expected. Conversely the pure "chase" situation ($\alpha_0 = + \pi/2$) is largely dependent on the value of k assumed for each path.

When the chase vehicle has its velocity vector ($\bar{V}_I$) orthogonal to the target's vector ($\bar{V}_T$), at the initial point, the distance traveled by the Target is slight more than one-half of the distance required for the pure chase case (based on a same

42
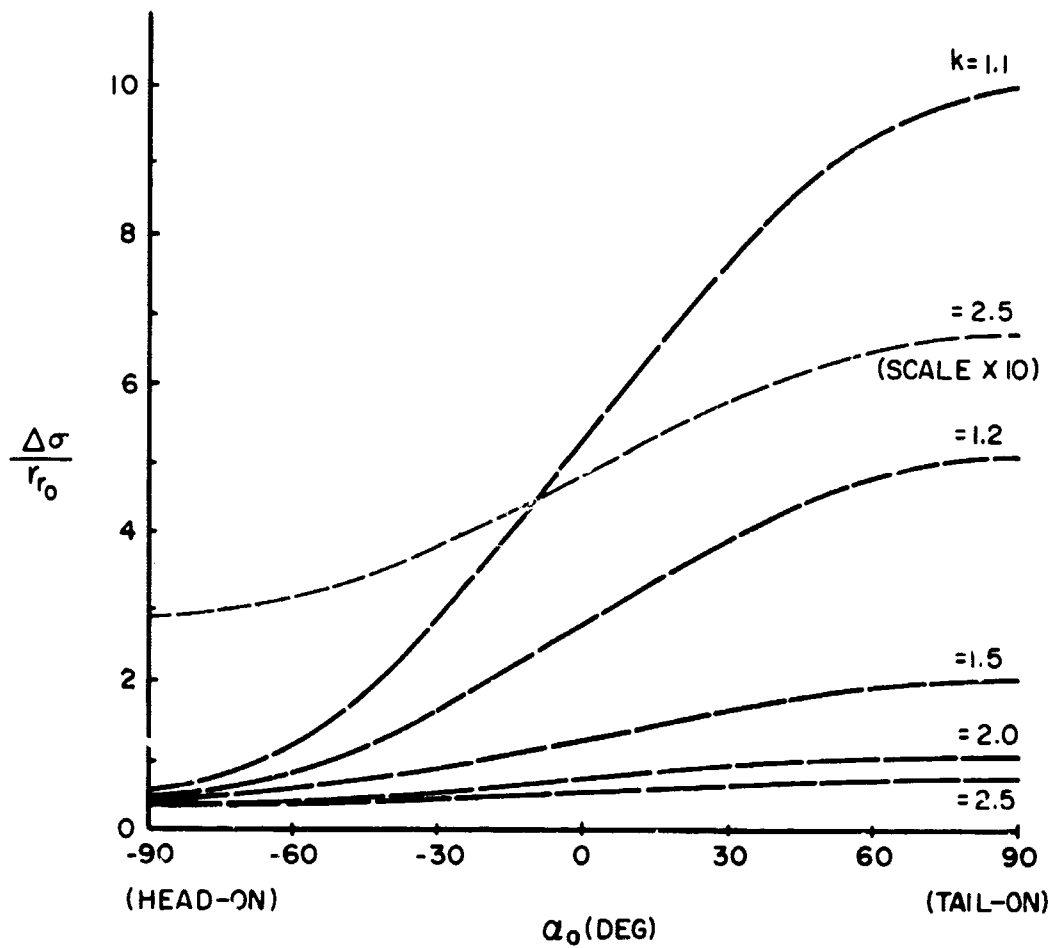
Fig. IV.3. Distance flown by the target during the pursuit, as a function of α_0, for several values of k.

initial separation, r_{r_0}). It is also interesting to note that so long as the initial direction for the interceptor lies between the "head-on" case ($\alpha_0 = -\pi/2$) and the orthogonal orientation ($\alpha = 0$), the distance that the Target flies is relatively small compared to the situation when α_0 is between 0 and $+\pi/2$. Evidentally, this latter path, which the pursuing vehicle flies, is basically a "turn-around" trajectory with the final segment being a simple "chase" maneuver.

IV.7. The Range-Rate Expression

As a mathematical operation, the range-rate expression could be ascertained by differentiating Eq. (IV.24); however this leads to some rather cumbersome algebraic manipulations.

Instead of proceeding in this straight forward fashion a different approach will be undertaken here; one which relies on a direct evaluation of the relative speed components.

IV.7a. The Relative Velocity

From the accompanying sketch it is evident that the range, or relative position, vector ($\bar{r}_r$) can be described as follows:

(1) at $t = t_0$,

$$\bar{r}_{r_0} = \bar{r}_{T_0} - \bar{r}_{I_0};$$

(2) for a general value of t,

$$\bar{r}_r = \bar{r}_T - \bar{r}_I.$$

Consequently the velocity relationship is immediately noted to be

$$\bar{V}_r = \bar{V}_T - \bar{V}_I$$

wherein the

$$\bar{V}_j \triangleq \frac{d\bar{r}_j}{dt} \quad (j = T, I, r).$$

44
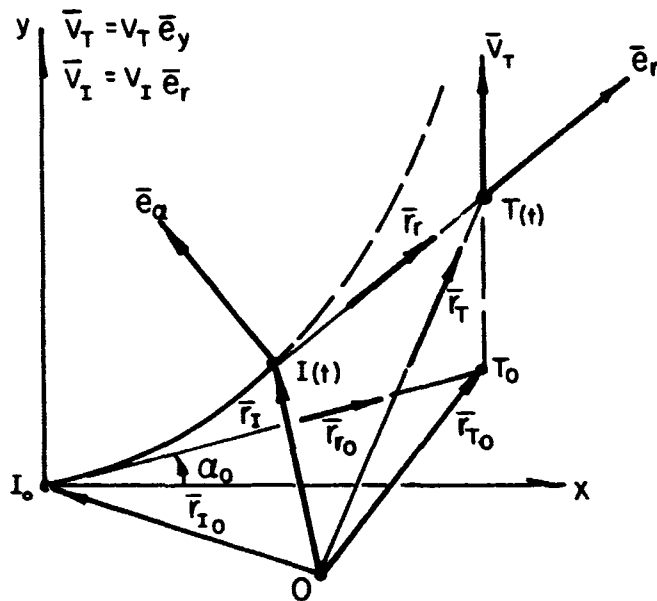
Sketch IV.4. Illustrating quantities needed to evaluate the relative speeds, thus the range rate ($\dot{r}_r$). The origin, "0", is inertial (in character); the vectors $\bar{r}_j$ ($j = I$, T) position the Interceptor and Target during the flight operation. Quantities ( )$_0$ refer to initial values. The vectors ($\bar{e}_r$, $\bar{e}_a$, $\bar{e}_z$) form a unit orthogonal traid at the interceptor. (Note that $\bar{e}_z = \bar{e}_r \times \bar{e}_a$.)

From kinematics, and definition, one can write

$$\bar{V}_r \triangleq \frac{d\bar{r}_r}{dt} = \dot{r}_r \, \bar{e}_r + r_r \, \dot{\bar{e}}_r$$

wherein

$$\bar{e}_r = \frac{\bar{r}_r}{|\bar{r}_r|},$$

and

$$\dot{\bar{e}}_r = \bar{\omega}_r \times \bar{e}_r,$$

with $\bar{\omega}_r$ describing the rate of turning of the triad ($\bar{e}_r$, $\bar{e}_a$, $\bar{e}_z$) at I.

45

It should be evident that for the planar motion considered here

$$\bar{\omega}_r = \dot{\alpha}\,\bar{e}_z$$

and, therefore,

$$\dot{\bar{e}}_r = \dot{\alpha}\,(\bar{e}_z \times \bar{e}_r) = \dot{\alpha}\,\bar{e}_\alpha\,.$$

As a consequence of this evaluation the <u>relative velocity vector</u> $(\bar{V}_r)$ can be expressed as,

$$\bar{V}_r = \dot{r}_r\,\bar{e}_r + r_r\,\dot{\alpha}\,\bar{e}_\alpha = \bar{V}_T - \bar{V}_I\,, \qquad\qquad \text{(IV.26)}$$

taking account of the mathematical statements above.

IV.7b. The Speed Components

In order to define the radial and transverse components of the relative velocity one can proceed in the following manner (referring to the accompanying sketch):
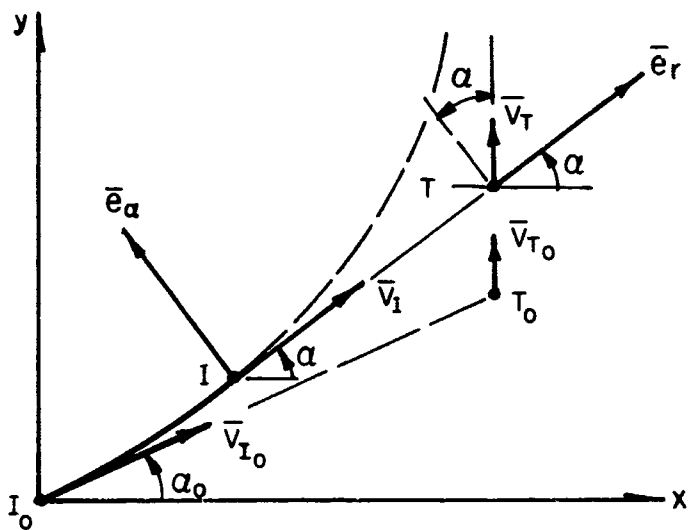
Sketch IV.5. Describing the kinematics of the pursuit problem, especially those related to the relative motion.

46

(a)   The radial component $(\dot{r}_r)$ is,

$$\dot{r}_r \triangleq \overline{V}_r \cdot \overline{e}_r = \overline{V}_T \cdot \overline{e}_r - \overline{V}_I \cdot \overline{e}_r = V_T \sin \alpha - V_I .$$

(b)   The transverse component $(r_r \dot{\alpha})$ is,

$$r_r \dot{\alpha} \triangleq \overline{V}_r \cdot \overline{e}_\alpha = \overline{V}_T \cdot \overline{e}_\alpha - \overline{V}_I \cdot \overline{e}_\alpha = V_T \cos \alpha .$$

Recalling that the speed ratio $k \triangleq V_I / V_T$, then the above relations are written as

$$\dot{r}_r = V_T (\sin \alpha - k),$$

and

$$r_r \dot{\alpha} = V_T \cos \alpha . \qquad\qquad (IV.27)$$

Recognizing that the slope of the pursuit curve (p_I) is

$$p_I = \tan \alpha$$

then

$$\cos \alpha = \frac{1}{\sqrt{1 + p_I^2}} \quad \text{and} \quad \sin \alpha = \frac{p_I}{\sqrt{1 + p_I^2}},$$

where p_I is defined by Eq. (IV.17); and, alternate forms for Eq. (IV.27) are,

$$\dot{r}_r = V_T \left(\frac{p_I}{\sqrt{1 + p_I^2}} - k \right),$$

and

$$r_r \dot{\alpha} = \frac{V_T}{\sqrt{1 + p_I^2}} . \qquad\qquad (IV.28)$$

47

IV.8. The Range-Rate

The first of the two expressions above (or the corresponding form in Eq. (IV.27)) is the "range-rate" for the interceptor during its pursuit of the target. From the physics of the problem it should be apparent that $\dot{r}_r < 0$ for $\cap$ successful operation; hence it would be necessary (here) that

$$\hbar > \frac{p_I}{\sqrt{1 + p_I^2}}; \quad \text{or,} \quad \hbar > \sin \alpha.$$

This requirement is not restrictive since $|\sin \alpha| \leq 1.0$; also, a premise for the entire pursuit problem has been that $\hbar > 1.0$.

Equations (IV.28) and (IV.24) describe two of the more useful quantities related to a flight operation — namely, the range-rate and the range of the interceptor-target combination. Figure (IV.4) plots these two quantities against one another, for several values of $\hbar$ and for selected initial positioning of the vehicles (α_0). As an indication of the limit values which these two expressions achieve, when $x_I \rightarrow 0$, one should note that $r_{r_{lim}} \rightarrow 0$ and $\dot{r}_{r_{lim}} \rightarrow V_T (1 - \hbar)$. These limits are located on the following graphs using dashed line segments to complete the curves.

The accompanying plots are indicative of a rather profound influence (for a given value of $\hbar$) attributed to the varying of α_0. However, a look at Eq. (IV.28) will verify that the limit value of the (dimensionless) range-rate is uninfluenced by this variable. Also, it is not immediately evident that as α_0 increases the variability of the range rate decreases (during the overall maneuver). The plot of these quantities, for $\alpha_0 = 75°$, shows the very nearly linear relationship between range and range-rate. Of course, as $\alpha_0 \rightarrow \pi/2$ this should not be unexpected.

When one reads the following figures it should be kept in mind that r_r/a attains its maximum value at $t = 0$, and diminishes to $r_r/a = 0$ at the termination of the maneuver.

IV.9. Turning Rate for the interceptor

The rate at which the interceptor's flight-path tangent must rotate during the pursuit of the Target (T) can be ascertained from the second expression in Eq. (IV.28). Thus the turning rate is,

48
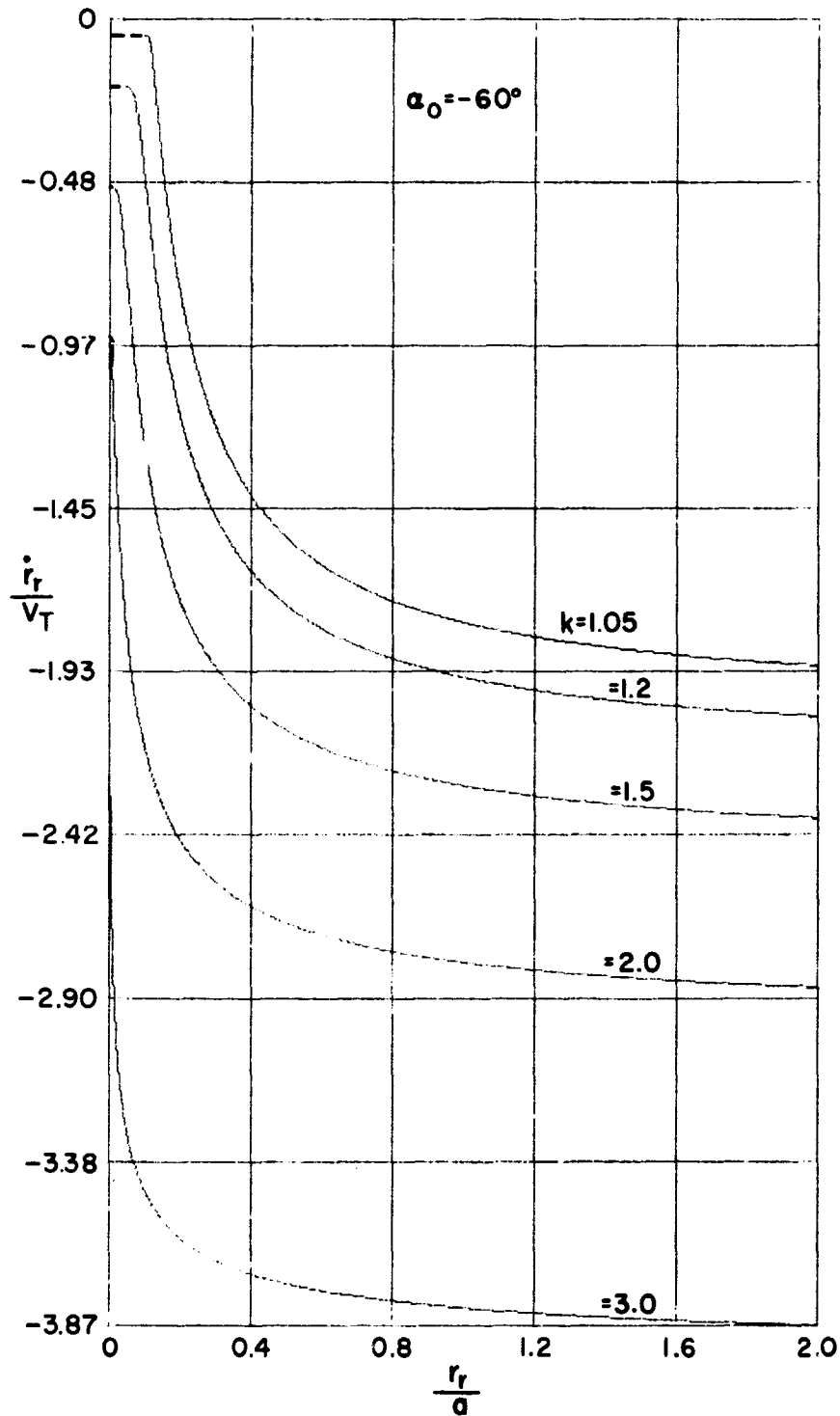
Fig. IV.4(a). Correlation of range-rate ($\dot{r}_r/V_T$) to rang (r_r/a) during the pursuit maneuver, for a_0 = -60°. The influence of k is illustrated by means of the several curves shown on this plot. It should be recognized that the lower limit of $\dot{r}_r/V_T$ (as r_r/a → 0) is (1 - k).
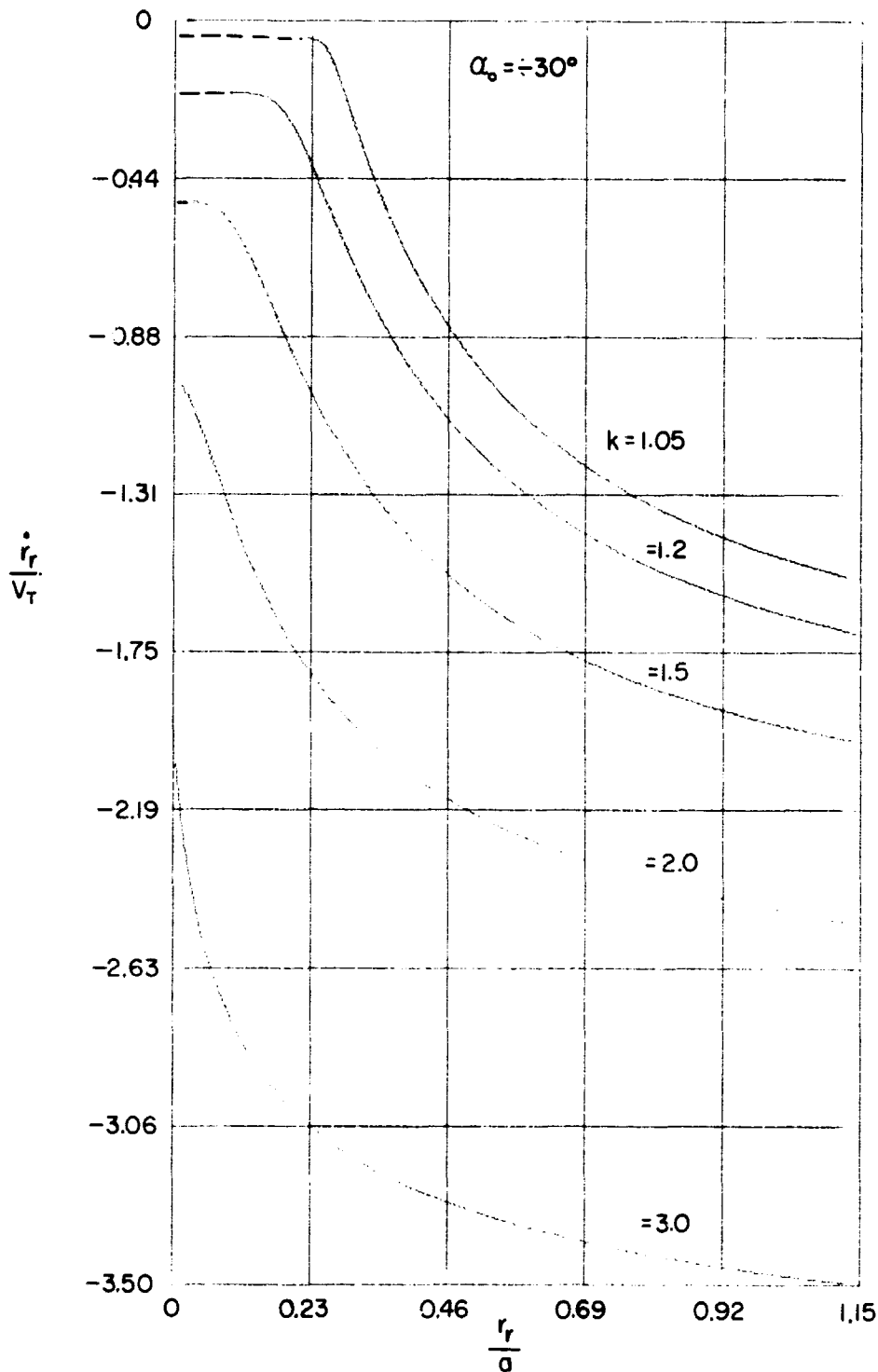
Fig. IV.4(b). Correlation of range-rate ($\dot{r}_r/V_T$) to range (r_r/a) during the pursuit maneuver. for a_0 = -30°. The influence of k is illustrated by means of the several curves shown on this plot. It should be recognized that the lower limit of $\dot{r}_r/V_T$ (as $r_r/a \Rightarrow 0$) is (1 - k).
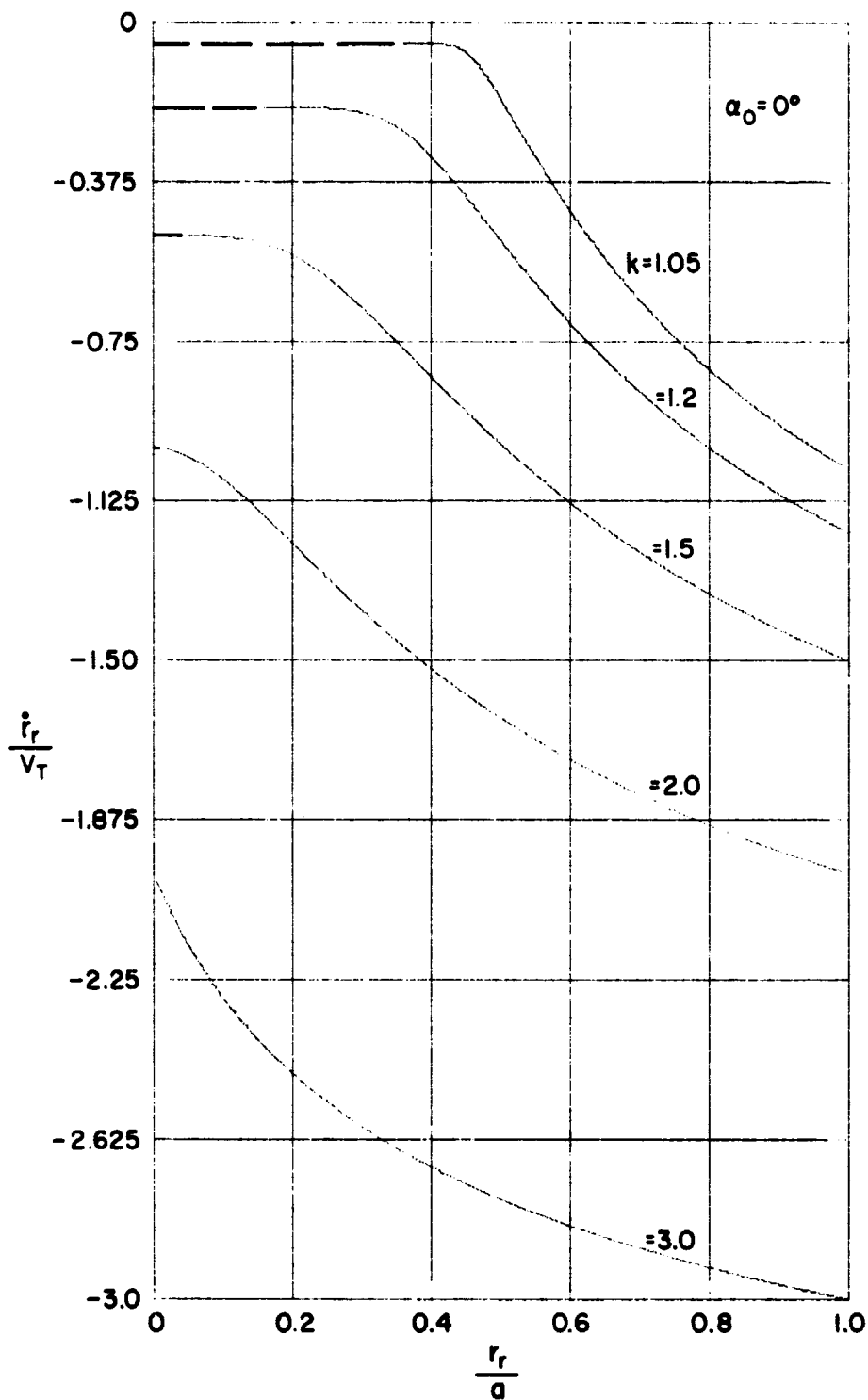
Fig. IV.4(c). Correlation of range-rate ($\dot{r}_r/V_T$) to range (r_r/a) during the pursuit maneuver, for $a_0 = 0°$. The influence of k is illustrated by means of the several curves shown on this plot. It should be recognized that the lower limit of $\dot{r}_r/V_T$ (as $r_r/a \rightarrow 0$) is $(1 - k)$.
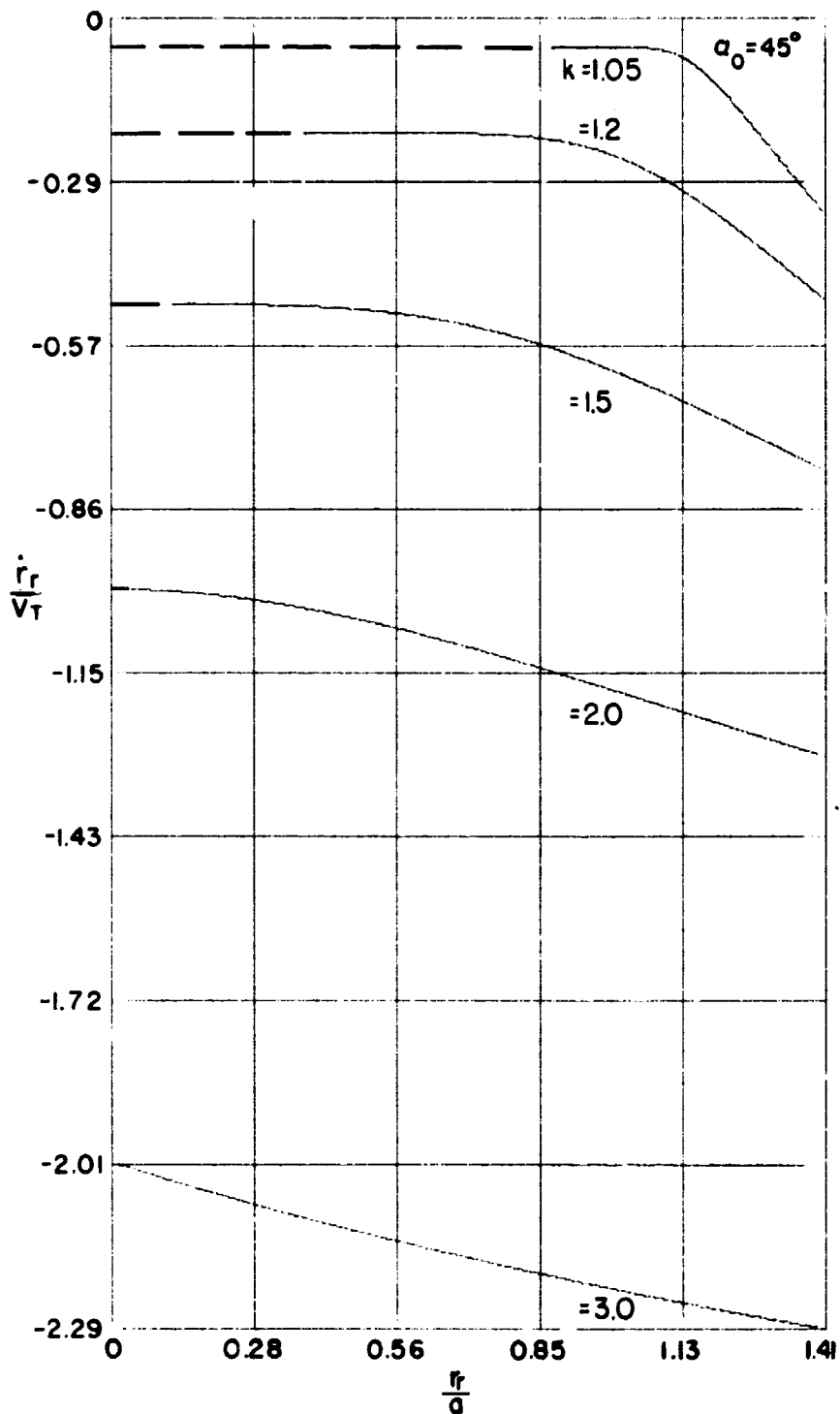
Fig. IV.4(d). Correlation of range-rate $(\dot{r}_r/V_T)$ to range (r_r/a) during the pursuit maneuver. for $a_0 = 45°$. The influence of k is illustrated by means of the several curves shown on this plot. It should be recognized that the lower limit of $\dot{r}_r/V_T$ (as $r_r/a \to 0$) is $(1 - k)$.
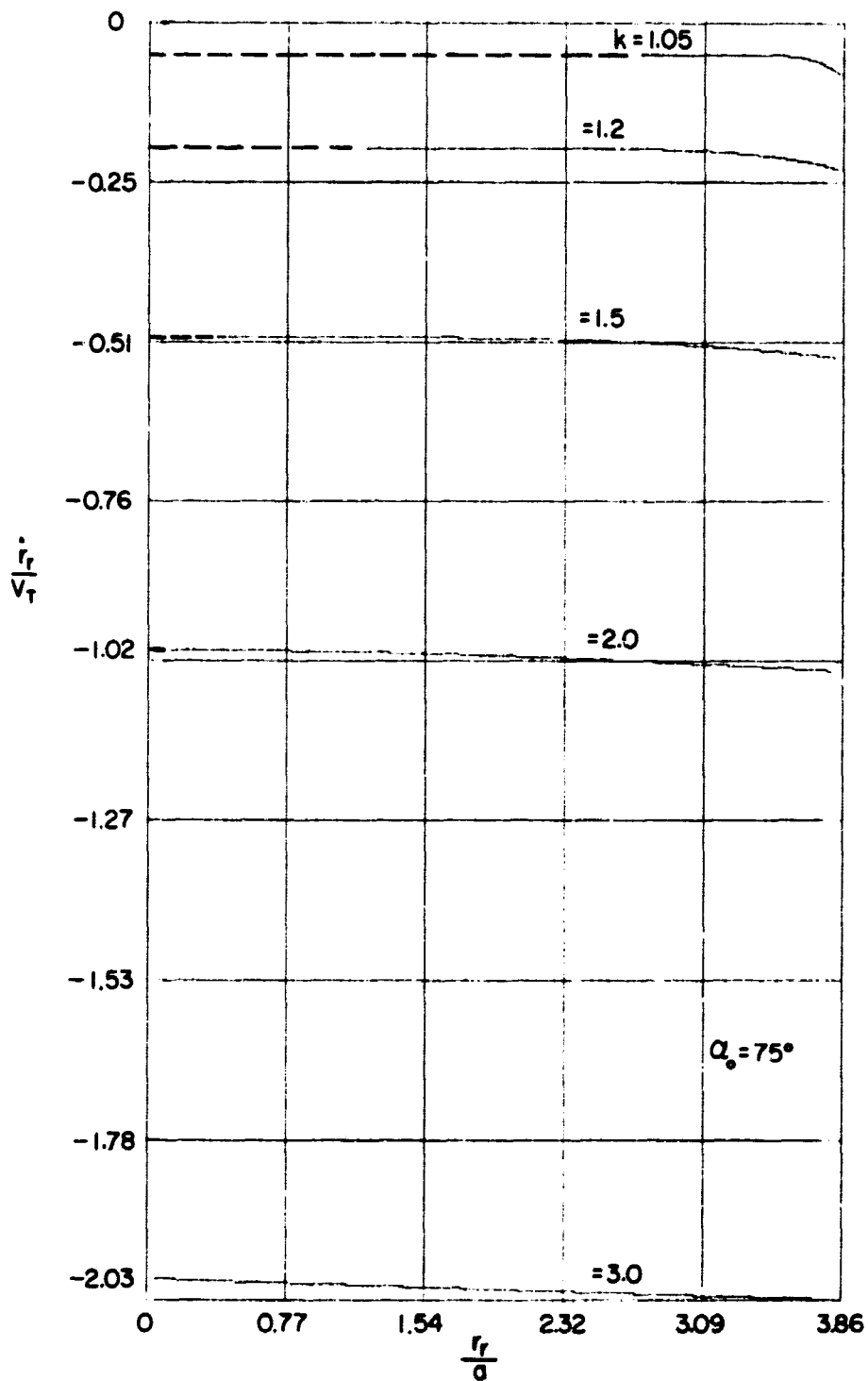
Fig. IV.4(e). Correlation of range-rate $(\dot{r}_r/V_T)$ to range (r_r/a) during the pursuit maneuver, for $a_0 = 75°$. The influence of k is illustrated by means of the several curves shown on this plot. It should be recognized that the lower limit of $\dot{r}_r/V_T$ (as $r_r/a \to 0$) is $(1 - k)$.

$$\dot{\alpha} = \frac{V_T}{r_r \sqrt{1 + p_I^2}} = \frac{V_T}{a \left(1 - \frac{x_I}{a}\right)\left(1 + p_I^2\right)} \qquad \text{(IV.29)}$$

accounting for Eq. (IV.24); and, wherein p_I would be obtained from Eq. (IV.17). Once more it is noted that the controlling variable is x_I/a.

In addition to describing how the slope angle (α) varies during the flight, $\dot{\alpha}$ is a parameter useful in determining the maneuverability requirements which will be placed on the interceptor (I).

Fig. IV.5, which follows as several graphs, presents the turning rate and the lateral acceleration*, as dimensionless quantities, expressed in terms of the dimensionless range for the two vehicles. On these graphs the several values of k serve as parameters, while each figure is for a given α_0. It should be evident that the singularities apparent to these dimensionless expressions do not allow one to conveniently extend the results completely to $x_I/a = 1.0$ (the position of intercept by the pursuit craft). Of course these limits may be ascertained by a manipulation of the governing equations.

It does not seem likely, at first glance, that there is a simple direct relationship between the two quantities in question here ($\dot{\alpha}$ and A_α). Yet, by a simple manipulation one can show that

$$\frac{\dot{\alpha} a}{V_T} \equiv \frac{A_\alpha a}{k V_T^2} = \frac{1}{\left(1 - \frac{x_I}{a}\right)\left(1 + p_I^2\right)}$$

wherein p_I describes the local tangent (to the interceptor's path) and x_I/a describes the pursuit's location as it moves along its trajectory.

A glance at the graphs included here will verify that the initial phases of the pursuit operation may or may not be too stringent; and that the interceptor could fly a rather "easy" path here. Yet, as the terminal phase of the maneuver is approached the pursuing vehicle may have to undergo some rather difficult gyrations, and may have to overcome comparatively large lateral forces, if the operation is to continue as desired.

---

*The lateral acceleration is developed in the next section (IV.10); only the connecting relationship between these parameters (nondimensionalized) is of consequence here.

54
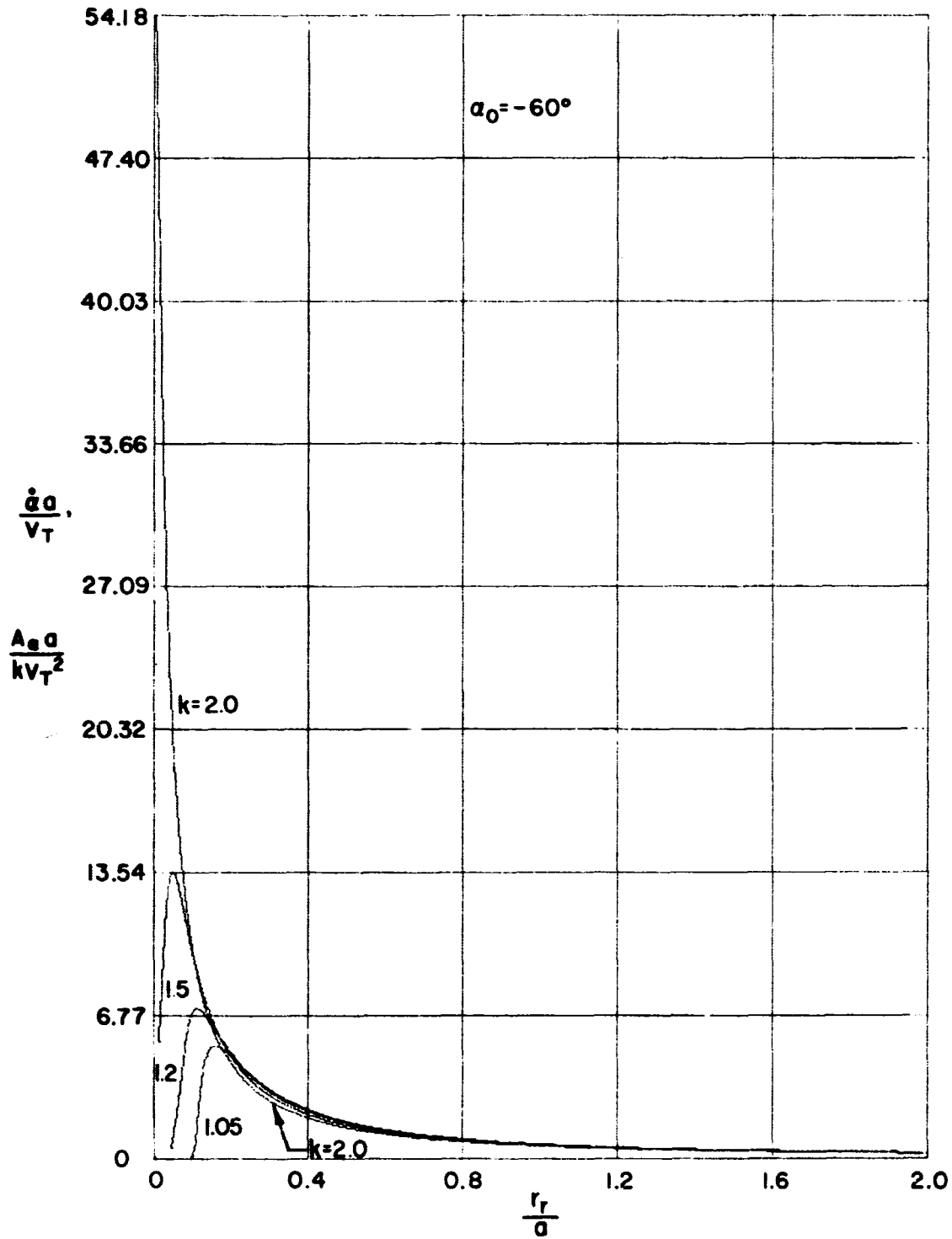
Fig. IV.5(a). Nondimensional turning rate and lateral acceleration experienced by the interceptor during pursuit, as a function of the dimensionless range (r_r/a); $a_0 = -60°$.
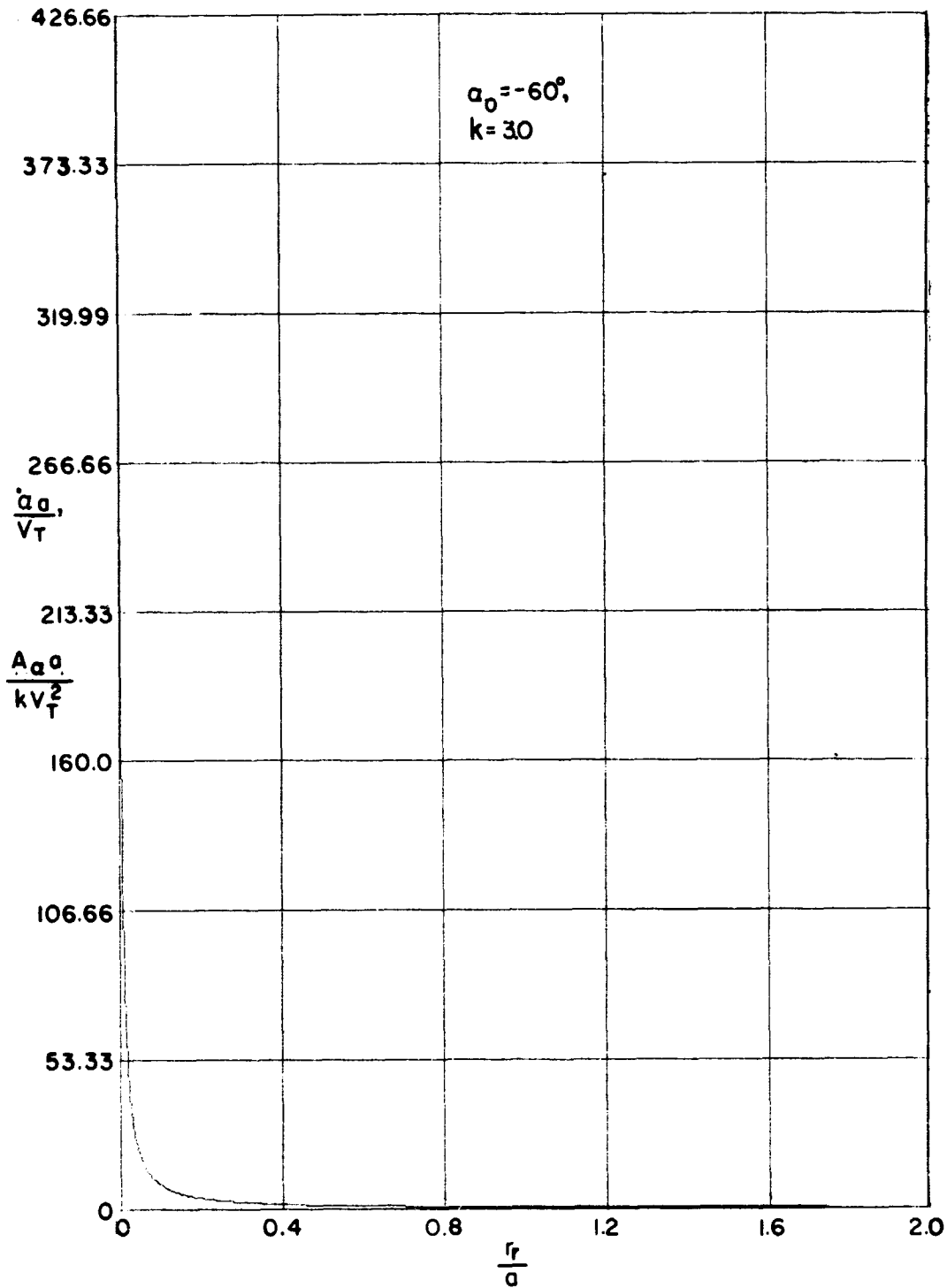
Fig. IV.5(a). Continued.
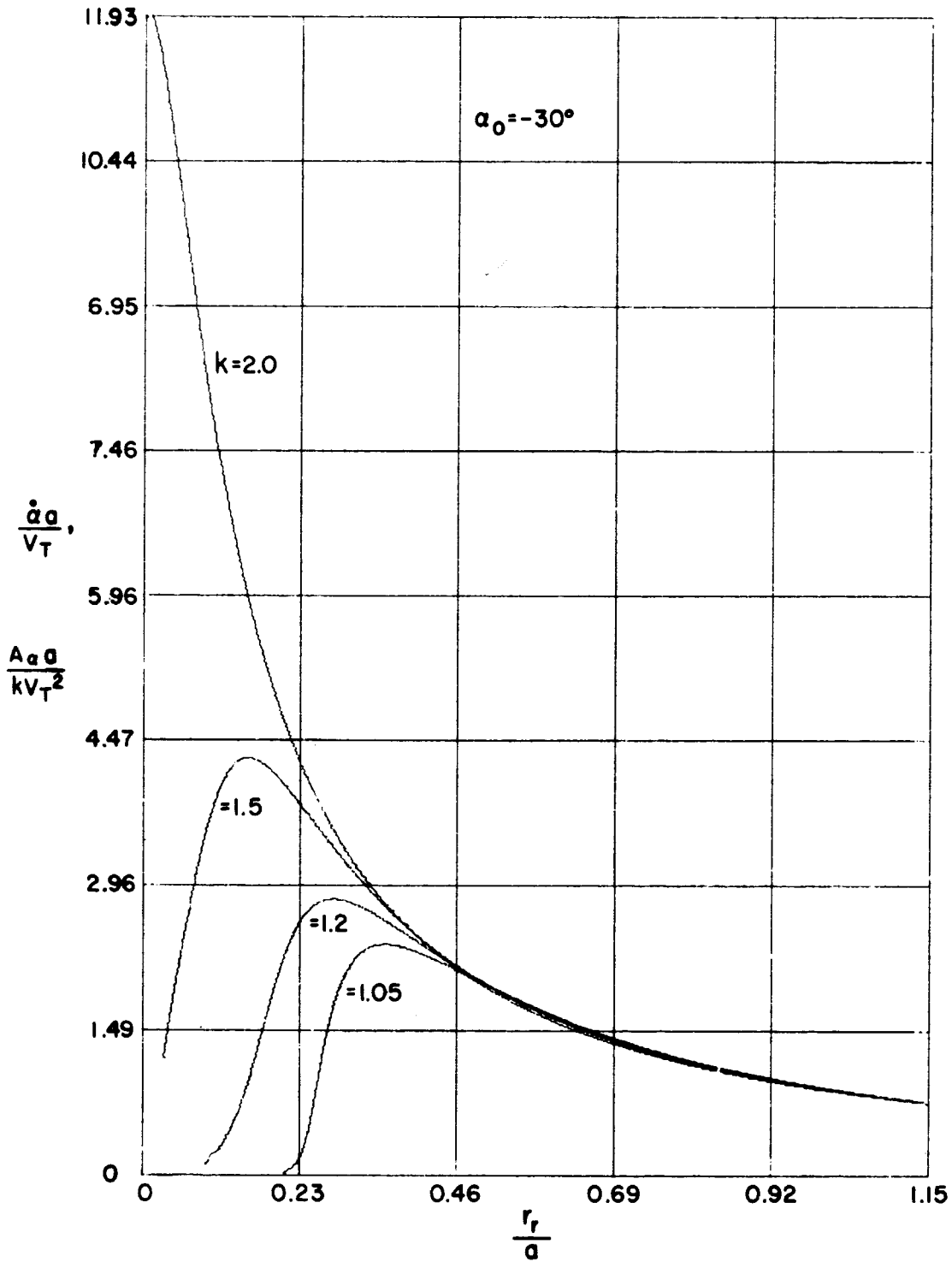
Fig. IV.5(b). Nondimensional turning rate and lateral acceleration experienced by the interceptor during pursuit, as a function of the dimensionless range (r_r/a); $a_0 = -30°$.
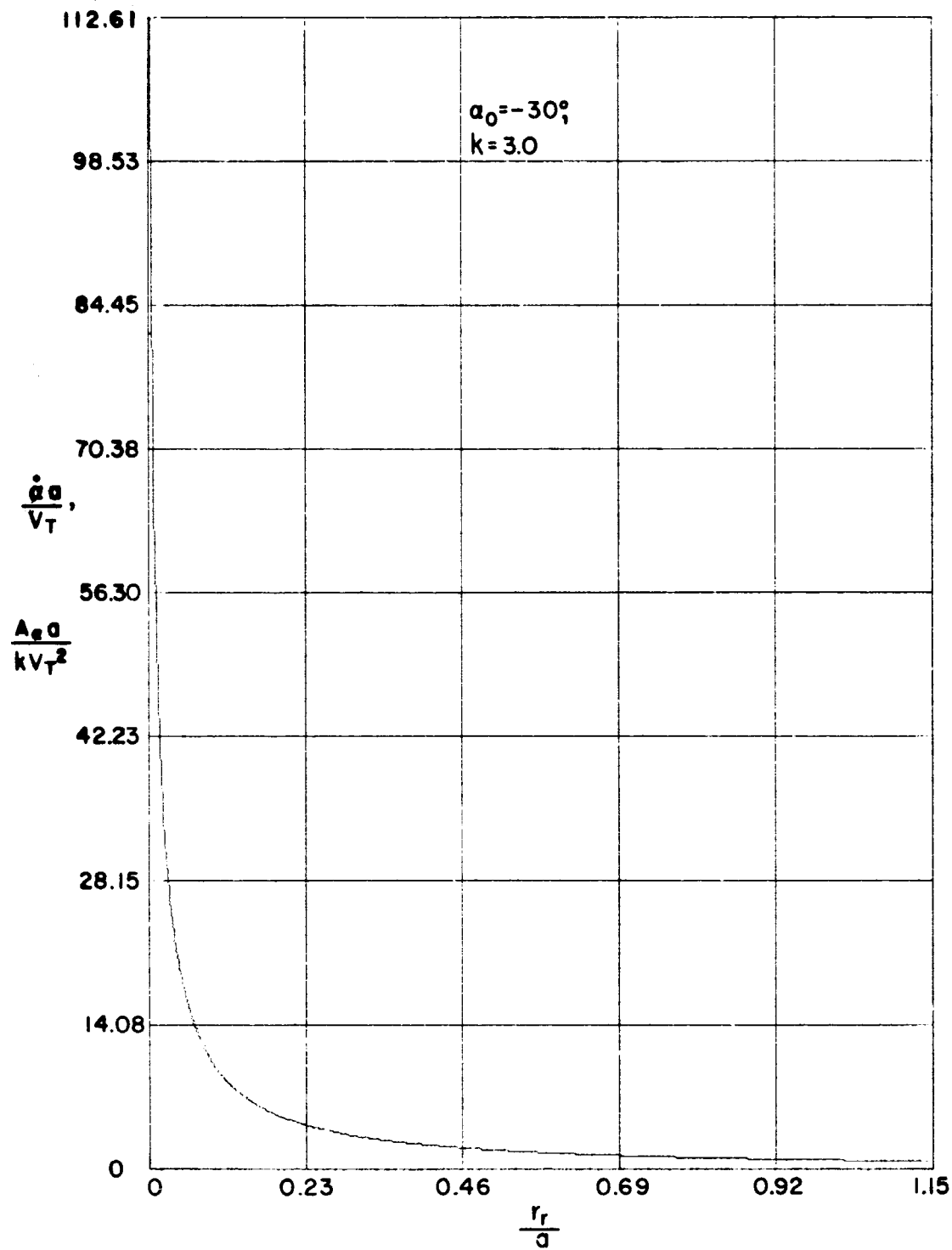
Fig. IV.5(b). Continued.
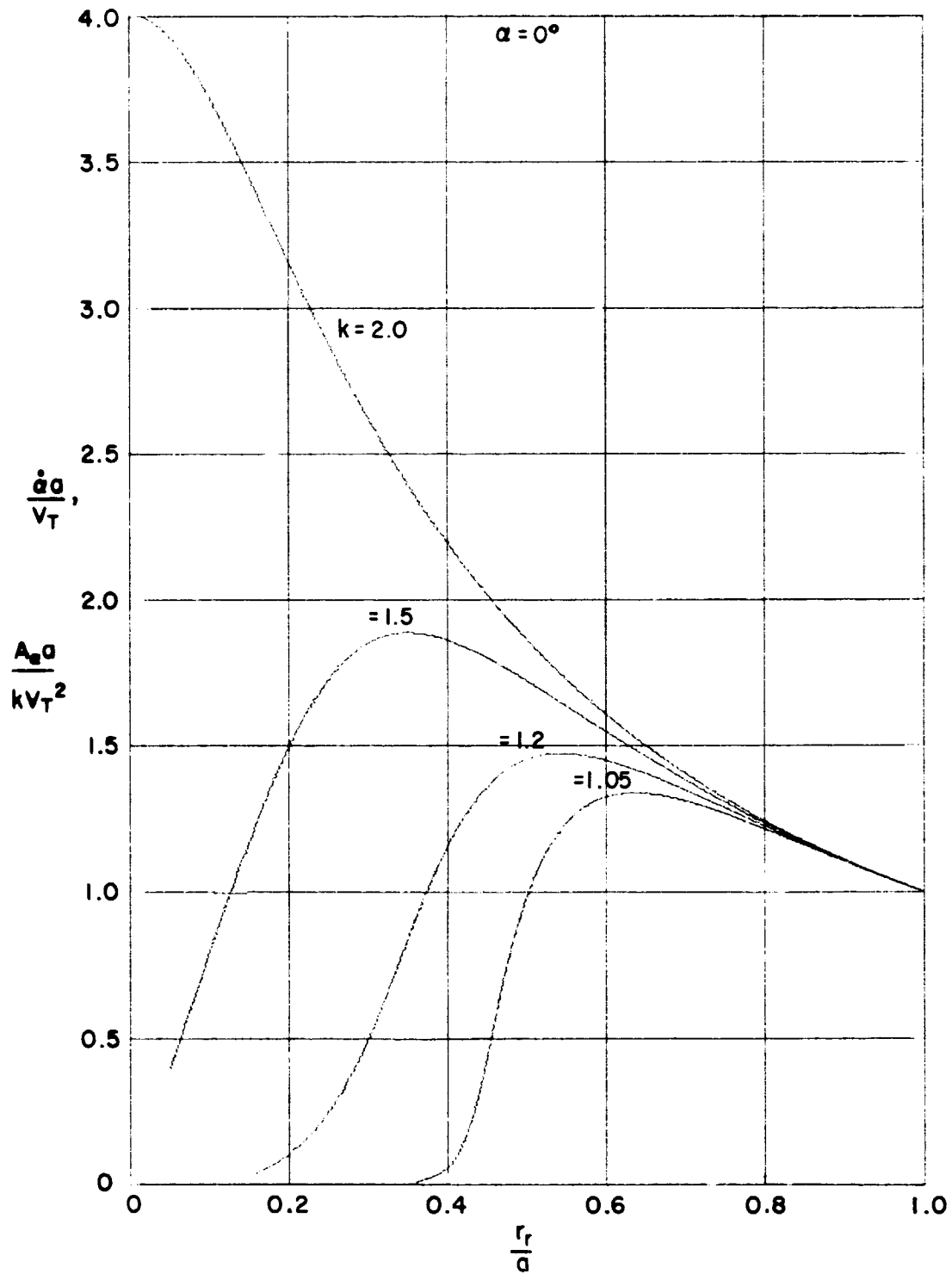
Fig. IV.5(c). Nondimensional turning rate and lateral acceleration experienced by the interceptor during pursuit, as a function of the dimensionless range (r_r/a); $a_0 = 0°$.
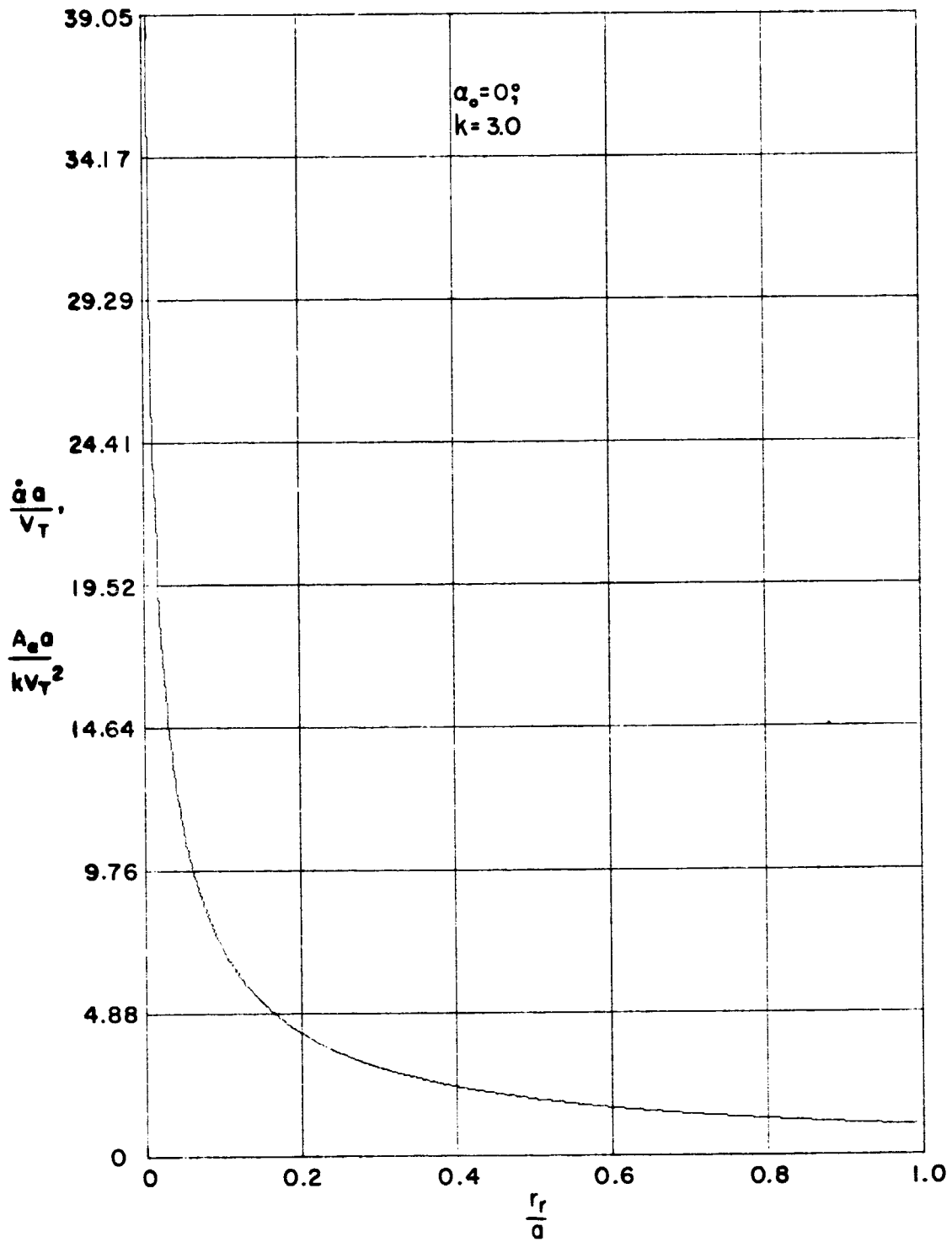
Fig. IV.5(c). Continued.
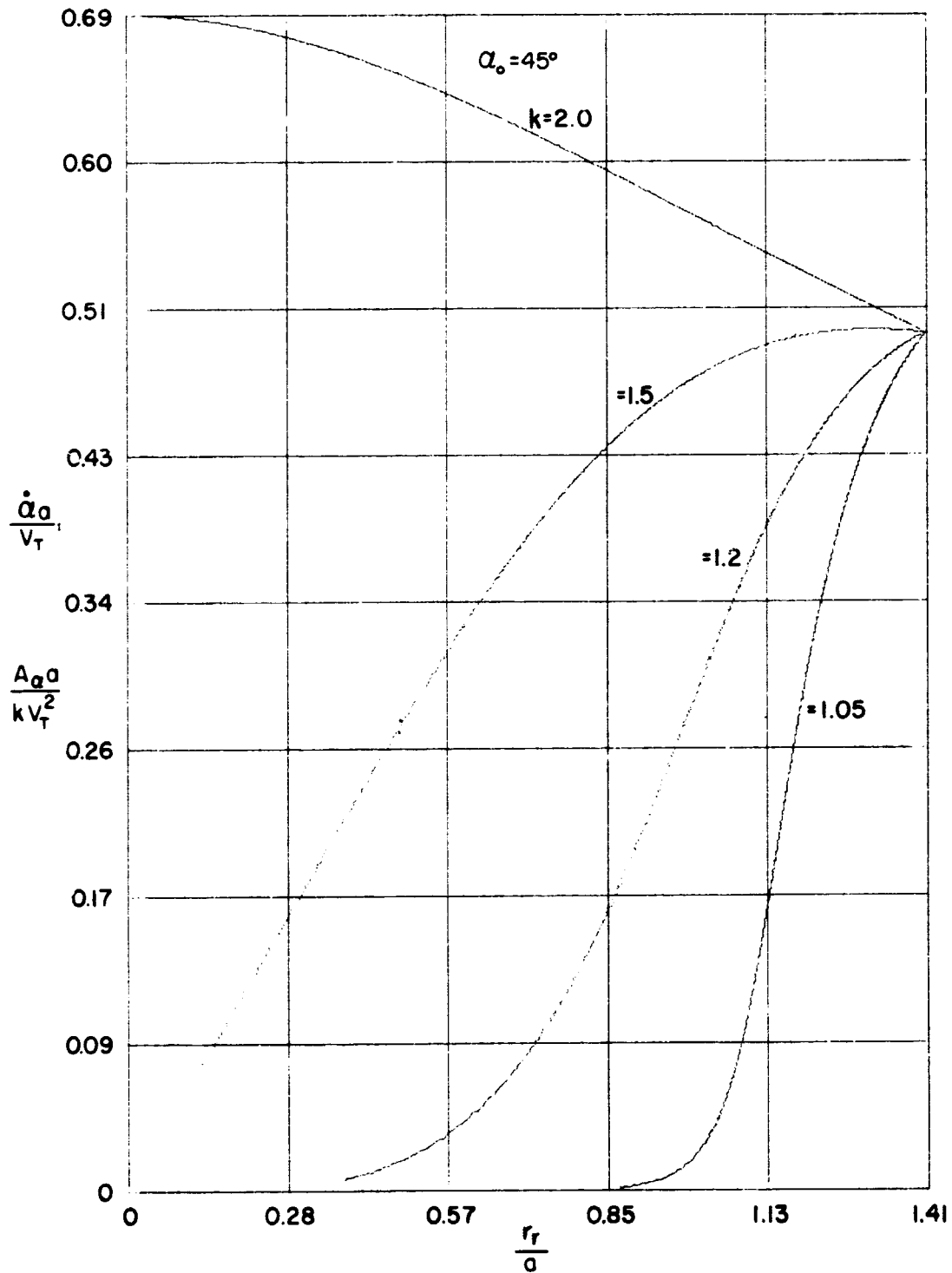
Fig. IV.5(d). Nondimensional turning rate and lateral acceleration experienced by the interceptor during pursuit, as a function of the dimensionless range (r_r/a); $\alpha_0 = 45°$.
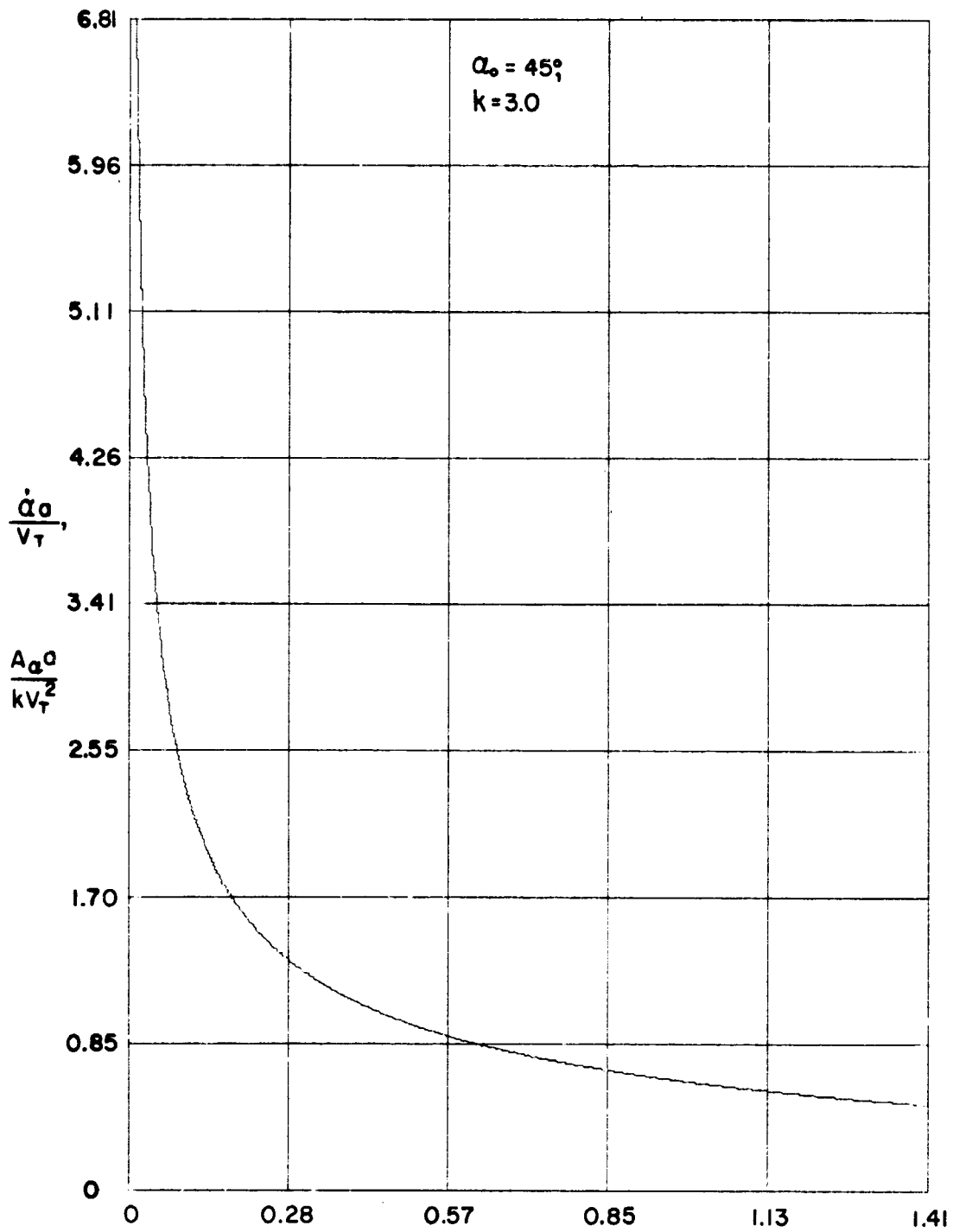
Fig. IV.5(d). Continued.
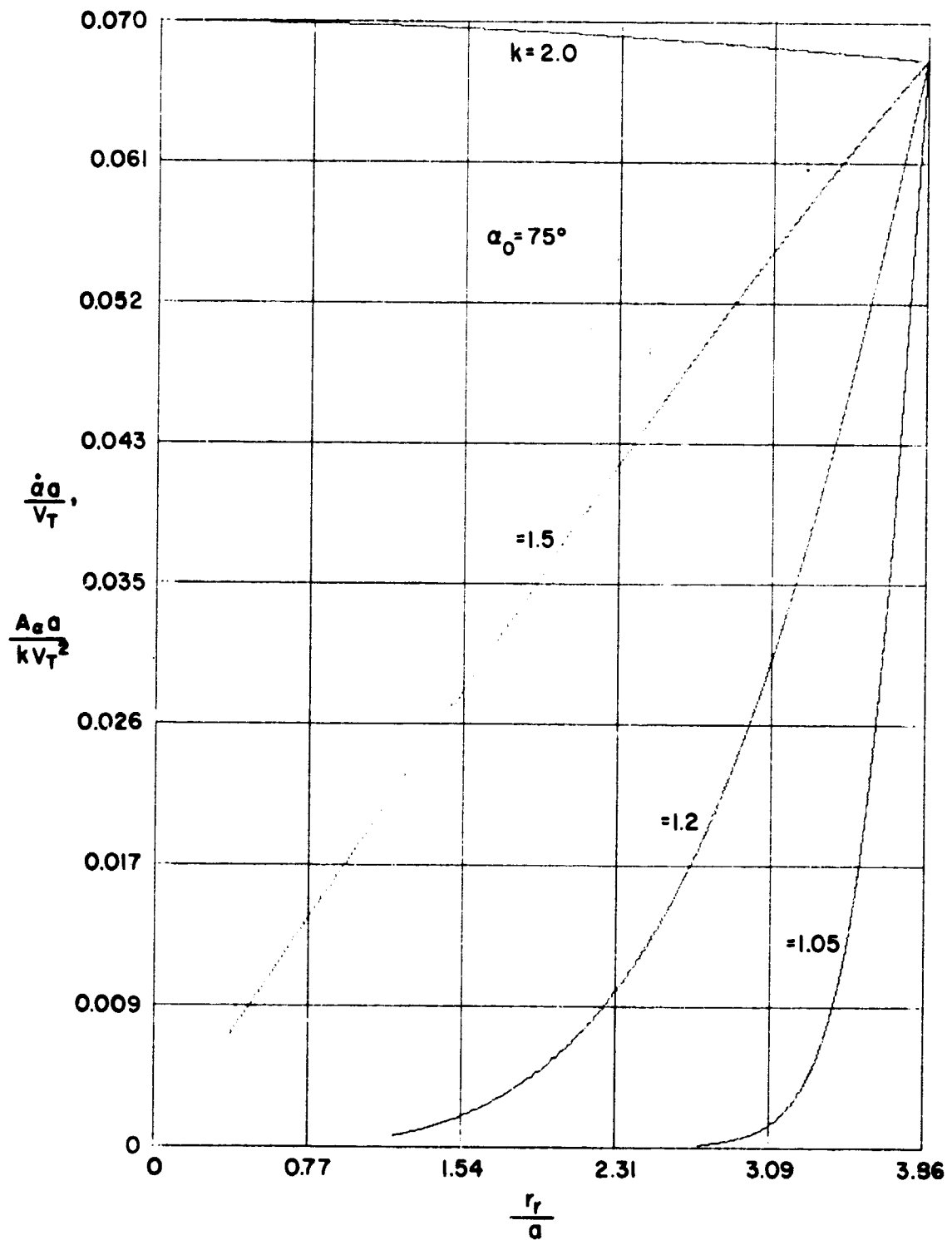
Fig. IV.5(e). Nondimensional turning rate and lateral acceleration experienced by the interceptor during pursuit, as a function of the dimensionless range (r_r/a); $a_0 = 75°$.
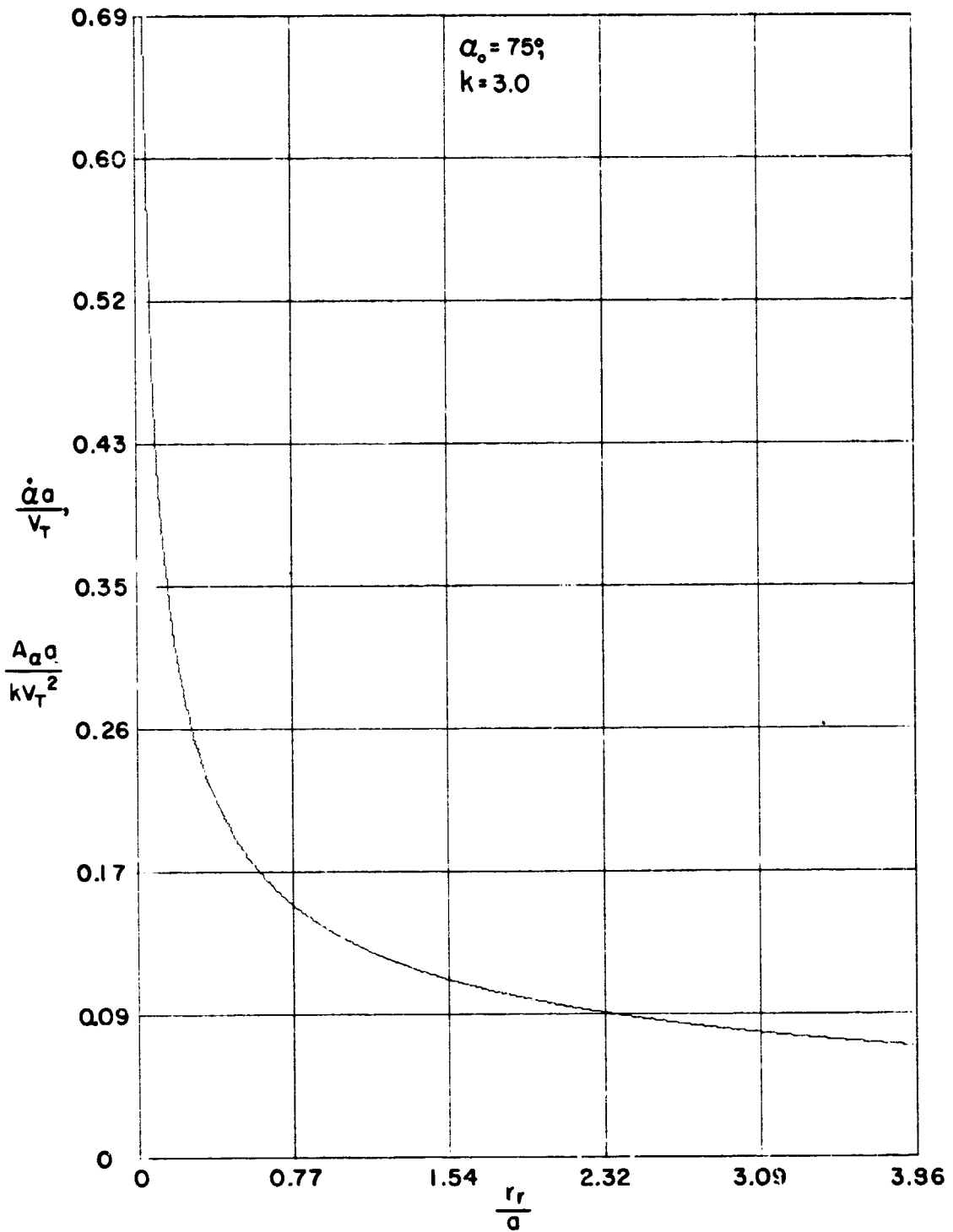
Fig. IV.5(e). Continued.

As one might expect there will be a fair to heavy influence exerted by the value of k (which is being experienced) and by the α_0 for the flight operation. Generally, the higher values of k lead to the most difficult operations in terms of turning rates, and lateral accelerations. As the pure chase maneuver is approached ($\alpha_0 = + \pi/2$) the interceptor is relieved of having to engage in the more difficult operational aspects of this flight type, provided $k \leq 2.0$. Here, as k increases ($k > 2.0$) the equations suggest a rather sharp rise in $\dot{\alpha}$ and A_α. Conversely, one could argue that as k becomes small, the relative (positional) accelerations quickly begin to vanish and the interceptor will be engaged in an almost pure chase operation.

IV.10. Interceptor Acceleration

In the foregoing section it was found that the interceptor's velocity vector underwent a continual rotation ($\dot{\alpha}$) which was dependent on the inclination (α) and the range (or separation distance) — see Eq. (IV.27).

Since the velocity vector ($\overline{V}_T$) has a fixed magnitude, then it can be shown that the only (kinematic) acceleration for the interceptor is one having a transverse component (normal to $\overline{V}_I$).

Since the velocity vector for the interceptor can be written as

$$\overline{V}_I = V_I \, \overline{e}_r \, ,$$

then it follows that the (kinematic) acceleration can be described by,

$$\overline{A} \triangleq \frac{d\overline{V}_I}{dt} = \dot{V}_I^{\,0} \overline{e}_r + V_I \, \dot{\overline{e}}_r$$

since $V_I \triangleq$ constant; thus

$$\overline{A} = V_I \dot{\overline{e}}_r = V_I \, (\overline{\omega}_r \times \overline{e}_r)$$

where, as before, $\overline{\omega}_r = \dot{\alpha} \, \overline{e}_z$. As a consequence the kinematic acceleration is found to be

$$\overline{A} = V_I \, \dot{\alpha} \, \overline{e}_\alpha \, ; \tag{IV.30}$$

which is a vector normal to $\overline{V}_I$, having only the transverse component (A_α).

65
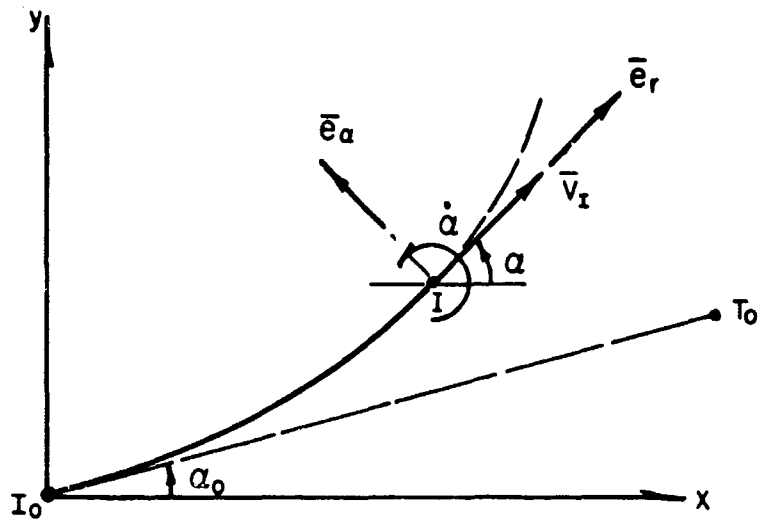
Sketch IV.6. To aid in the evaluation of Interceptor's acceleration. Shown is a part of the unit triad attached to the interceptor — this is the moving triad $(\bar{e}_r, \bar{e}_\alpha, \bar{e}_z)$; $\bar{e}_z$ is normal to the plane of motion (shown); $\bar{e}_r$ is aligned with $\bar{V}_I$, instantaneously.

That is,

$$A_\alpha = V_I \, \dot{\alpha},$$

which, after incorporation Eq. (IV.27), can be written as

$$A_\alpha = \frac{k V_I^2 \cos \alpha}{r_r} \tag{IV.31a}$$

taking account of the definition for k, and substituting for $\dot{\alpha}$.

Expressing r_r, the "range," from Eq. (IV.24a) then

$$A_\alpha = \frac{k\,V_I^2}{a\left(1 - \dfrac{x_I}{a}\right)\left(1 + p_I^2\right)} \equiv \frac{k\,V_I^2}{r_{r_0}\left(1 - \dfrac{x_I}{a}\right)\sqrt{1 + p_I^2}} \qquad \text{(IV.31b)}$$

using Eq. (IV.23); recall that r_{r_0} is the initial "range." (Note: a plot, using Eq. (IV.31b), is included here on Fig. IV.5, as noted earlier. Of course, the acceleration is graphed in dimensionless form, as was the turning rate.)

In the interest of recasting the description of the acceleration this quantity is rewritten below, after noting that r_r can be alternately expressed as

$$r_r = r_{r_0}\left(\frac{\sec \alpha}{\sec \alpha_0}\right)\left(\frac{\sec \alpha_0 + \tan \alpha_0}{\sec \alpha + \tan \alpha}\right)^k$$

In this regard Eq. (IV.31a) can be rewritten into the form,

$$A_\alpha = \frac{k\,V_I^2}{r_{r_0}}\frac{(\sec \alpha_0)^{1-k}}{(1 + \sin \alpha_0)^k}\left[(\cos \alpha)^{2-k}(1 + \sin \alpha)^k\right] \qquad \text{(IV.32)}$$

wherein the range on α is:

$$-\frac{\pi}{2} \le \alpha \le +\frac{\pi}{2}\,!$$

In the interest of gathering information regarding this acceleration, a natural question to ask is one concerning the extremal(s) for this quantity. Thus, after taking the derivative of Eq. (IV.32) (wrt α) the condition for an extremal to exist is found to be,

$$\sin \alpha = \frac{k}{2}. \qquad \text{(IV.33)}$$

67

Quite naturally this suggests some constraint on k (necessarily, now, $1 \leq k \leq 2$ for the extremals). This does not imply that $k \not> 2.0$, but does suggest the existing conditions for a finite maximum acceleration.

The condition noted in Eq. (IV.33) does not restrict the initial angle (a_0); this parameter, in the expression for acceleration, is free in its choice. Physically, however, if $a_0 > a$ (= $\sin^{-1} k/2$), then it should be apparent that the vehicle will not experience the maximum acceleration (corresponding to its value of k). Also, it should be evident to the reader that a is an increasing quantity for the intercepting pursuit problem.

Another interesting fact, regarding the normal acceleration, becomes apparent if one looks at the quantity inside the squared brackets in Eq. (IV.32). Noting that when $a = 0$ (that is, when the interceptor (I) has its velocity vector directed orthogonal to the velocity vector for the target (T)) this quantity becomes unity regardless of the value for (k). Hence, for any launch where $a_0 < 0$, the acceleration experienced by the vehicle (as it passes through $a = 0$) is heavily dependent on the initial conditions and the value of k (provided, of course, $1 < k \leq 2.0$).

One last remark regarding this acceleration: When the angle of inclination (a) is at its lowest limit ($- \pi/2$), then in order for the vehicle to experience any acceleration it is necessary that $a_0 = - \pi/2$ (also)). As a consequence, the transverse acceleration given to the vehicle at this inclination angle is found to be zero. Of course, this is a natural consequence arising from the orientation of the two vehicles relative to each other.

IV.11. A Figure of Merit

A "Figure of Merit" for the pursuit problem will be defined in terms of the interceptor's ability to affect a collision, in comparison to a collision by means of a "direct intercept." It is easy to visualize that the direct intercept, being a straight line path, will yield a smallest time for a collision to occur based on a prescribed set of initial values and a given value of k. As a corresponding situation, for the same values of k and initial range, the pursuit path will take longer to accomplish the collision; how much longer this mode of operation requires will be measured by the figure of merit. For those special cases wherein the times to intercept are identical, the figure of merit is unity; the larger the discrepancy between the two methods the greater the value for the figure of merit.

In establishing this quantity, the time of reference — that for a direct intercept — has been obtained previously as Eq. (III.11); that is, the time to intercept (directly) is,

$$t_i = \frac{r_{r_0}}{V_T \ [\sqrt{k^2 - \sin^2 \theta_T} + \cos \theta_T]}$$

Now, for this expression it can be shown that

$$\theta_T = \frac{\pi}{2} + a_0$$

(See the appropriate sketches); hence, this time, expressed in terms of a_0, is

$$t_i = \frac{r_{r_0}}{V_T \ [\sqrt{k^2 - \cos^2 a_0} - \sin a_0]} \qquad \text{(IV.34)}$$

with r_{r_0} being the initial "range", or separation distance, between I and T.

Now, defining the figure of merit as $M \triangleq t_m/t_i$, then

$$M = \frac{k + \sin a_0}{k^2 - 1} \ (\sqrt{k^2 - \cos^2 a_0} - \sin a_0) \qquad \text{(IV.35)}$$

after manipulation, and after using Eq. (IV.23), (IV.22), and (IV.34). The range of a_0 applicable here is, of course,

$$-\frac{\pi}{2} \leq a_0 \leq +\frac{\pi}{2} \ ;$$

this takes into account all flight paths from the direct "head-on" collision course to the simpler "chase" of the target (T) by the interceptor (I).

69

From a study of Eq. (IV.35) one can deduce that $M \to 1.0$ as $\alpha_0 \to -\pi/2$, and as $\alpha_0 \to +\pi/2$, regardless of the value given to $k(k > 1.0)$. At these limit values of α_0 the pursuit problem reduces to the corresponding intercept case.

Also, one can see that as $k \to 1.0$ the figure of merit (M) becomes quite large (in the vicinity of $\alpha_0 = 0$) indicating a very substantial increment in the time needed to effect an intercept by the pursuit maneuver. Actually there is no finite solution for M when $k \equiv 1.0$.

Also, one notes that for $\alpha_0 \simeq -30°$ the values of M are comparatively large for values of k not too different from unity. This would indicate that the Figure of Merit peaks (or, is maximized) in the region near to $\alpha_0 \simeq -30°$; and as increases, from this level, the values for M decrease. Apparently the lowest values of M occur at the extreme limits of α_0 (as indicated above).

It is equally evident that as k becomes large (say $k \simeq 10$, or greater) the value for M does not vary much from unity. This would indicate that the pursuit trajectories and the direct intercept paths do not differ, substantially, in geometric form.

As an aid toward understanding these remarks, and to gather other information concerning these two modes for bringing about a collision, a plot of Eq. (IV.35) has been prepared and is presented on Fig. IV.6, on following page. The various features of such a graph (as noted above) are immediately evident; and, as mentioned earlier, the computations were terminated at $|\alpha_0| = 80°$ in order to avoid the singularity which appears at the limit angle (s). This cut-off does not produce any difficulty since it is easy to recognize that $M \to 1.0$ as $|\alpha_0| \to \pi/2$.

IV.12. Line of Sight

One means of describing the location of one vehicle relative to the other is by a "line-of-sight" angle. In the pursuit problem the target is always directly ahead of the interceptor; however, the position of the interceptor relative to the target is a variable. Of course, as noted earlier, the range of variation for this line-of-sight angle can be described, a priori. What is of interest here is the history of this quantity as the pursuit maneuver progresses toward the final collision.

As a definition the line-of-sight angle, measured from (say) the direction of $\overline{V}_T$, can be expressed as

$$\angle (LOS)_T = \frac{3\pi}{2} - \alpha, \qquad (IV.35)$$
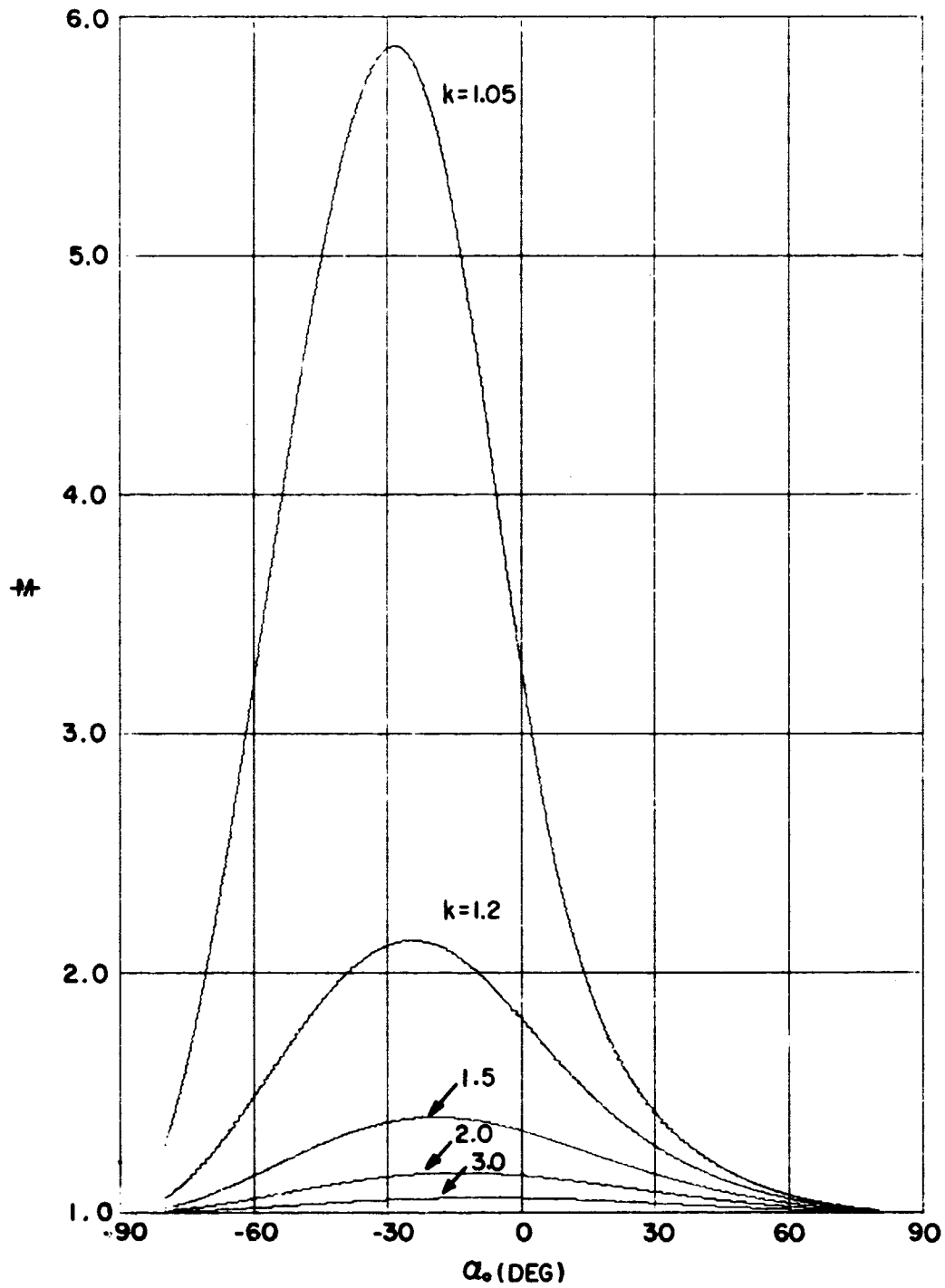
Fig. IV.6. A plot describing the Figure of Merit (M) as a function of Initial Position (a_0) and Speed Ratio (k)

where a is described from p_I in Eq. (IV.17). It is quite apparent that initially $\lambda\,(LOS)_T = 3\pi/2 - a_0$, and that the terminal value is $\lambda\,(LOS) = 3\pi/2 - (\pi/2)$ $\equiv \pi$, which is equivalent to one of the terminal requirements for the pursuit maneuver. Necessarily the history of this angle can be obtained directly from the variability of p_I which, in turn, depends explicitly on x_I/a, the independent variable for this study.

Figure IV.7 have been prepared to illustrate the behavior of the line-of-sight angle, during this flight mode, and is presanted as a function of a_0 and k. Generally speaking this angle has its most regular variation for the lower values of k (considering the several a_0 conditions selected here). As k increases the "elbow" in the curves becomes more pronounced — especially for the lowest values of a_0 — and, would approach a no-variation condition as $a_0 \rightarrow \pi/2$. For small k and large a_0 (but $< \pi/2$) this linearity is approached by the $\lambda\,(LOS)_T$. It is readily reckoned that as k becomes large ($k > 3.0$), and/or $a_0 \rightarrow -\pi/2$, the graphing of $\lambda\,(LOS)_T$ would approach the condition where the graph could be composed of two straight lines, orthogonal to one another. The first segment would appear as a horizontal line on the figure, and the last segment would be a vertical (parallel to the ordinate).

V. THE PURSUIT PROBLEM FOR A TARGET ON A CIRCULAR PATH

V.I. Introduction

A variation of the pursuit problems investigated in the previous sections would be one which considers the target vehicle to be traveling along a circular path; thus, the study to be conducted here is aimed again at defining a trajectory for the pursuit particle.

Remembering that the pursuing interceptor is always "looking" at the target, then the tangent to its flight path continually and instantaneously points to the (known) position of the target.

Since the circular path is predefined, then it is apparent that the position angle for the target can serve, quite adequately, as an independent variable in the solution. Thus, with suitable definitions, one should be able to formulate and, in principle, solve for the interceptor's chase path during the entire maneuver. Of course, as might be expected, this formulation becomes non-linear and is somewhat complicated in form — much too much so for an analytic evaluation.

72
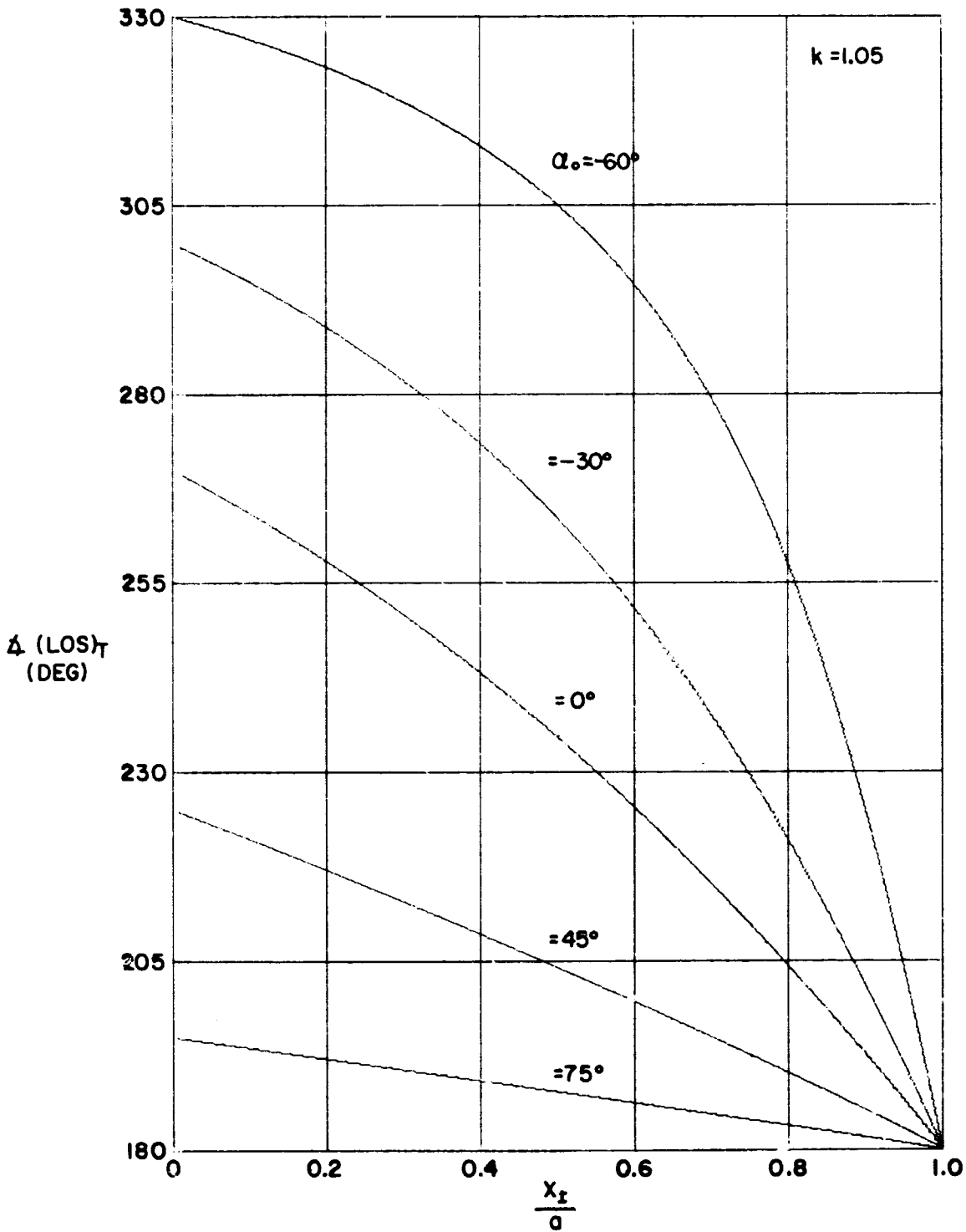
Fig. IV.7(a). Graph showing the Line-of-Sight (angle position of I relative to T) as a function of Initial Position (α_0) and Track Coordinate (x/a), for k = 1.05.

73
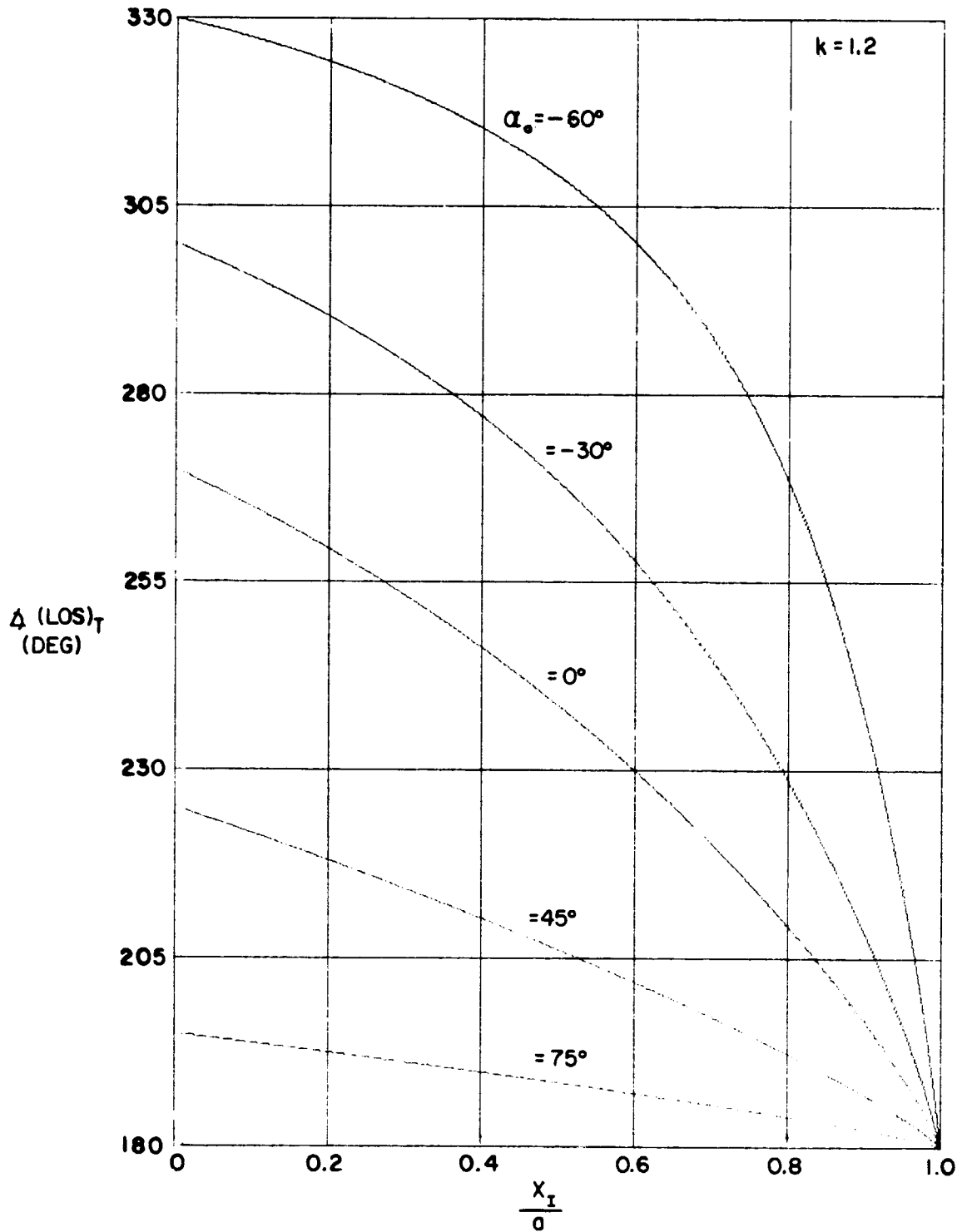
Fig. IV.7(b). Graph showing the Line-of-Sight (angle position of I relative to T) as a function of Initial Position (a_0) and Track Coordinate (x/a), for k = 1.2.

74
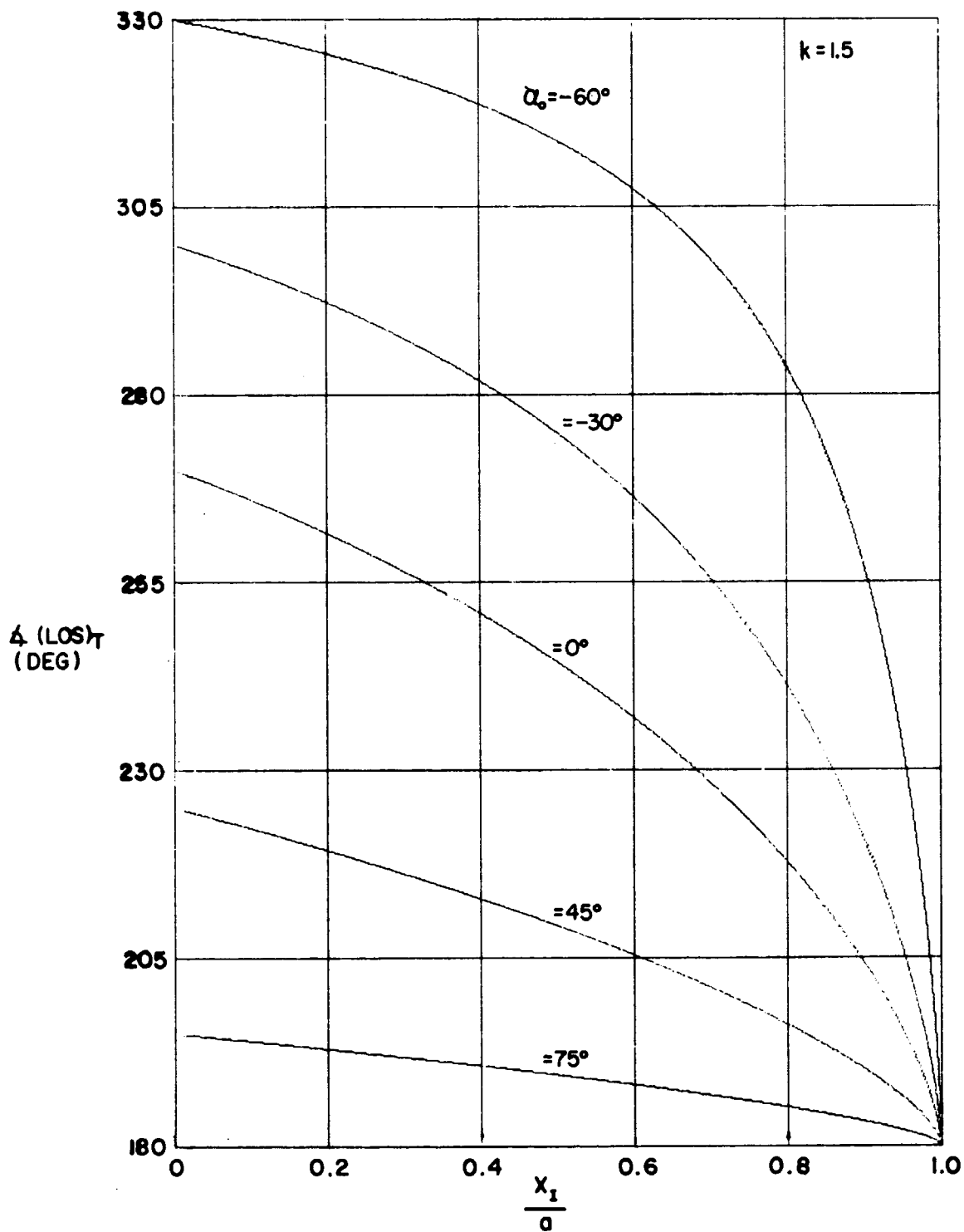
Fig. IV.7(c). Graph showing the Line-of-Sight (angle position of I relative to T) as a function of Initial Position (a_0) and Track Coordinate (x/a), for k = 1.5.
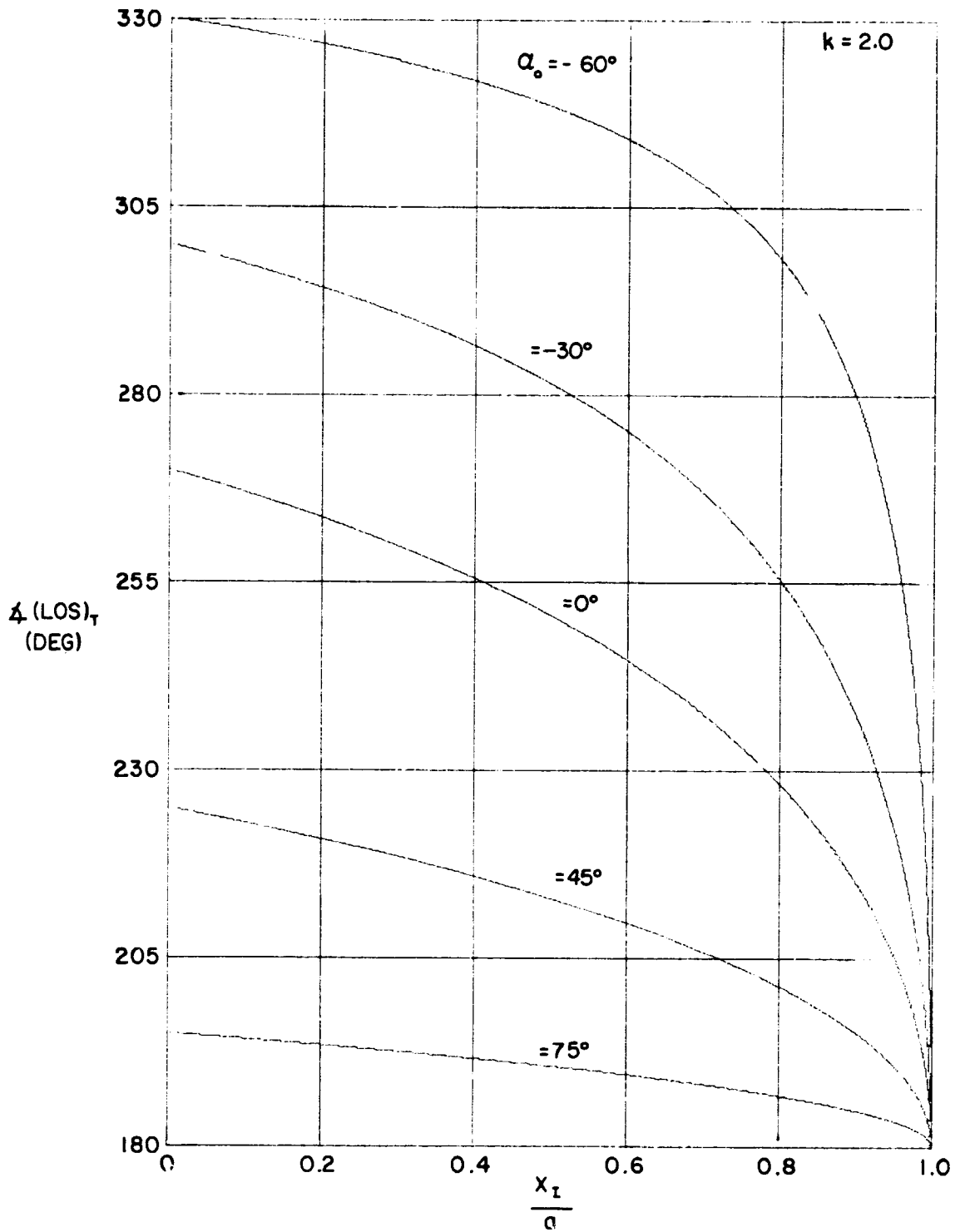
Fig. IV.7(d). Graph showing the Line-of-Sight (angle position of I relative to T) as a function of Initial Position (a_0) and Track Coordinate (x/a), for k = 2.0.
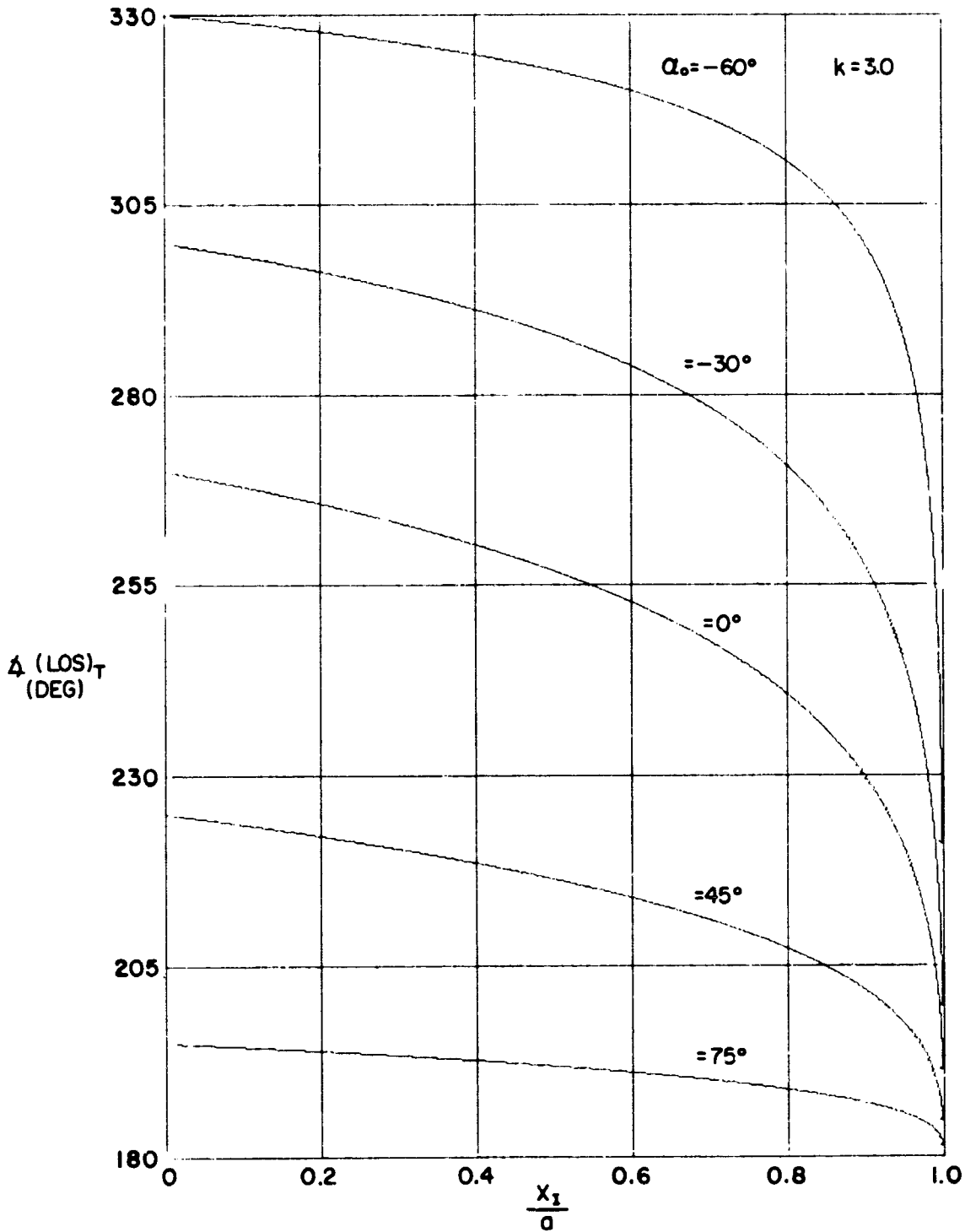
Fig. IV.7(e). Graph showing the Line-of-Sight (angle position of I relative to T) as a
function of Initial Position (a_0) and Track Coordinats (x/a), for k = 3.0.

V.2. General Description

It will be evident, shortly, that the geometry of this investigation could be viewed as the pursuit of an orbiting vehicle by a second craft which has the required maneuvering capability needed to negotiate the chase path. Since this problem is essentially a kinematic study the assumption of a central force field in this case would be secondary, and of consequence only when defining the target's velocity. Also, it should be apparent that this problem has other aerospace applications, it could serve equally well to describe the path of a seeker missile as it chases a target along a pursuit course.

In the following sketch a general, instantaneous situation is depicted. The target (T) is moving along its circular trajectory (of radius a); its position is located, relative to an inertial x-axis, by the position angle, θ_T. The interceptor (I) flies along the chase path, which is to be determined, at an assumed fixed speed (V_I) which is some multiple (k) of the target's speed. Thus, once again the speed ratio is introduced and defined as

$$k \triangleq \frac{V_I}{V_T}. \qquad (V.1)$$
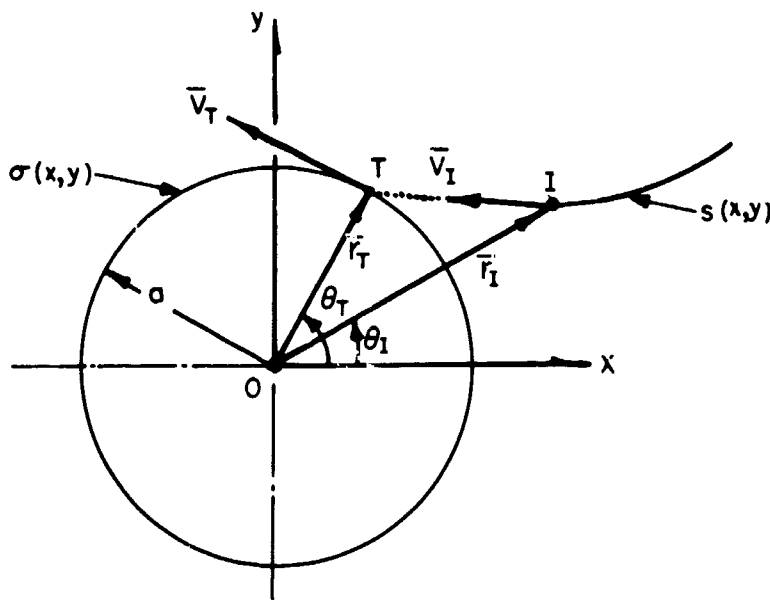
Sketch V.I. Showing the basic geometry of the pursuit problem for a target flying along a circular path, σ. The x, y axes are inertial; O is the origin, and the r_i, θ_i are plane polar coordinates.

78

Recognizing that the time rate of the displacement along these two trajectories defines each vehicle's speed, then $V_T \overset{\Delta}{=} d\sigma/dt$ and $V_I \overset{\Delta}{=} ds/dt$, where $\sigma(x, y)$ = 0 and $s(x, y) = 0$ denote the two space paths. In order to be fully cognizant of the specifics required here an added sketch (V.2), with the needed detail, is presented below.
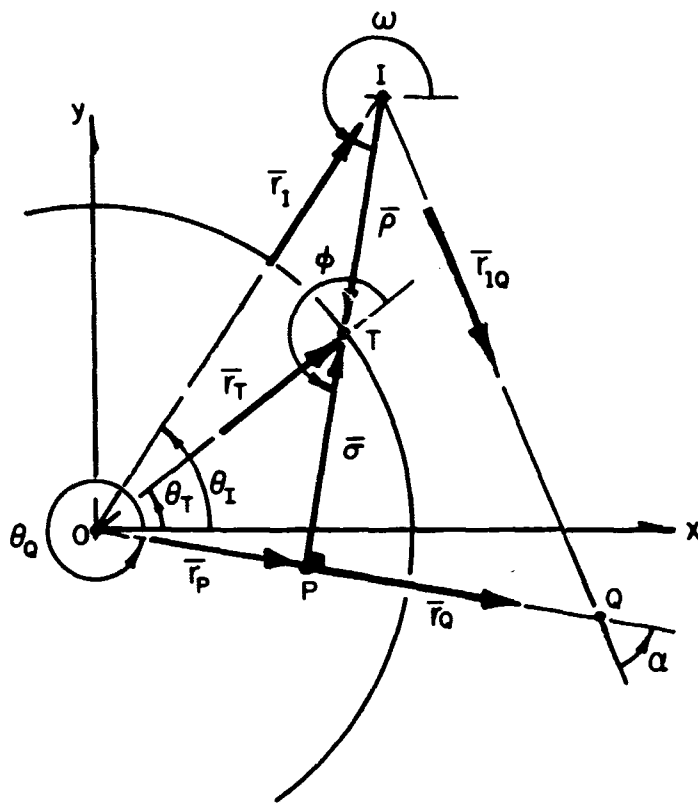
Sketch V.2. Defining the specific geometry of the pursuit problem. Shown here are vectors and angles necessary for a more complete description.

V.3. A Detailed Description

As an aid to the proper description of the geometry for this problem, it is necessary to introduce several quantities not shown in the diagram on preceding page (Sketch V.1). There, the basic geometric requirements were aluded to; in the sketch above the more detailed geometries are defined.

Several vectors needed in the problem's formulation are shown on this sketch. In order to describe these vectors best, use will be made of the various lettered positions as a means of denoting the vector lengths. Also, the letters are arranged, under an overscore, in an <u>order</u> which signifies the "from" and "to" of each vector. For instance the position vector $\bar{r}_T$ may be "defined" as

$$\bar{r}_T \overset{\Delta}{=} \overline{OT},$$

denoting a <u>vector</u> originating at "0" and terminating at "T", as shown. Following this scheme one sees on the figure the following vectors:

Name	Notation	Description
Position vector for the interceptor (I)	$\bar{r}_I$	$\overline{OI}$
Position vector of the geometry point, P	$\bar{r}_P$	$\overline{OP}$
Position vector of the geometry point, Q	$\bar{r}_Q$	$\overline{OQ}$
Line of sight vector (from I to T)	$\bar{\rho}$	$\overline{IT}$
Vector locating T from P	$\bar{\sigma}$	$\overline{PT}$
Vector locating Q from I	$\bar{r}_{IQ}$	$\overline{IQ}$

It will be assumed herein that the problem is confined to a single given plane of motion (x, y); thus the inertial reference triad will be $(\bar{e}_x, \bar{e}_y, \bar{e}_z)$ – where $\bar{e}_z \overset{\Delta}{=} \bar{e}_x \times \bar{e}_y$ following the conventional right hand rule.

The several angles shown on the sketch on preceding page are positive valued, and are necessary to the problem's formulation and solution. In addition, it is essential to establish, as definitions, certain directions, lengths, etc. as noted below.

For a description of the vector $\bar{\sigma}$ one needs to: first, locate point P; second, describe the line length OQ, and last to ascertain a direction for $\bar{r}_Q$. In this regard, the point P is found by extending the vector $\bar{\rho}$ (forward or backward, as needed) and drawing a line through O normal to $\bar{\rho}$; the intersection of these two lines locates P. The line OQ will be <u>given</u> a length* which is k times larger than the circular radius, a; that is,

---

*The reasoning behind this selection will be evident in a subsequent development.

$$OQ \overset{\Delta}{=} ka.$$

For the sake of consistency in notation the vector $\bar{r}_Q$ will be defined as follows,

$$\bar{r}_Q \overset{\Delta}{=} \frac{\bar{e}_z \times \bar{\rho}}{|\bar{\rho}|} \; (OQ).$$

This is a vector having a fixed length ($ka = OQ$), but a direction which varies according to the relative positions of T and I; its direction is obtained from the vector multiplication, $(\bar{e}_z \times \bar{\rho})/|\bar{\rho}|$.

The several angles which are significant here are described in the following table, and according to the operations noted there:

Description of the Angle	Operation	Notation
Angular location of $\bar{r}_T$ relative to the x-axis	$\frac{1}{|\bar{r}_T|} [\bar{e}_x \cdot \bar{r}_T]$	θ_T
Angular location of $\bar{r}_Q$ relative to the x-axis*	$\frac{1}{OQ} [\bar{e}_x \cdot \bar{r}_Q]$	θ_Q
Angular location of $\bar{\rho}$ measured from $\bar{r}_T$	$\frac{1}{|\bar{r}_T| \, |\bar{\rho}|} [\bar{r}_T \cdot \bar{\rho}]$	φ
Angular location of $\bar{\rho}$ measured from the x-axis	$\frac{1}{|\bar{\rho}|} [\bar{e}_x \cdot \bar{\rho}]$	ω
Angular location of $\bar{r}_Q$ relative to $\bar{r}_{IQ}$	$\frac{1}{|\bar{r}_{IQ}| \, OQ} [\bar{r}_{IQ} \cdot \bar{r}_Q]$	α

and, from a study of the sketch: $\omega - \varphi \equiv \theta_T.$

---

*A positive angle is shown; this particular representation is not contrary to vector descriptions.

81

The reference angle, θ_T, can be obtained by means of the integral,

$$\theta_T = \theta_{T_0} + \dot{\theta} \int_0^t dt ,$$

since $\dot{\theta} \equiv V_I / a$ (a constant); θ_{T_0} corresponds to $t = 0$.

Two vectors, $\overline{PI}$ and $\overline{PQ}$, have a particular use in this study; these are defined from the sketch as

$$\overline{PI} = \bar{\sigma} - \bar{\rho} ,$$

$$\overline{PQ} = \bar{r}_Q - \bar{r}_p ;$$

also, note that

$$\left| \overline{PI} \right| = \left| \bar{\sigma} - \bar{\rho} \right| \equiv \left| \left| \bar{\rho} \right| - a \cos \varphi \right| ,$$

and

$$\left| \overline{PQ} \right| = \left| \overline{OQ} - \bar{r}_p \right| \equiv \left| k a - a \sin \varphi \right| .$$

In order to demonstrate that the above definitions and descriptions are consistent, several general and specific cases have been investigated; three added sketches are shown on following pages for the purpose of more fully illustrating the generalities mentioned earlier. Note that the interceptor (I) may fly paths which lie either inside or outside of the target circle (radius a).

V.4. Formulation of the Pursuit Problem

The last sketch shown on page 84, is descriptive of the displacements which occur during a time lapse (δt); herein the target and interceptor will traverse path segments $\delta\sigma$ and δs, respectively. According to Eq. (V.1), and accounting for the definitions noted in the foregoing sections, it is seen that

$$\delta s = k \, \delta \sigma \equiv k a \, \delta \theta_T , \tag{V.2a}$$
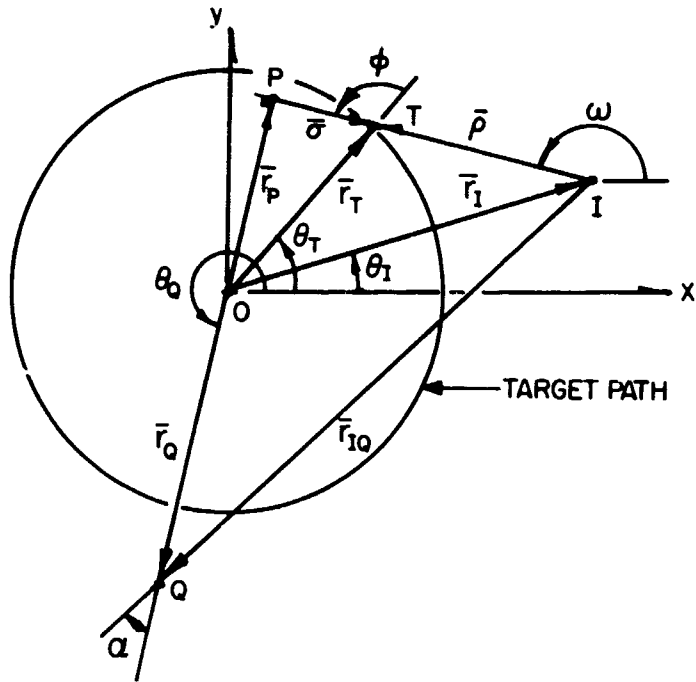
Sketch V.3. Showing I outside of circle (a); $\theta_T > \theta_I$.
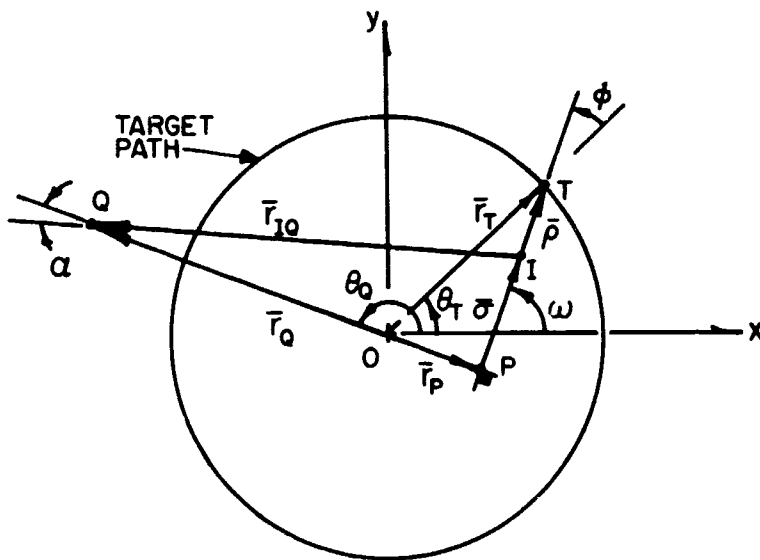
Sketch V.4. Showing I inside the circle (a); $\theta_I > \theta_T$.

83

Sketch V.5. Showing I inside the circle (a); $\theta_T < \theta_I$. (Compare this to the previous sketch to see the influence of $\theta_I > \theta_T$).

Sketch V.6. Showing the basic geometry necessary for the formulation of the circular pursuit problem.

or

$$\delta s = \delta x_I \sqrt{1 + \left(\frac{\delta y_I}{\delta x_I}\right)^2} \; ; \qquad\qquad \text{(V.2a)}$$

wherein

$$\delta x_I \simeq \delta s \cos \omega,$$

$$\delta y_I \simeq \delta s \sin \omega. \qquad\qquad \text{(V.2b)}$$

As a consequence of the above statements, and for the limit as $\delta t \to 0$ (also selecting the positive radical),

$$\frac{ds}{dx_I} = \sqrt{1 + \tan^2 \omega} = \sec \omega; \qquad\qquad \text{(V.3a)}$$

or

$$\frac{ds}{d\theta_T} = \hbar a = (\sec \omega) \frac{dx_I}{d\theta_T} . \qquad\qquad \text{(V.3b*)}$$

V.5. Cartesian Coordinate Representation, and the Governing Equations

With reference to the (inertial) cartesian axes it is noted that the points T and I are located by:

$$x_T = |\bar{r}_T| \cos \theta_T \equiv a \cos \theta_T,$$

$$y_T = |\bar{r}_T| \sin \theta_T \equiv a \sin \theta_T; \qquad\qquad \text{(V.4a)}$$

and

$$x_I = x_T + |\bar{\rho}| \sin\left(2\pi - \omega - \frac{\pi}{2}\right) = x_T - |\bar{\rho}| \cos \omega, \qquad\qquad \text{(V.4b)}$$

---

*This is the length assigned to the vector $\overline{OQ}$ (shown previously).

85

Sketch V.7.   Illustrating position geometry required to
formulate this problem.

$$y_I = y_T - |\overline{\rho}| \sin \omega,$$

respectively.

In addition, it should be apparent that:

$$|\overline{\sigma}| = |\overline{r}_T| \cos \varphi' = |- a \cos \varphi|; \qquad \qquad \text{(V.5)}$$

$$|\overline{r}_p| = |\overline{r}_T| \sin \varphi' = |a \sin \varphi|;$$

and, as a check on these lengths, recall that

$$|\overline{r}_T| = a = \sqrt{|\overline{\sigma}|^2 + |\overline{r}_p|^2} .$$

86

From Eq. (V.2) it is evident that

$$dx_I \sin \omega - dy_I \cos \omega = 0,$$

whereas, from Eq. (V.4),

$$dx_I = - (a \sin \theta_T) d\theta_T + \rho \sin \omega \, d\omega - (\cos \omega) \, d\rho,$$

$$dy_I = (a \cos \theta_T) d\theta_T - \rho \cos \omega \, d\omega - (\sin \omega) \, d\rho;$$

hence, it is easy to demonstrate that

$$dx_I \sin \omega - dy_I \cos \omega = 0 \equiv - a \cos (\omega - \theta_T) d\theta_T + \rho d\omega$$

or

$$\rho \frac{d\omega}{d\theta_T} = a \cos \varphi, \qquad (V.6)$$

since $(\omega - \theta_T) \equiv \varphi$.

In addition, from Eq. (V.2), one notes that

$$ds = dx_I \cos \omega + dy_I \sin \omega,$$

or

$$ds \equiv ka \, d\theta_T = a \sin (\omega - \theta_T) - d\rho \equiv a \sin \omega - d\rho,$$

leading directly to

$$\frac{d\rho}{d\theta_T} + ka = a \sin \varphi. \qquad (V.7)$$

Equations (V.6) and (V.7) describe the behavior of ρ and ω in terms of the most convenient independent variable (θ_T); unfortunately these quantities are expressed in terms of still another variable, φ. Consequently, in order to obtain a system of equations which can be solved (at least in principle) to yield the pursuing interceptor's path, these expressions must be further manipulated and altered.

87

Differentiating Eq. (V.6) provides the second order relation,

$$\rho \frac{d^2\omega}{d\theta_T^2} + \frac{d\rho}{d\theta_T} \frac{d\omega}{d\theta_T} + a \sin\varphi \frac{d\varphi}{d\theta_T} = 0, \qquad (V.8)$$

which can be altered by including Eq. (V.7) and using the relation $\omega = \varphi + \theta_T$ (as an aid in correlating the variables, ω, φ and θ_T) to obtain,

$$\frac{d\omega}{d\theta_T} = 1 + \frac{d\varphi}{d\theta_T}. \qquad (V.9)$$

Also, Eq. (V.6), per se, can be introduced to eliminate the variant ρ from Eq. (V.8). The end result of these operations leads directly to

$$\frac{d^2\omega}{d\theta_T^2} \cos\varphi + \left(\frac{d\omega}{d\theta_T}\right)^2 (2 \sin\varphi - \hbar) - \frac{d\omega}{d\theta_T} \sin\varphi = 0. \qquad (V.10)$$

Eq. V.10) can be solved to obtain $\omega = \omega(\theta_T)$; or it may be altered, again, to describe a governing relation for φ. To this end use Eq. (V.9), noting that

$$\frac{d^2\omega}{d\theta_T^2} = \frac{d^2\varphi}{d\theta_T^2};$$

then it is easy to show that this result is,

$$\frac{d^2\varphi}{d\theta_T^2} \cos\varphi + 2\left(\frac{d\varphi}{d\theta_T}\right)^2 \left(\sin\varphi - \frac{\hbar}{2}\right) + 3 \frac{d\varphi}{d\theta_T} \left(\sin\varphi - \frac{2\hbar}{3}\right)(\sin\varphi - \hbar) = 0. \qquad (V.11)$$

Eq. (V.11) suggests an alternate scheme for obtaining one of the unknowns found in $\omega = \varphi + \theta_T$ — hence either of the above expre: ;ions can be employed during the formal mathematical solution process.

88

There remains the need to describe $\rho = \rho(\theta_T)$ in order to complete a description of the interceptor's trajectory. Such an expression may be obtained by differentiating Eq. (V.7), and using Eqs (V.6) and (V.9) to reduce the variable dependencies. After performing these operations it is found that,

$$\frac{d^2 \rho}{d\theta_T^2} - a \cos \varphi \left(\frac{a \cos \varphi}{\rho} - 1 \right) = 0. \qquad (V.12a)$$

However, rather than use Eq. (V.12a) a somewhat more convenient form can be had by substituting for the trigonometric terms from Eq. (V.7). The resultant obtained from this substitution is,

$$\rho \frac{d^2 \rho}{d\theta_T^2} + \rho \sqrt{a^2 - \left(\frac{d\rho}{d\theta_T} + ka \right)^2} - \left[a^2 - \left(\frac{d\rho}{d\theta_T} + ka \right) \right] = 0. \qquad (V.12b)$$

Now Eq. (V.12), and (V.10) or (V.11), form a set which may be solved to describe a flight path for the pursuit problem being studied here. Necessarily the finding of the path, per se, will have to be performed by numerical means; and most likely with the aid of a computer, due to the essential non-linearity of these governing expressions. Unfortunately the basic character of these differential equations does not lend to an easy geometric representation of them; consequently the results will most conveniently be viewed simply as the numerical solutions produced for whatever case is being investigated.

V.6. Solution Procedure

In order to "start" the solution procedure one needs to know, or specify, a set of initial conditions. Those quantities needed are ρ_0, θ_{T0} (and $\dot{\theta}_T$), φ_0 (or ω_0), $(d\rho/d\theta_T)_0$ and (say) $(d\varphi/d\theta_T)_0$. The geometric initial values may be simply stated as a priori information; however, the derivative terms are found by using the same (a priori) information, with other known quantities, plus the appropriate mathematical statements. For instance, Eq. (V.7) can be used to obtain

$$\left(\frac{d\rho}{d\theta_T} \right)_0 = a (\sin \varphi_0 - k); \qquad (V.13a)$$

while Eqs. (V.9) and (V.6) are employed to give

$$\left(\frac{d\varphi}{d\theta_T}\right)_0 = \frac{a \cos \varphi_0 - \rho_0}{\rho_0} ,$$

(V.13b)

which, incidentally, is equivalent to writing a ratio of the initial lengths,

$$\left(\frac{d\varphi}{d\theta_T}\right)_0 \equiv \frac{(IP)_0}{\rho_0} ;$$

(V.13c)

where the length $(IP)_0$ is defined as,

$$(IP)_0 \overset{\Delta}{=} |\overline{IP}|_0 = |\overline{\rho}_0 - \overline{\sigma}_0| .$$

(See Sketch V.7).

V.7. Graphical Results

A graphical representation of the results obtained from this investigation is most conveniently presented as a trace of the interceptor's path of motion, along with that of the target. Unfortunately, the solutions described from the section above are not obtained in terms of the most desired variables. Rather than present the paths as abstractions (say plots of $\rho = \rho(\varphi)$), a more revealing situation would be to show the actual trajectories plotted in terms of the cartesian coordinates for the two vehicles during flight. Consequently, Eq. (V.4) is recommended for use in reproducing these traces. As a convenience, these expressions are noted below:

(1) the path of the target can be described from

$$x_T = a \cos \theta_T, \quad y_T = a \sin \theta_T$$

(V.14a)

and,

(2) the path of the interceptor from,

90

$$x_I = x_T - \rho \cos \omega \equiv a \cos \theta_T - \rho \cos (\varphi + \theta_T),$$

$$y_I = y_T - \rho \sin \omega \equiv a \sin \theta_T - \rho \sin (\varphi + \theta_T), \qquad \text{(V.14b)}$$

wherein the independent variable, θ_T, is obtained from

$$\theta_T = \theta_{T_0} + \dot{\theta}_T \int_0^t dt, \qquad \text{(V.14c)}$$

since $\dot{\theta}_T = V_T / a$ (a constant).

As an aid to understanding and illustrating the results obtained here, several cases will be presented from a more complete collection of material gathered during the study of this overall problem. Also, included with each trace of the two paths of motion there will be accompanying plots of the lateral acceleration and the range-rate and the range, in dimensionless form, for the pursuit vehicle. These latter graphs are presented as functions of the independent variable, θ_T (for convenience of reference).

It was mentioned that all graphs are presented in terms of dimensionless quantities. The purpose in doing so is to be able to represent a much larger family of results, and to do this without having to consider the attendant larger number of variables encountered in dimensional representations. Because of the uniformity of the non-dimensional expressions, this scheme is not only desirable but contributes to the conciseness of results.

Generally for the figures shown here, lengths are nondimensionalized by placing them in ratio to "a" (the target path's radius); speeds are expressed in ratio to V_T (the target's speed); and, the lateral acceleration (A_I) is ratioed to the centrifugal acceleration for the target vehicle (V_T^2/a). For each set of graphs the initial values for that case are noted on the plot indicating the two trajectories; each of the associated plots will have other pertinent notations inscribed on them to aid in comparing cases and to illustrate the influence of initial values on the problem.

V.8. Dimensionless Representations

For presenting the results obtained (here) it was suggested that transformations of the variables, leading to dimensionless quantities, should be used with the plot routines.

91

For such a representation let the variable ρ be replaced by χ, where

$$\chi \overset{\Delta}{=} \rho/a; \tag{V.15}$$

then Eq. (V.12b) can be rewritten as

$$\chi \frac{d^2\chi}{d\theta_T^2} + \chi \sqrt{1 - \left(\frac{d\chi}{d\theta_T} + k\right)^2} - \left[1 - \left(\frac{d\chi}{d\theta_T} + k\right)^2\right] = 0. \tag{V.16}$$

Next, the initial quantity $(d\rho/d\theta_T)_0$ is transformed to

$$\left(\frac{d\chi}{d\theta_T}\right)_0 = \sin \varphi_0 - k; \tag{V.17}$$

and, similarly, Eq. (V.13b) is replaced by

$$\left(\frac{d\varphi}{d\theta_T}\right)_0 = \frac{\cos \varphi_0 - \chi_0}{\chi_0}. \tag{V.18}$$

For the graphical results, per se, the cartesian variables will be non-dimensionalized, also, as noted below (refer to Eqs. (V.14)): that is, defining

$$\xi_T \overset{\Delta}{=} \frac{x_T}{a} = \cos \theta_T$$

$$\eta_T \overset{\Delta}{=} \frac{y_T}{a} = \sin \theta_T; \tag{V.19}$$

and

$$\xi_I \overset{\Delta}{=} \frac{x_I}{a} = \xi_T - \chi \cos \omega = \cos \theta_T - \chi \cos (\varphi + \theta_T),$$

$$\eta_I \overset{\Delta}{=} \frac{y_I}{\rho} = \eta_T - \chi \sin \omega = \sin \vartheta_T - \chi \sin (\varphi + \theta_T), \qquad \text{(V.20)}$$

then these last expressions will be used for the presentation of trajectories flown by the target and the interceptor, respectively.

V.9. The Acceleration, or A Control Requirement

The interceptor, during its pursuit operation, may have to undertake some rather rigorous maneuvers, theoretically. Whether or not the vehicle can successfully perform these has not been a constraint imposed on this problem. In view of the possible restrictions which could arise some insight into (say) the accelerations which the interceptor might encounter would be illuminating and helpful to the investigator.

In order to define the interceptor's accelerations it is advantageous to introduce a moving triad, attached to the interceptor, designated as the triad ($\bar{e}_\rho$, $\bar{e}_\omega$, $\bar{e}_z$). Here the unit vectors are described as:

$\bar{e}_\rho$, parallel to the relative position vector, $\bar{\rho}$;

$\bar{e}_z$, normal to the plane of motion ($\bar{e}_z = \bar{e}_x \times \bar{e}_y$);

and

$\bar{e}_\omega$, normal to $\bar{e}_\rho$: thus, $\bar{e}_\omega = \bar{e}_z \times \bar{e}_\rho$; (Note, say, sketch V.7).

Recognizing that the interceptor's velocity vector can be expressed as

$$\bar{V}_I = V_I \bar{e}_\rho, \quad (V_I \overset{\Delta}{=} \text{a constant}), \qquad \text{(V.21)}$$

then the acceleration vector may be written as

$$\bar{A}_I = \frac{d\bar{V}_I}{dt} = \dot{V}_I \bar{e}_\rho + V_I \dot{\bar{e}}_\rho,$$

wherein $\dot{V}_I \equiv 0$, and

$$\dot{\bar{e}}_\rho = \bar{\Omega} \times \bar{e}_\rho.$$

93

Here $\bar{\Omega}$ is the rotational-rate vector describing the triad's angular motion. For this problem, $\bar{\Omega} \triangleq \dot{\omega}\, \bar{e}_z$, thus it follows that

$$\bar{A}_I = V_I\, \dot{\omega}\, \bar{e}_\omega \qquad (V.22)$$

which states that there is a <u>transverse</u> acceleration (only); or, that this is a requirement which must be met by the maneuvering capability of the intercept vehicle in a realistic case.

Making substitutions from the analysis section — recalling the definitions for $\dot{\theta}_T$, k, and $d\omega/d\theta_T$ — it is easy to show that

$$A_I = \frac{k V_T^2 \cos\varphi}{\rho}\; ; \qquad (V.23)$$

where ρ, φ are functions of θ_T, while k and V_T are preselected constants.

This quantity could very well be viewed as a constrait imposed on whatever vehicle is being represented here. As a convenience in understanding the behavior of this term, as the pursuit maneuver progresses, it is included among the several graphic presentations appended to this section.

V.10. The Time for the Pursuit Maneuver

The time required to complete the pursuit maneuver is readily calculated from a knowledge of the target vehicle's path. Since this particle moves at a fixed speed along a given (fixed geometry) path, then it is evident that when the total arc ($\Delta\sigma$) is known, the time of the motion is obtained from

$$\Delta t = \frac{\Delta\sigma}{V_T} \equiv \frac{a(\theta_f - \theta_0)}{V_T} \qquad (V.24)$$

where a is the radius of the target's path, and θ_i ($i = 0$, f) denotes the angular position of the target initially $((\ )_0)$ and finally $((\ )_f)$. It is obvious that this is the time of flight for the interceptor, as well, according to the definition of the pursuit operation.

94

Since this is an almost trivial resultant, there is no need to present any results in tabular and/or graphic form; simple analytic answers may be obtained from Eq. (V.24), directly.

V.11. Path Length for the Pursuit Maneuver

Similar to the case discussed above, a determination of path length for this operation is actually of minor consequence. In view of the basic assumptions made for this maneuver, the path length for the target is known — at the completion of the problem. That is, with $\Delta\sigma \triangleq$ the path length for the target, then

$$(\Delta\sigma)_{TOT} = a(\theta_f - \theta_i).$$ (V.25)

Also, the definition, $k \triangleq V_I/V_T$ infers that

$$ds = k \, d\sigma$$

where $s \triangleq$ path of the pursuit vehicle; therefore,

$$(\Delta s)_{TOT} = k(\Delta\sigma)_{TOT},$$ (V.26)

thus the <u>length</u> of this trajectory is known, also.

Needless to say the presentation of this result will result in very little additional information; hence this will not be undertaken here.

V.12. Range and Range-Rate

Two of the primary measurable quantities in the pursuit (and intercept) problem are the range (ρ) and range-rate $(\dot{\rho})$ for the vehicles. Normally this information is obtained from (say) on-board radar systems, and is used in the navigational and guidance logic needed by the maneuvering vehicle.

The range (ρ) is obtained from the solution of Eq. (V.12b), as a part of the general solution, while the range rate $(\dot{\rho})$ must be acquired from (V.7); that is, this quantity is acquired from,

$$\frac{d\rho}{dt} = \frac{d\rho}{d\theta_T} \frac{d\theta_T}{dt} = -a(k - \sin\varphi)\,\dot{\theta}_T;$$

which, can be rewritten as

$$\dot{\rho} = V_T \, (\sin \varphi - k), \qquad\qquad (V.27)$$

implying that $\rho = \rho \, (\theta_T)$ through $\varphi = \varphi \, (\theta_T)$.

These two quantities are also included in the graphical representations appended to this section. Each trajectory represented on the figures will have, accompanying it, one plot for the dimensionless range (ρ / a) variation, and one for the dimensionless range-rate $(\dot{\rho}/V_T)$, both as functions of the position angle (θ_T).

Rather than chance being too repetitious in the discussions of each plot, some general comments are offered as a beginning. These are accompanied with the suggestion that one should look at the several different graphs in order to gain a better insight into the behavior of these quantities for the various cases presented.

As one expects the range is a continually decreasing function of time (or θ_T), being almost linear in many cases, but normally having some non-linearity. Actually this parameter is not the most interesting of those considered in the full investigation, and warrents very little general discussion.

The range-rate is the more fascinating topic to discuss. It is evident (here) that this dimensionless parameter can undergo rather large excursions during a given pursuit operation; and, it appears that, categorically, the cases have similar characteristics as shown on these plots. Normally, those cases which are not close to a pure chase-flight type are those which exhibit the largest range-rate changes. And, frequently, those paths which have a larger k value are also those which give the more variable range-rates.

V.13. General Remarks from Observations of the Graphs

Lateral accelerations are noted to be largest, generally, for those cases which initiate as a head-on (or near head-on) configuration. When the approach to pursuit is from ahead, and k is large, the lateral accelerations are also large. To some degree of expectation, those operations which originate from beside and close to the target, even for small k values, also undergo relatively elevated levels of lateral acceleration. It is apparent that the more "head-on" oriented situations would be much better performed as "intercepts" than as "pursuits." If this mode for operation was followed then the more restrictive aspects of this flight type would be alleviated.

96

It would seem, from this overall study, that the more likely "optimum" cases would be those which were allowed to select between the simple intercept and the pursuit modes, coupled with a capability of being able to switch from one mode to the other in order to meet changing collision requirements as they arise. The pursuit mode could be used to account for course deviations — not accounted for in a priori considerations — while the simple intercept operation could be utilized to overcome restrictions imposed by large turning rates and lateral accelerations when a near-to-head-on approach becomes apparent. Such a selectivity has not been attempted in this study, nor is it within the scope of the present formulations; such a problem as this must be deferred to a subsequent investigation.

A review of the figures produced during this study will indicate that rather distinctive patterns arise for the geometry describing the lateral acceleration, the range-rate and the range, as one varies the speeds (or k) and the initial positioning of the vehicles (φ_0, ρ_0).

When k is small (near unity), and ρ_0 is of the order of "a", or greater, then the lateral accelerations may undergo one or more cycles of variation; but, the value ultimately tends to a level approaching $k^2 V_T$! As k grows this level naturally increases, but only to the extent that the "catch-up" occurs more quickly and the maneuver does not fully tend to the "hound-and-hare" type of terminal condition.

For those cases where $\varphi_0 < \pi/2$ the lateral accelerations are positive throughout the maneuver (both vehicles have the same type of path curvature); for $\pi \geq \varphi_0 \geq \pi/2$ the initial phase of the operation has a negative acceleration, but the terminal portion again approaches the same type of condition as that experienced when $\varphi_0 < \pi/2$. As φ_0 is increased, from $\pi/2$ to $3\pi/2$, the initial excursion of the acceleration is negative; while those cases where $\varphi_0 > 3\pi/2$ are characterized by large (negative valued) "spikes" appearing on these plots. These situations are noted to occur when $\rho_0 = 0(a)$; however, when φ_0 is significantly increased (or decreased) the patterns are altered and the variations can be noted best by looking at the figures.

Characteristically the Range-Rate parameter ($\dot{\rho}/V_T$) will generally experience one to two excursions as the value of φ_0 is incremented from 0 to π. Above $\varphi_0 = \pi$ this quantity returns to a single excursion, as a general statement. It is also demonstrated that when large ρ_0/a values are included, and the flight path is not "direct," but akin to a sinusoid, then the range-rate may undergo multiple excursions — (see figures where $\rho_0/a >> 1.0$) -- this is to be expected since the target would likely fly along its path for more than one circuit, necessitating the flight condition for the interceptor as observed and reported here.

A study of the dimensionless range (ρ/a) graphs shows that there are (again) distinctive patterns developed for the several classes of pursuit approaches (ρ_0, φ_0) which are included among the plots appended to this section. Generally speaking, "kinks" will appear in the range curves whenever there is a decided ($\pm$) spike evident on the acceleration curve(s). An excursion in the acceleration is accompanied by a non-linearity on the range picture; and, an influence, due to the spread in θ_T over which this excursion occurs, is noted. That is, so long as the variation in acceleration does not approach the "spike" configuration then the non-linearity in range is rather gentle and does not tend to the "kink." (Compare Fig. 2 and Fig. 4, for instance.) The long range $(\rho_0/a \gg 1.0)$ and short range $(\rho_0/a \ll 1.0)$ cases behave in a rather similar fashion to the situations discussed here; consequently, after one becomes familiar with these various maneuvers it would be relatively easy to predict what should be expected in the variations for a given set of initial values. Also, it becomes evident, immediately, that for certain of the pursuit cases the accelerations are rather unmanageable; and, that in a real situation there are maneuvering requirements which are not likely to be realized by actual pursuing vehicles.

The graphs which follow this section are, as indicated earlier, presented in dimensionless form, but as functions of θ_T as a most convenient variable. Of course θ_T and t are interchangeable variables due to the constancy of $\dot{\theta}_T$.

As an aid to the reader the several parameters which are plotted, and the initial orientations (φ_0) are clarified and noted below:

The quantities indicated on the ordinates of the graphs are:

(a) Dimensionless Lateral Acceleration Parameter = $A_I a/V_T^2$, (see Eq. (V.23));

(b) Dimensionless Range-Rate Parameter = $\dot{\rho}/V_T$, (see Eq. (V.27));

(c) Dimensionless Range Parameter = ρ/a $(\equiv \chi)$, (A solution resultant).

For the purpose of identifying where the Target (T) and Pursuit Interceptor (I) are located, relative to one another for various φ_0 values, the following sketch indicates this positioning of I relative to T. The numbers, enclosed in parens, ( ), indicate the value assigned to φ_0, in degrees, corresponding to these several positions; the distance, ρ_0, describes the straight line displacement of I_0 relative to T_0.

THE
TARGET'S
PATH ——→

(270°)
I_0
(0) I_0 T_0 I_0 (180)
I_0
(90)

T_0 IS GENERALLY LOCATED
AS SHOWN HERE

I_0 SIGNIFIES THE POSITION(S)
ASSIGNED TO INTERCEPTOR,
INITIALLY.
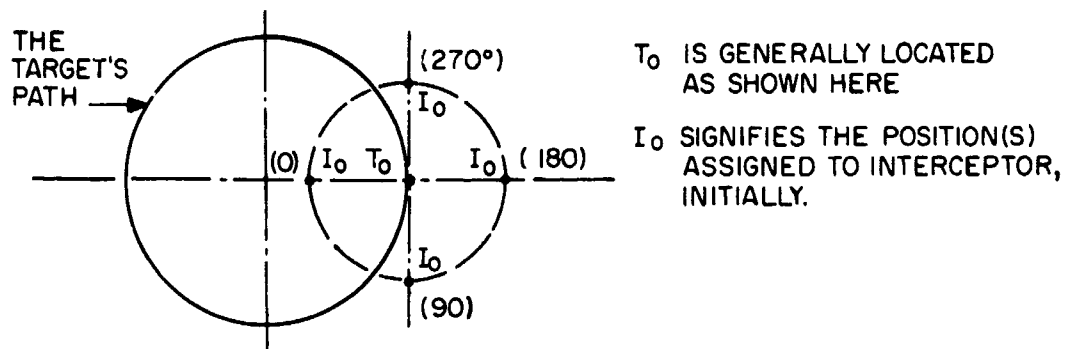
In many of the figures there are notations included to aid in the understanding
of how the variations in these parameters occur, how these may be correlated
to the appropriate trajectory figure, and how they relate to one another for the
various cases described.
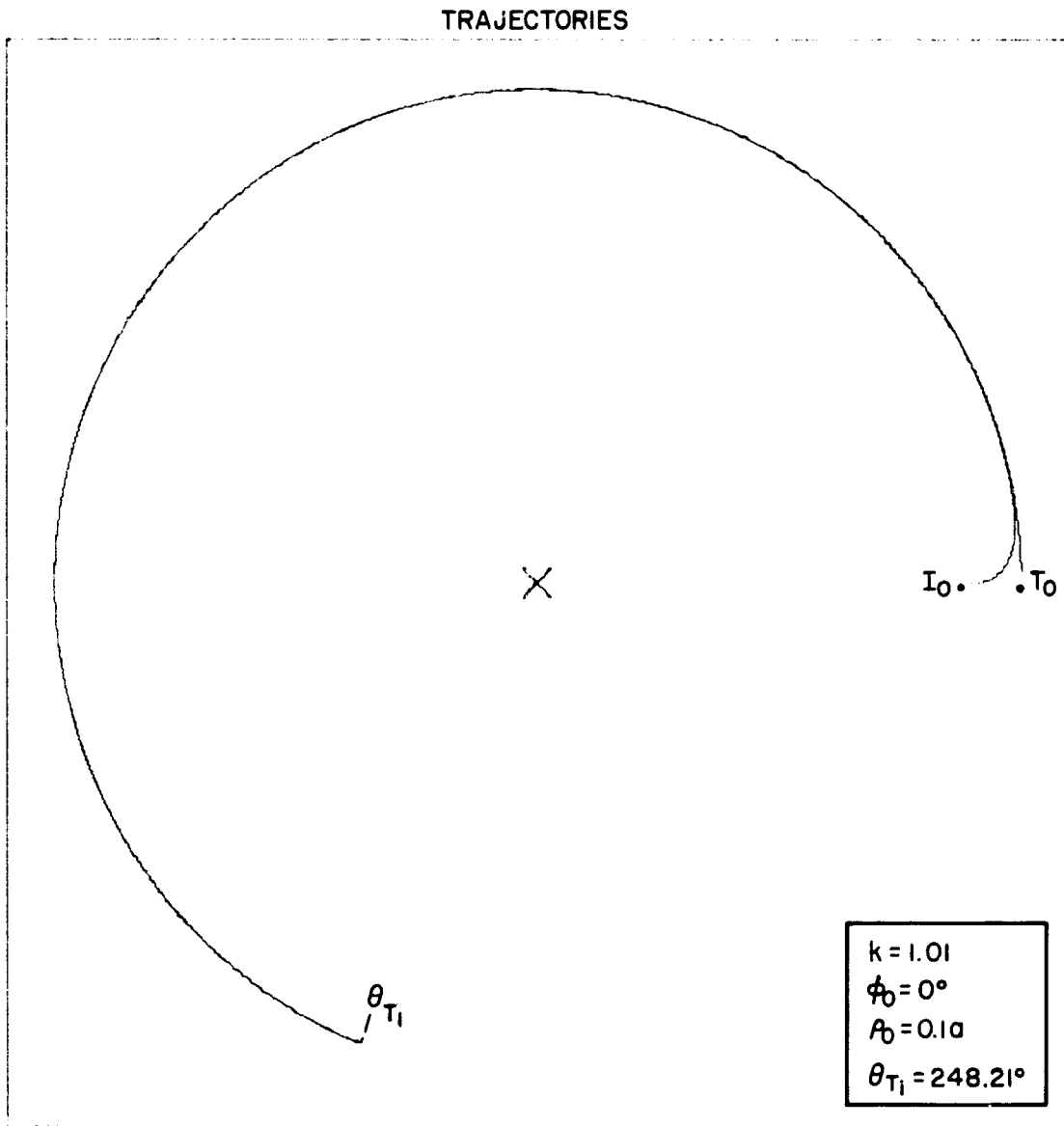
TRAJECTORIES

k = 1.01
ϕ_0 = 0°
P_0 = 0.1a
θ_{T_i} = 248.21°

Fig. V.1(a).   Trajectories for the Target (T) and Interceptor (I) during the circular pursuit maneuver (for k = 1.01, φ_0 = 0°, ρ_0 = 0.1a).

100

LATERAL ACCELERATION

POSIT	COORD
A	(0°, 10.09)
B	(2.68°, 13.703)
C	(248.21°, 1.02)
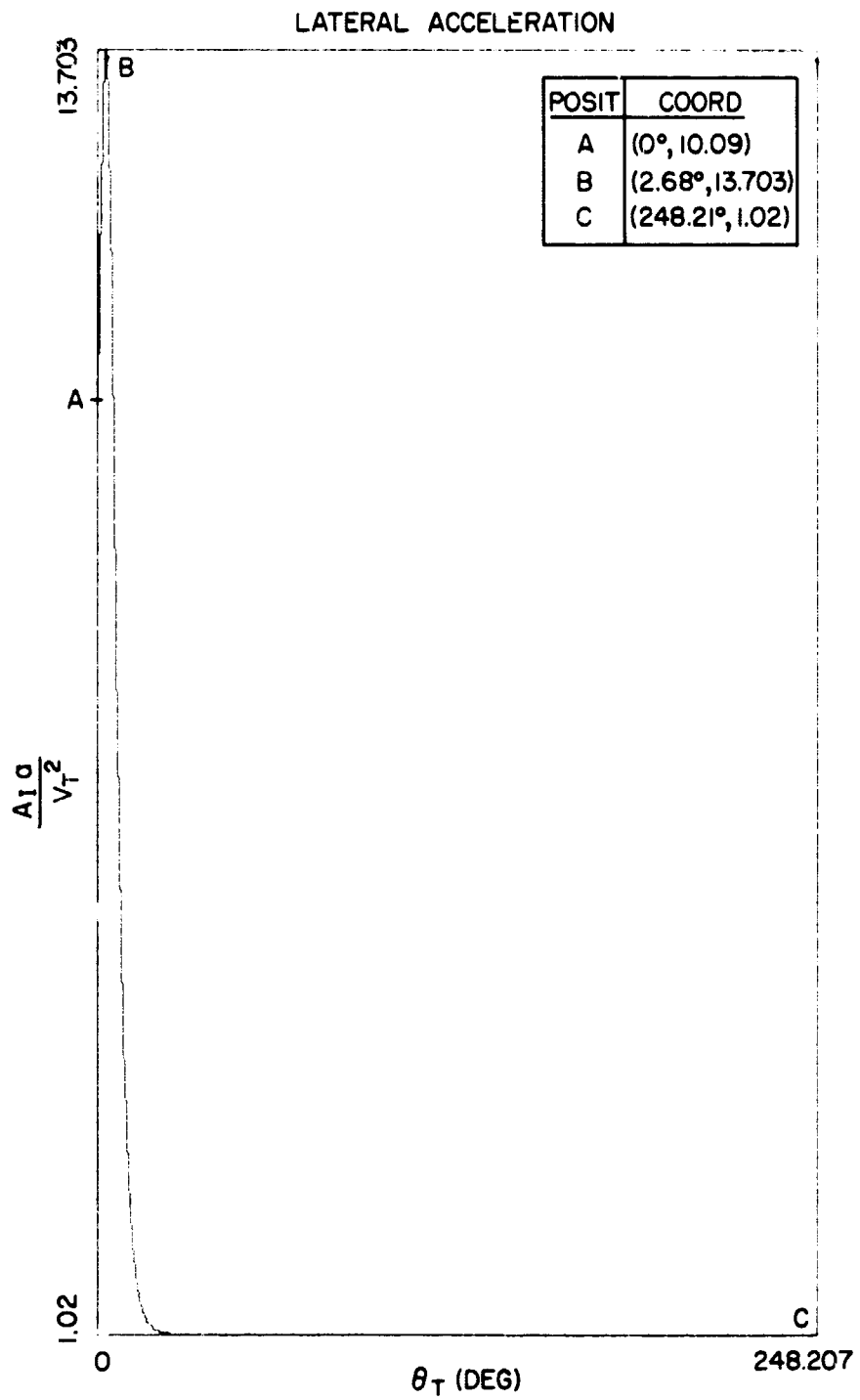
Fig. V.1(b). Dimensionless Lateral Acceleration experienced by the Interceptor during the Circular Pursuit Maneuver (for $k = 1.01$, $\varphi_0 = 0°$, $\rho_0 = 0.1a$) as a function of θ_T.

RANGE RATE

$\dot{\rho}/v_T$

θ_T (DEG)

POSIT	COORD
A	$(0°, -1.01)$
B	$(21.0°, -0.02)$
C	$(248.21°, -0.01)$

-0.01

-1.01

0

248.207
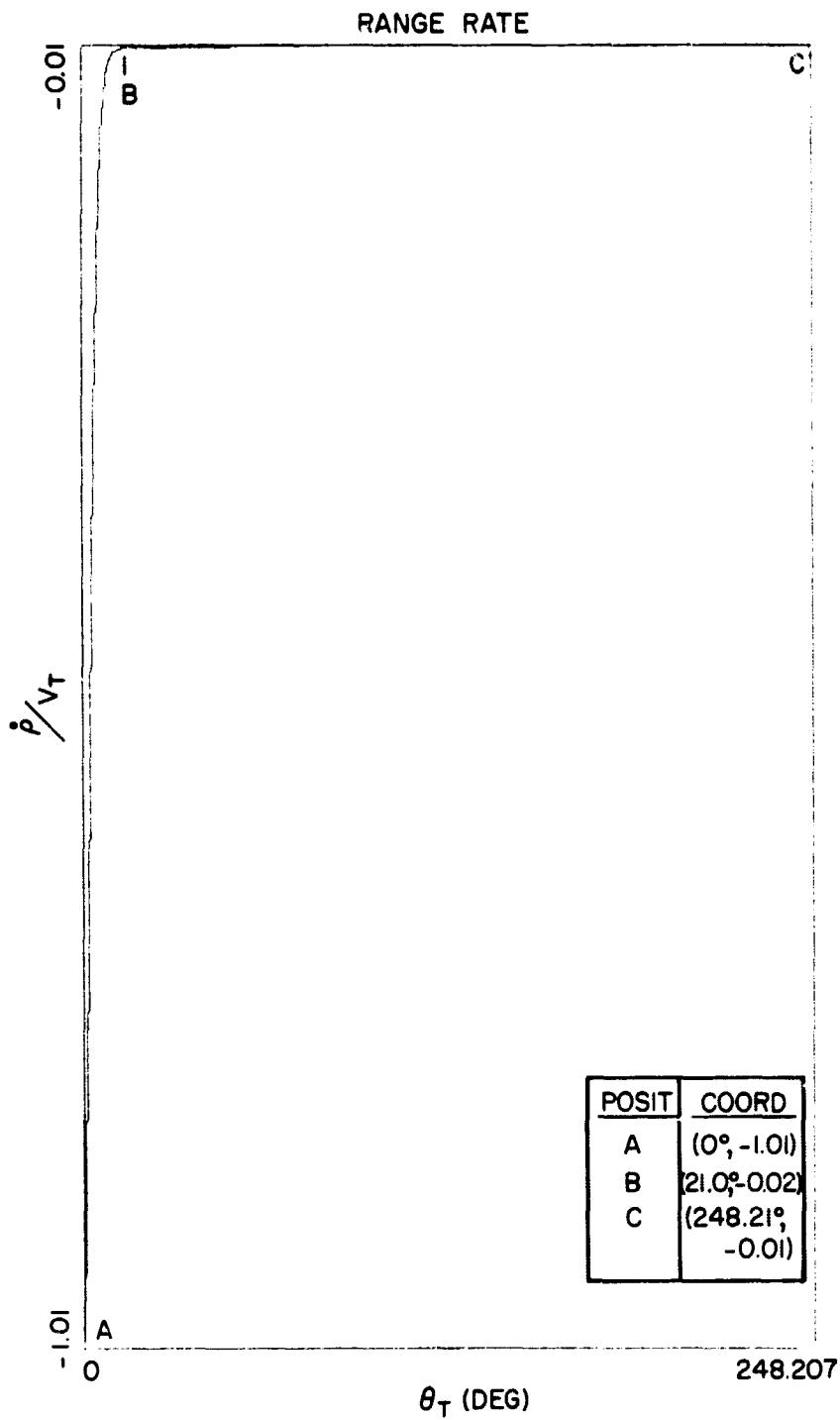
Fig. V.1(c). Dimensionless range-rate for the circular pursuit maneuver as a function of θ_T $(k = 1.01, \varphi_0 = 0°, \rho_0 = 0.1a)$.
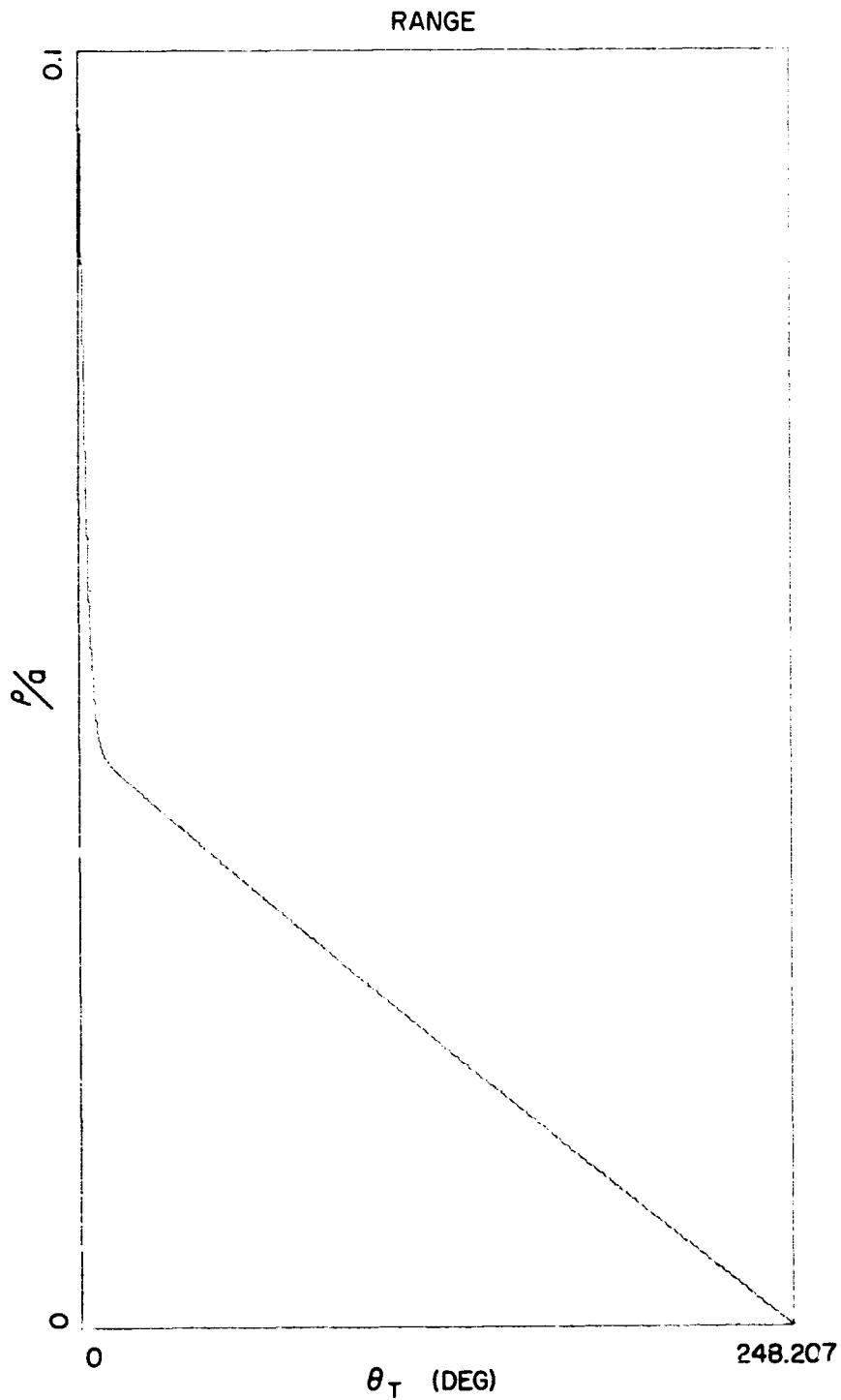
Fig. V.1(d). Dimensionless Range for the Circular Pursuit Maneuver as a function of θ_T ($k = 1.01$, $\varphi_0 = 0°$, $\rho_0 = 0.1a$).

$k = 1.05$
$\phi_0 = 0°$
$\rho_0 = a$
$\theta_{T_i} = 260.96°$

Fig. V.2(a.   Trajectories for the Target (T) and Interceptor (I) during the circular
pursuit maneuver (for $k = 1.05$, $\varphi_0 = 0°$, $\rho_0 = a$).

LATERAL ACCELERATION

POSIT	COORD
A	(48°.56, 2.893)
B	(260.96° 1.105)

$\frac{A_i a}{V_T^2}$

θ_T (DEG)
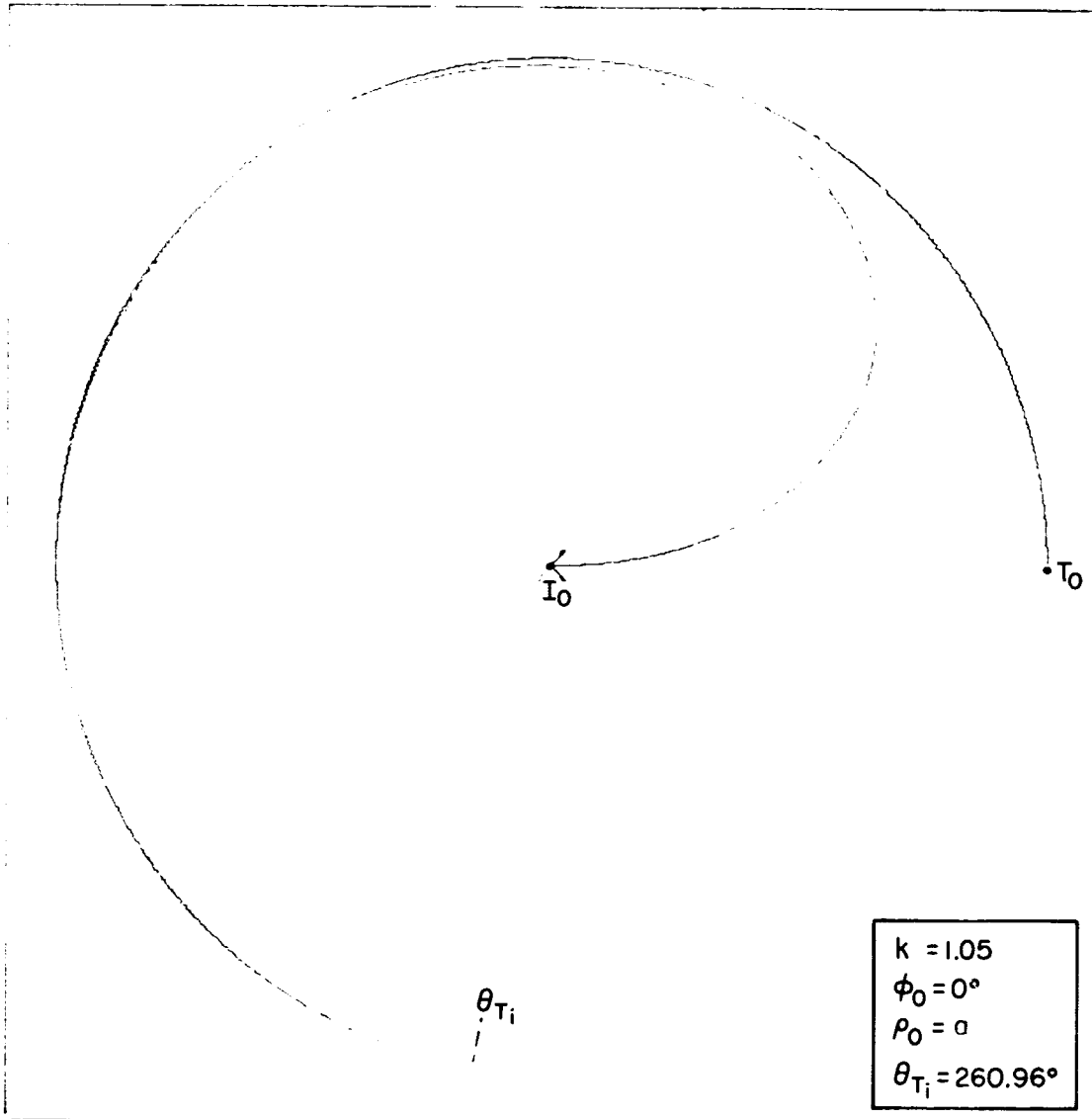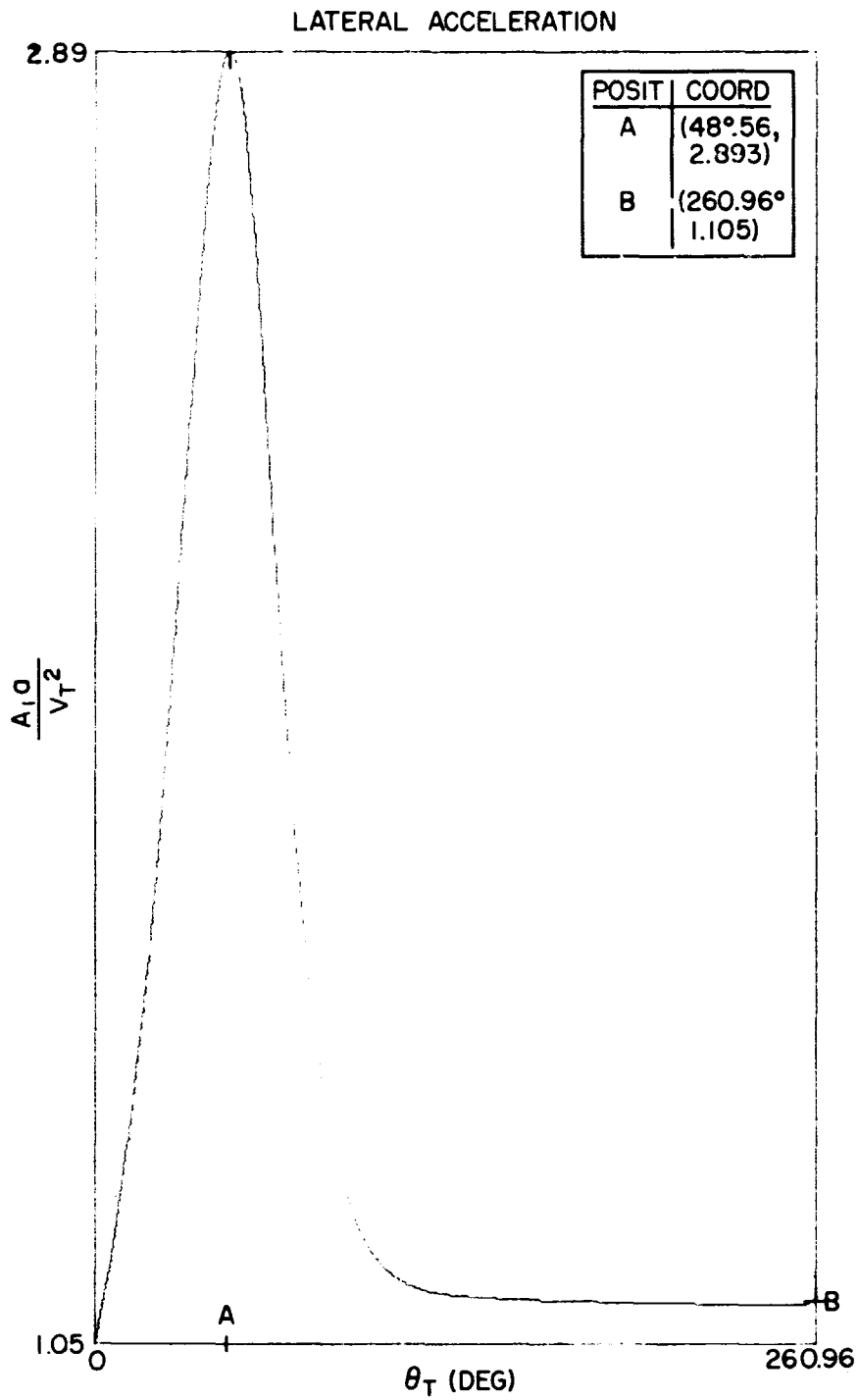
Fig. V.2(b). Dimensionless Lateral Acceleration experienced by the Interceptor during the Circular Pursuit Maneuver (for k = 1.05, $\varphi_0 = 0^\circ$, ρ_0 = a) as a function of θ_T.
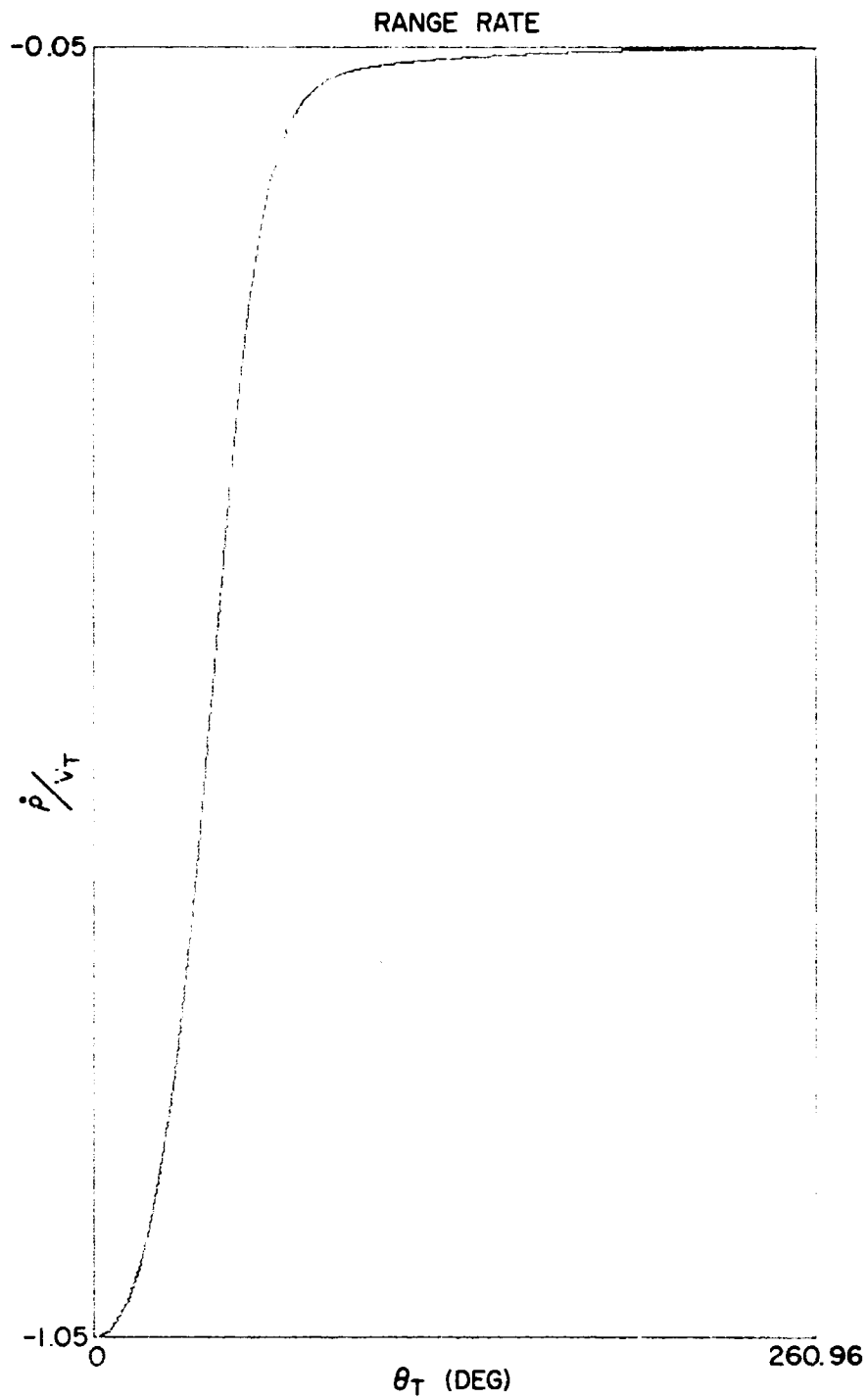
Fig. V.2(c). Dimensionless Range-Rate for the Circular Pursuit Maneuver as a function of θ_T (k= 1.05, φ_0 = 0°, ρ_0 = a).
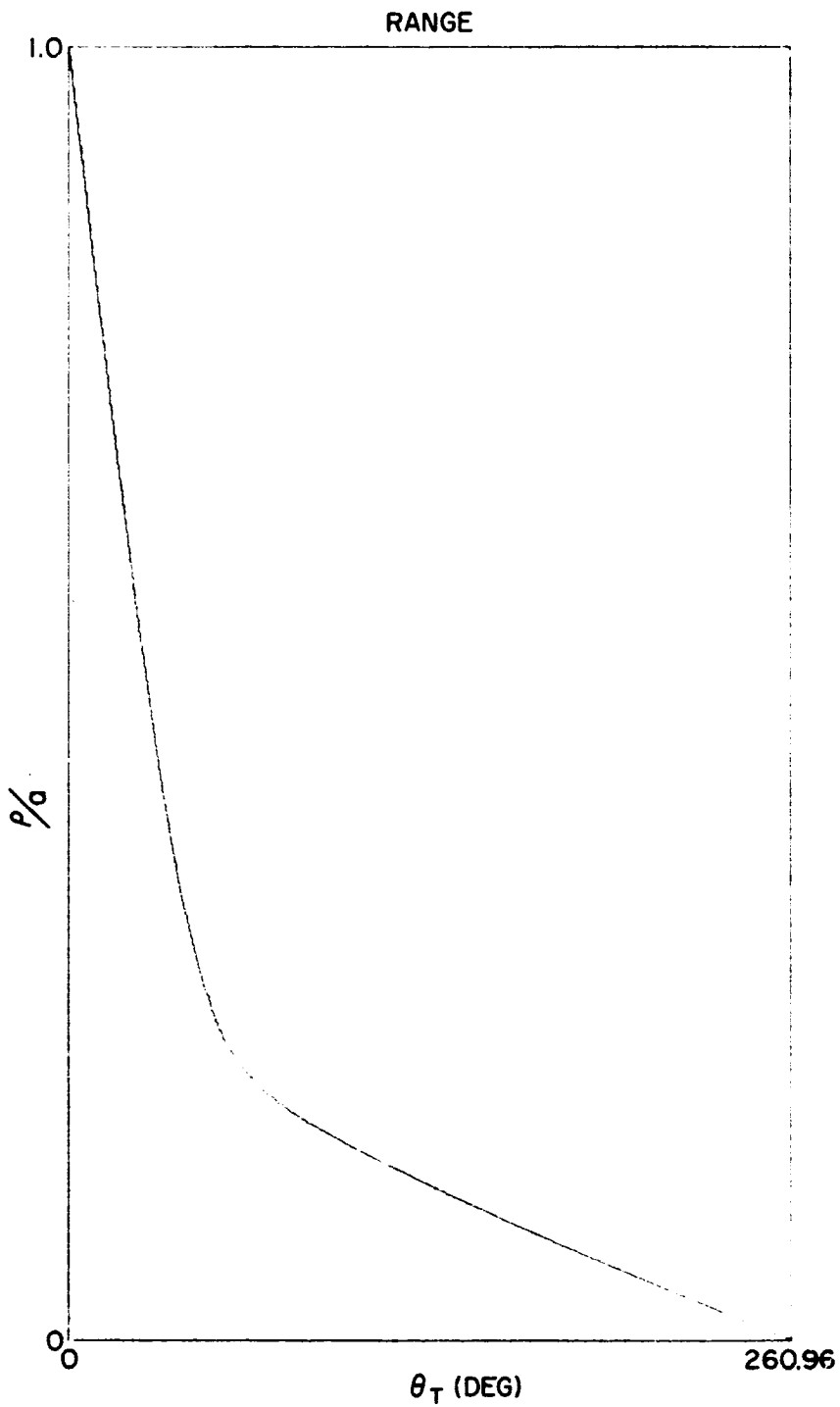
RANGE

Fig. V.2(d). Dimensionless Range for the Circular Pursuit Maneuver as a function of θ_T ($k = 1.05$, $\varphi_0 = 0°$, $\rho_0 = a$).

107
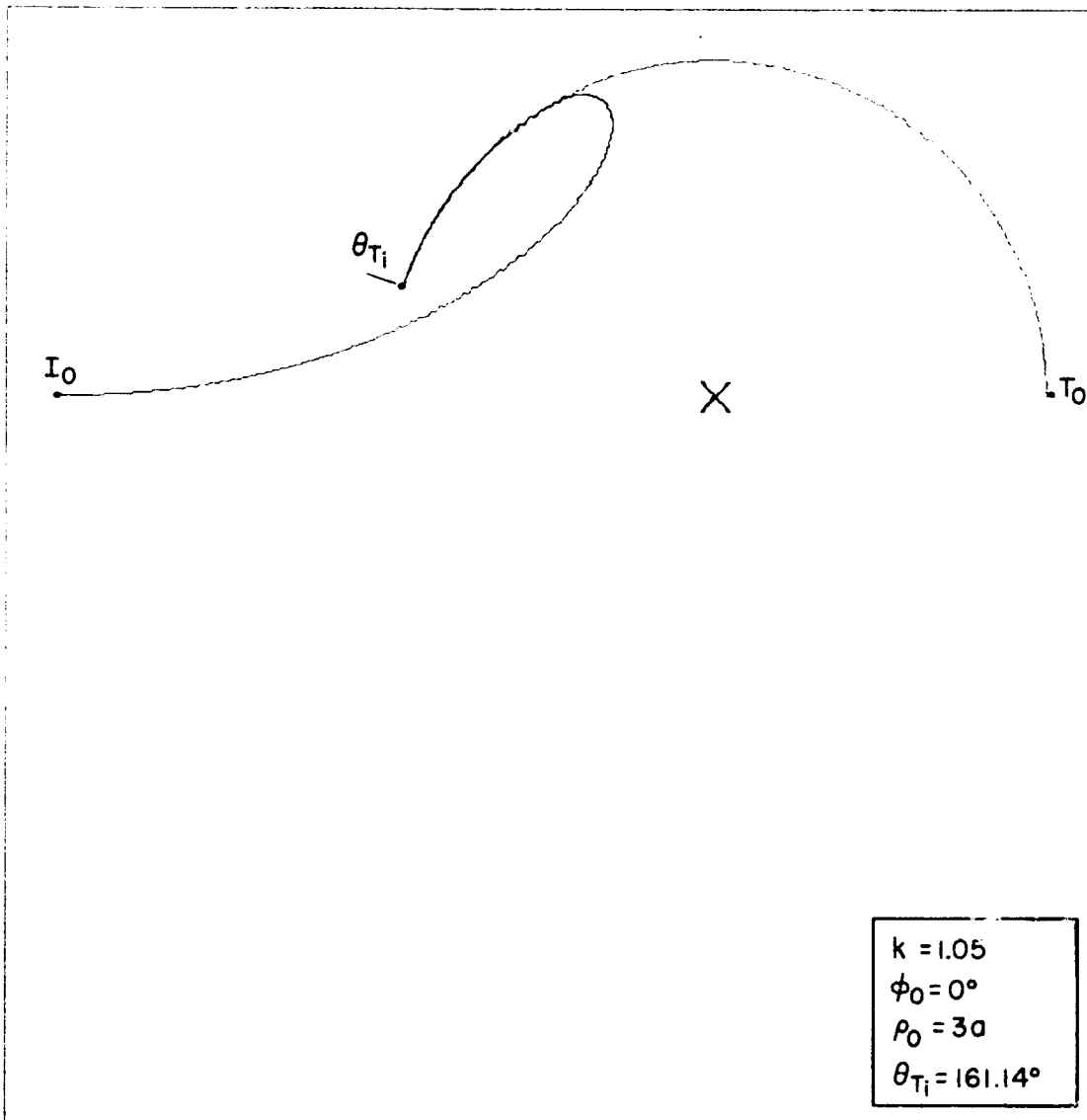
Fig. V.3(a). Trajectories for the Target (T) and Interceptor (I) during the circular pursuit maneuver (for $k = 1.05$, $\varphi_0 = 0°$, $\rho_0 = 3a$).

Figure annotations: θ_{T_i}; I_0; T_0; X

$k = 1.05$
$\phi_0 = 0°$
$\rho_0 = 3a$
$\theta_{T_i} = 161.14°$

LATERAL ACCELERATION

POSIT	COORD
A	(113°.24, 15.9)
B	(161.14°, 1.105)

$\dfrac{A_I a}{V_T^2}$

θ_T (DEG)

Fig. V.3(b). Dimensionless Lateral Acceleration experienced by the Interceptor during the Circular Pursuit Maneuver (for $k = 1.05$, $\varphi_0 = 0°$, $\rho_0 = 3a$) as a function of θ_T.

109

RANGE RATE

POSIT	COORD
A	(0°, -1.05)
B	(88°.63, -1.753

$\dot{\rho}/V_T$

A

B

-0.05

-1.75

0

161.14

θ_T (DEG)
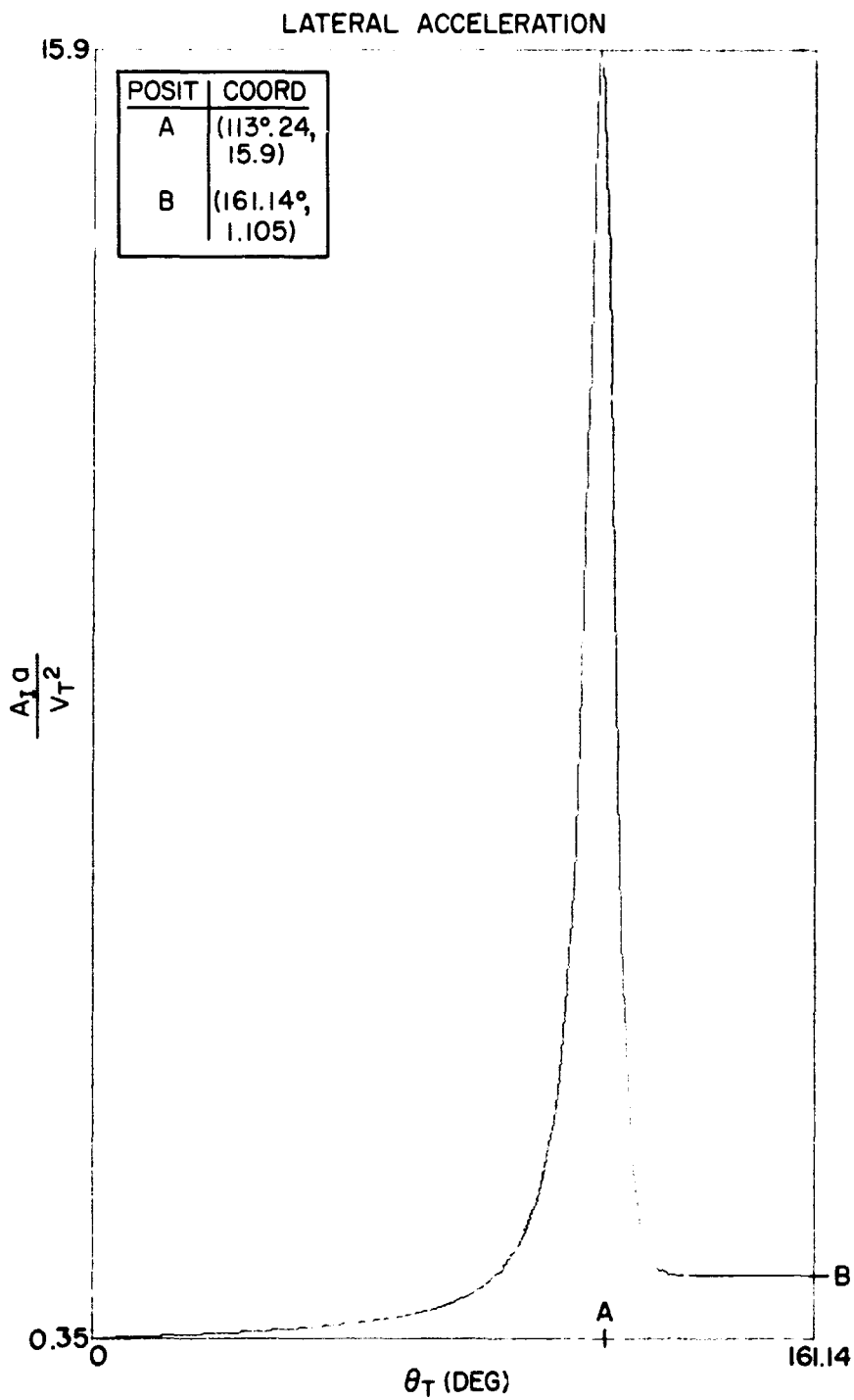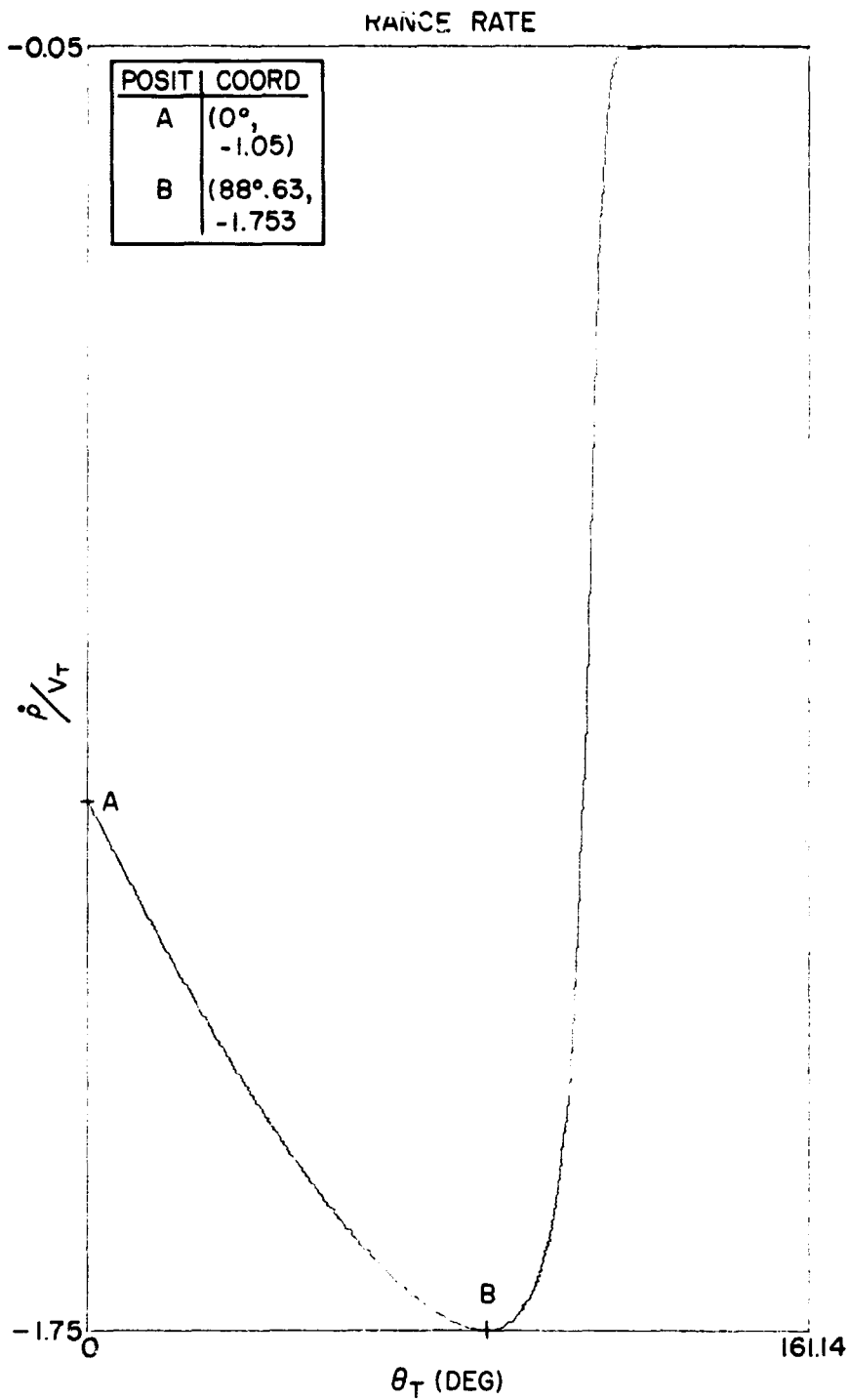
Fig. V.3(c). Dimensionless Range-Rate for the Circular Pursuit Maneuver as a function of θ_T ($k = 1.05$, $\varphi_0 = 0°$, $\rho_0 = 3a$).

110
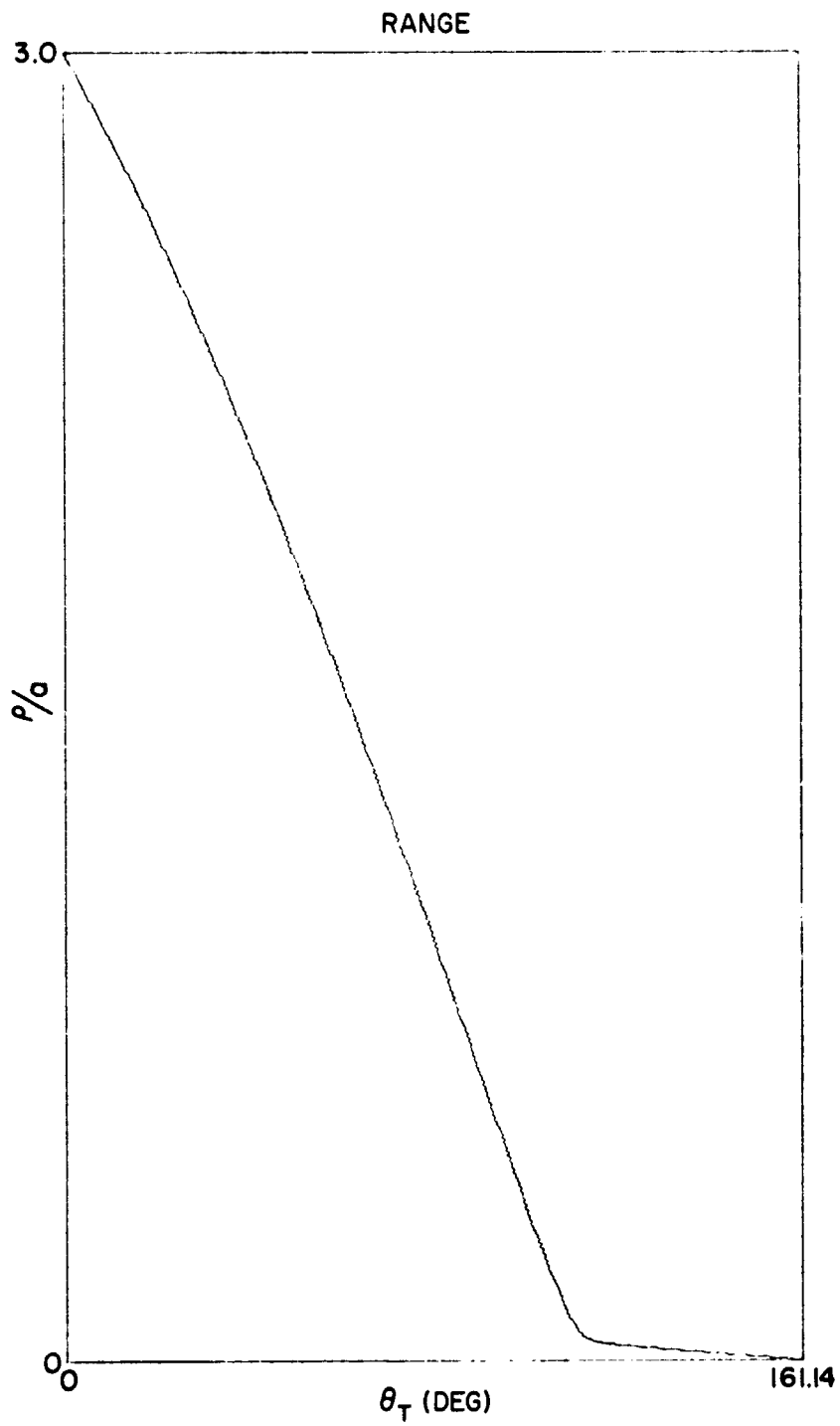
RANGE

Fig. V.3(d). Dimensionless Range for the Circular Pursuit Maneuver as a function of θ_T (k= 1.05, $\varphi_0 = 0°$, $\rho_0 = 3a$).

111
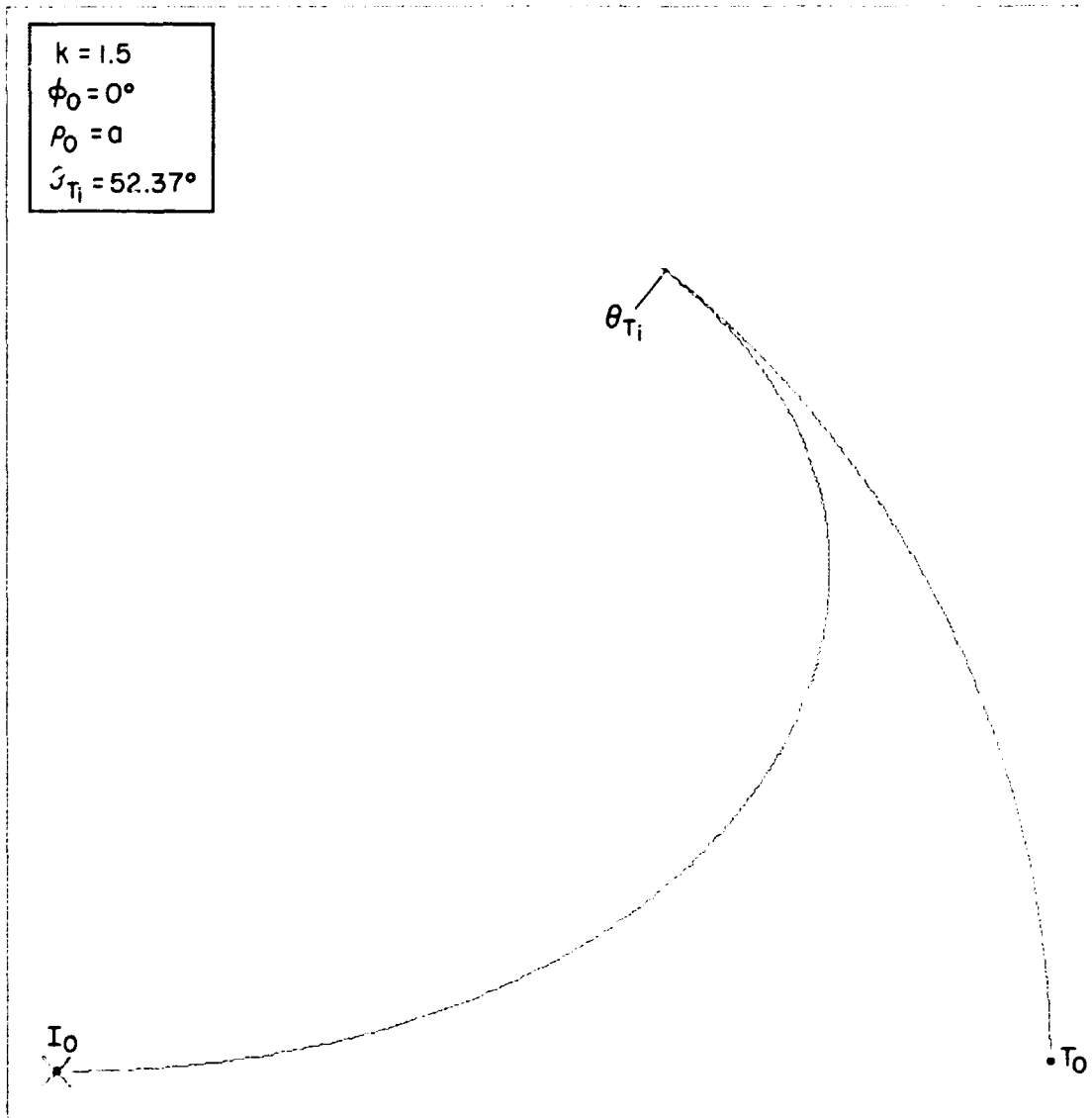
Fig. V.4(a). Trajectories for the Target (T) and Interceptor (I) during the circular pursuit maneuver (for $k = 1.50$, $\varphi_0 = 0°$, $\rho_0 = a$).
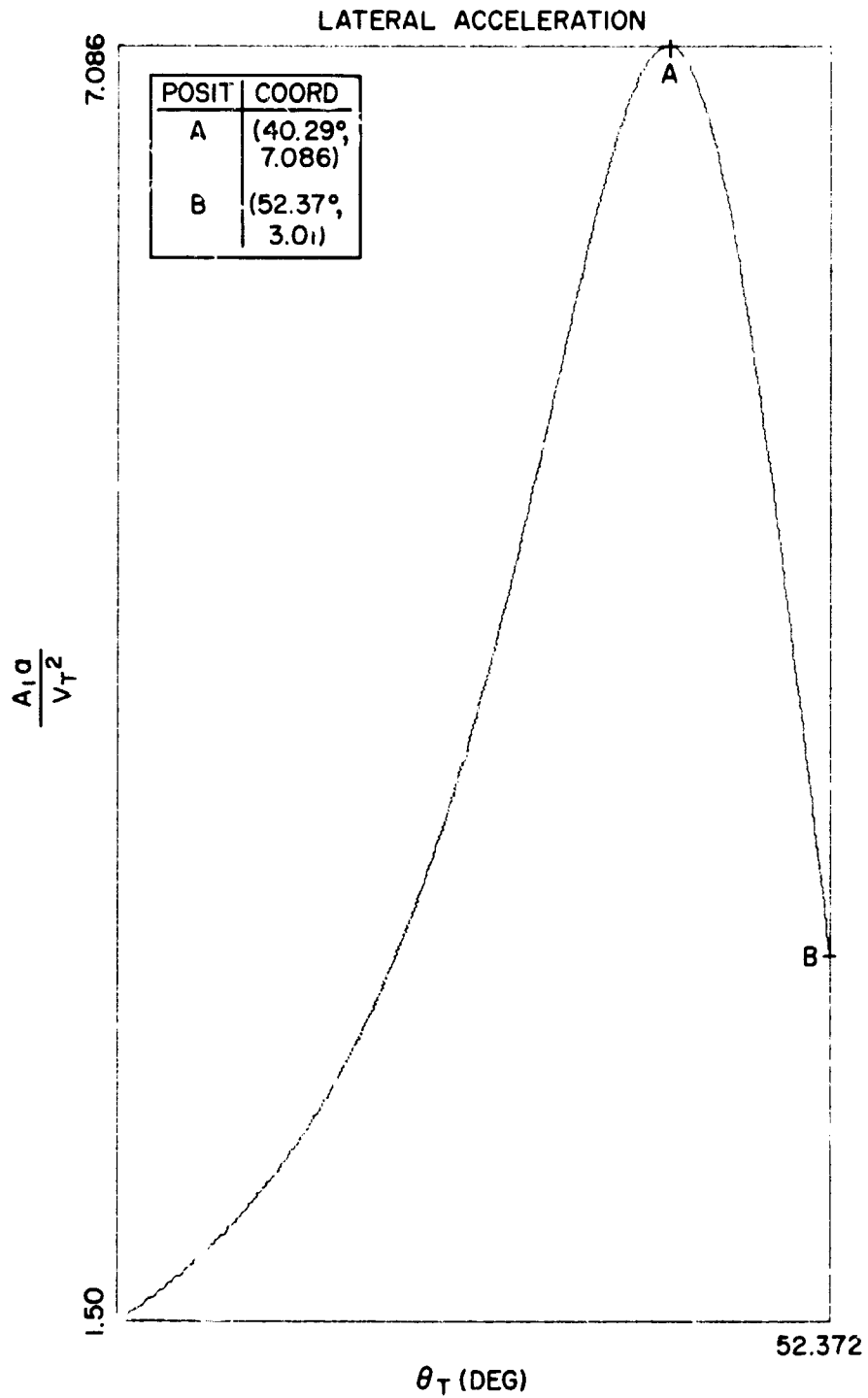
Fig. V.4(b). Dimensionless Lateral Acceleration experienced by the Interceptor during the Circular Pursuit Maneuver (for $\hat{k}$ = 1.50, φ_0 = 0°, ρ_0 = a) as a function of θ_T.
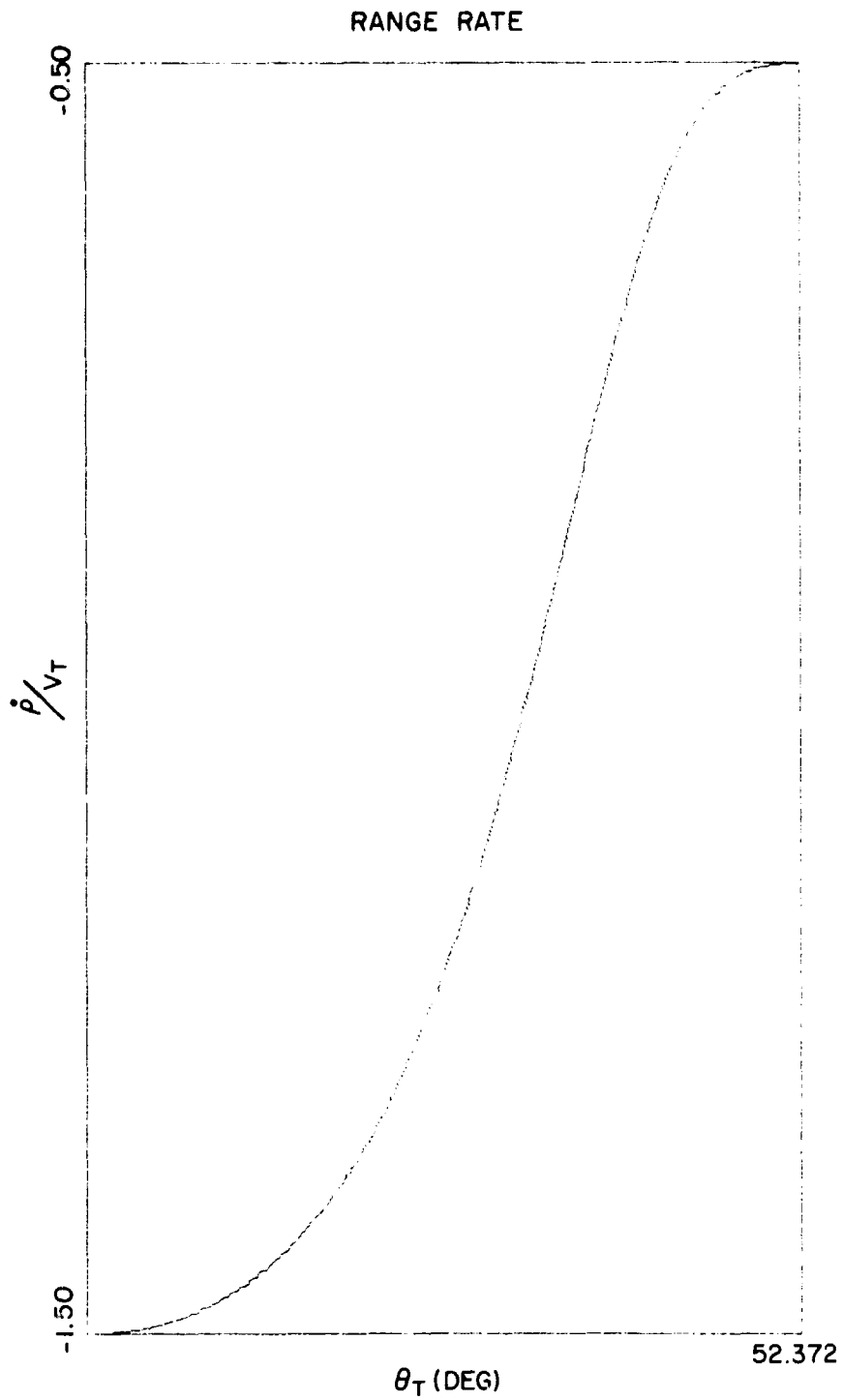
RANGE RATE

Fig. V.4(c). Dimensionless Range-Rate for the Circular Pursuit Maneuver as a function of θ_T (k = 1.50, $\varphi_0 = 0°$, ρ_0 = a).

114
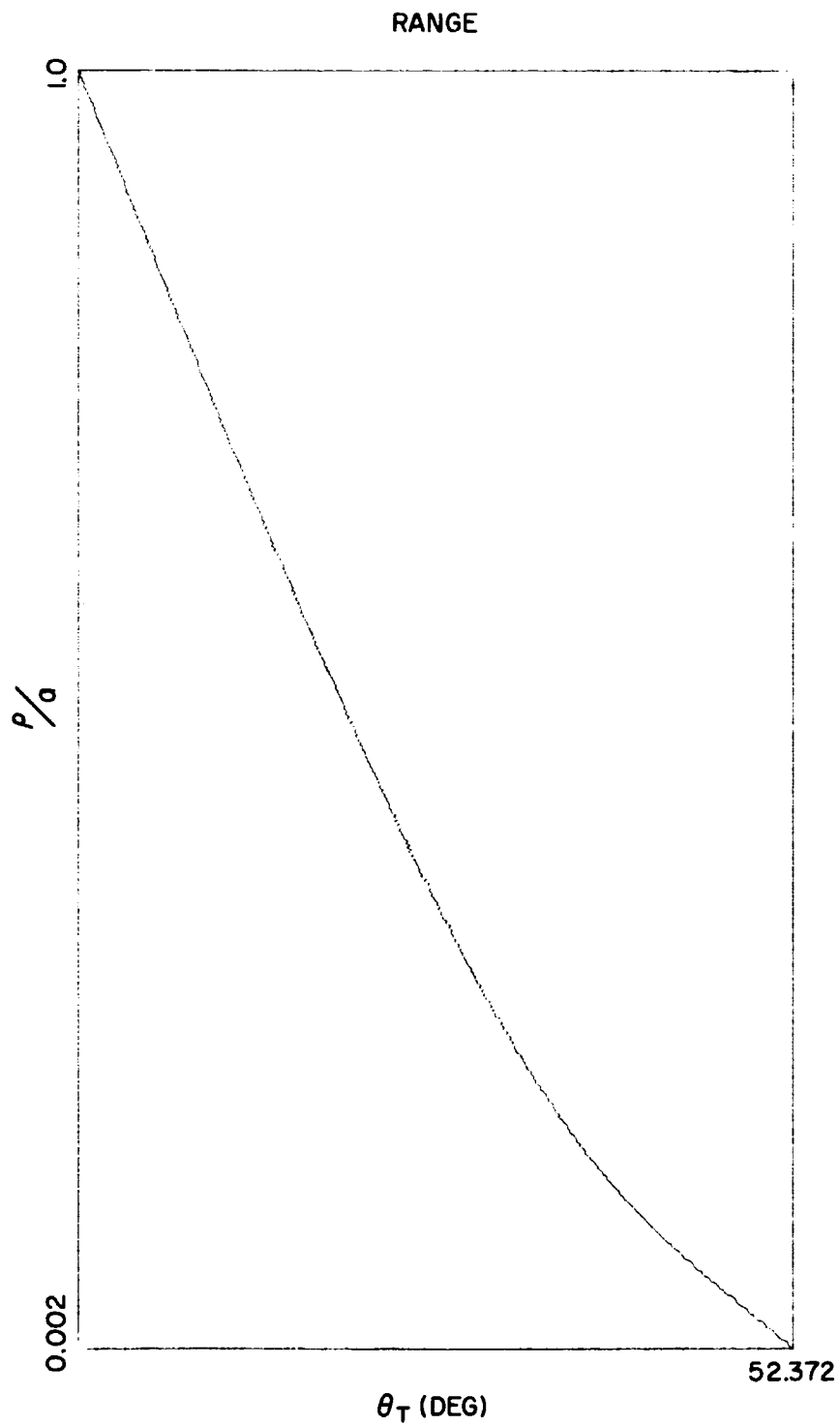
RANGE

Fig. V.4(d). Dimensionless Range for the Circular Pursuit Maneuver as a function
of θ_T (k = 1.50, $\varphi_0 = 0°$, ρ_0 = a).

115

θ_{T_i}

I_0

T_0

k = 2.0
$\phi_0 = 0°$
$\rho_0 = 6.25a$
$\theta_{T_i} = 133.39°$
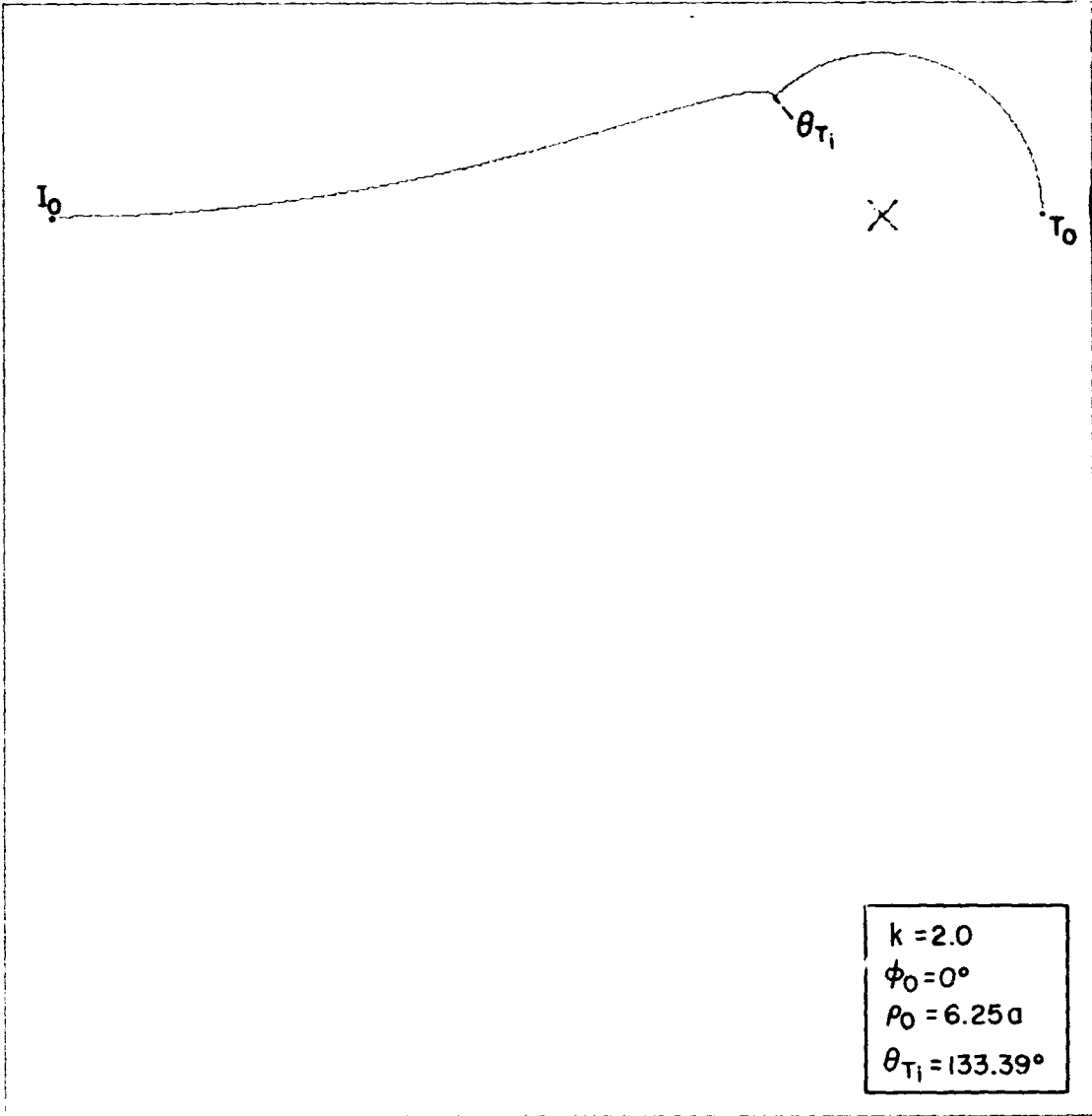
Fig. V.5(a).   Trajectories for the Target (T) and Interceptor (I) during the circular
pursuit maneuver (for k = 2.00, $\varphi_0 = 0°$, $\rho_0 = 6.25a$).

116

LATERAL ACCELERATION

$\frac{A_{ID}}{V_T^2}$

0.36

-361.62

POSIT	COORD
A	(0°, 0.32)
B	(40.96°, 0.36)
C	(106.3°, 0.0)

0   θ_T(DEG)   133.392
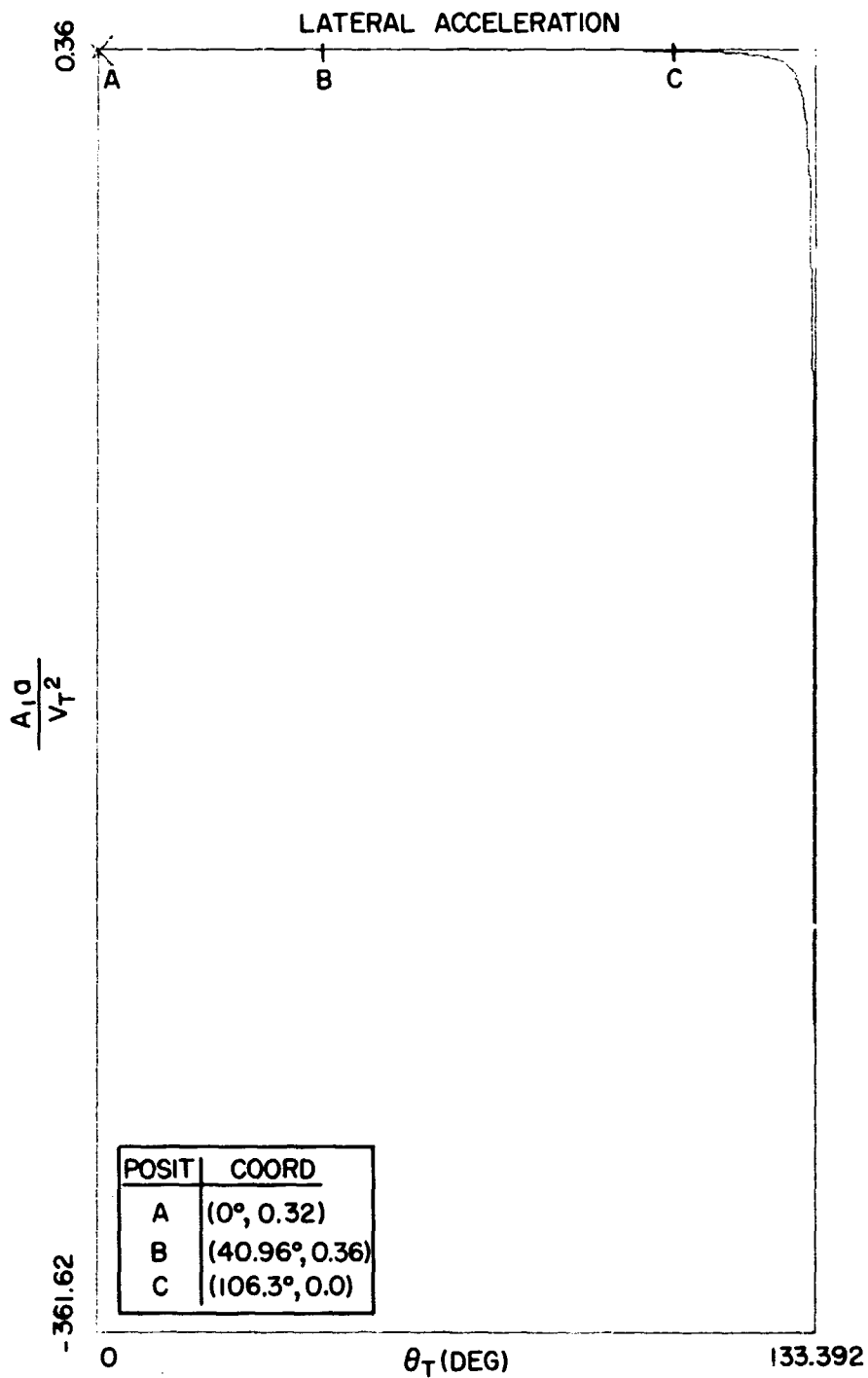
Fig. V.5(b). Dimensionless Lateral Acceleration experienced by the Interceptor during the Circular Pursuit Maneuver (for k = 2.0, φ_0 = 0°, ρ_0 = 6.25a) as a function of θ_T.

117

RANGE RATE

POSIT	COORD
A	(0°, -2.0)
B	(106.3°, -3.0)
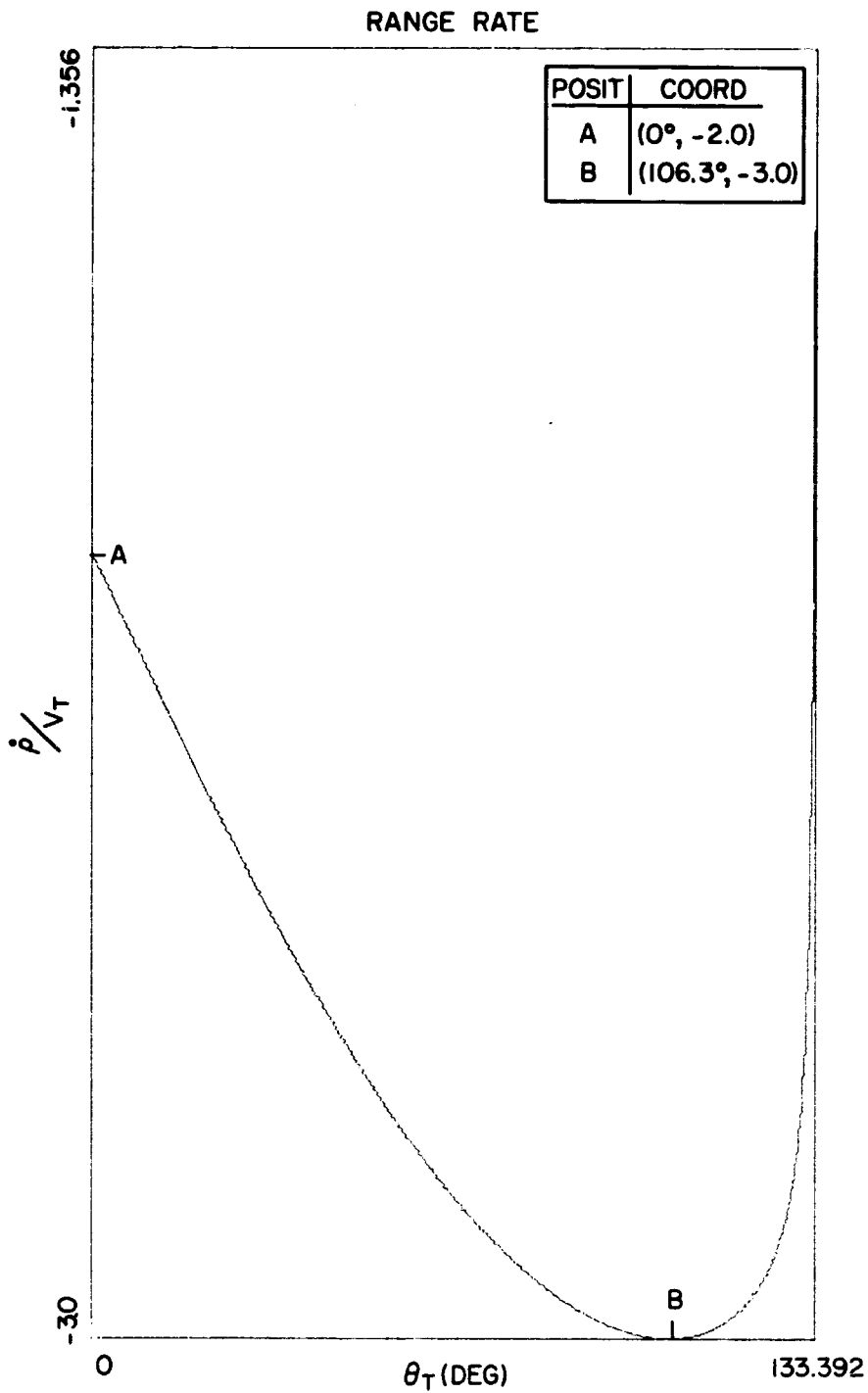
Fig. V.5(c). Dimensionless Range-Rate for the Circular Pursuit Maneuver as a function of θ_T ($k = 2.0$, $\varphi_0 = 0°$, $\rho_0 = 6.25a$).
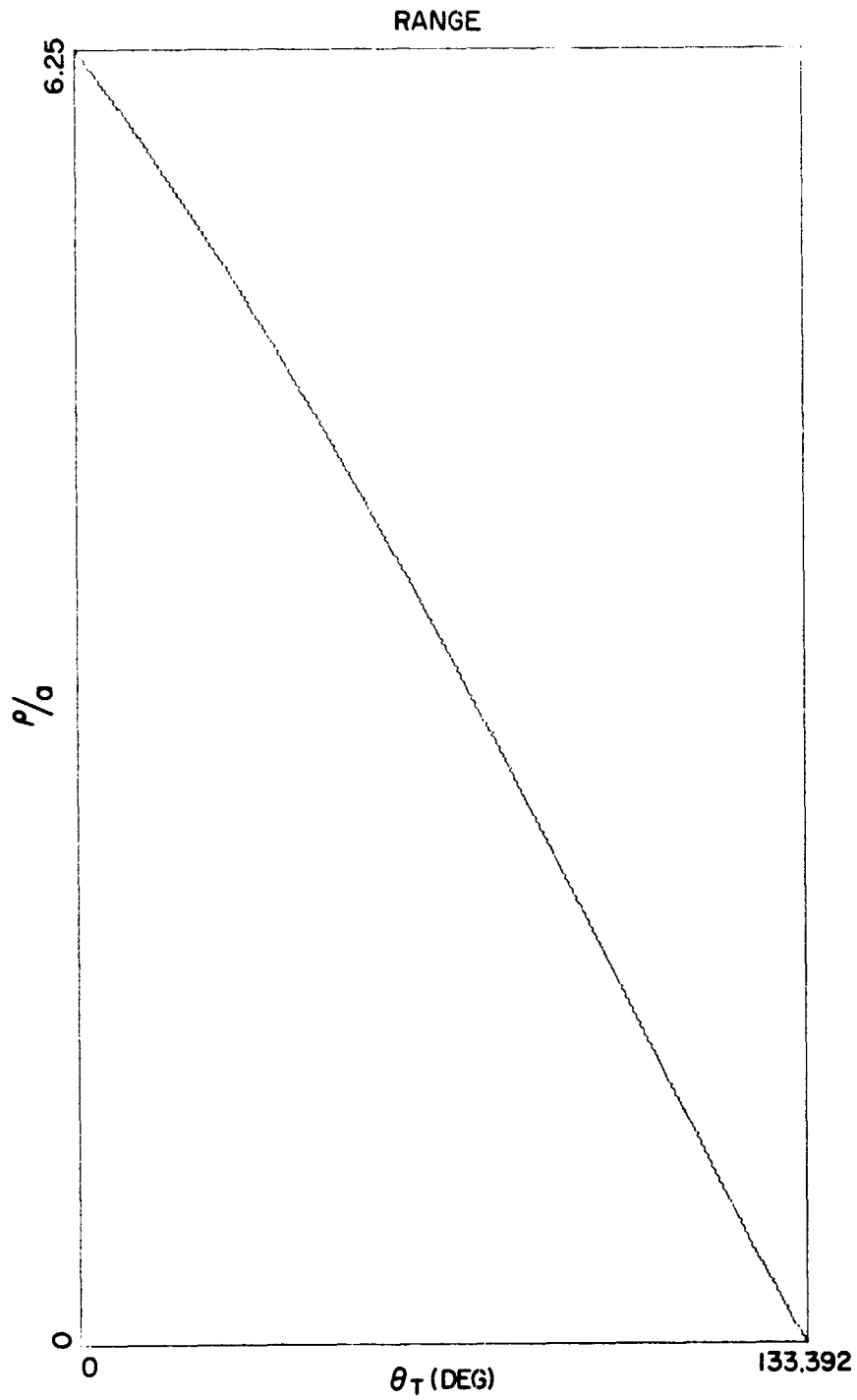
RANGE

Fig. V.5(d). Dimensionless Range for the Circular Pursuit Maneuver as a function of θ_T ($k= 2.0$, $\varphi_0 = 0°$, $\rho_0 = 6.25a$).

k = 1.5
$\phi_0 = 60°$
$\rho_0 = a$
$\theta_{T_i} = 89.52°$
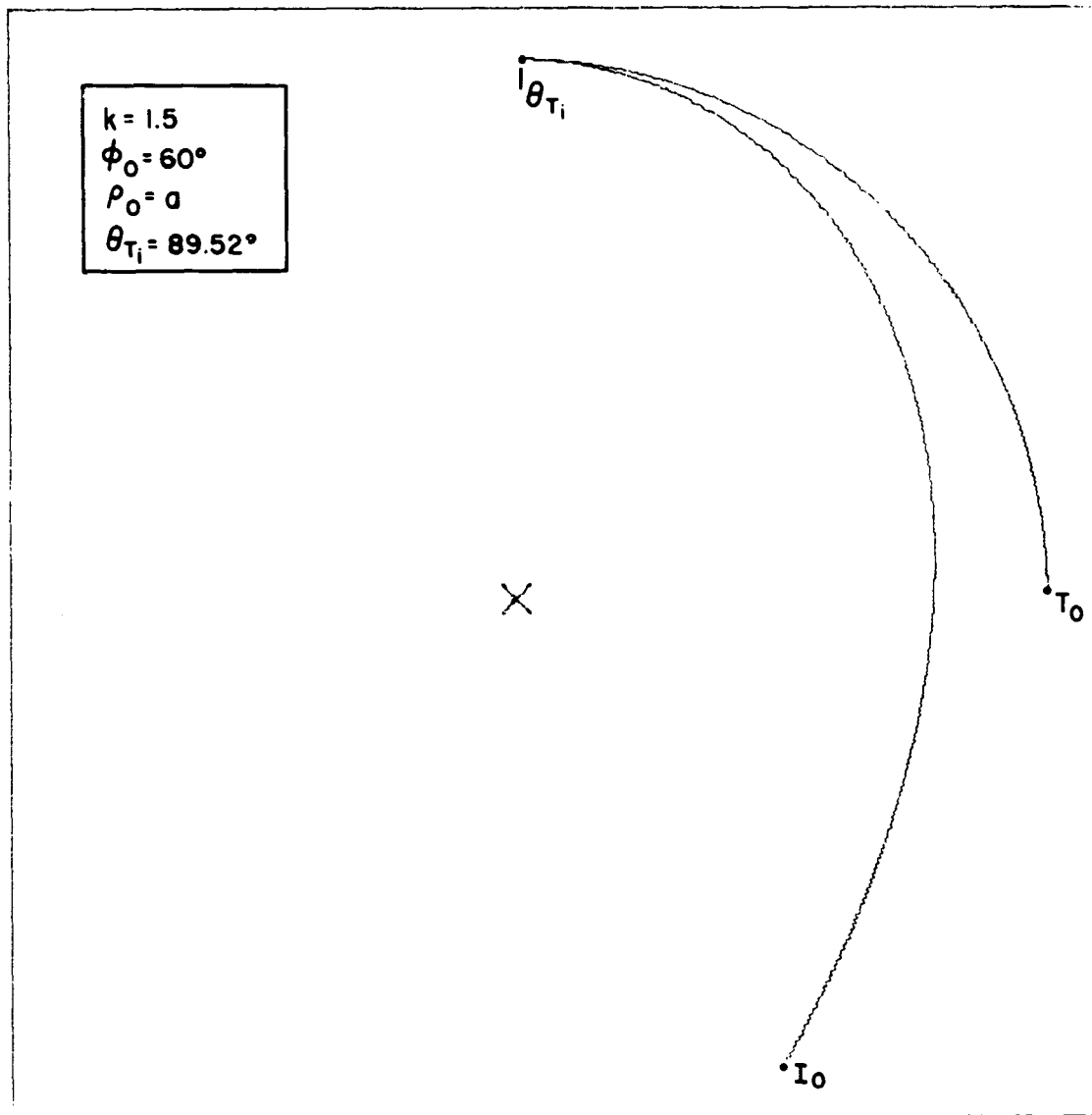
Fig. V.6(a). Trajectories for the Target (T) and Interceptor (I) during the circular pursuit maneuver (for k = 1.50, $\varphi_0 = 60°$, $\rho_0 = a$).
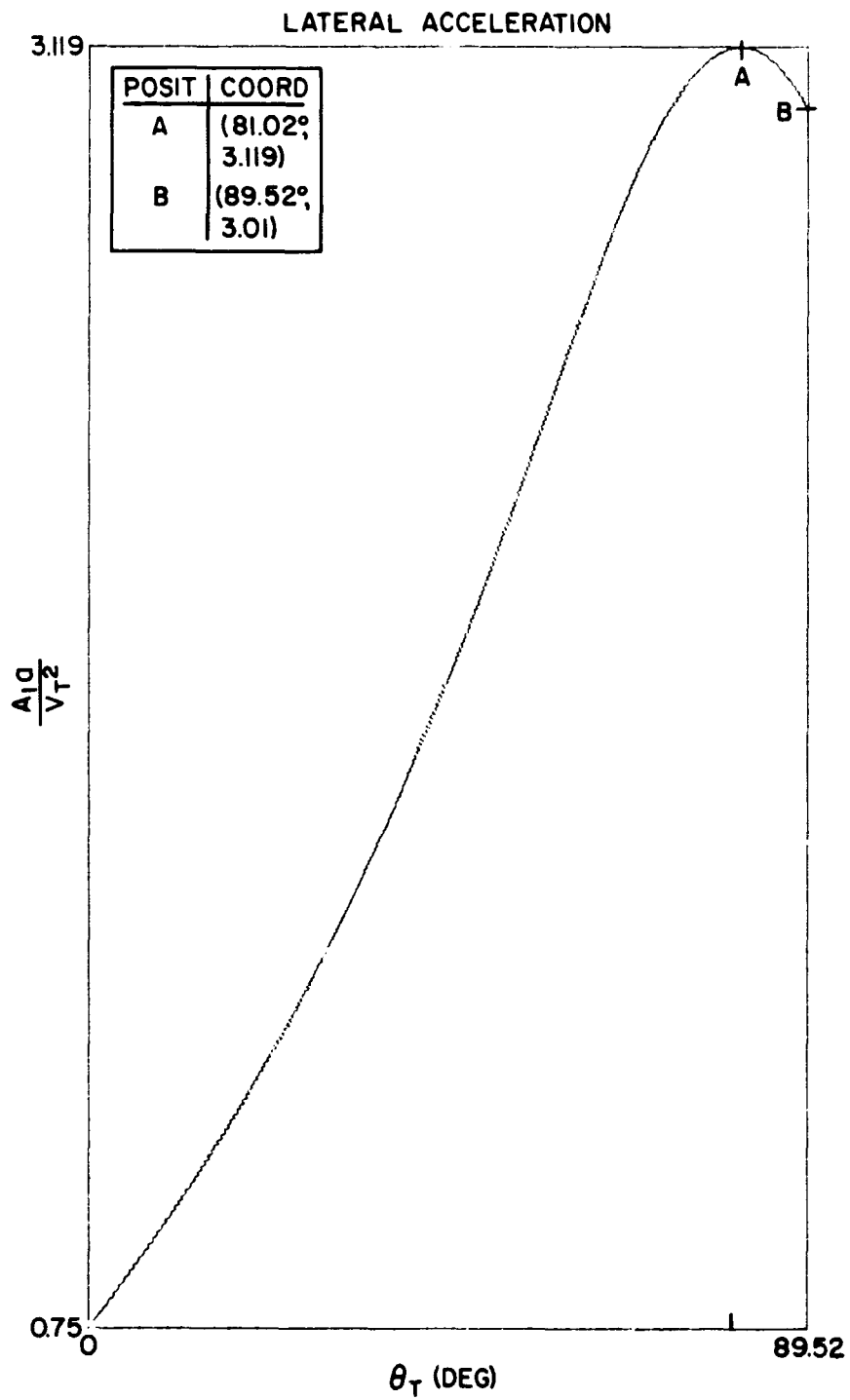
Fig. V.6(b). Dimensionless Lateral Acceleration experienced by the Interceptor during the Circular Pursuit Maneuver (for $k = 1.50$, $\varphi_0 = 60°$, $\rho_0 = a$) as a function of θ_T.

121

RANGE RATE

POSIT	COORD
A	(0°, −0.634)
B	(31.56°, −0.717)

$\dot{\rho}/V_T$

−0.5

A

B

− 0.72

O

89.52

θ_T (DEG)
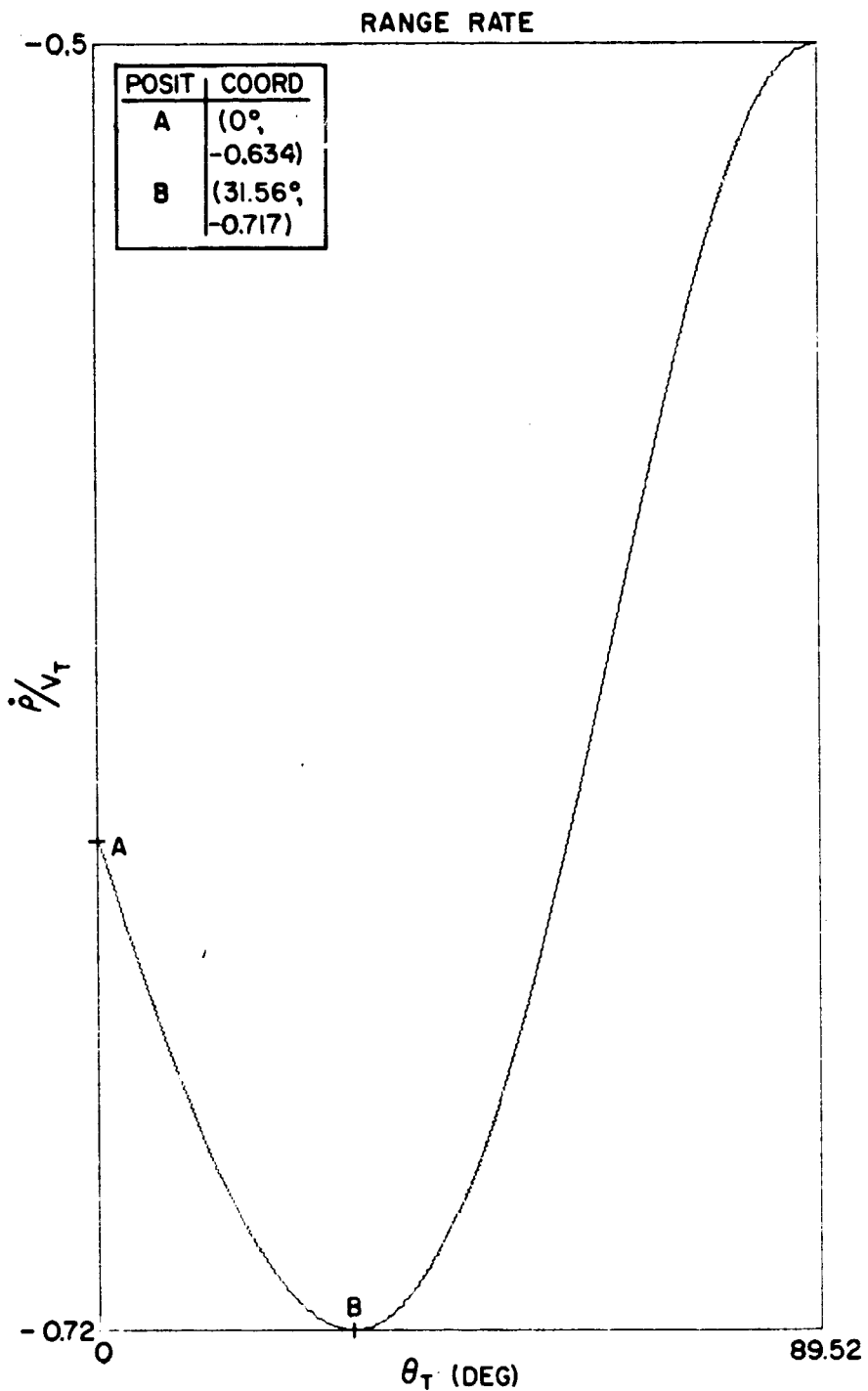
Fig. V.6(c). Dimensionless Range-Rate for the Circular Pursuit Maneuver as a function of θ_T (k= 1.50, φ_0 = 60°, ρ_0 = a).

122
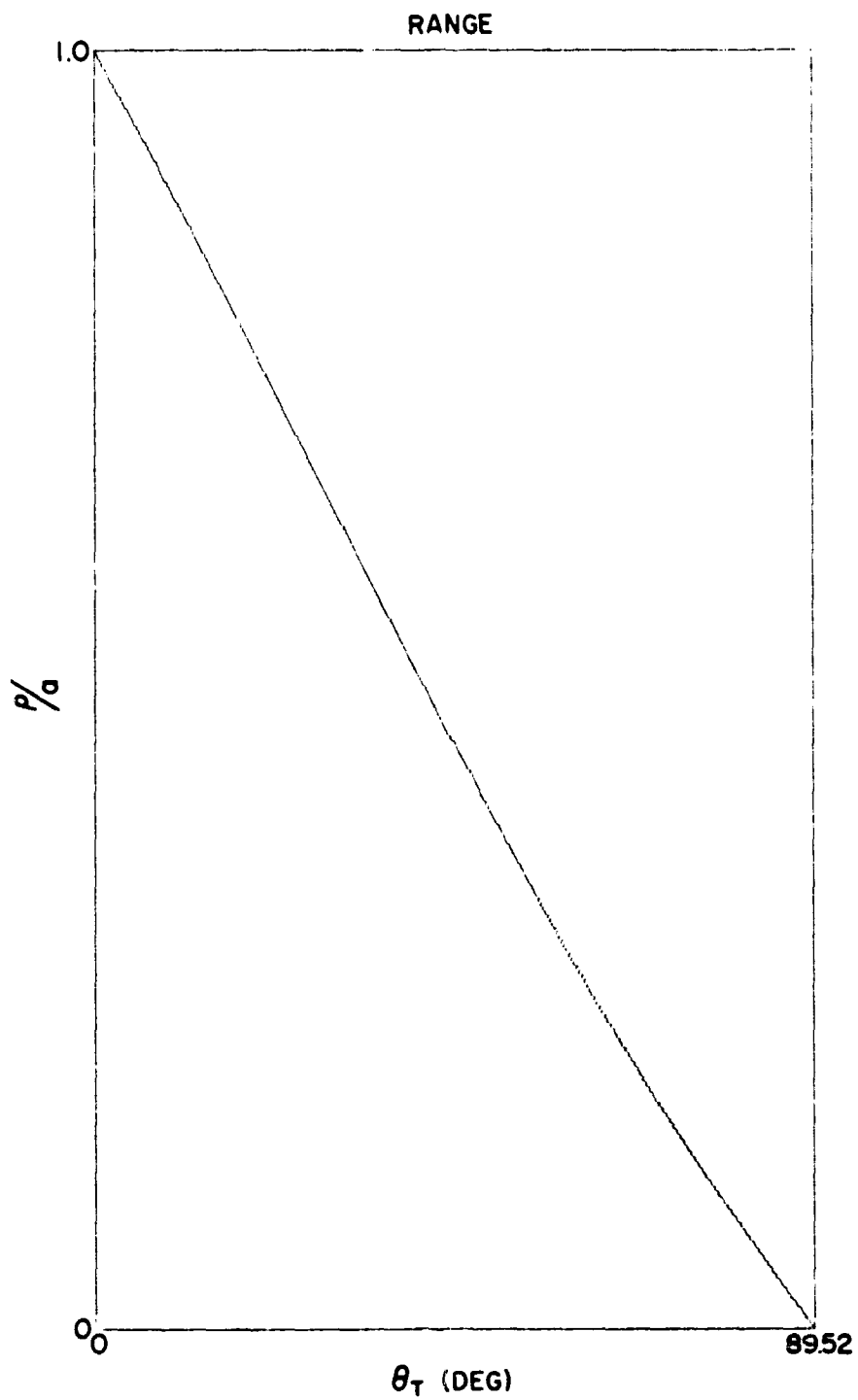
Fig. V.6(a) Dimensionless Range for the Circular Pursuit Maneuver as a function of θ_T (k = 1.50, φ_0 = 60°, ρ_0 = a).
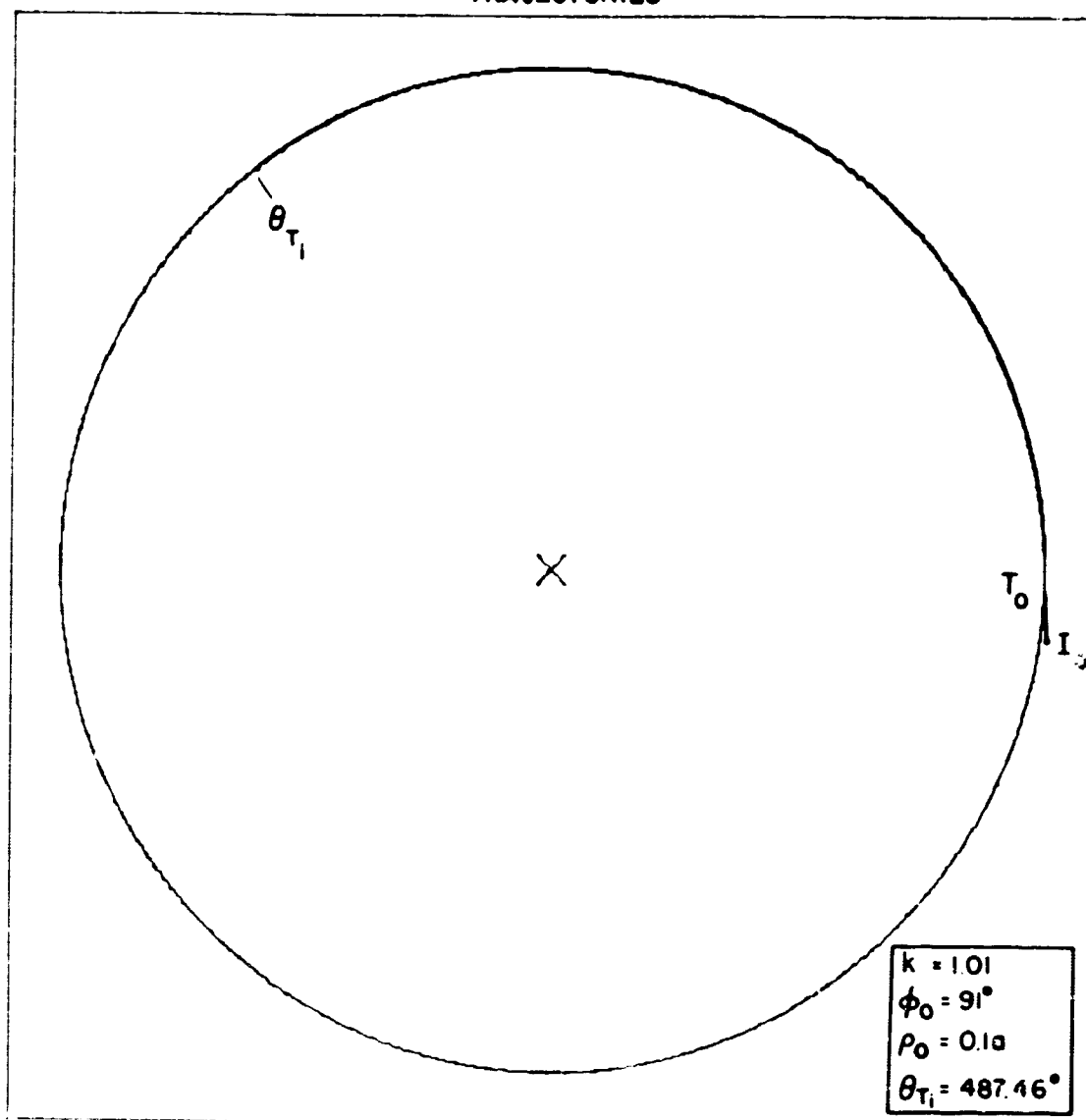
Fig. V.7(a). Trajectories for the Target (T) and Interceptor (I) during the circular pursuit maneuver (for k = 1.01, φ_0 = 91°, ρ_0 = 0.1a).
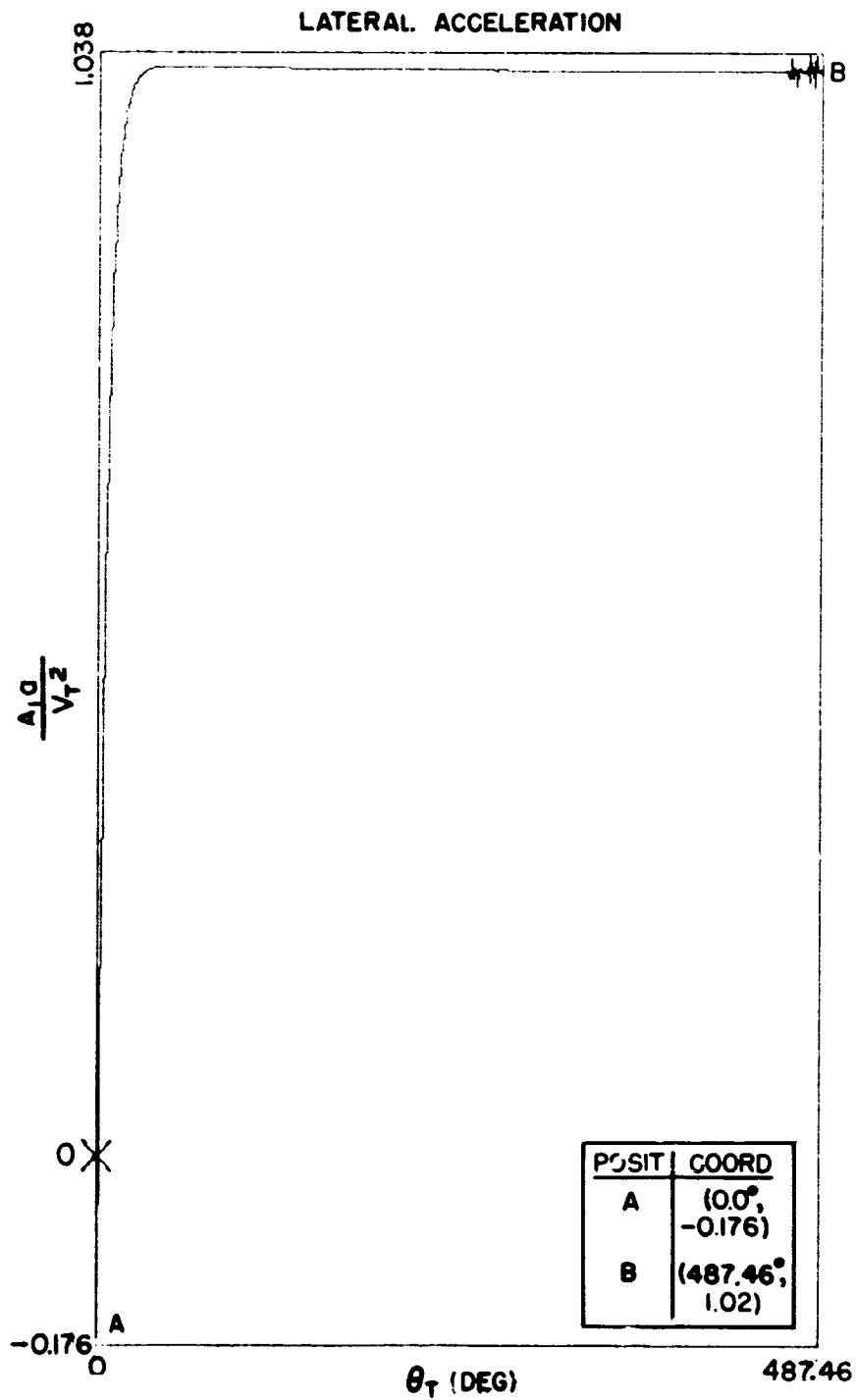
Fig. V.7(b). Dimensionless Lateral Acceleration experienced by the Interceptor during the Circular Pursuit Maneuver (for k = 1.01, ψ_0 = 91°, ρ_0 = 0.1a) as a function of θ_T.
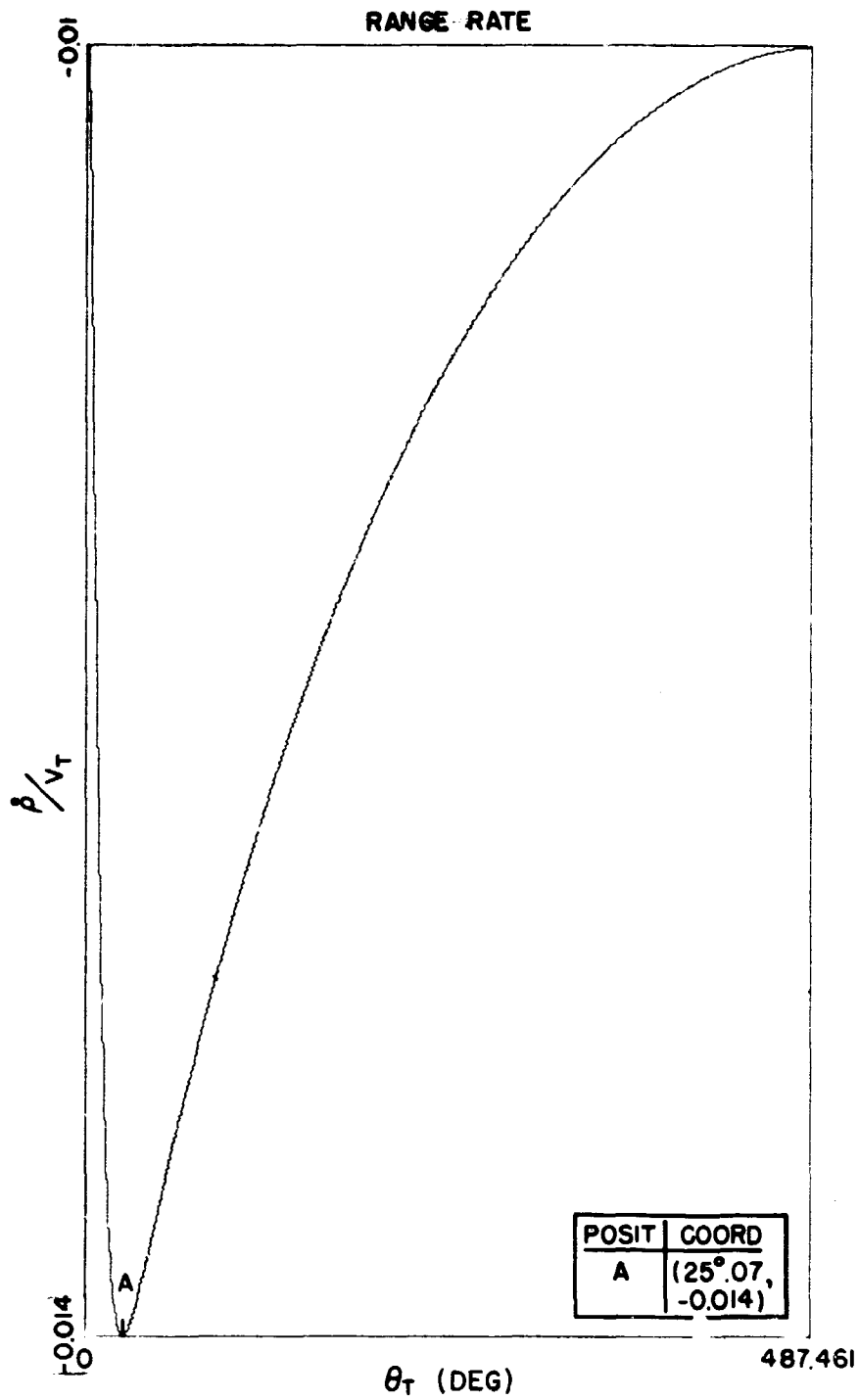
Fig. V.7(c). Dimensionless Range-Rate for the Circular Pursuit Maneuver as a
function of θ_T (k = 1.01, φ_0 = 91°, ρ_0 = 0.1a).

126
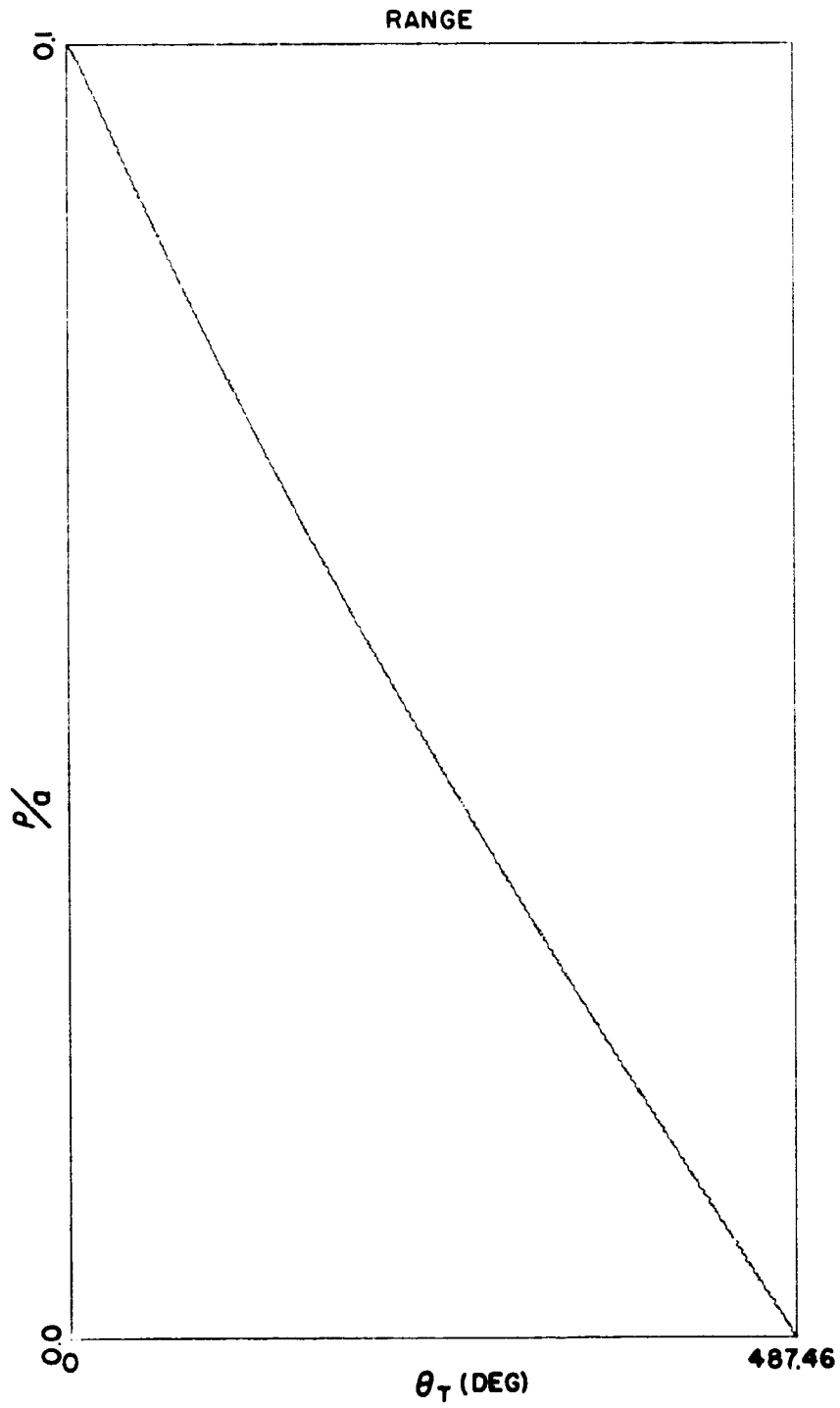
RANGE

Fig. V.7(d). Dimensionless Range for the Circular Pursuit Maneuver as a function of θ_T ($k = 1.01$, $\varphi_0 = 91°$, $\rho_0 = 0.1a$).

127
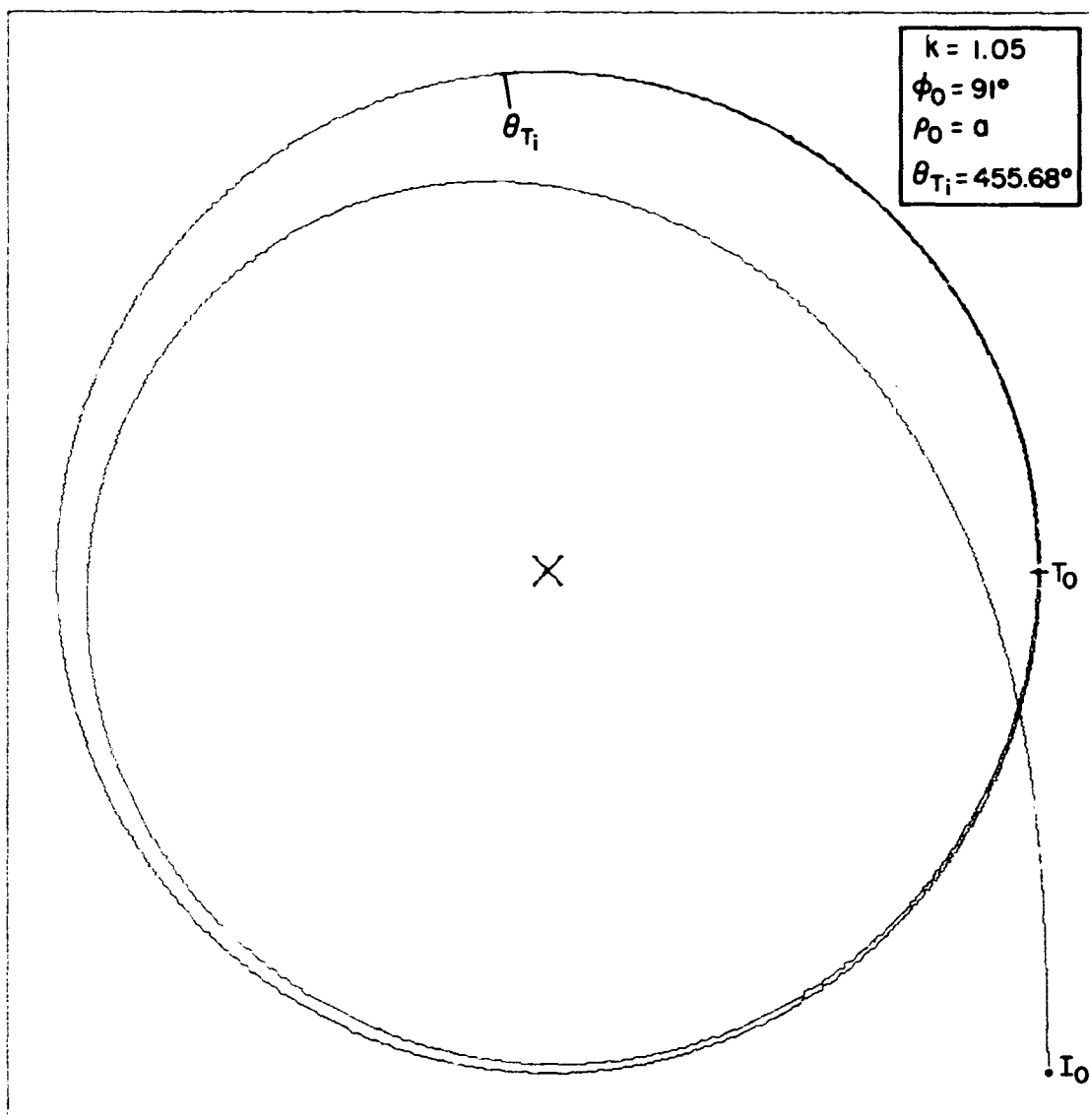
Fig. V.8(a). Trajectories for the Target (T) and Interceptor (I) during the circular
pursuit maneuver (for $k = 1.05$, $\varphi_0 = 91°$, $\rho_0 = a$).
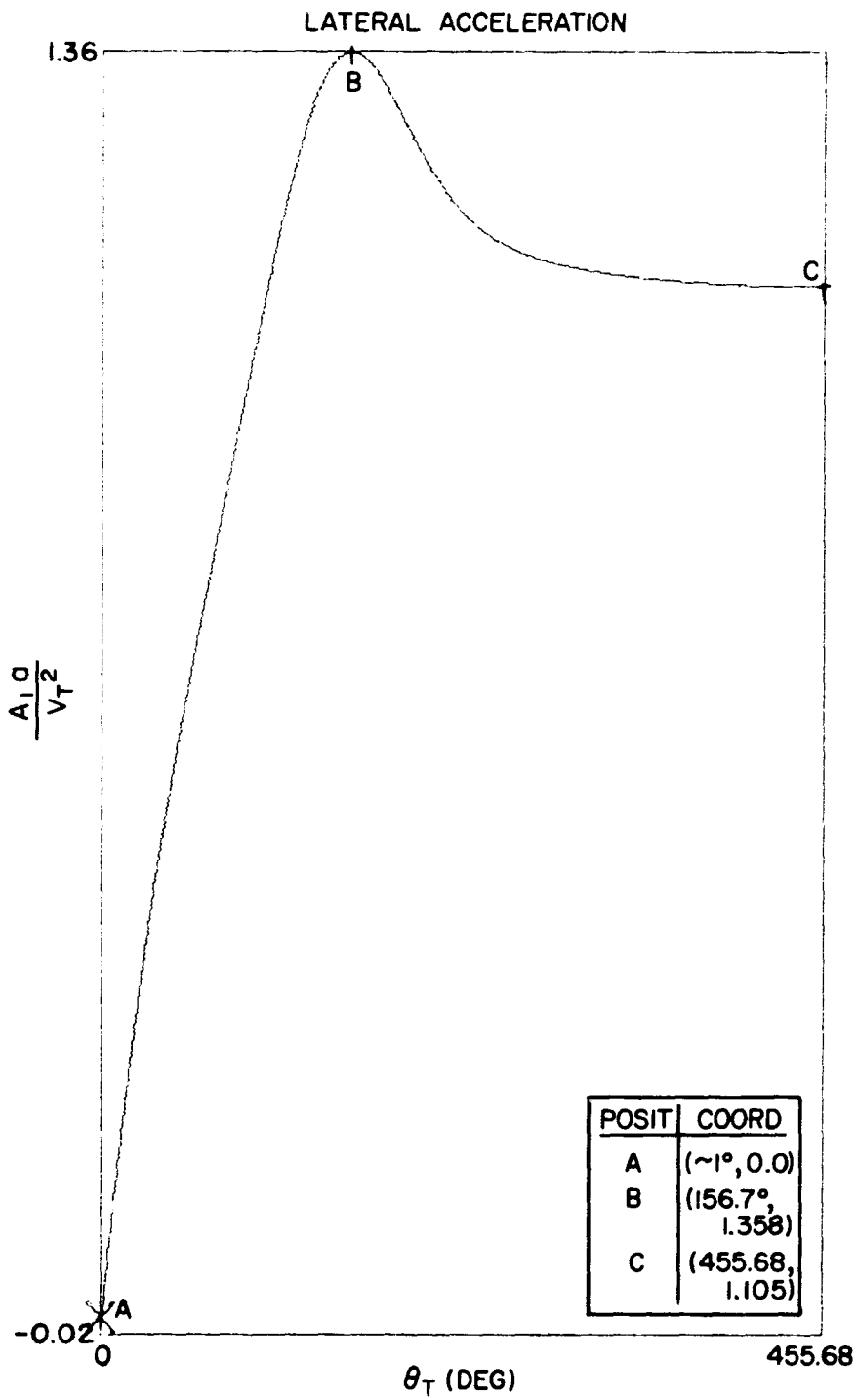
Fig. V.8(b). Dimensionless Lateral Acceleration experienced by the Interceptor during the Circular Pursuit Maneuver (for $\hbar$ = 1.05, φ_0 = 91°, ρ_0 = a) as a function of θ_T.

RANGE RATE

POSIT	**COORD**
A	98.03°, -0.308
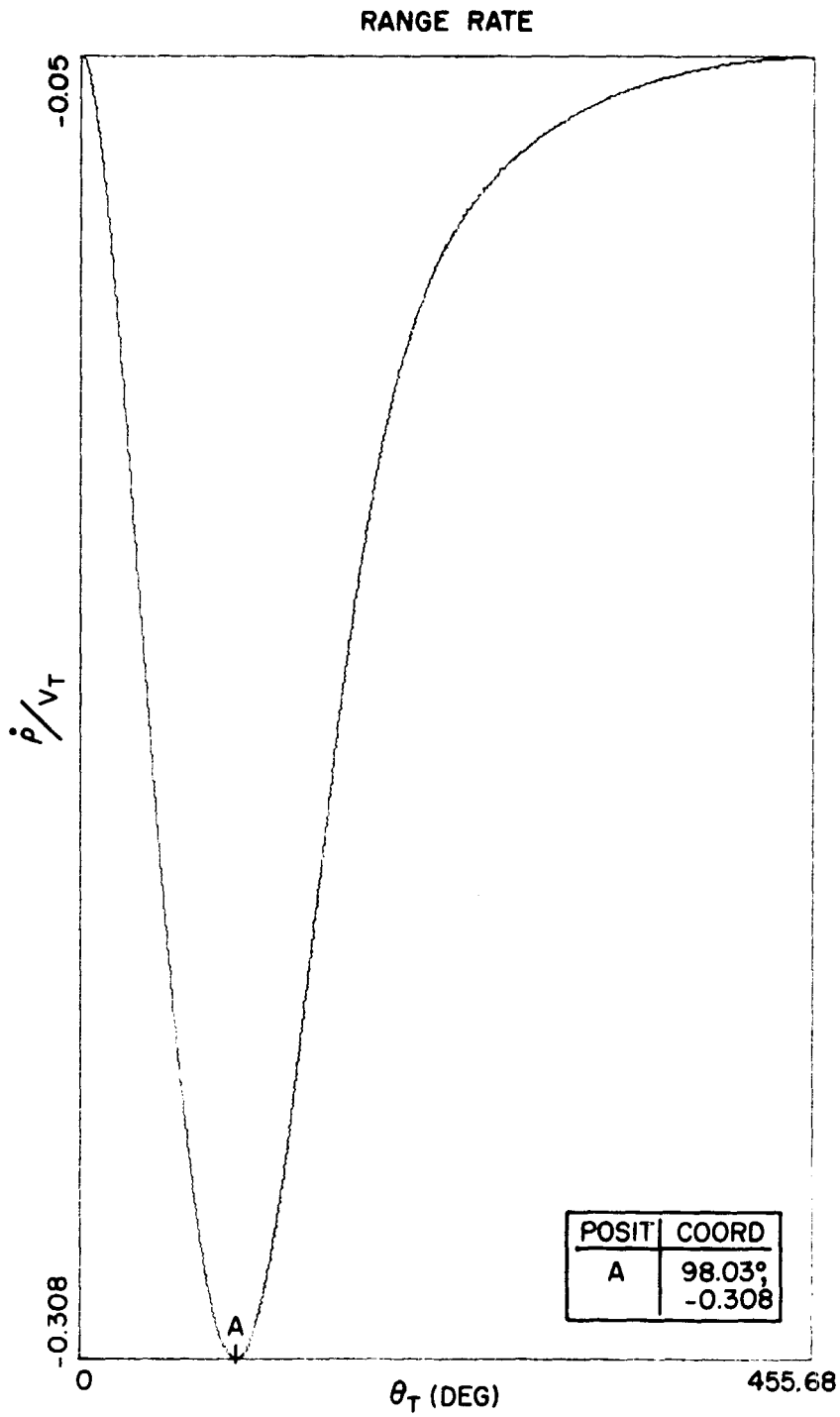
Fig. V.8(c). Dimensionless Range-Rate for the Circular Pursuit Maneuver as a function of θ_T ($\hat{k}$ = 1 05, φ_0 = 91°, ρ_0 = a).
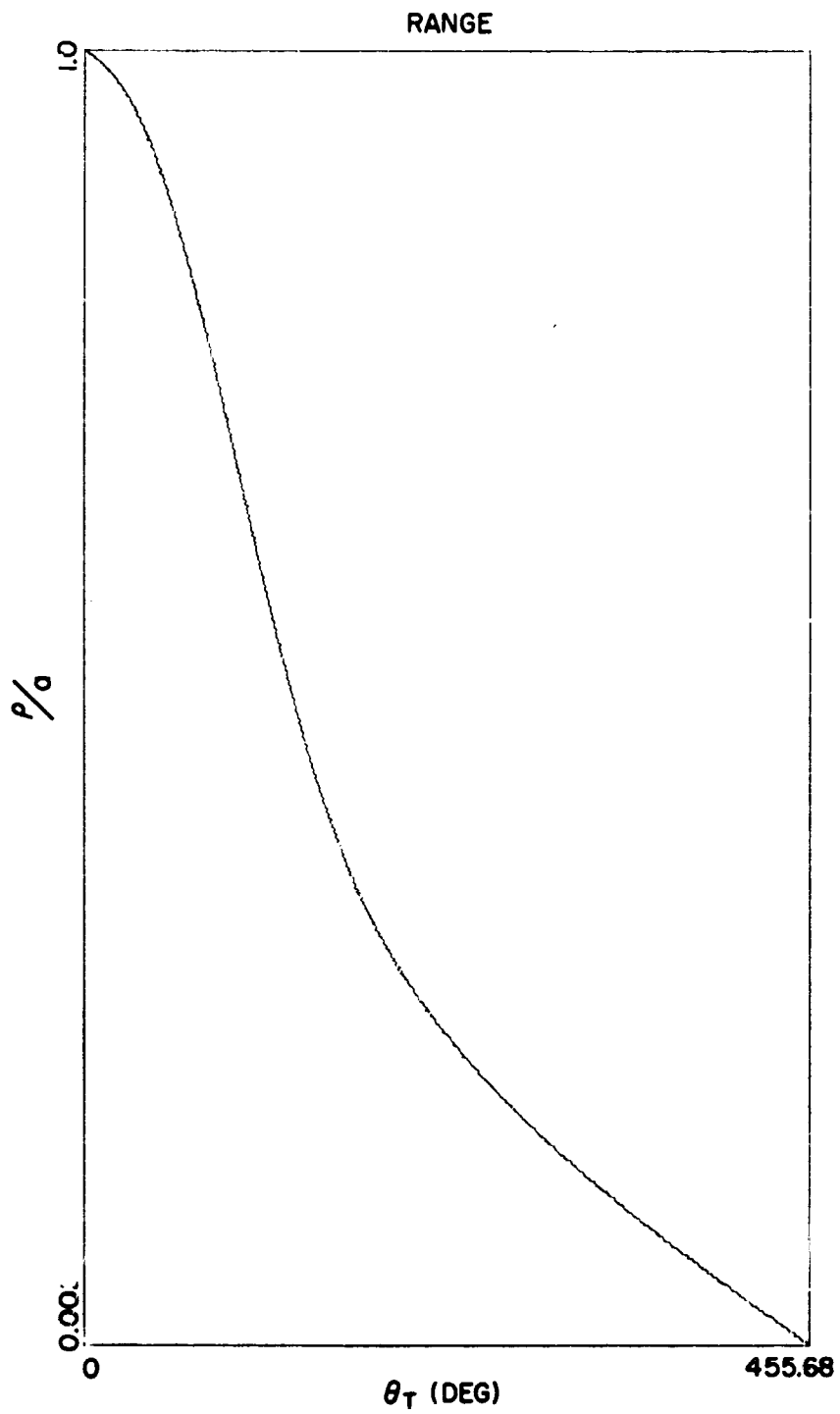
RANGE

Fig. V.8(d). Dimensionless Range for the Circular Pursuit Maneuver as a function of θ_T ($k = 1.05$, $\varphi_0 = 91°$, $\rho_0 = a$).

Fig. V.9(a). Trajectories for the Target (T) and Interceptor (I) during the Circular Pursuit Maneuver (for k = 1.05, φ_0 = 150°, ρ_0 = a).

132

LATERAL ACCELERATION

POSIT	COORD
A	$(40.9°, 0.0)$
B	$(188.2°, 1.3)$
C	$(486.12, 1.105)$

$\frac{A_I a}{V_T^2}$

θ_T (DEG)
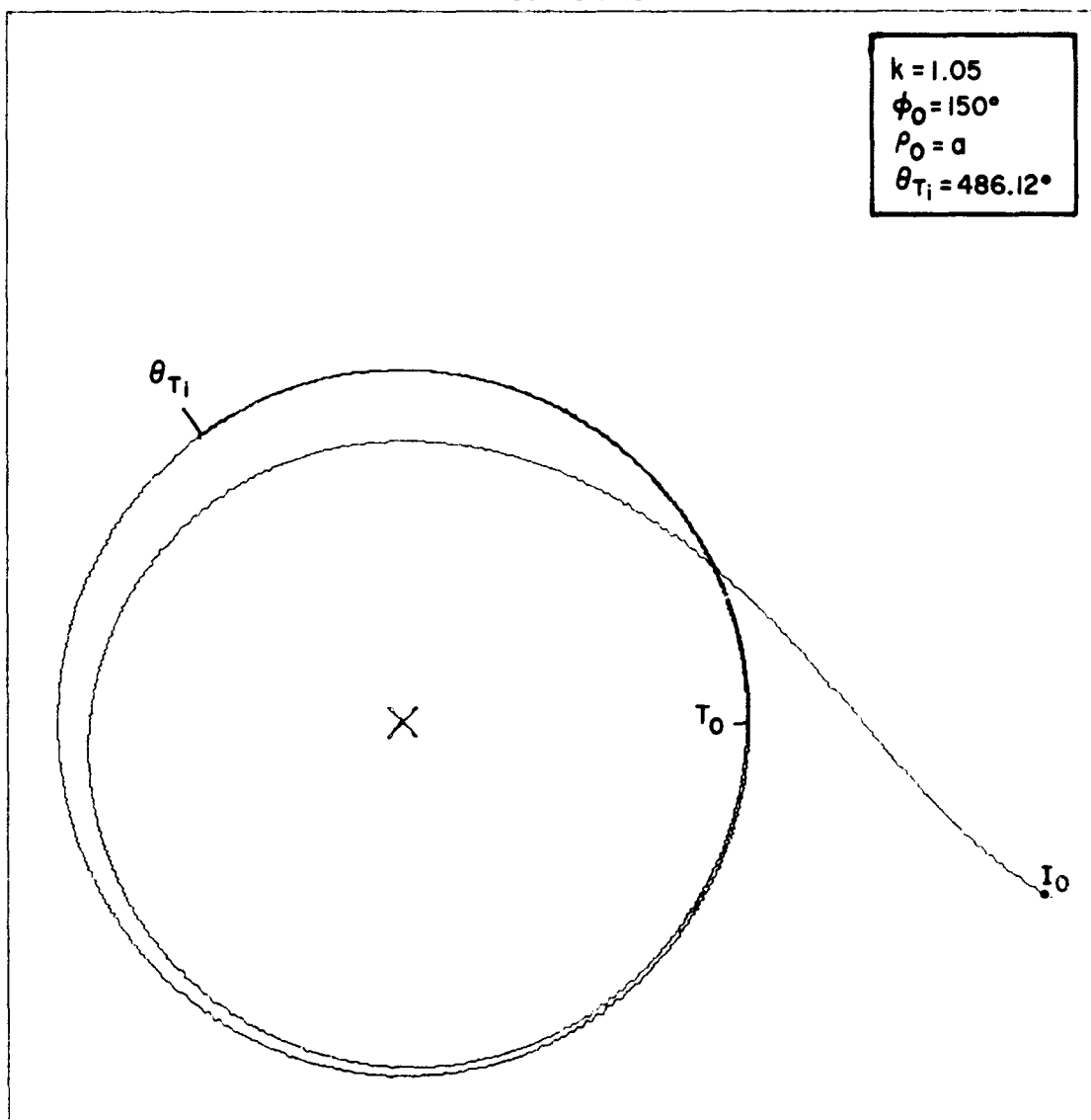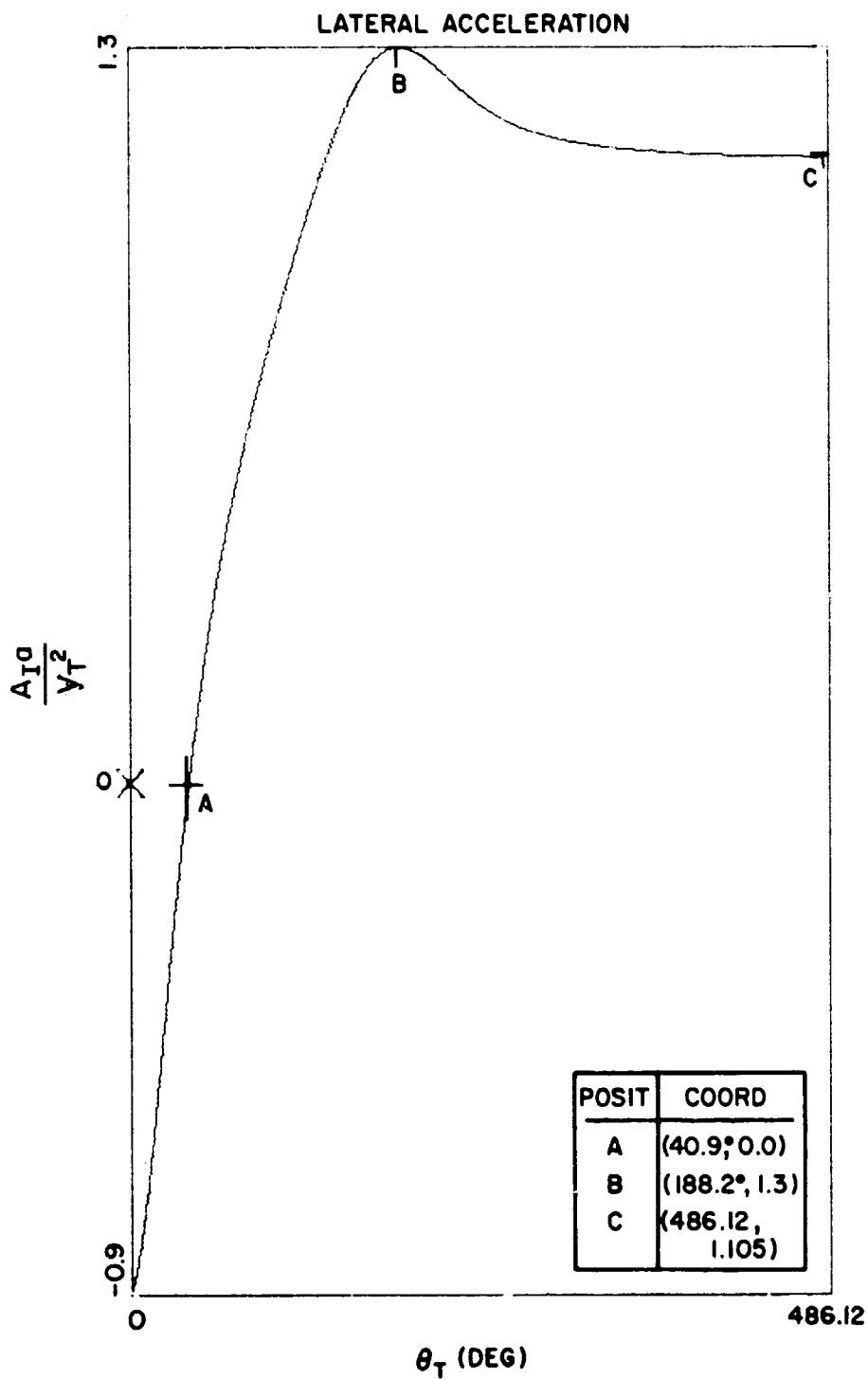
Fig. V.9(b). Dimensionless Lateral Acceleration experienced by the Interceptor during the Circular Pursuit Maneuver (for $k = 1.05$, $\varphi_0 = 150°$, $\rho_0 = a$) as a function of θ_T.
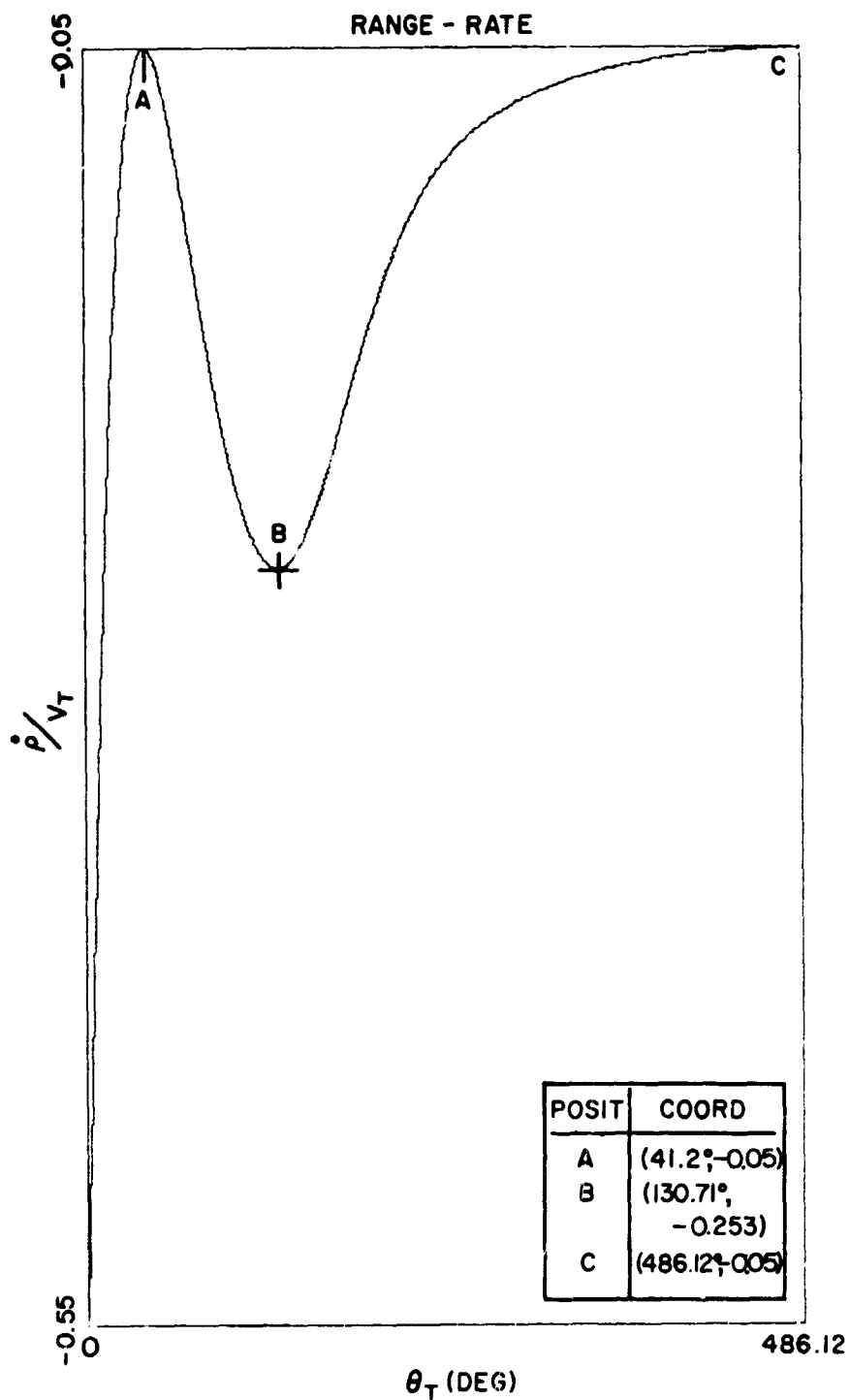
Fig. V.9(c). Dimensionless Range-Rate for the Circular Pursuit Maneuver as a function of θ_T (k = 1.05, φ_0 = 150°, ρ_0 = a).

POSIT	COORD
A	(41.2°,−0.05)
B	(130.71°, −0.253)
C	(486.12,−0.05)

134

RANGE

θ_T (DEG)
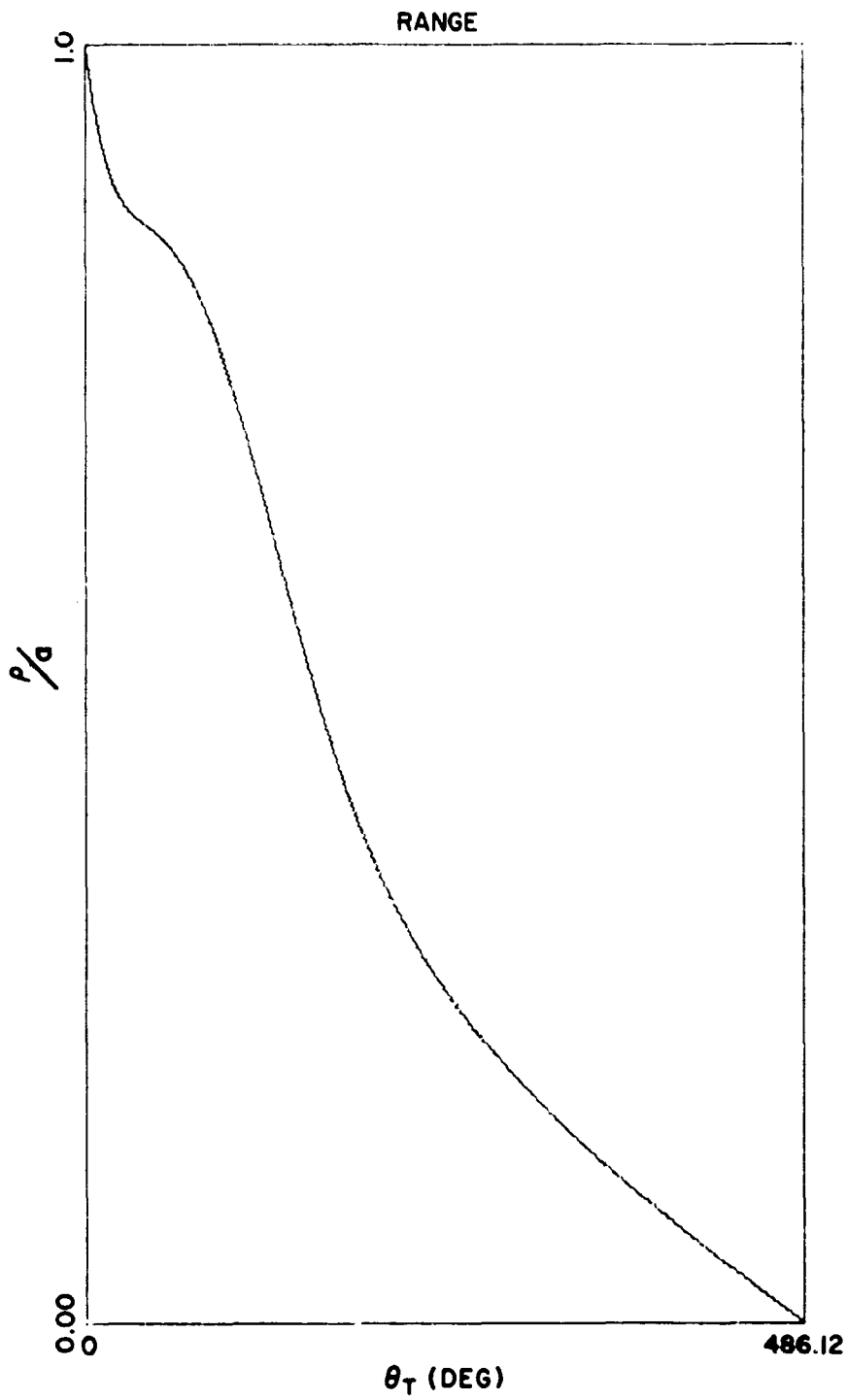
Fig. V.9(d). Dimensionless Range for the Circular Pursuit Maneuver as a function of θ_T (k = 1.05, φ_0 = 150°, ρ_0 = a).

135

$$k = 1.1$$
$$\phi_0 = 150°$$
$$\rho_0 = 4a$$
$$\theta_{T_i} = 309.31°$$
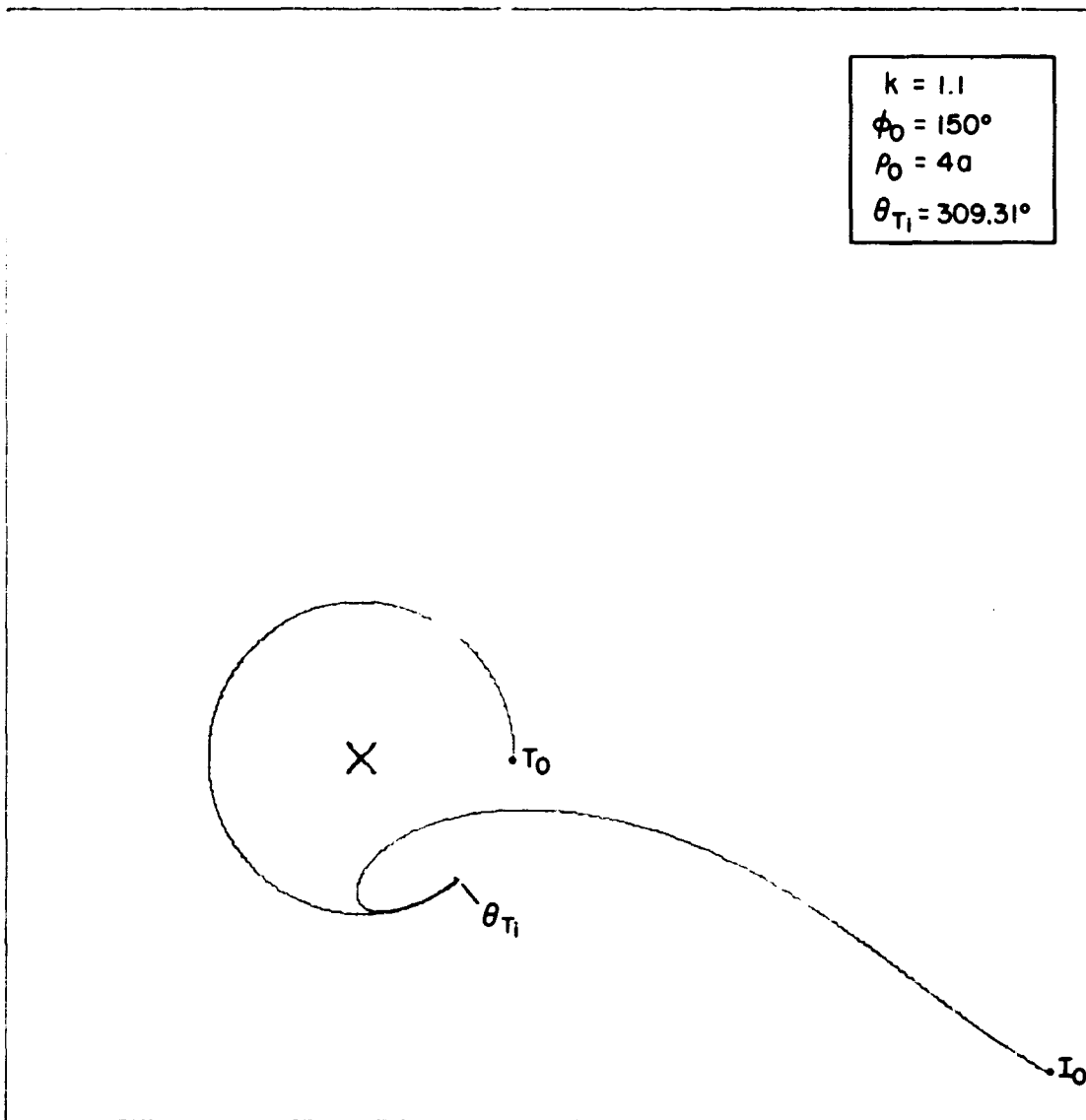
Fig. V.10(a). Trajectories for the Target (T) and Interceptor (I) during the Circular Pursuit Maneuver (for $k = 1.10$, $\varphi_0 = 150°$, $\rho_0 = 4a$).

LATERAL ACCELERATION

ыT	COORD
A	(53.5°, 0.0)
B	(272.6°, 10.8)
C	(309.31°, 1.22)

10.8

$\dfrac{A_1 a}{V_T^2}$

-0.24

0

θ_T (DEG)

309.31
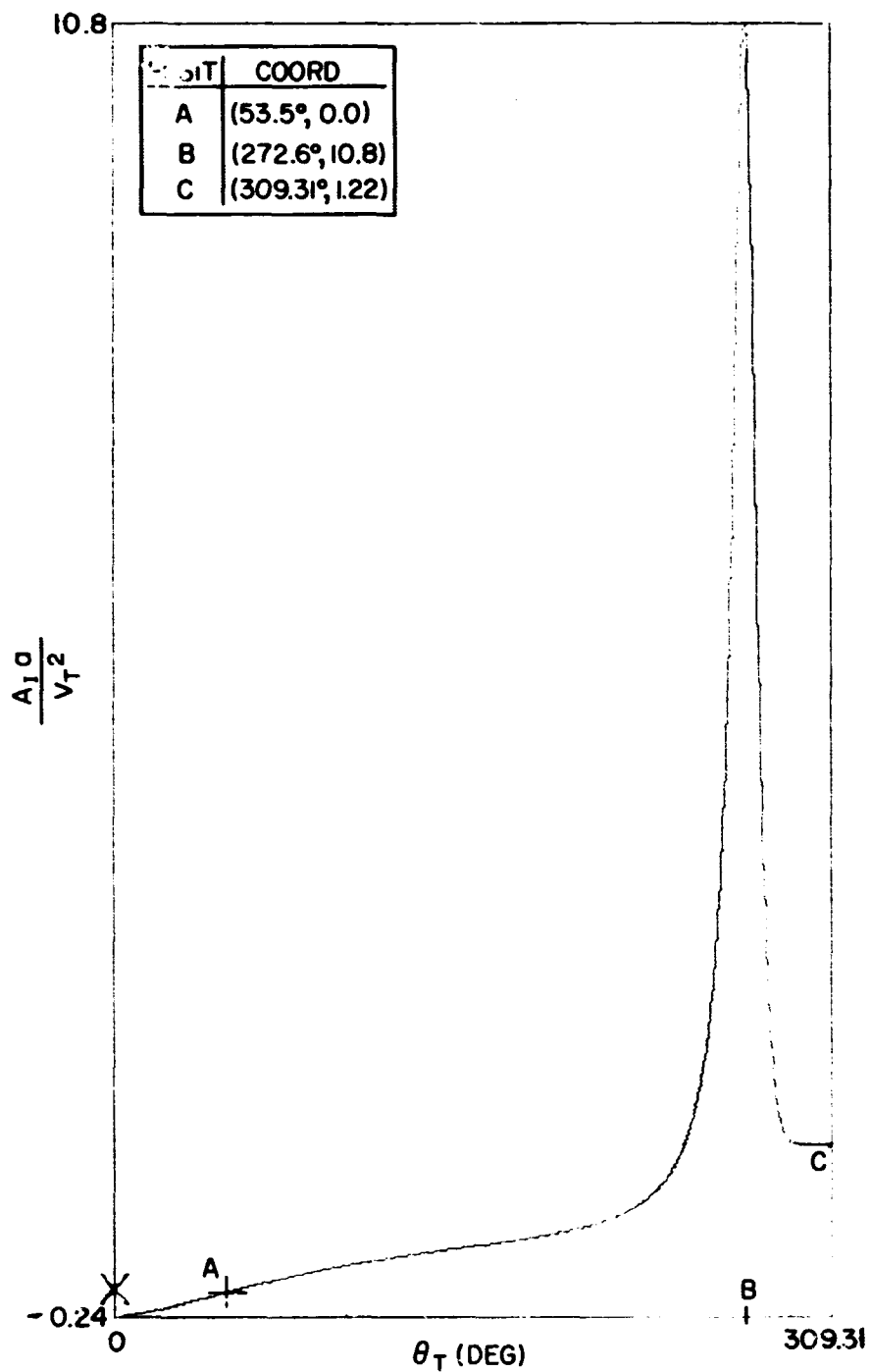
Fig. V.10(b). Dimensionless Lateral Acceleration experienced by the Interceptor during the Circular Pursuit Maneuver (for k = 1.10, φ_0 = 150°, ρ_0 = 4a) as a function of θ_T.

137

RANGE RATE

POSIT	COORD
A	(0°, -0.6)
B	(53.71°, -0.1)
C	(248.87°, -1.677)
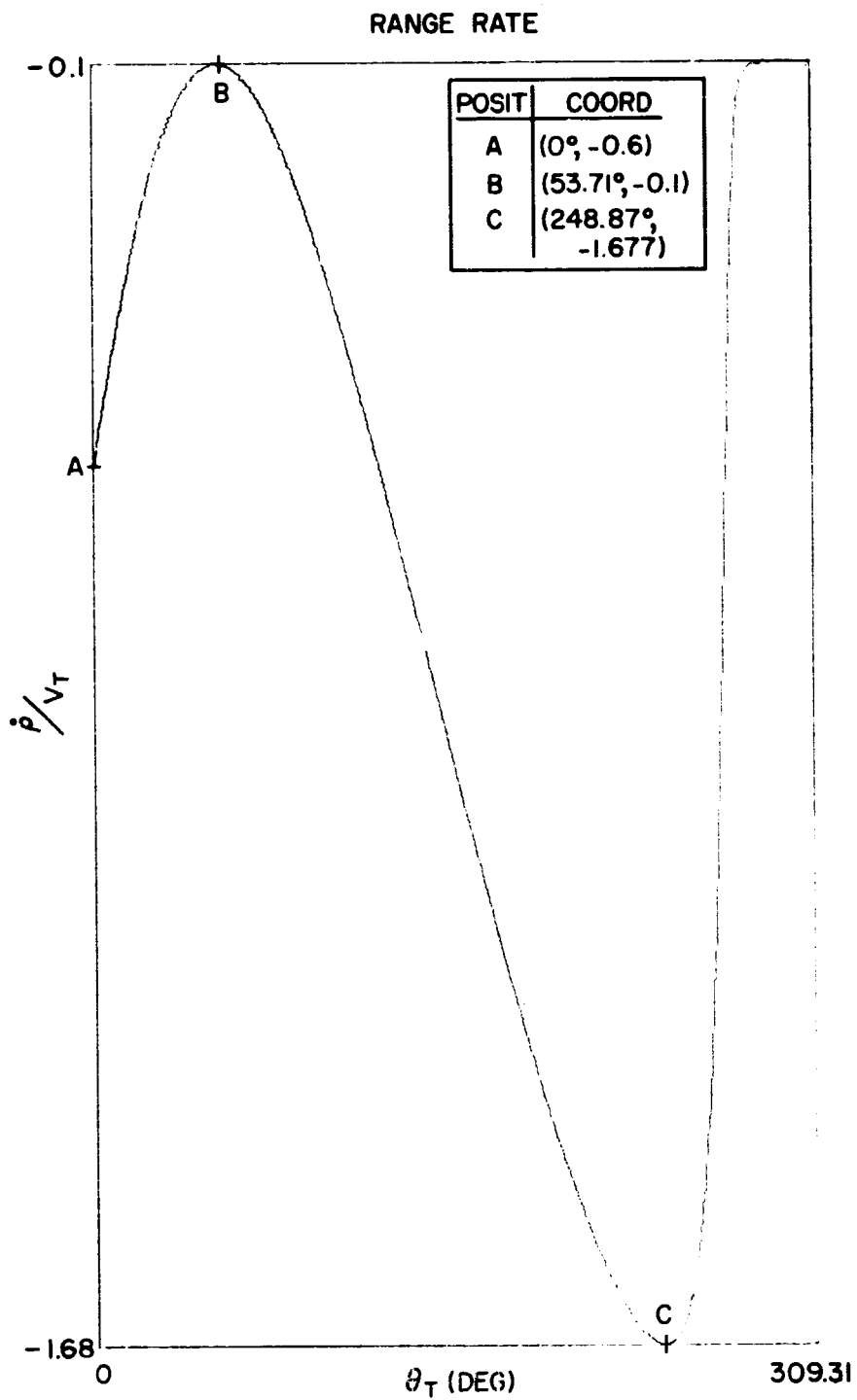
Fig. V.10(c). Dimensionless Range-Rate for the Circular Pursuit Maneuver as a function of θ_T (k = 1.10, φ_0 = 150°, ρ_0 = 4a).

138
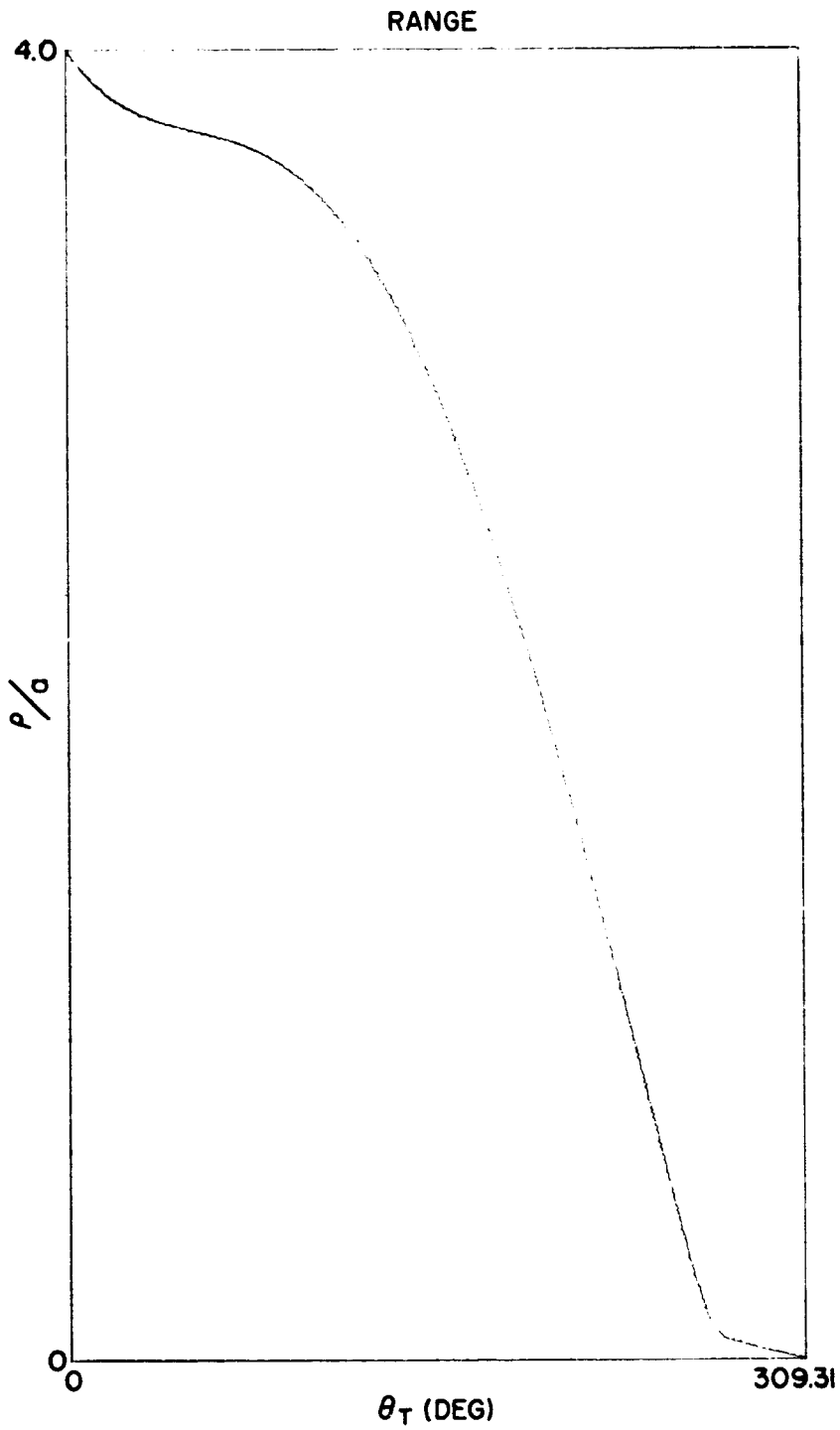
RANGE

Fig. V.10(d). Dimensionless Range for the Circular Pursuit Maneuver as a function of θ_T ($k = 1.10$, $\varphi_0 = 150°$, $\rho_0 = 4a$).

139
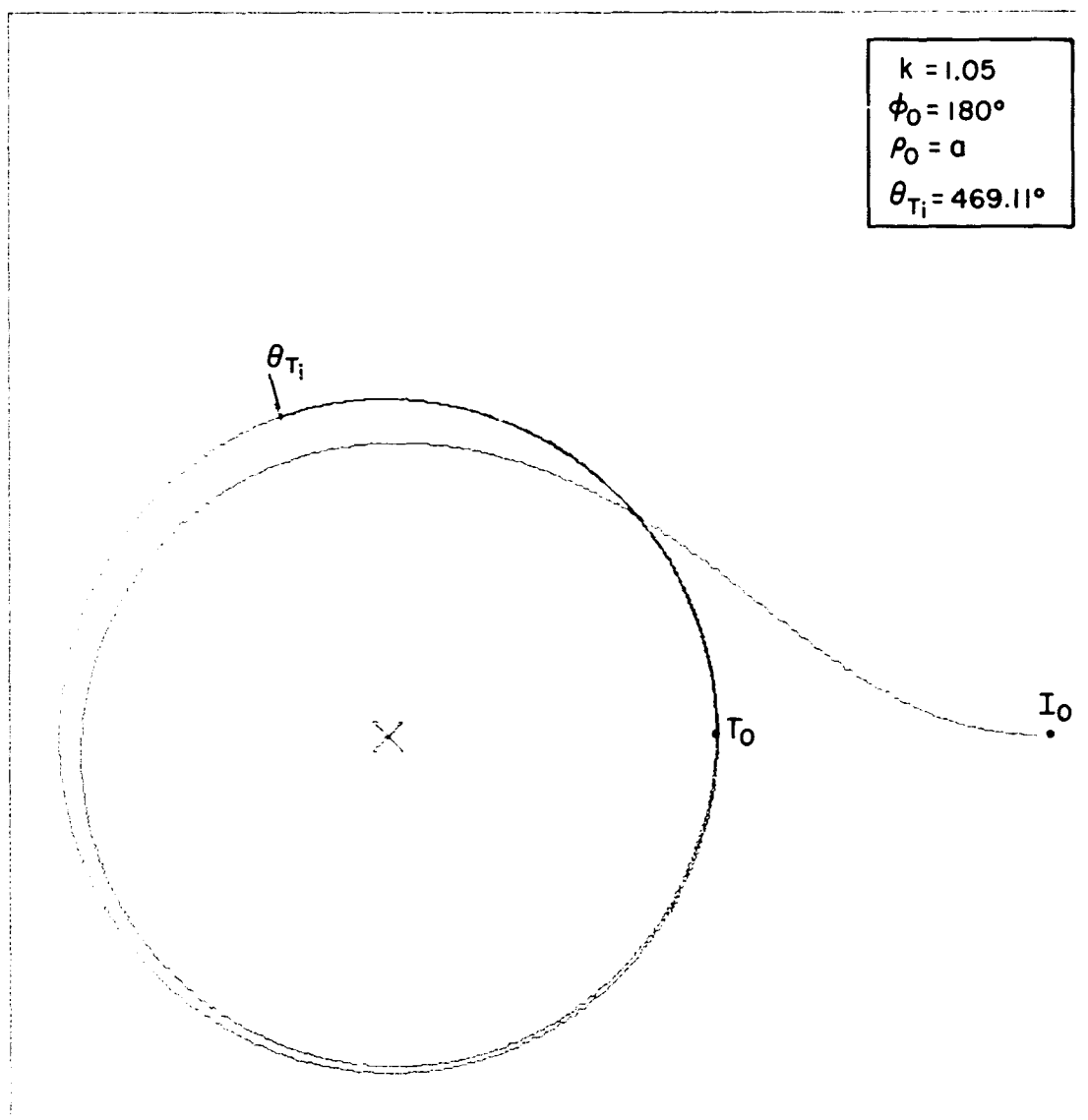
TRAJECTORIES

Fig. V.11(a). Trajectories for the Target (T) and Interceptor (I) during the circular
pursuit maneuver (for k = 1.05, φ_0 = 180°, ρ_0 = a).
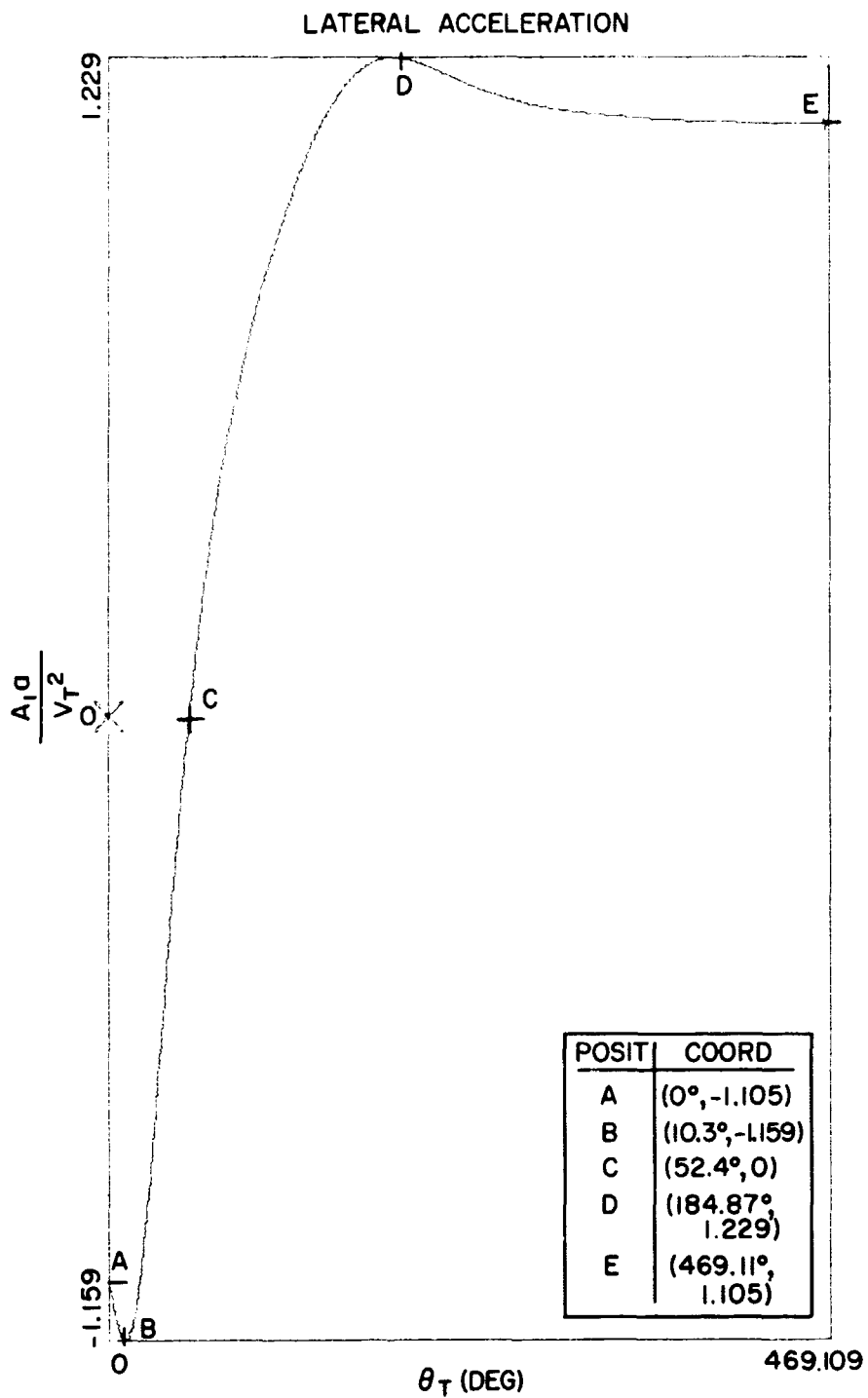
Fig. V.11(b). Dimensionless Lateral Accelerating experienced by the Interceptor during the Circular Pursuit Maneuver (for $k = 1.05$, $\varphi_0 = 180°$, $\rho_0 = a$) as a function of θ_T.
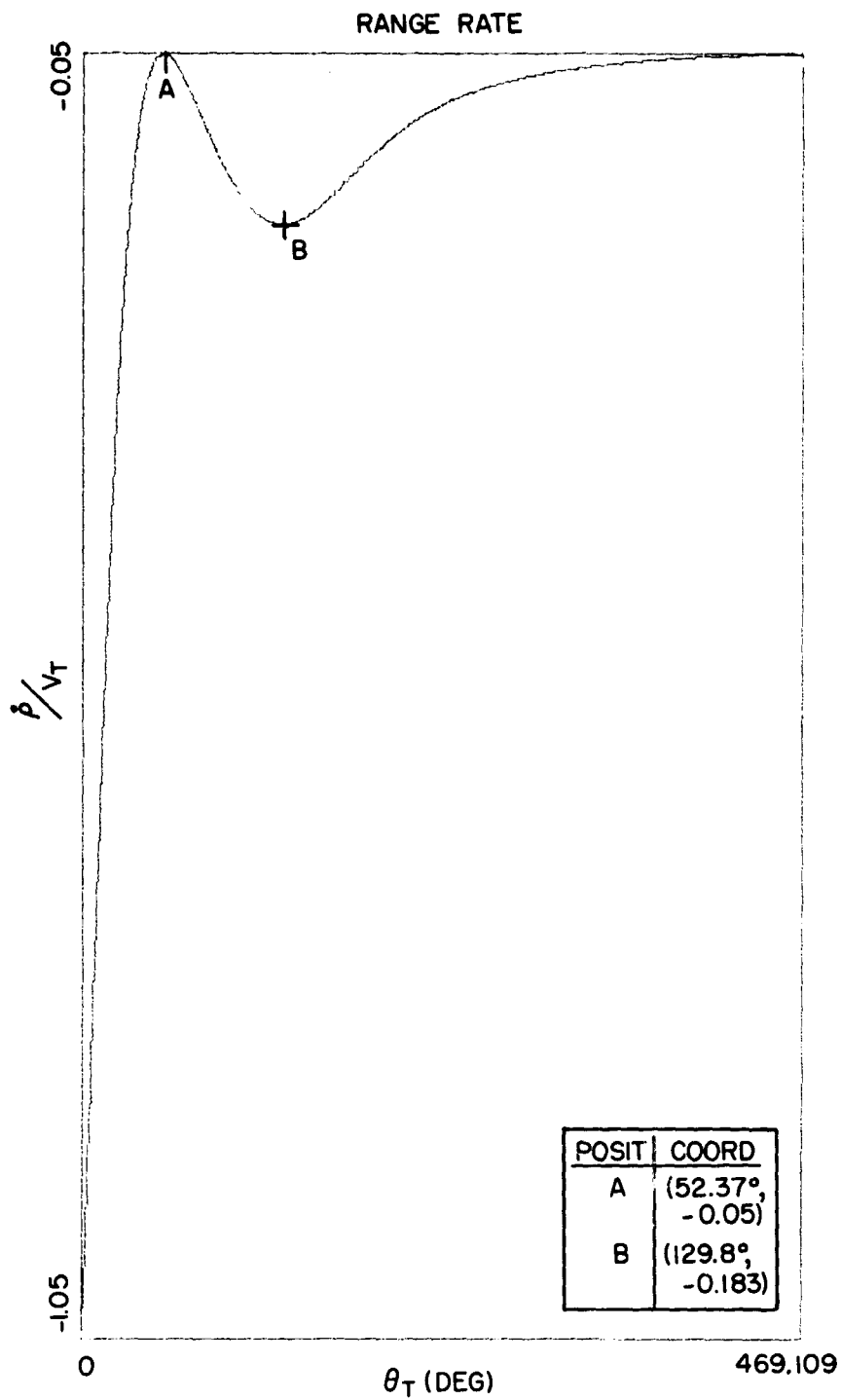
141

RANGE RATE

$\dot{\rho}/v_T$

θ_T (DEG)

POSIT	COORD
A	(52.37°, -0.05)
B	(129.8°, -0.183)

Fig. V.11(c). Dimensionless Range-Rate for the Circular Pursuit Maneuver as a function of θ_T (k= 1.05, φ_0 = 180°, ρ_0 = a).

142

RANGE

ρ/a

θ_T (DEG)

1.0

0

0

0

469.109
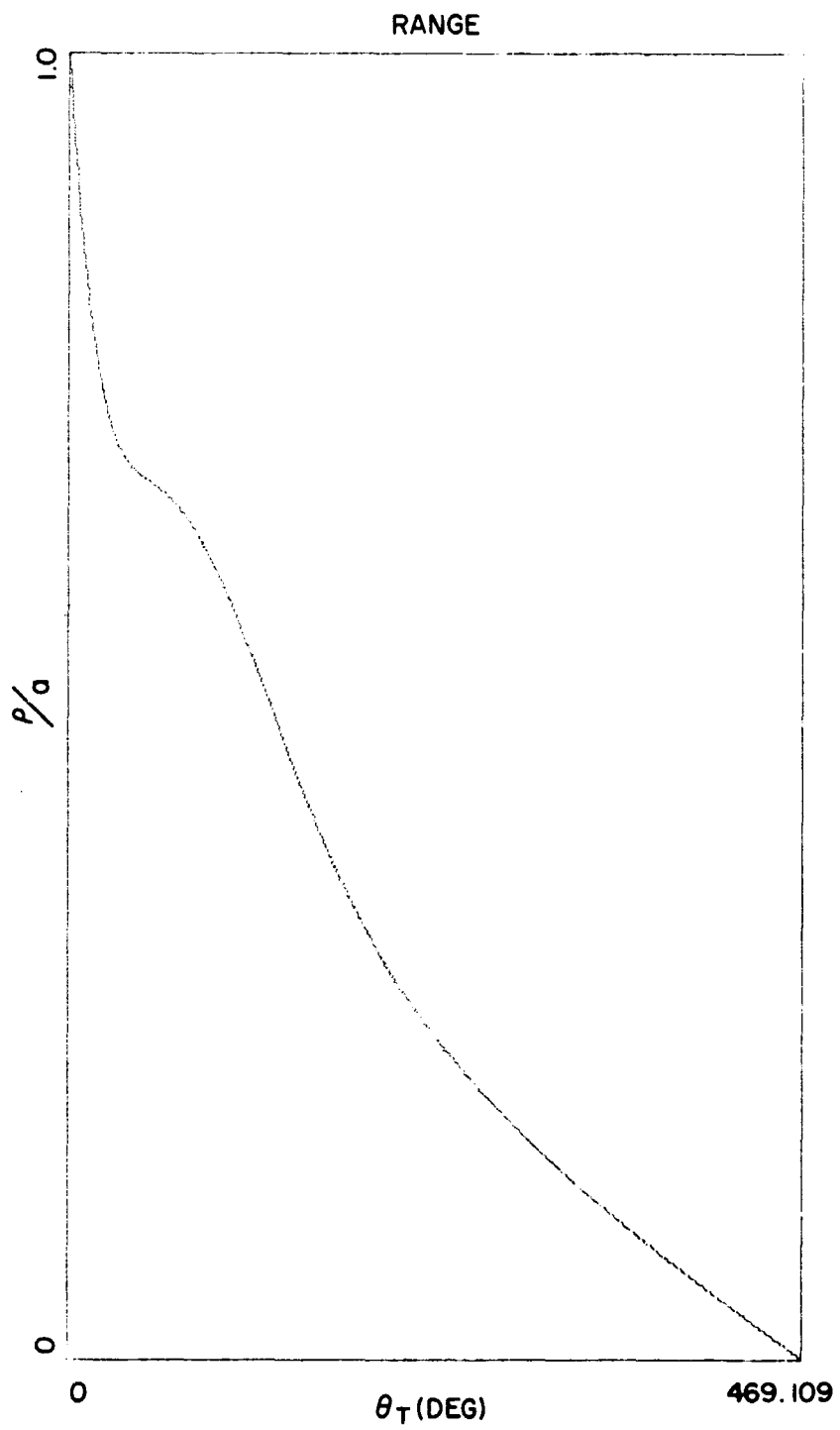
Fig. V.11(d).   Dimensionless Range for the Circular Pursuit Maneuver as a
function of θ_T (k= 1.05, φ_0 = 180°, ρ_0 = a).

143

Fig. V.12(a). Trajectories for the Target (T) and Interceptor (I) during the circular pursuit maneuver (for k = 1.05, φ_0 = 180°, ρ_0 = 7.8a).

LATERAL ACCELERATION

POSIT	COORD
A	(0°,-0.135)
B	(83.26°, 0)
C	(198.74°, 0.17)
D	(284.6°, 0)
E	(364.36°, -0.807)
F	(413.5°, 0)
G	(570.3°, 1.36)
H	(871.1°, 1.105)

1.363

$\dfrac{A_I a}{V_T^2}$

O'

-0.807

O   871.074

θ_T (DEG)
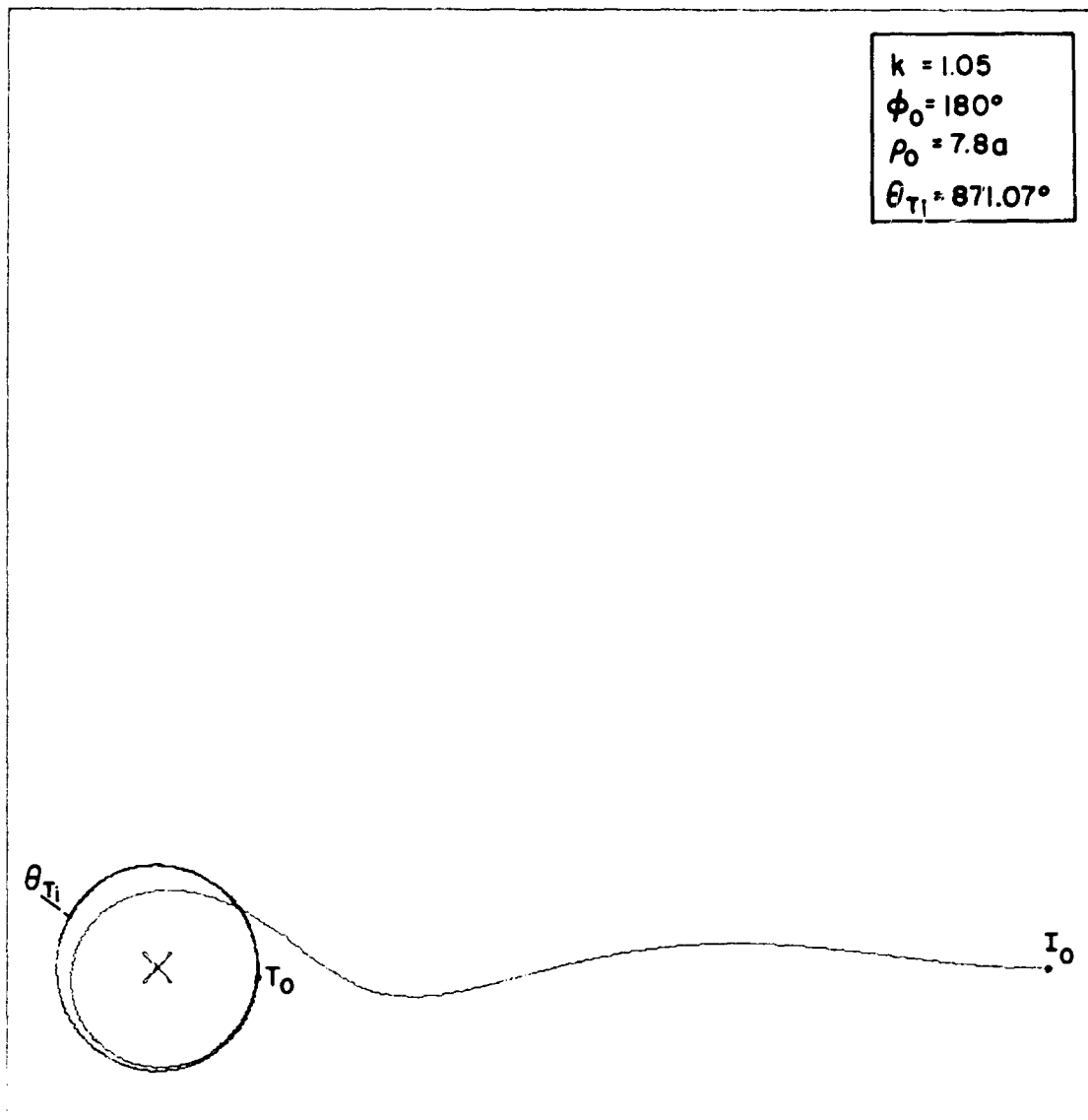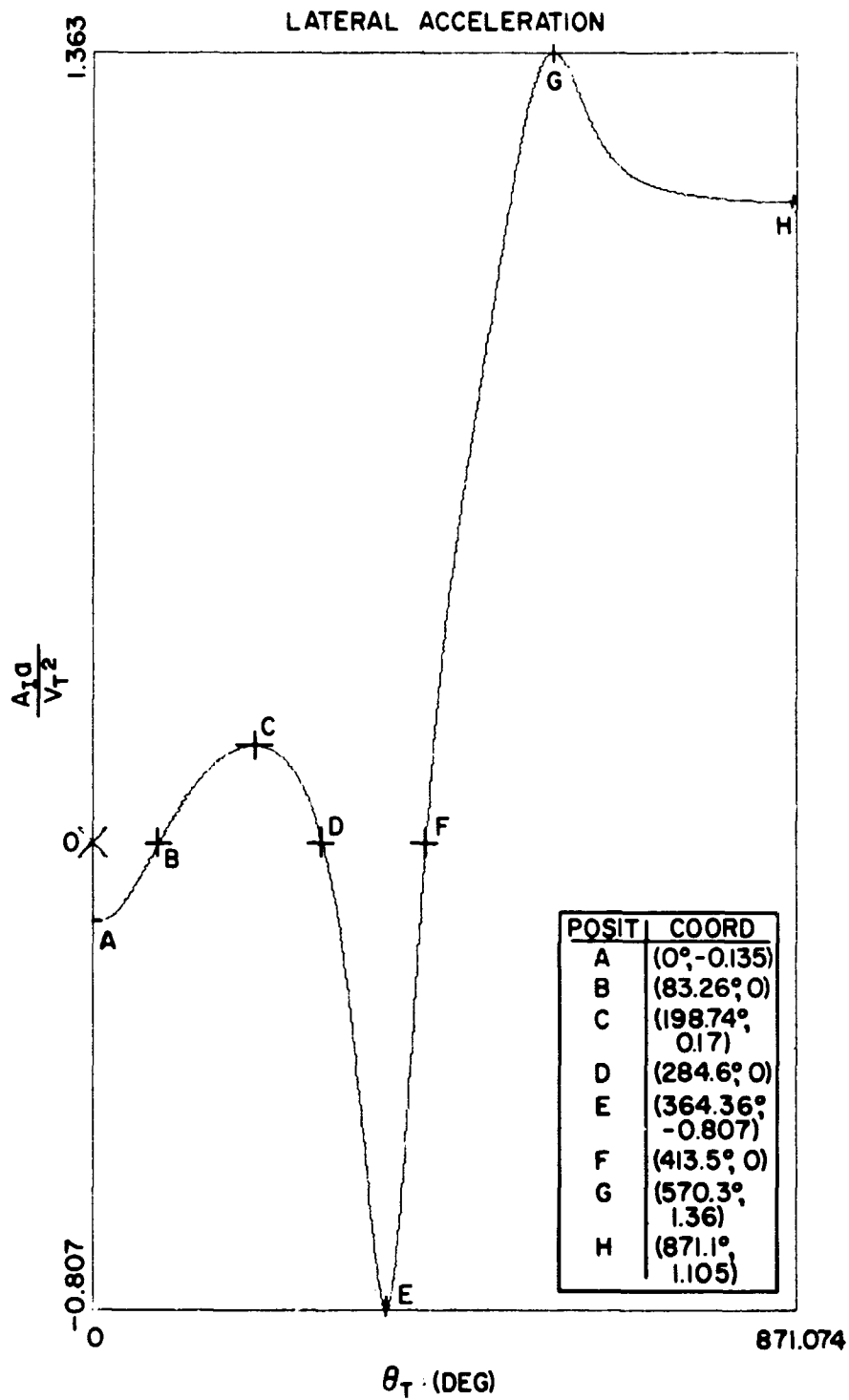
Fig. V.12(b). Dimensionless Lateral Acceleration experienced by the Interceptor during the Circular Pursuit Maneuver (for k = 1.05, φ_0 = 180°, ρ_0 = 7.8a) as a function of θ_T.

145
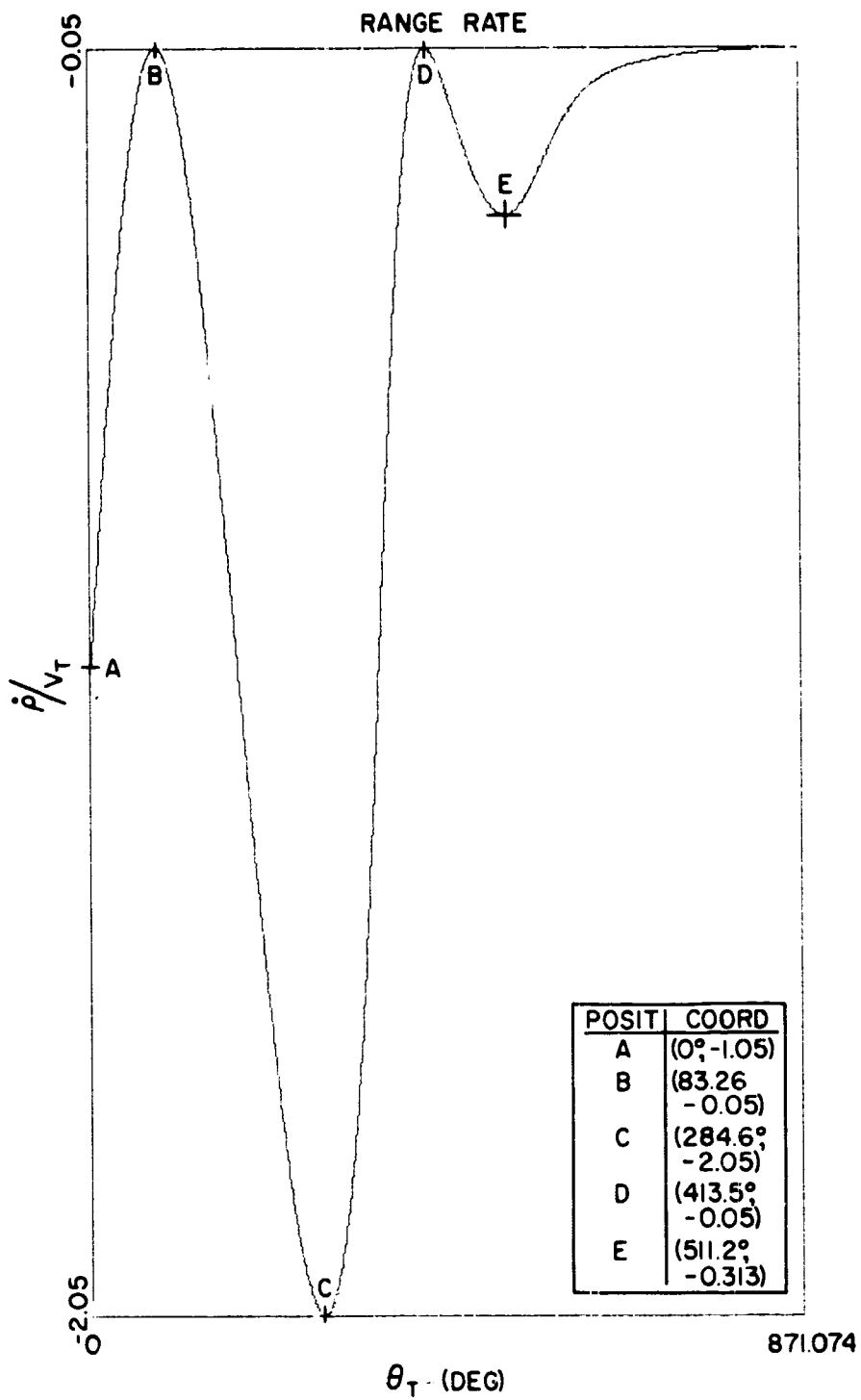
Fig. V.12(c). Dimensionless Range-Rate for the Circular Pursuit Maneuver as a function of θ_T ($\hat{k} = 1.05$, $\varphi_0 = 180°$, $r_0 = 7.8a$).

146

RANGE

ρ/a

$\theta_T = (DEG)$
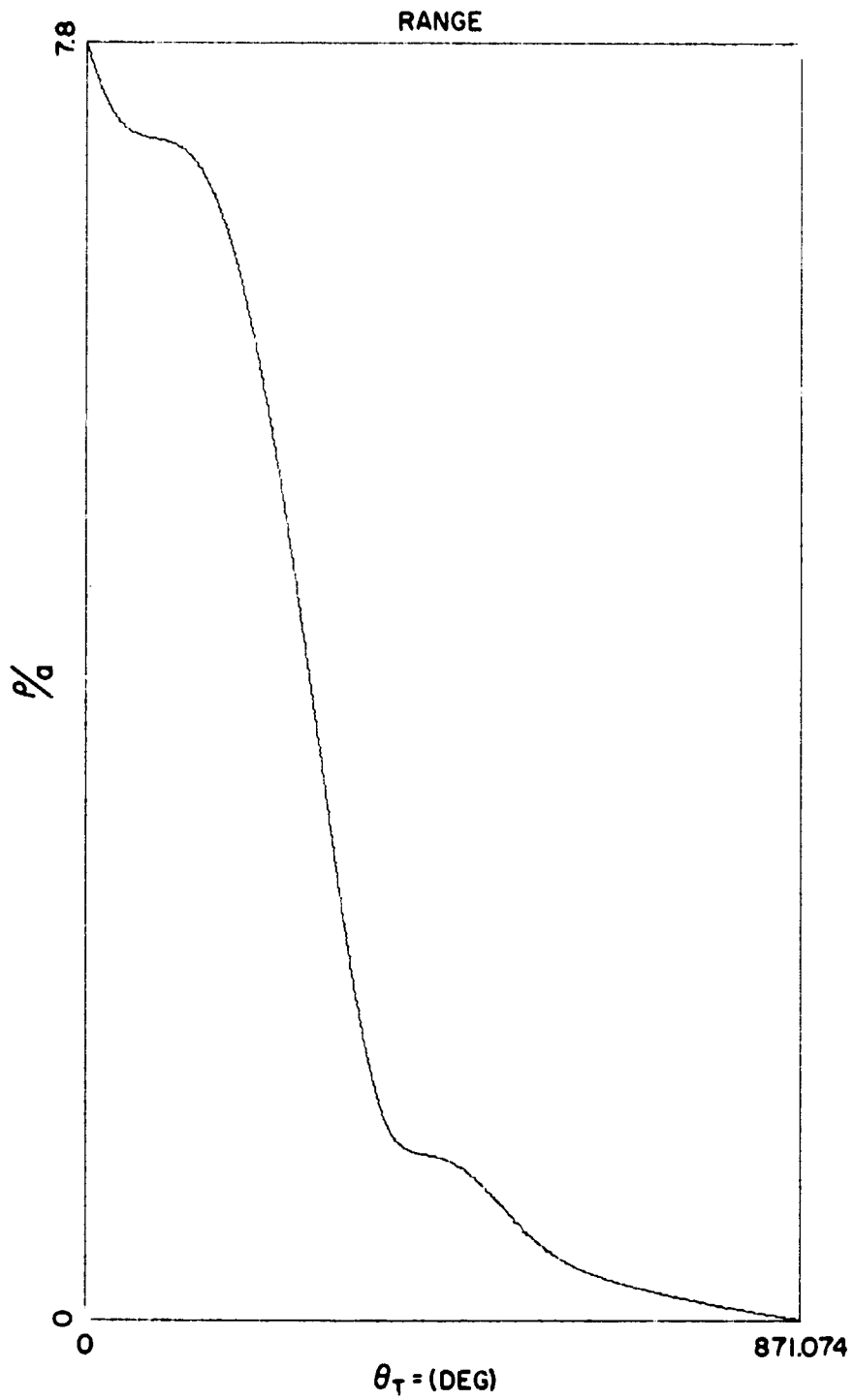
Fig. V.12(d). Dimensionless Range for the Circular Pursuit Maneuver as a function of θ_T (k= 1.05, φ_0 = 180°, ρ_0 = 7.8a).

147

Fig. V.13(a). Trajectories for the Target (T) and Interceptor (I) during the circular pursuit maneuver (for k = 1.50, φ_0 = 180°, ρ_0 = a).

LATERAL ACCELERATION

POSIT	COORD
A	(0.0°, −1.5)
B	(15.0°, −1.87)
C	(47.5°, 0.)

$\dfrac{A_{Ia}}{V_T^2}$

2.985

O ✕

+C

A

B

−1.869

O

83.258

θ_T (DEG)
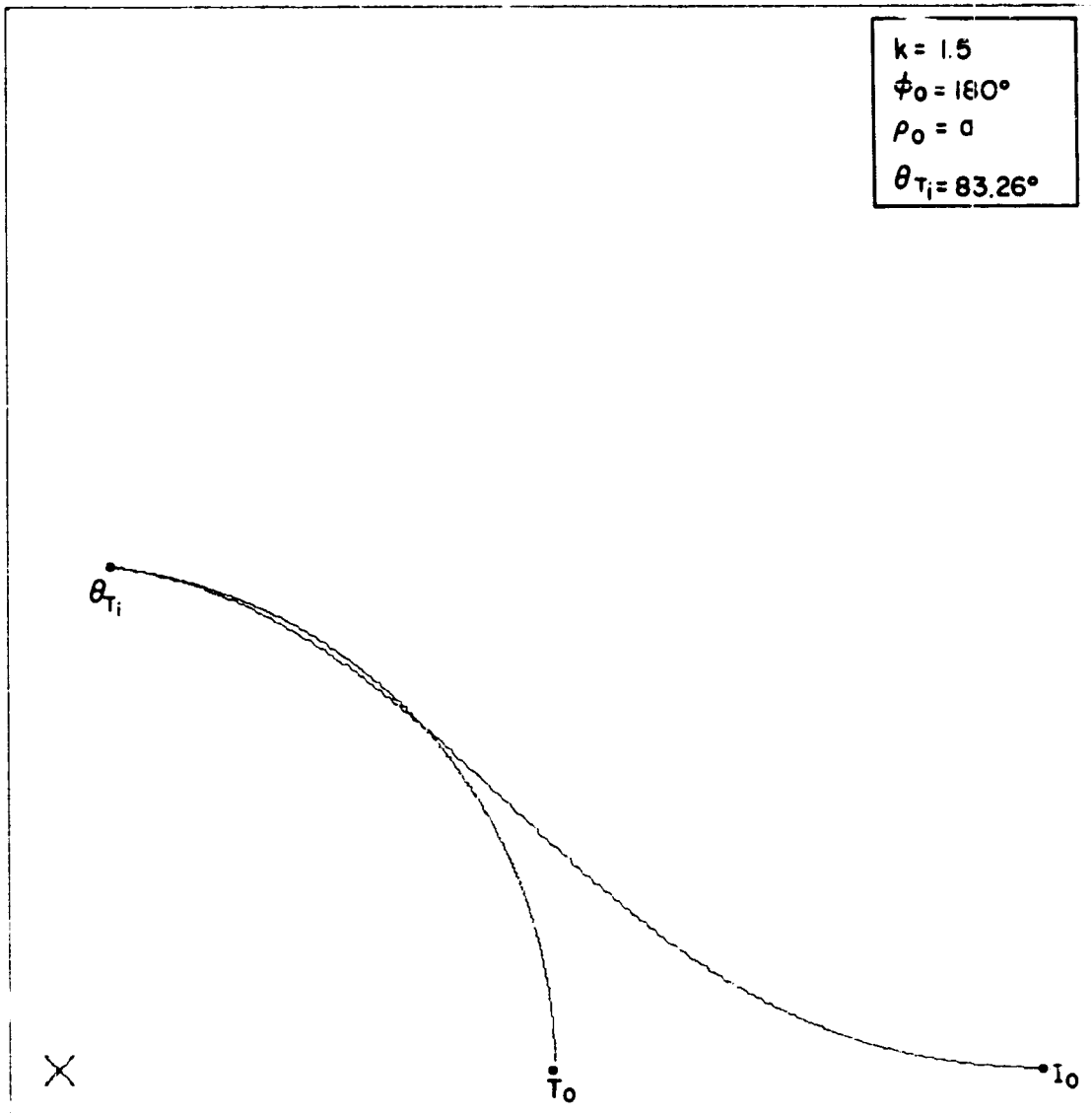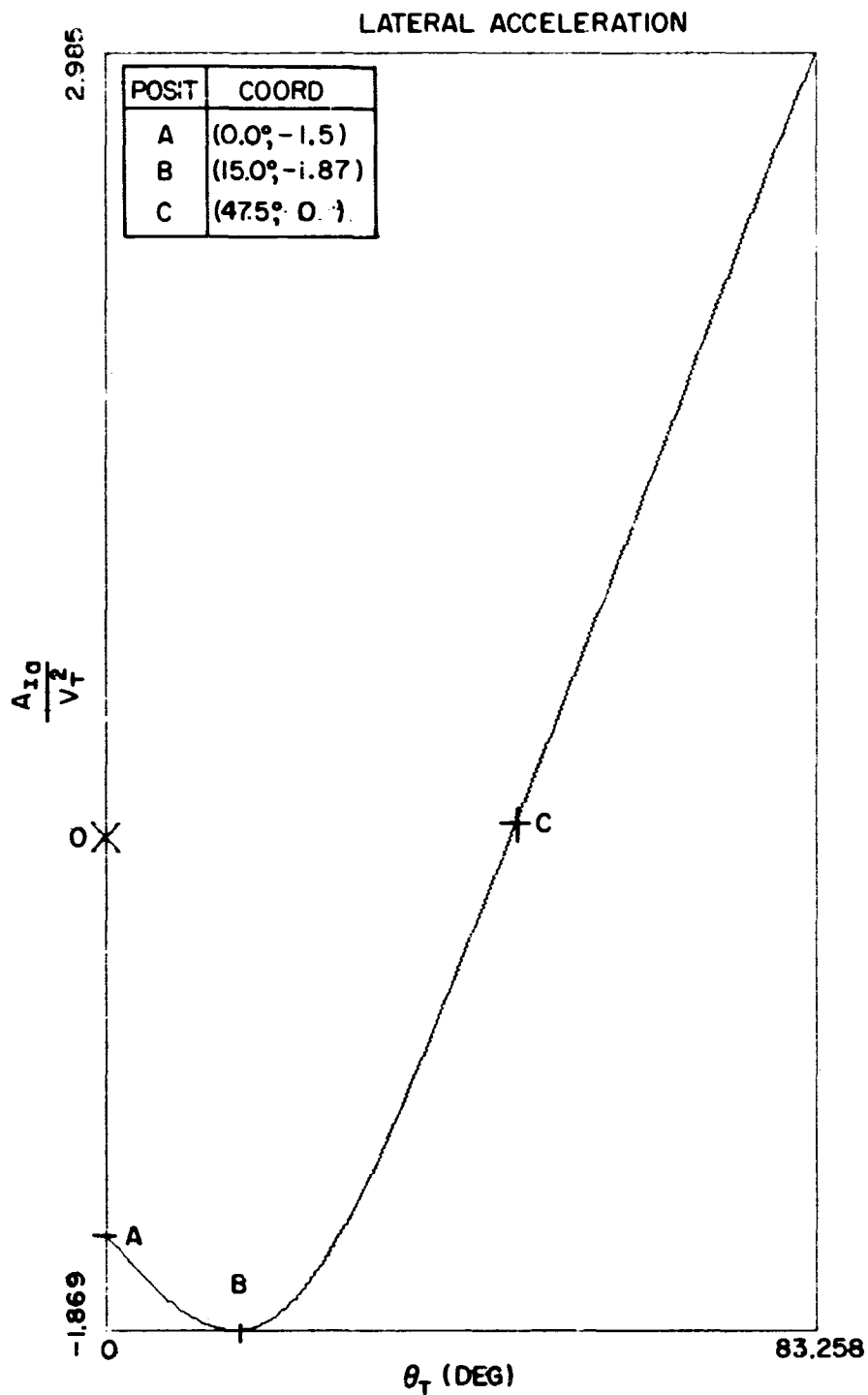
rig. V.13(b). Dimensionless Lateral Acceleration experienced by the Interceptor during the Circular Pursuit Maneuver (for $k = 1.50$, $\varphi_0 = 180°$, $\rho_0 = a$) as a function of θ_T.

149
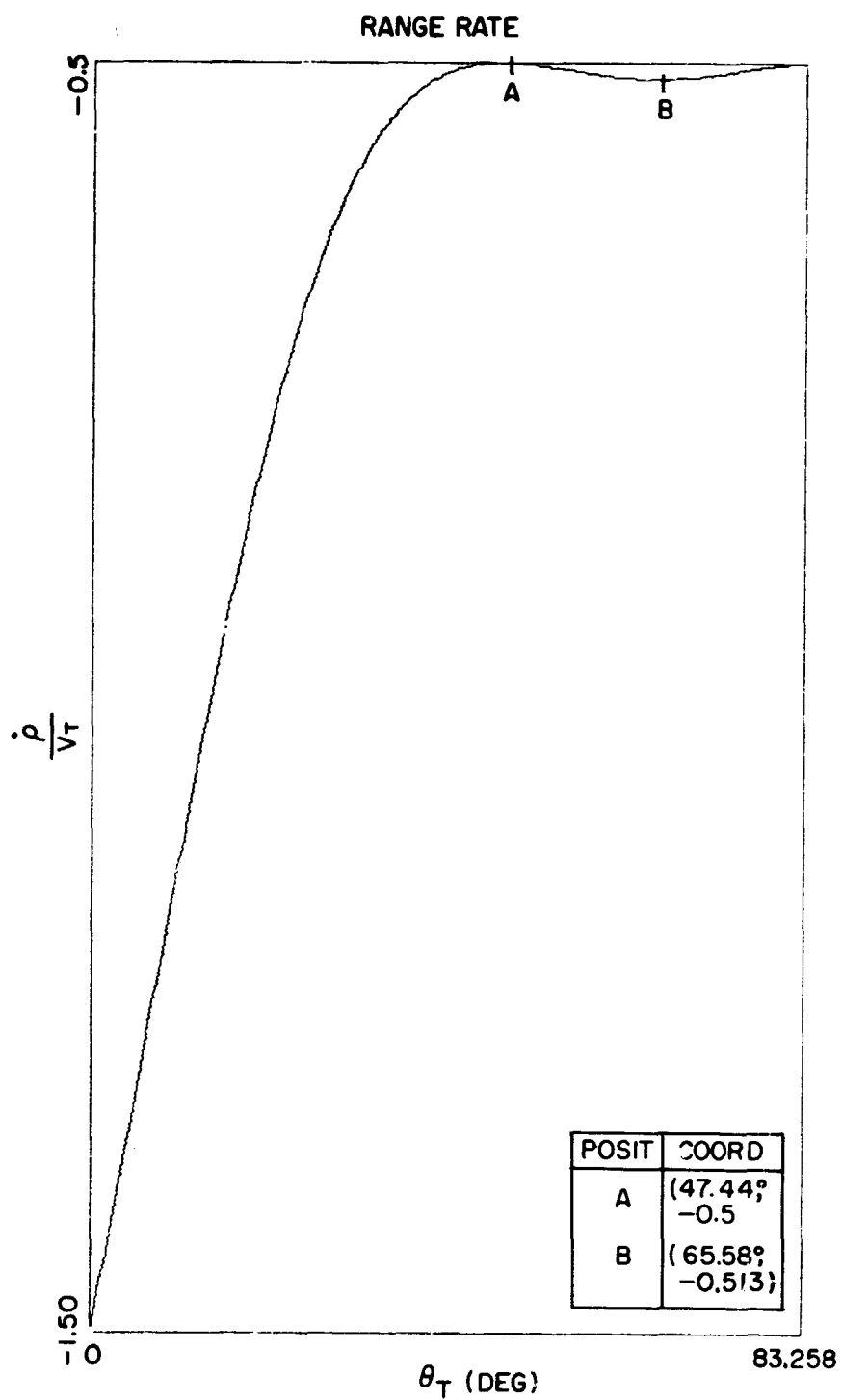
Fig. V.13(c). Dimensionless Range-Rate for the Circular Pursuit Maneuver as a function of θ_T (k = 1.50, φ_0 = 180°, ρ_0 = a).

150
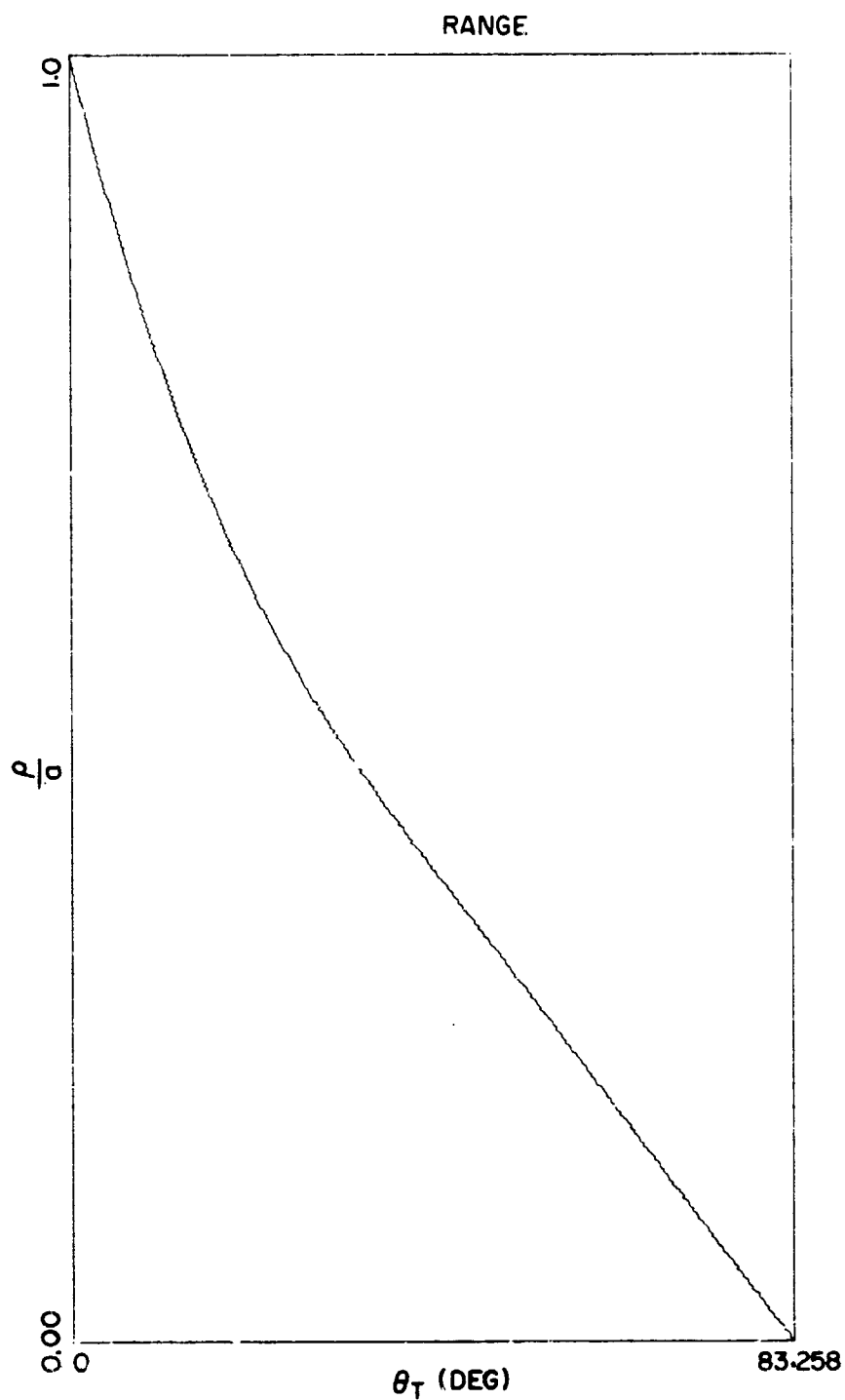
RANGE.

Fig. V.13(d). Dimensionless Range for the Circular Pursuit Maneuver as a function of θ_T (k= 1.50, φ_0 = 180°, ρ_0 = a).

151

Fig. V.14(a). Trajectories for the Target (T) and Interceptor (I) during the circular
pursuit maneuver (for k = 1.05, φ_0 = 210°, ρ_0 = a).

LATERAL ACCELERATION

$\frac{A_l a}{V_T^2}$

θ_T (DEG)

POSIT	COORD
A	(0°,−0.909)
B	(23.05°,−1.759)
C	(57.4°, 0)
D	(162.1°, 1.157)
E	(398.61°, 1.105)

Fig. V.14(b). Dimensionless Lateral Acceleration experienced by the Interceptor during the Circular Pursuit Maneuver (for k = 1.05, φ_0 = 210°, ρ_0 = a) as a function of θ_T.

153

RANGE – RATE

POSIT	COORD
A	(57.3°, 0.05)
B	(114°, -0.074)

Fig. V.14(c). Dimensionless Range-Rate for the Circular Pursuit Maneuver as a function of θ_T ($\hat{k} = 1.05$, $\varphi_0 = 210°$, $\rho_0 = a$).

154

RANGE

ρ/a

θ_T (DEG)

0

398.608
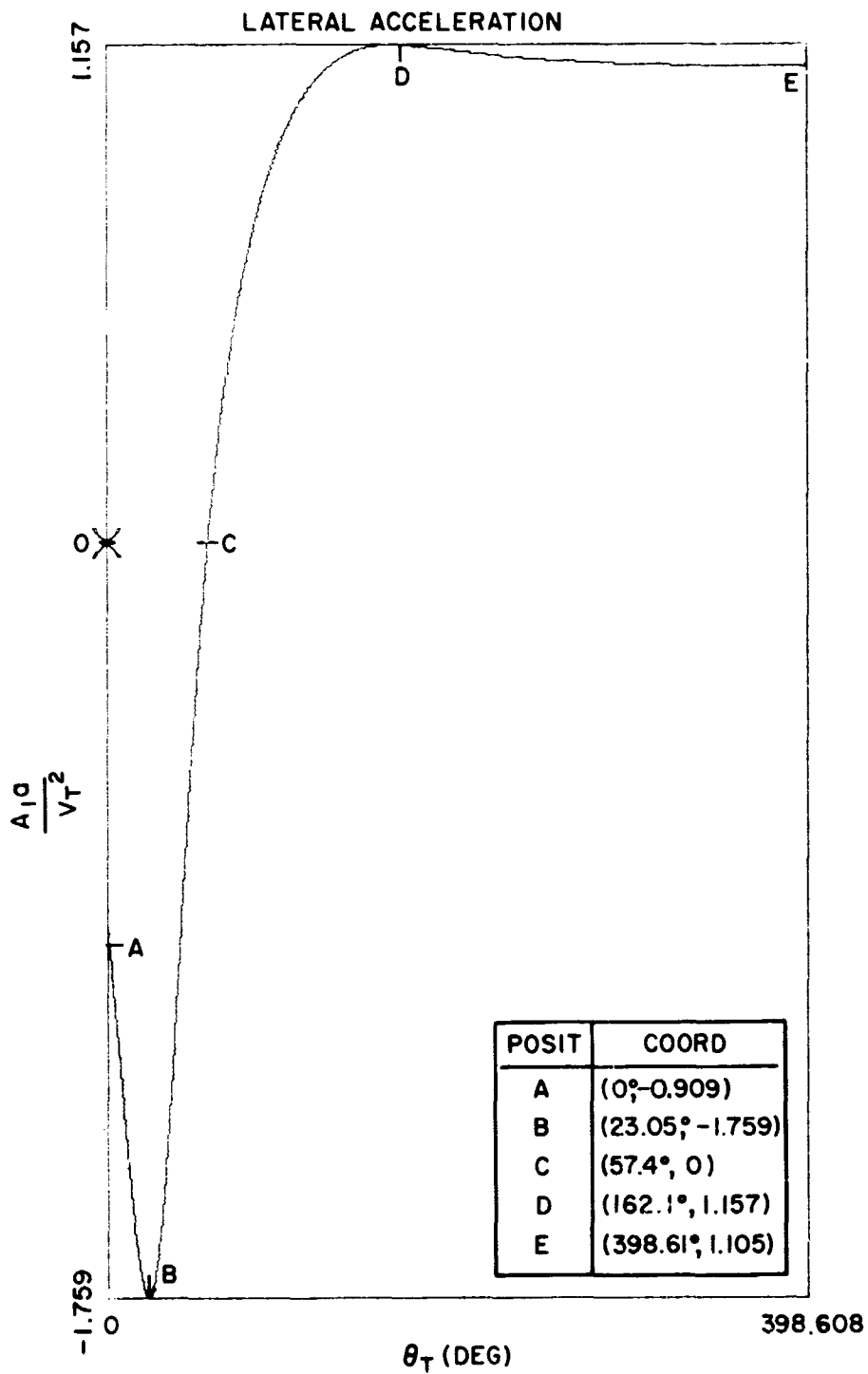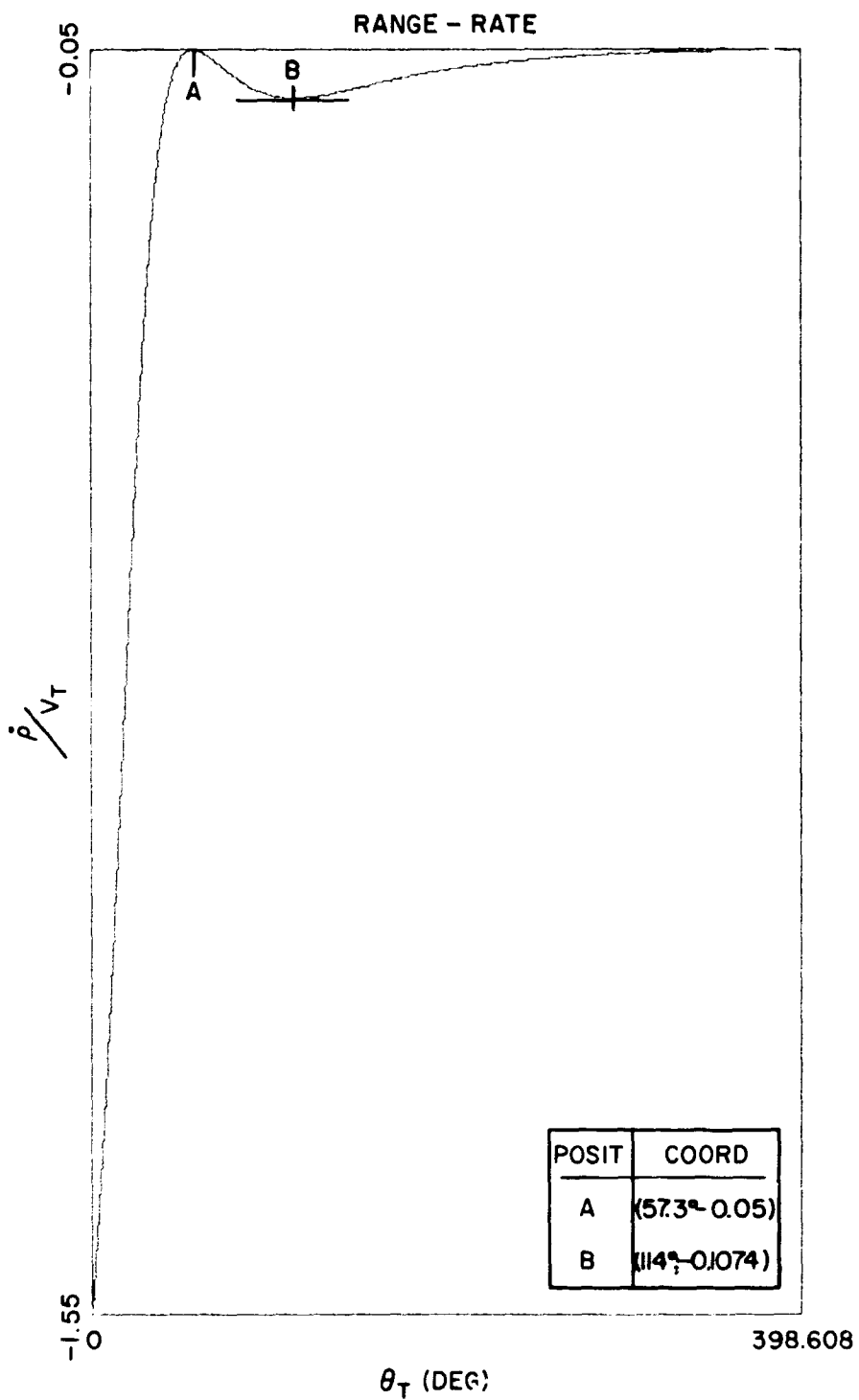
Fig. V.14(d).   Dimensionless Range for the Circular Pursuit Maneuver as a
function of θ_T (k= 1.05, φ_0 = 210°, ρ_0 = a).

155

TRAJECTORIES

Fig. V.15(a). Trajectories for the Target (T) and Interceptor (I) during the circular pursuit maneuver (for k = 1.01, φ_0 = 269°, ρ_0 = a).

LATERAL ACCELERATION

POSIT	COORD
A	(0.0°-0.018)
B	(30.21°, -21.18)
C	(___, 0.0)
D	(189.57° 1.0205)

$\dfrac{A_T a}{V_T^2}$

θ_T (DEG)
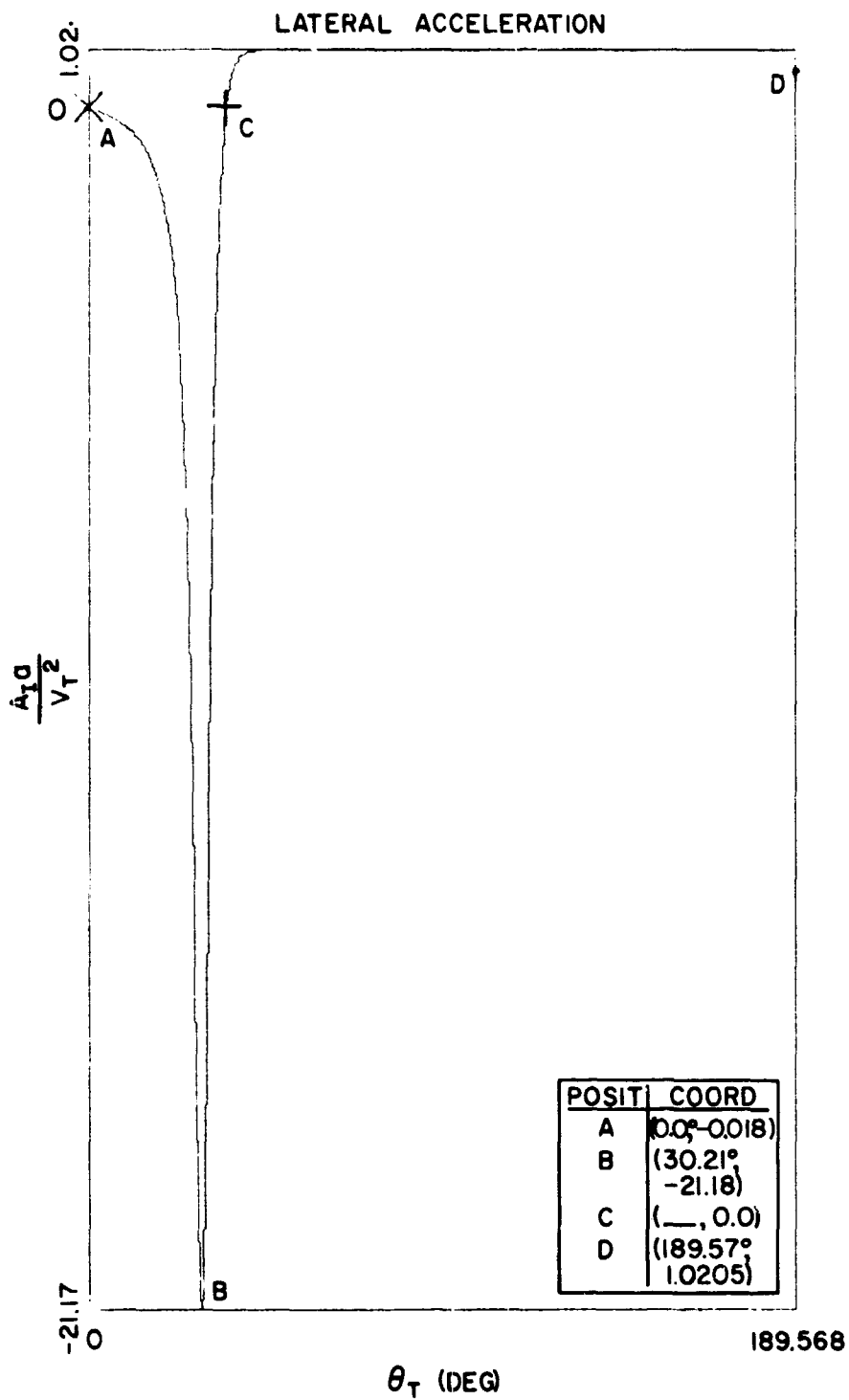
Fig. V.15(b). Dimensionless Lateral Acceleration experienced by the Interceptor during the Circular Pursuit Maneuver (for $k = 1.01$, $\varphi_0 = 269°$, $\rho_0 = a$) as a function of θ_T.

157
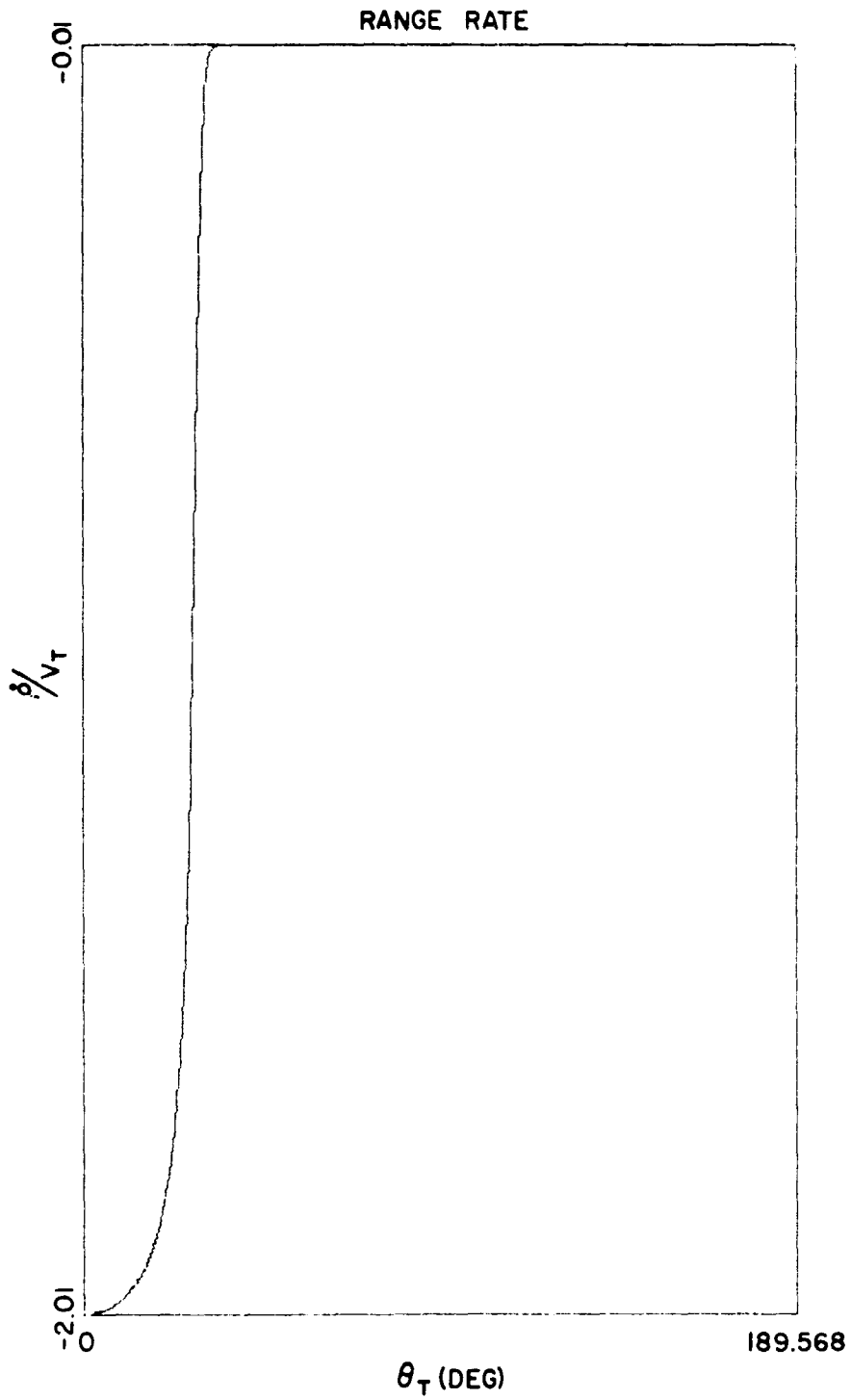
Fig. V.15(c). Dimensionless Range-Rate for the Circular Pursuit Maneuver as a function of θ_T ($\tilde{k}$ = 1.01, φ_0 = 269°, ρ_0 = a).

158
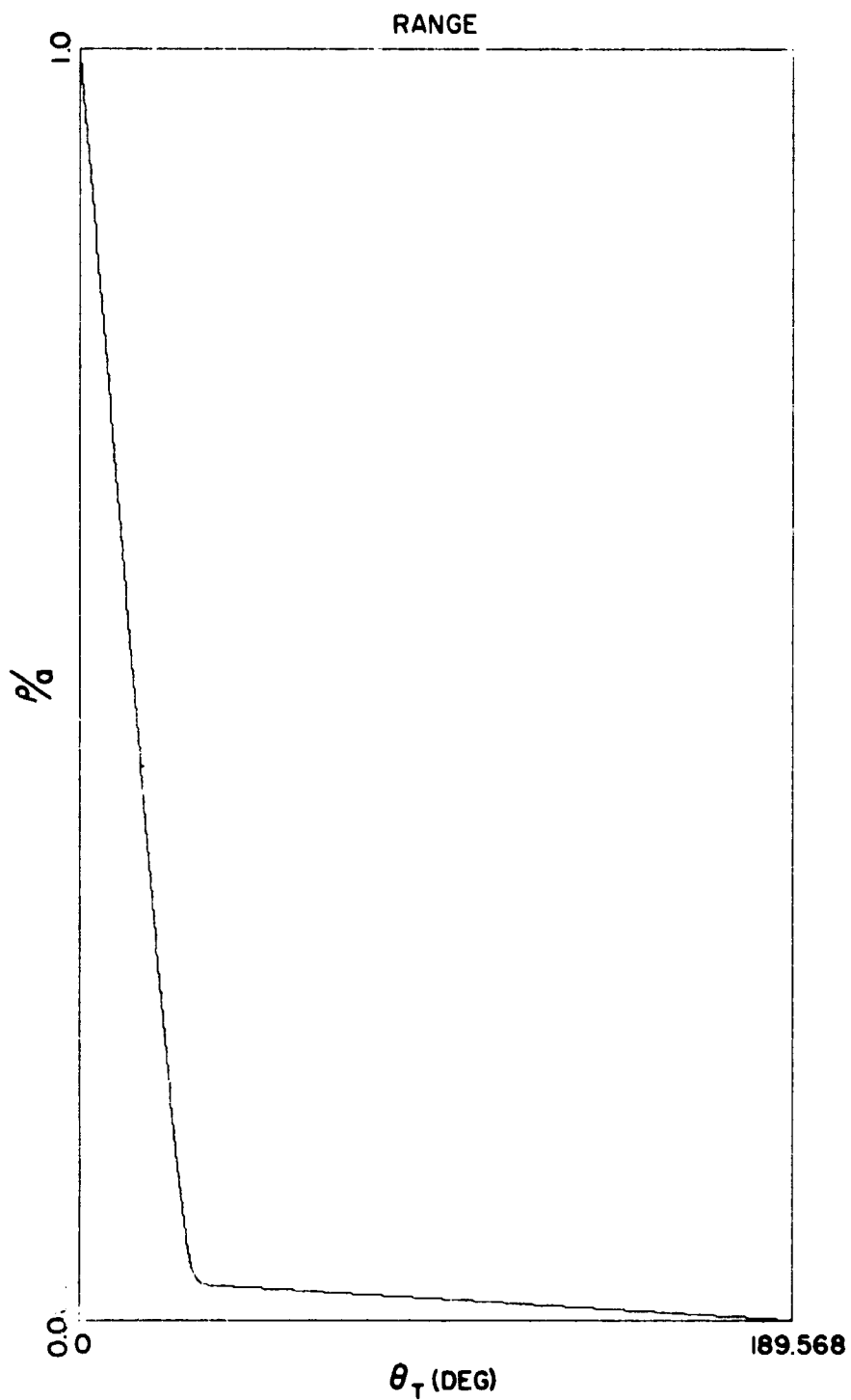
Fig. V.15(d). Dimensionless Range for the Circular Pursuit Maneuver as a function of θ_T ($k = 1.01$, $\varphi_0 = 269°$, $\rho_0 = a$).

159
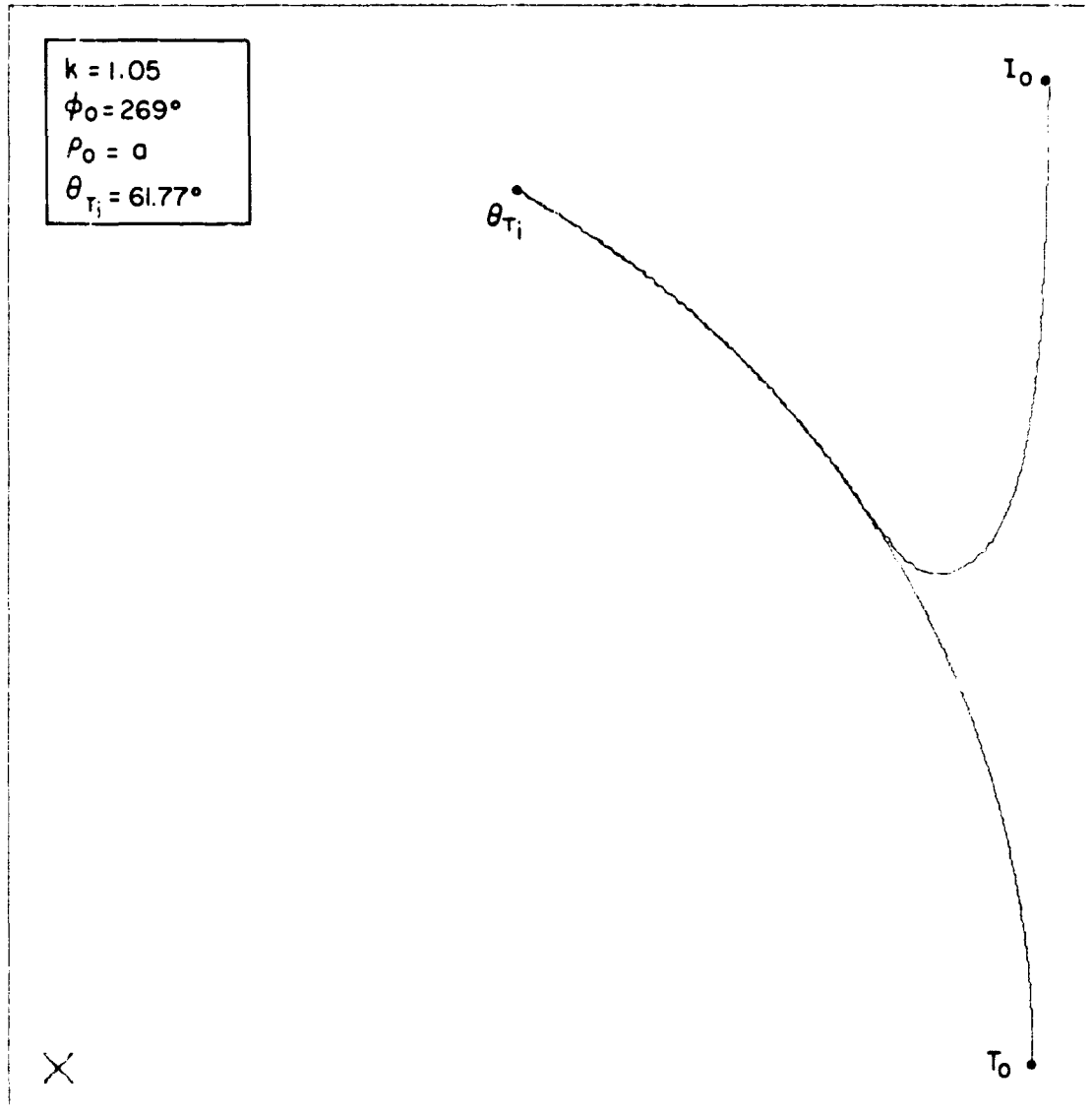
TRAJECTORIES

Fig. V.16(a). Trajectories for the Target (T) and Interceptor (I) during the circular
pursuit maneuver (for $k = 1.05$, $\varphi_0 = 269°$, $\rho_0 = a$).

160
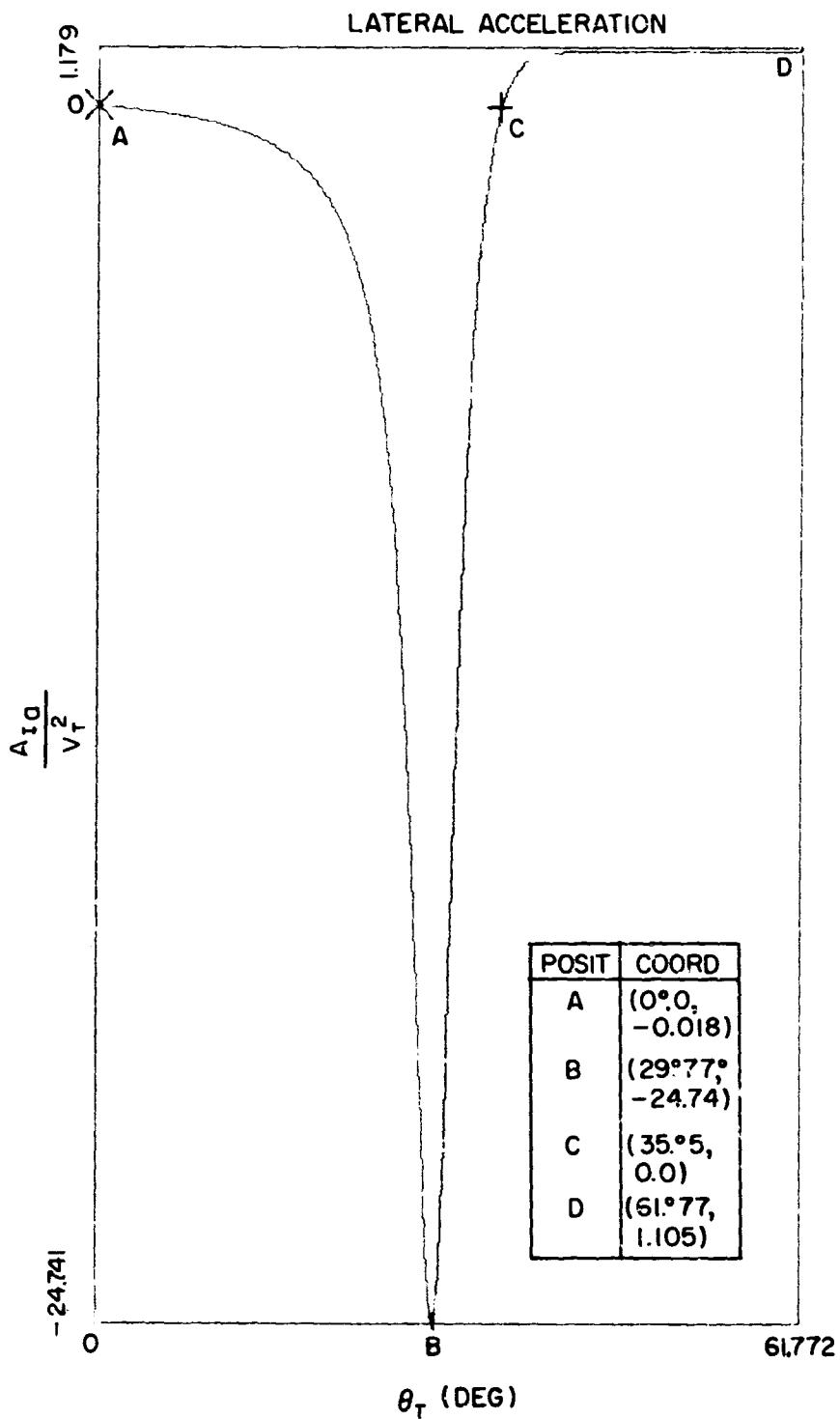
Fig. V.16(b). Dimensionless Lateral Acceleration experienced by the Interceptor during the Circular Pursuit Maneuver (for k = 1.05, φ_0 = 269°, ρ_0 = a) as a function of θ_T.

161
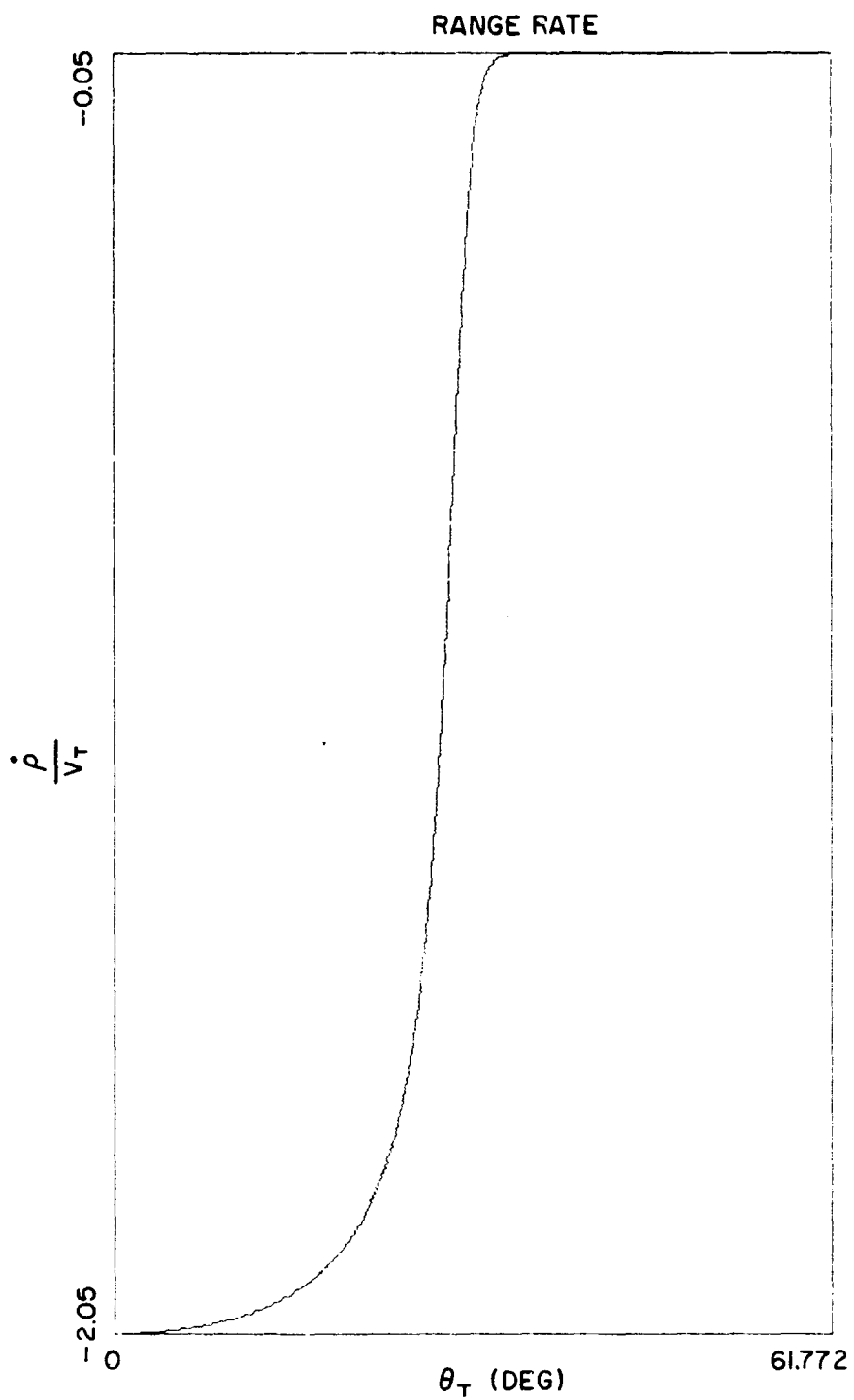
Fig. V.16(c). Dimensionless Range-Rate for the Circular Pursuit Maneuver as a function of θ_T ($k = 1.05$, $\varphi_0 = 269°$, $\rho_0 = a$).

162
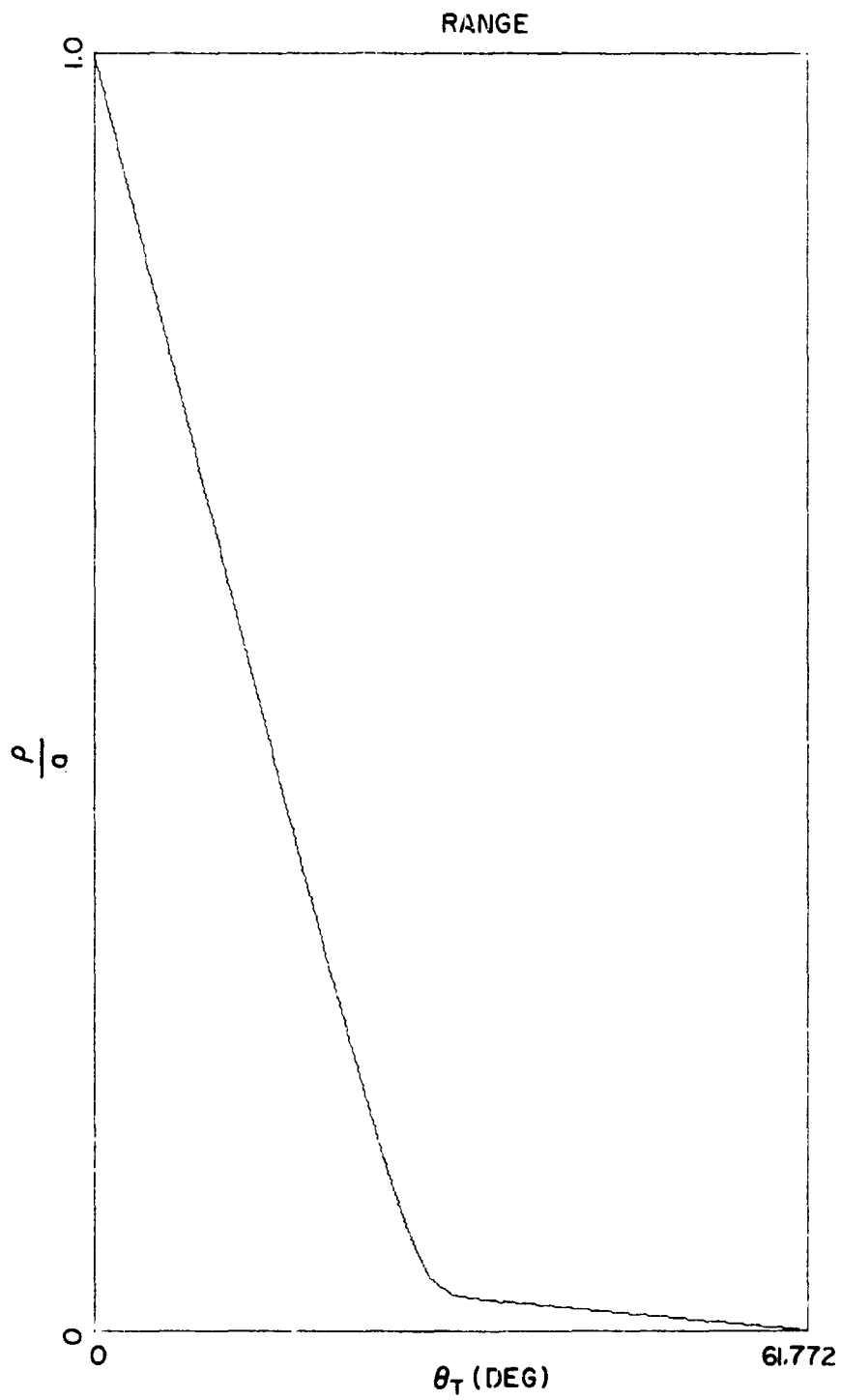
Fig. V.16(d)   Dimensionless Range for the Circular Pursuit Maneuver as a function of θ_T (k = 1.05, φ_0 = 269°, ρ_0 = a).

163

Fig. V.17(a). Trajectories for the Target (T) and Interceptor (I) during the circular pursuit maneuver (for $k = 1.05$, $\varphi_0 = 269°$, $\rho_0 = 2a$).

LATERAL ACCELERATION

$\dfrac{A_{rd}}{V_T^2}$

11.73

O ╳ A   ╋ C

POSIT	COORD
A	$(0^\circ.0,$ $-0.092)$
B	$(58^\circ.19,$ $-3.18)$
C	$(82^\circ.5,$ $0.0)$
D	$(301^\circ.7,$ $1.105)$

-3.179

O   B θ_T (DEG)   301.698
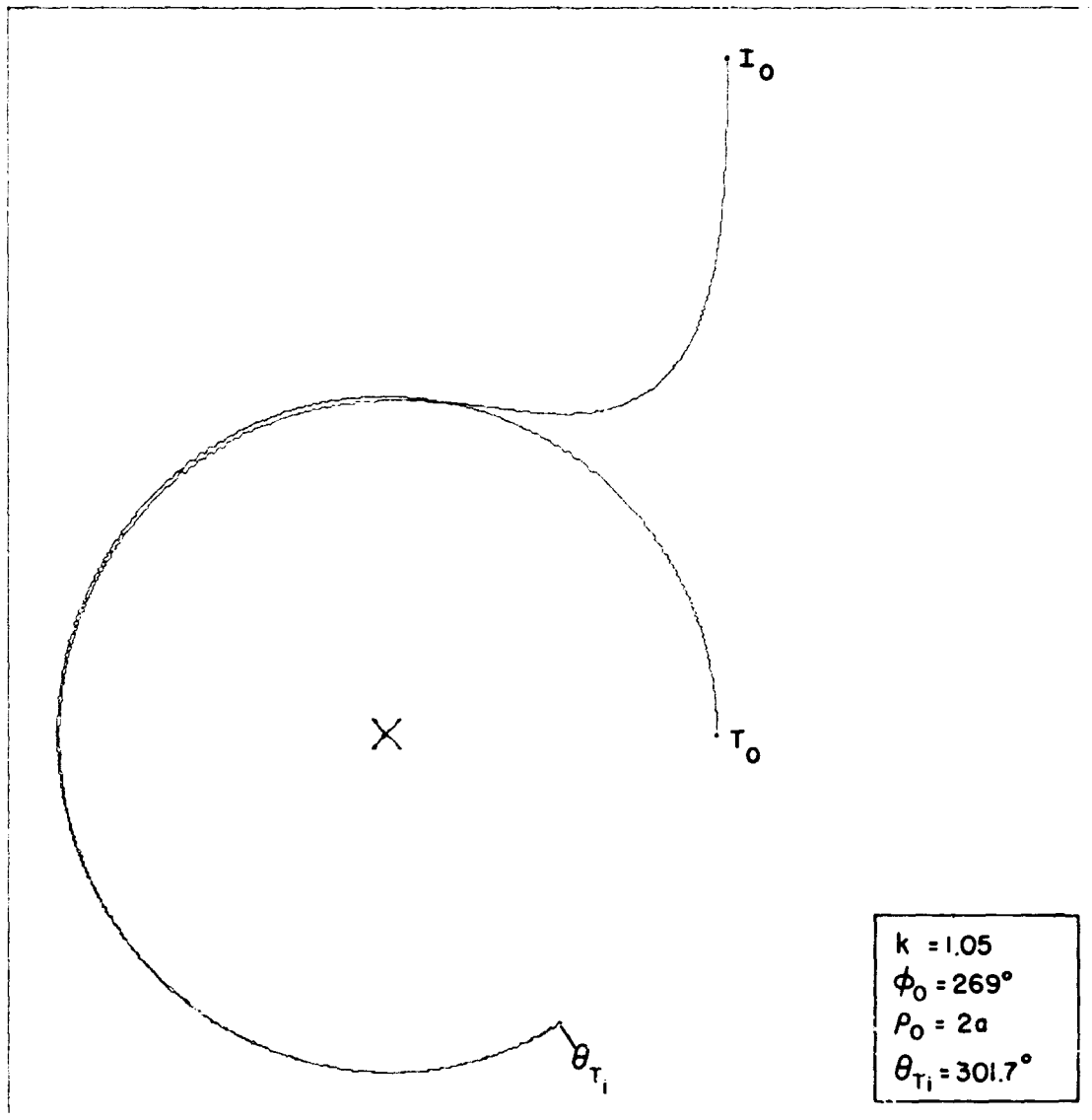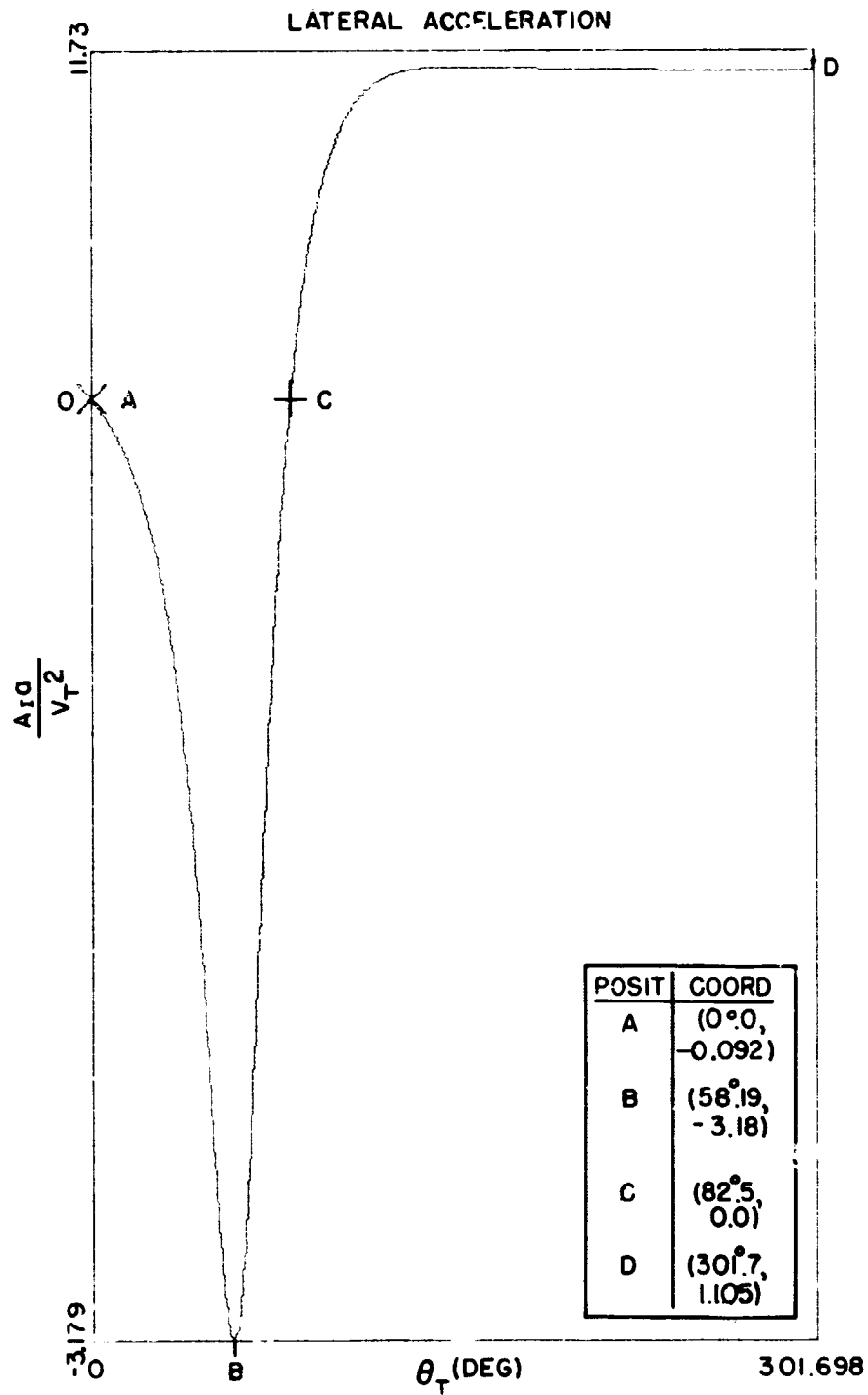
Fig. V.17(b). Dimensionless Lateral Acceleration experienced by the Interceptor during the Circular Pursuit Maneuver (for $k = 1.05$, $\varphi_0 = 269^\circ$, $\rho_0 = 2a$) as a function of θ_T.
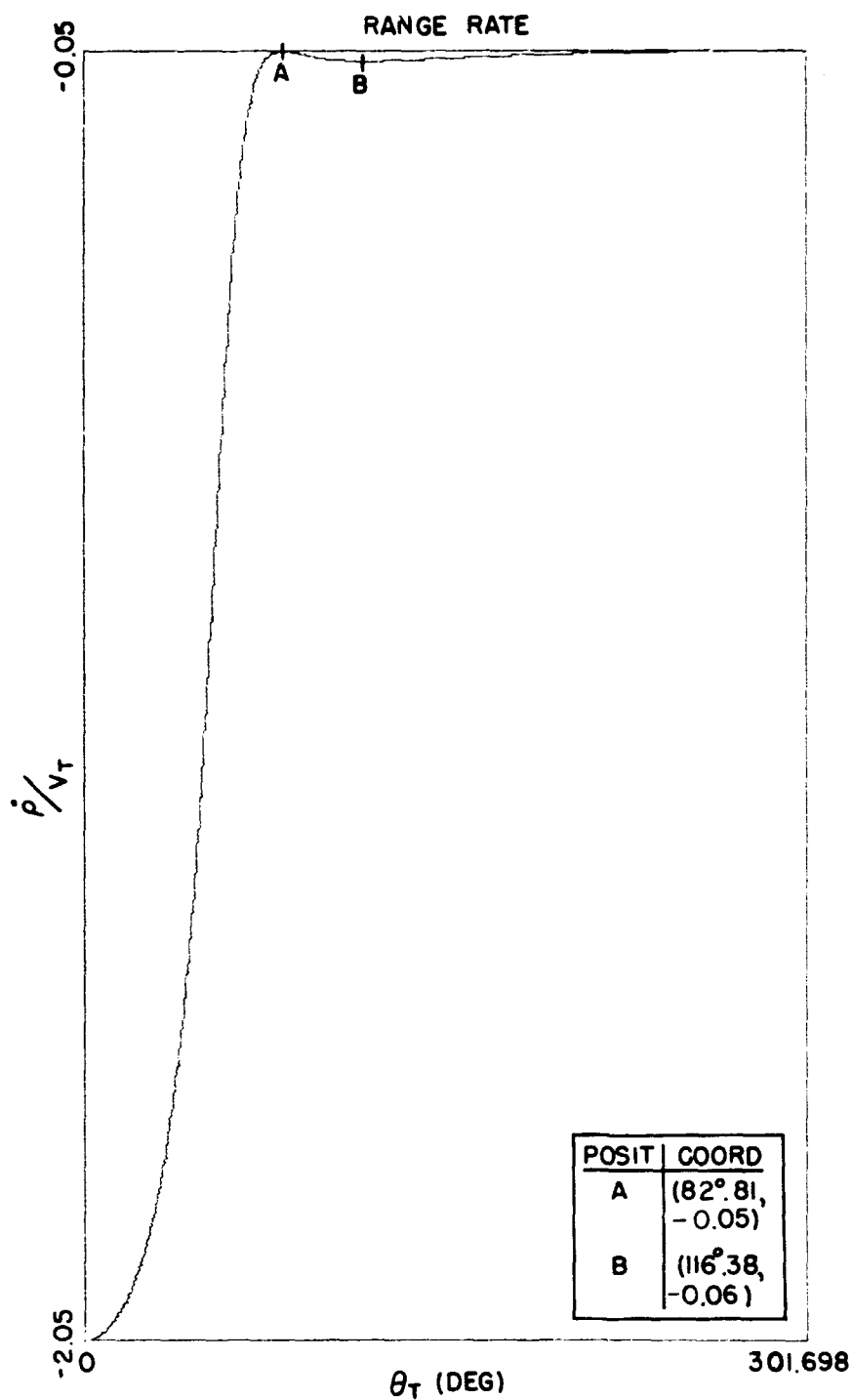
Fig. V.17(c). Dimensionless Range-Rate for the Circular Pursuit Maneuver as a function of θ_T (k = 1.05, φ_0 = 269°, ρ_0 = 2a).

166
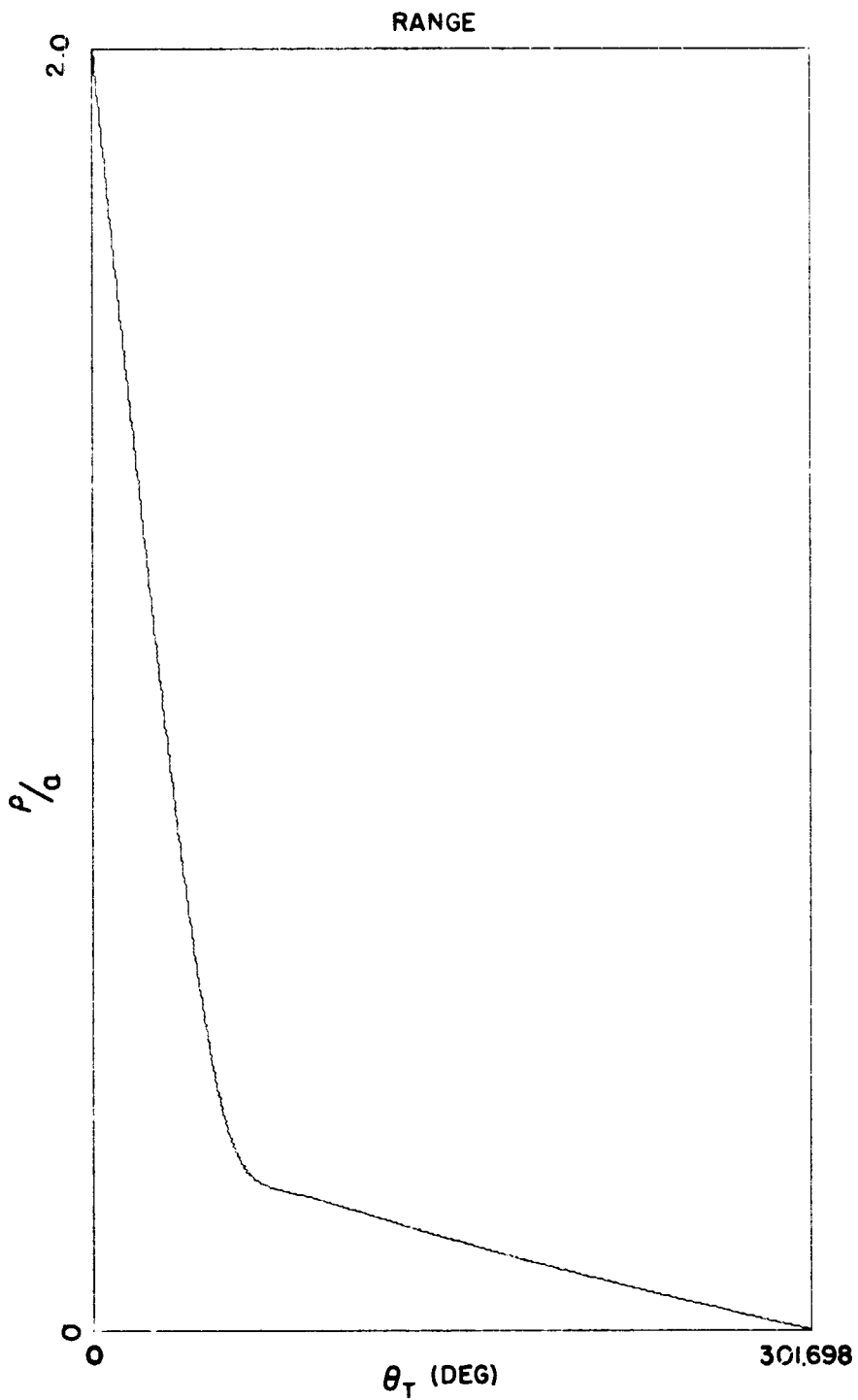
Fig. V.17(d).   Dimensionless Range for the Circular Pursuit Maneuver as a
function of θ_T (k= 1.05, φ_0 = 269°, ρ_0 = 2a).

167

I_0

θ_{T_i}

T_0

k = 2.0
$\phi_0 = 269°$
$\rho_0 = 2a$
$\theta_{T_i} = 41.85°$
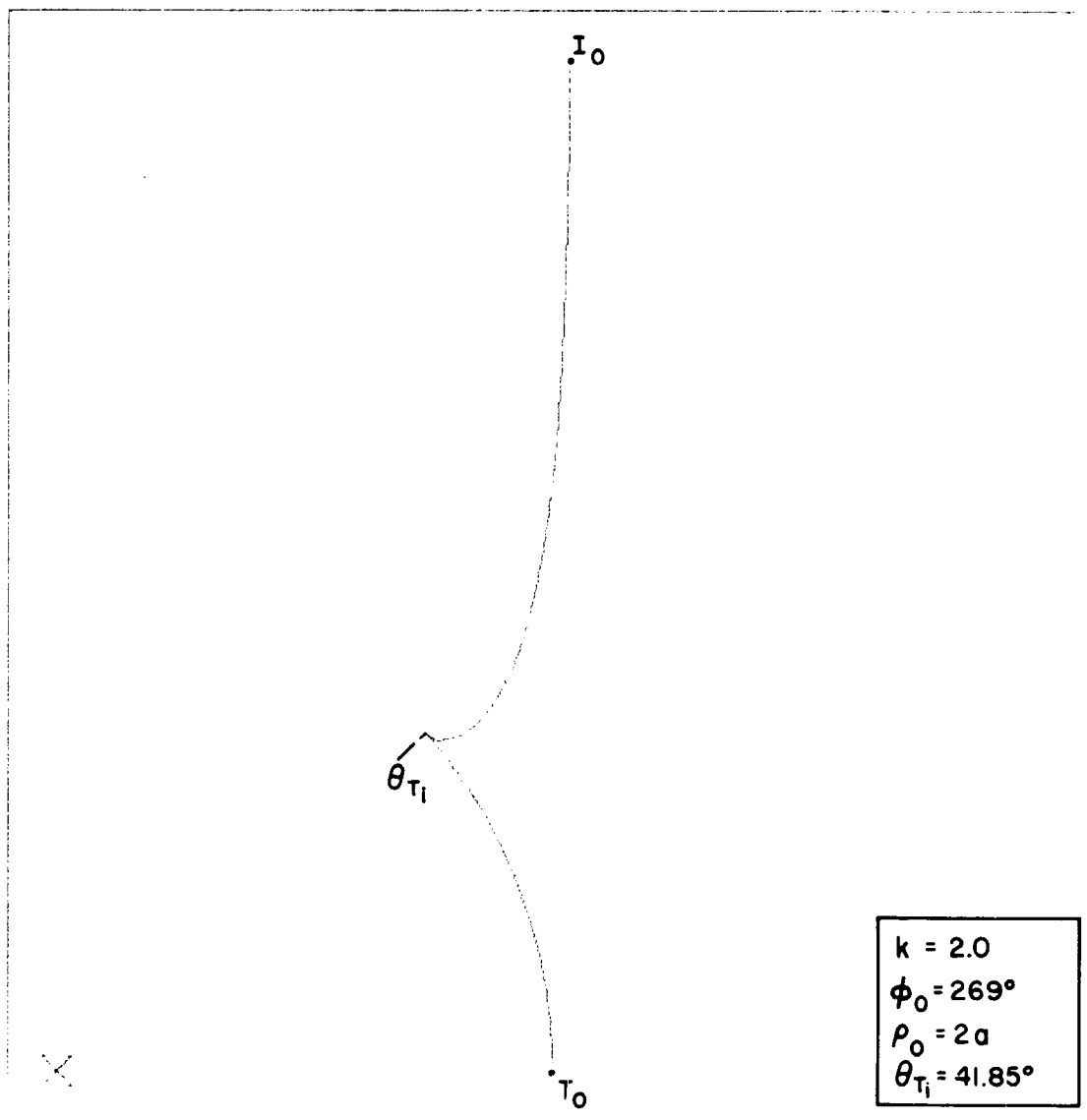
Fig. V.18(a). Trajectories for the Target (T) and Interceptor (I) during the circular
pursuit maneuver (for $k = 2.00$, $\varphi_0 = 269°$, $\rho_0 = 2a$).

168

LATERAL ACCELERATION

$\dfrac{A_I a}{V_T^2}$

-0.017

-93.38

0

41.853

θ_T (DEG)
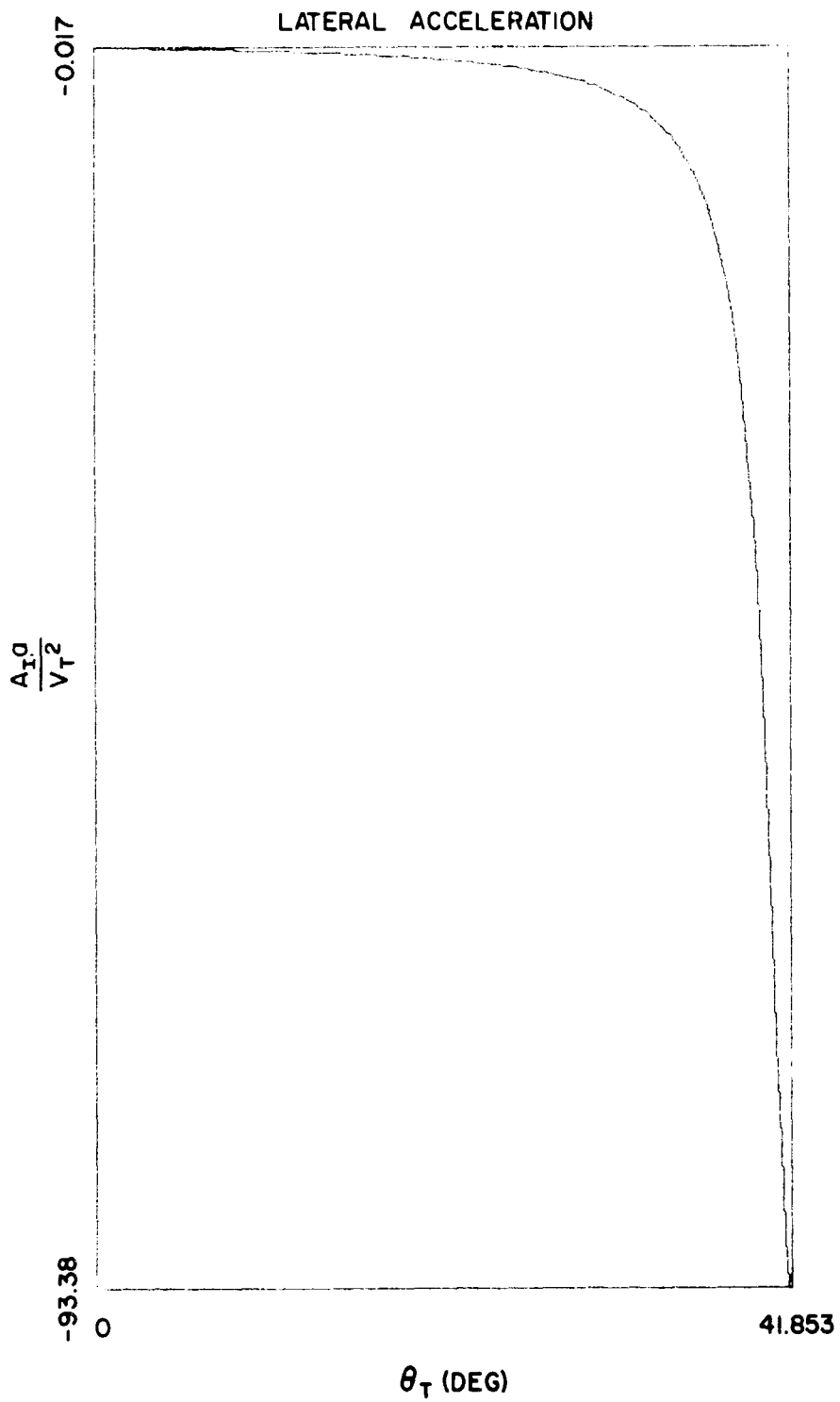
Fig. V.18(b). Dimensionless Lateral Acceleration experienced by the Interceptor during the Circular Pursuit Maneuver (for k = 2.0, φ_0 = 269°, ρ_0 = 2a) as a function of θ_T.

169
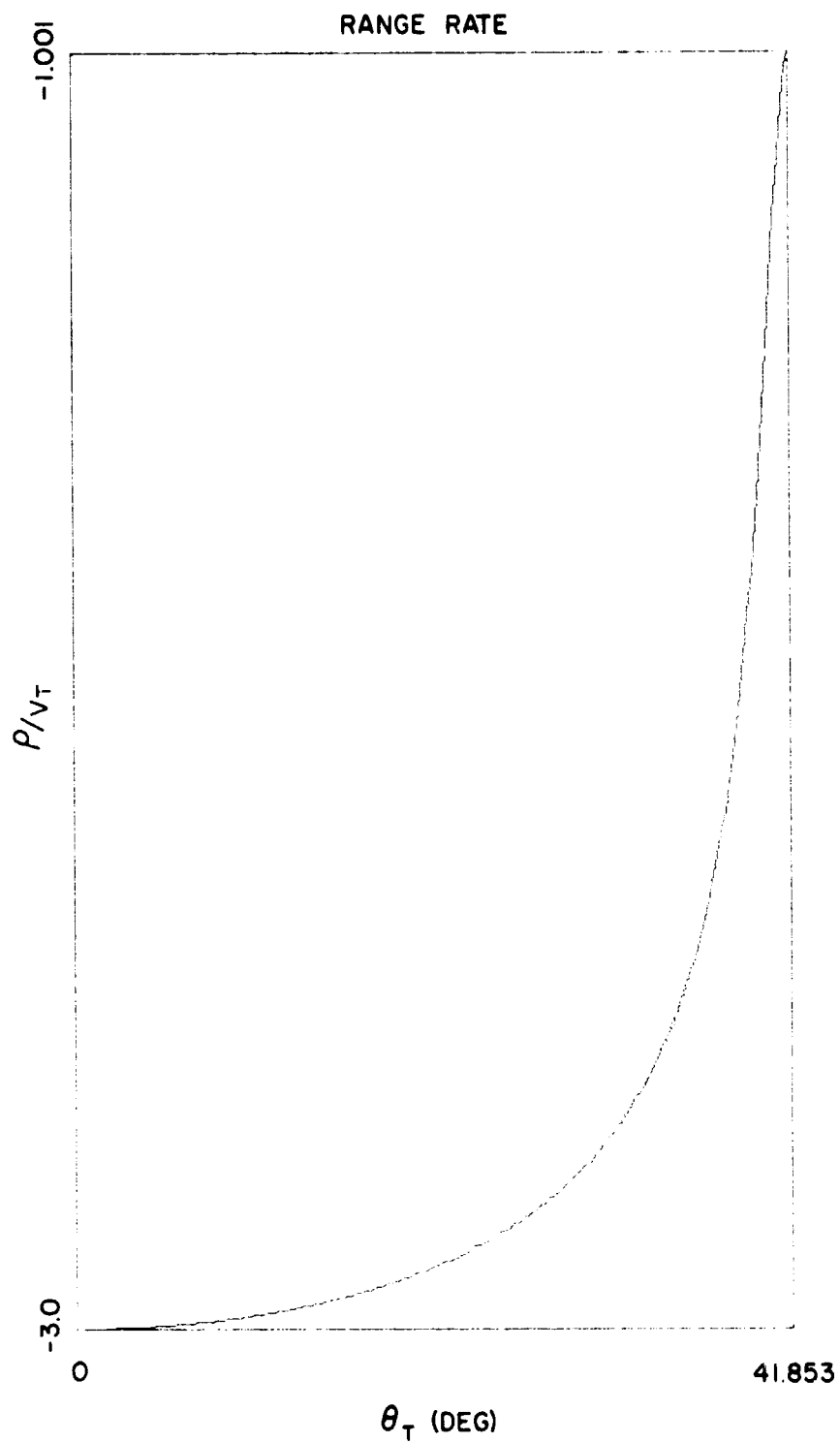
Fig. V.18(c). Dimensionless Range-Rate for the Circular Pursuit Maneuver as a function of θ_T ($k = 2.0$, $\varphi_0 = 269°$, $\rho_0 = 2a$).

170
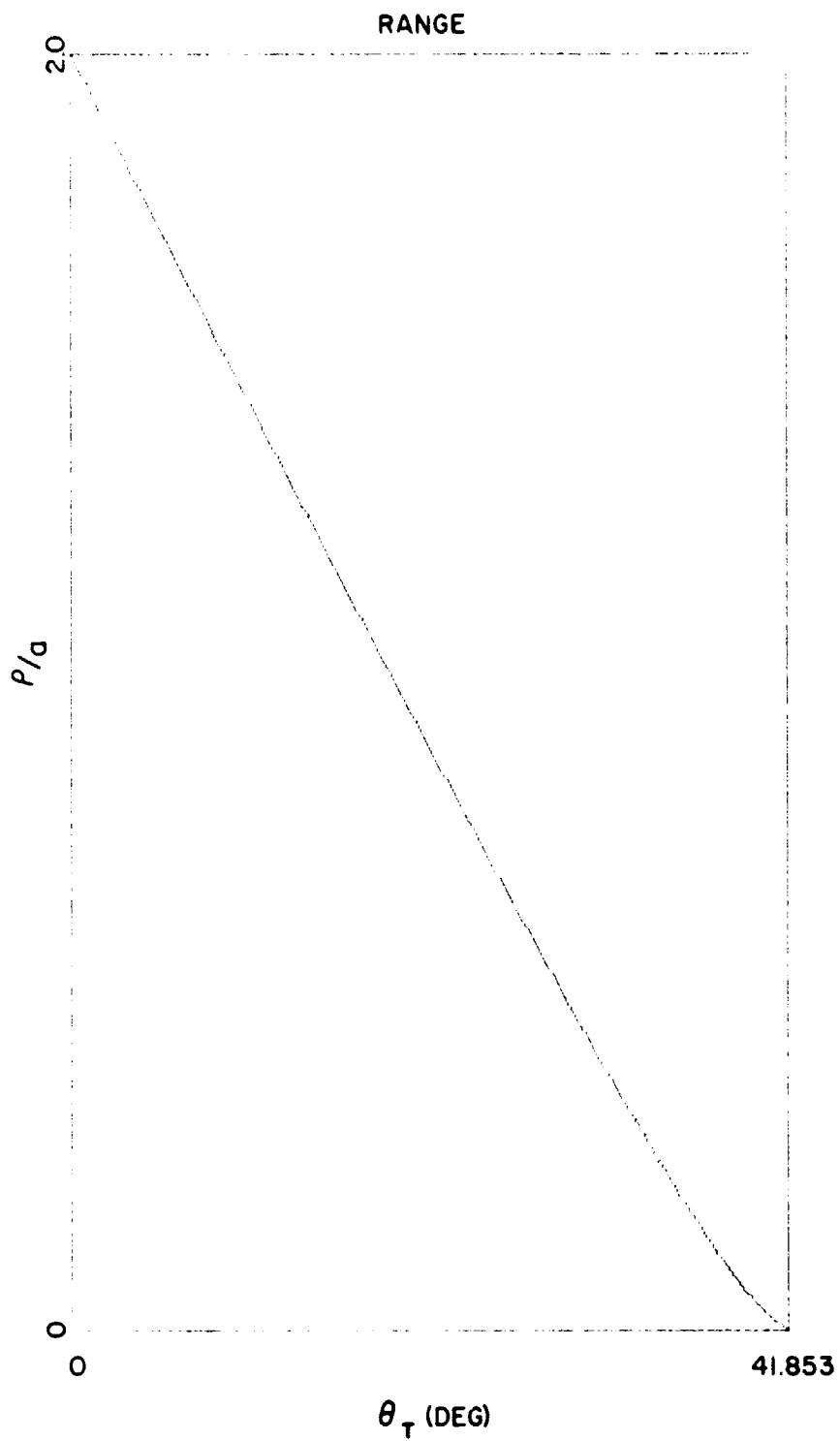
Fig. V.18(d). Dimensionless Range for the Circular Pursuit Maneuver as a function of θ_T ($\ell = 2.0$, $\varphi_0 = 269°$, $\rho_0 = 2a$).

171

$k = 1.5$
$\phi_0 = 300°$
$\rho_0 = a$
$\theta_{T_i} = 24.4°$
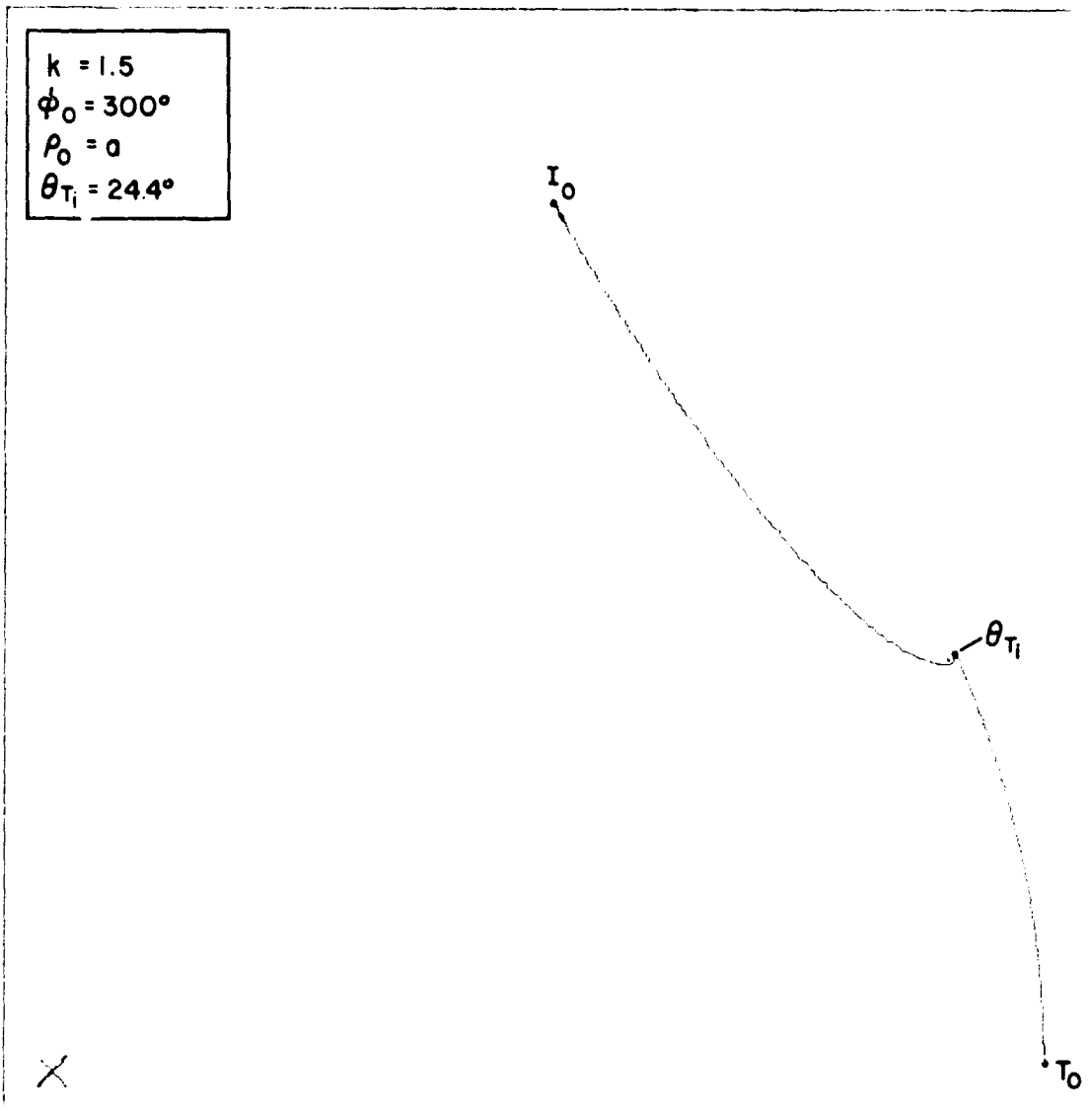
Fig. V.19(a). Trajectories for the Target (T) and Interceptor (I) during the circular
pursuit maneuver (for $k = 1.50$, $\varphi_0 = 300°$, $\rho_0 = a$).

172
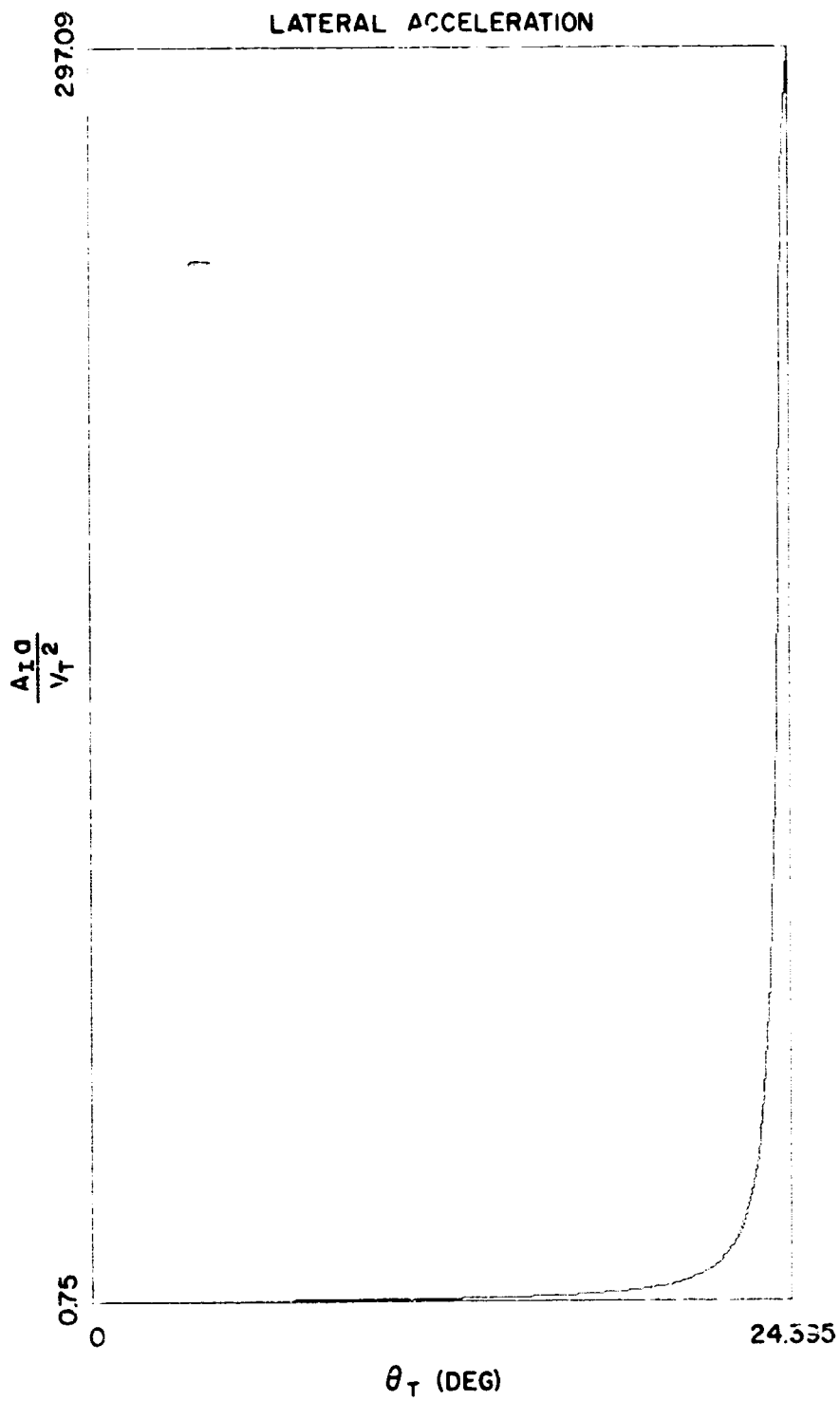
Fig. V.19(b). Dimensionless Lateral Acceleration experienced by the Interceptor during the Circular Pursuit Maneuver (for $k = 1.50$, $\varphi_0 = 300°$, $\rho_0 = a$) as a function of θ_T.

173

RANGE RATE

POSIT	COORD
A	(0°.0, -2.37)
B	(13°.65, -2.403)

-0.581

$\dot{\rho}/v_T$

-2.403

A

B

-2.0 O

24.395

θ_T (DEG)
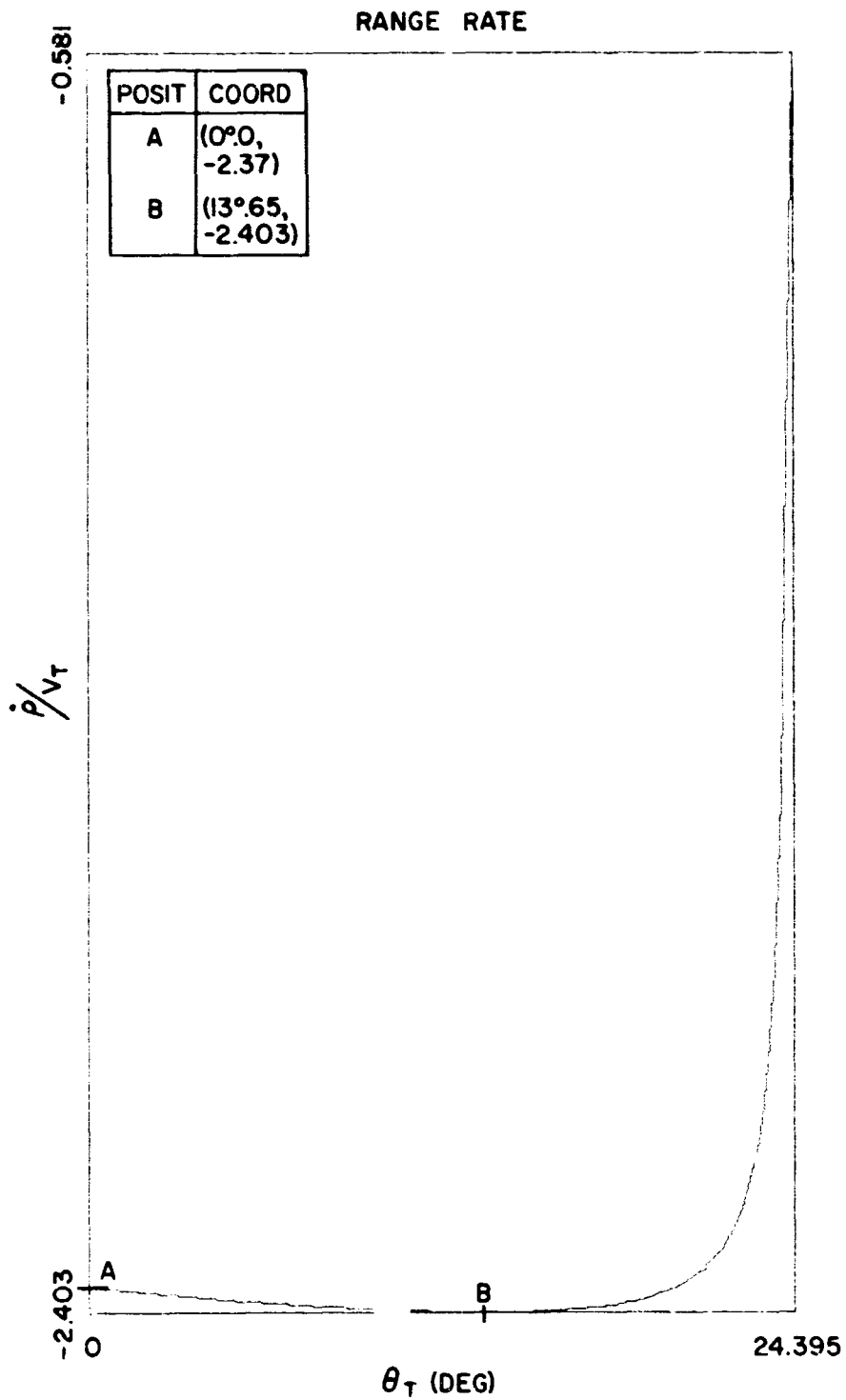
Fig. V.19(c). Dimensionless Range-Rate for the Circular Pursuit Maneuver as a function of θ_T ($k = 1.50$, $\varphi_0 = 300°$, $\rho_0 = a$).

174
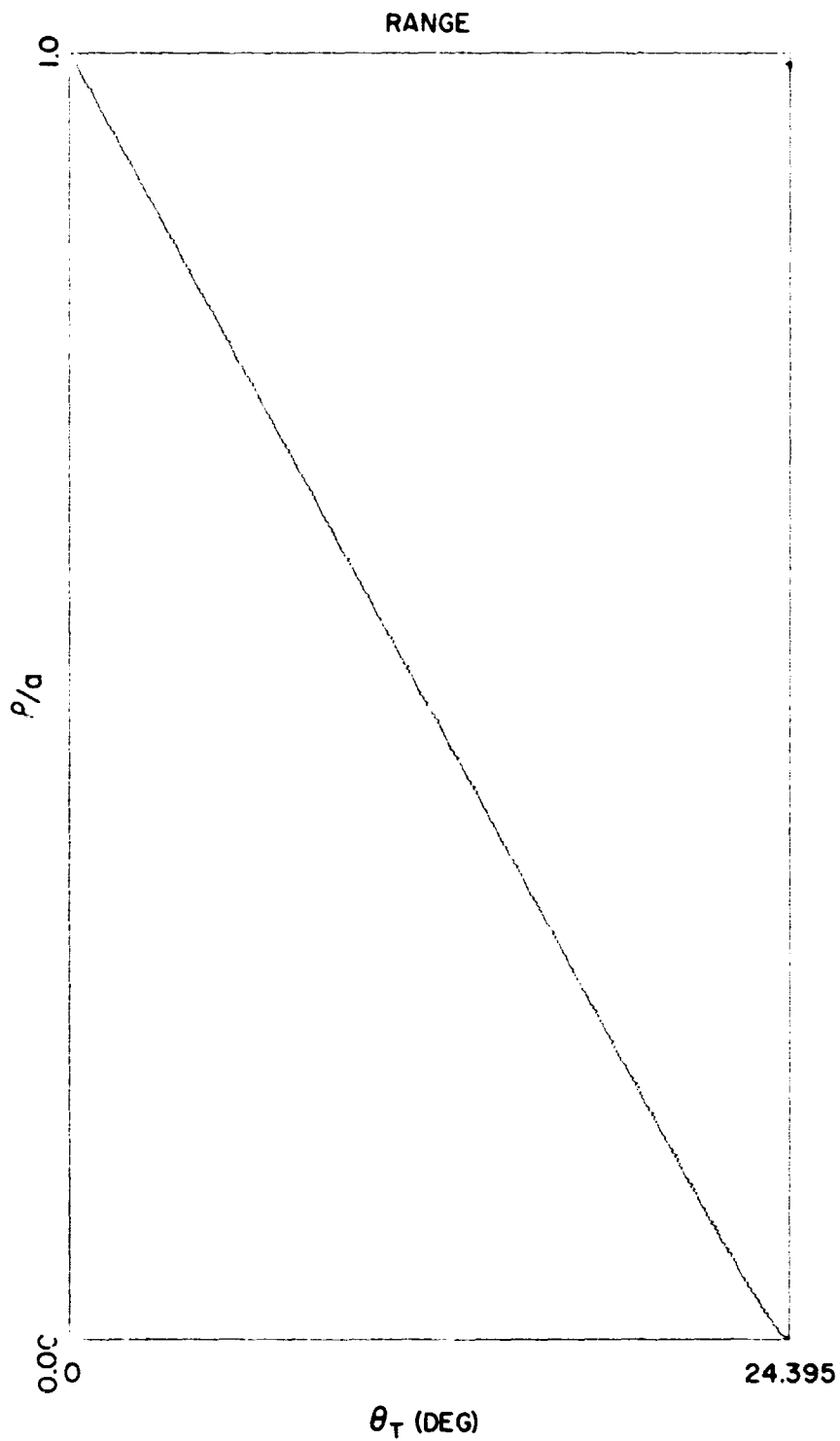
RANGE

Fig. V.19(d). Dimensionless Range for the Circular Pursuit Maneuver as a function of θ_T ($\overset{2}{k}$ = 1.50, $\varphi_0 = 300°$, ρ_0 = a).

Fig. V.20(a). Trajectories for the Target (T) and Interceptor (I) during the circular pursuit maneuver (for $k = 1.05$, $\varphi_0 = 330°$, $\rho_0 = a$).

176

LATERAL ACCELERATIONS

POSIT	COORD
A	(37°.82, 7.69)
B	(132.72°, 1.106)
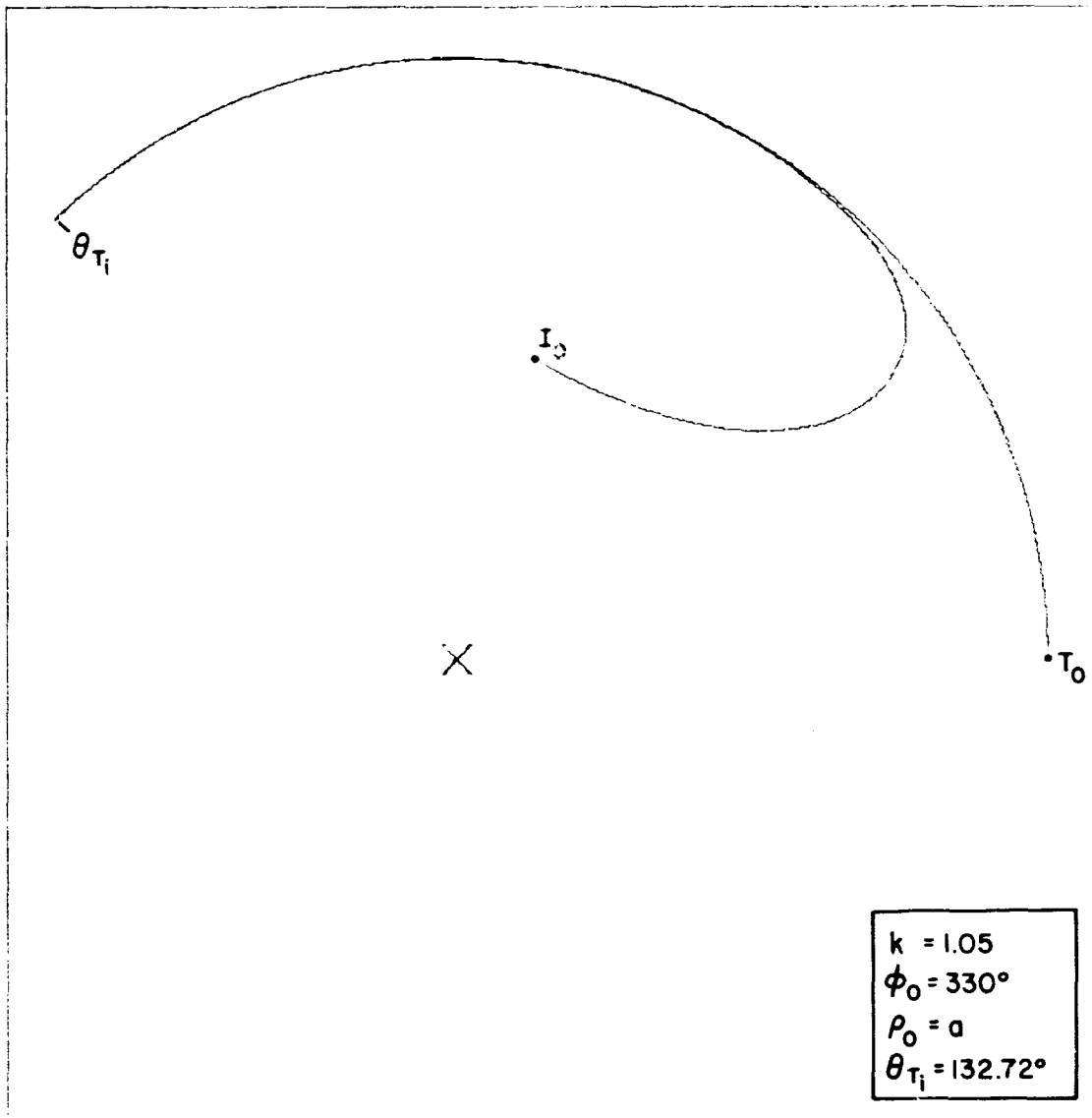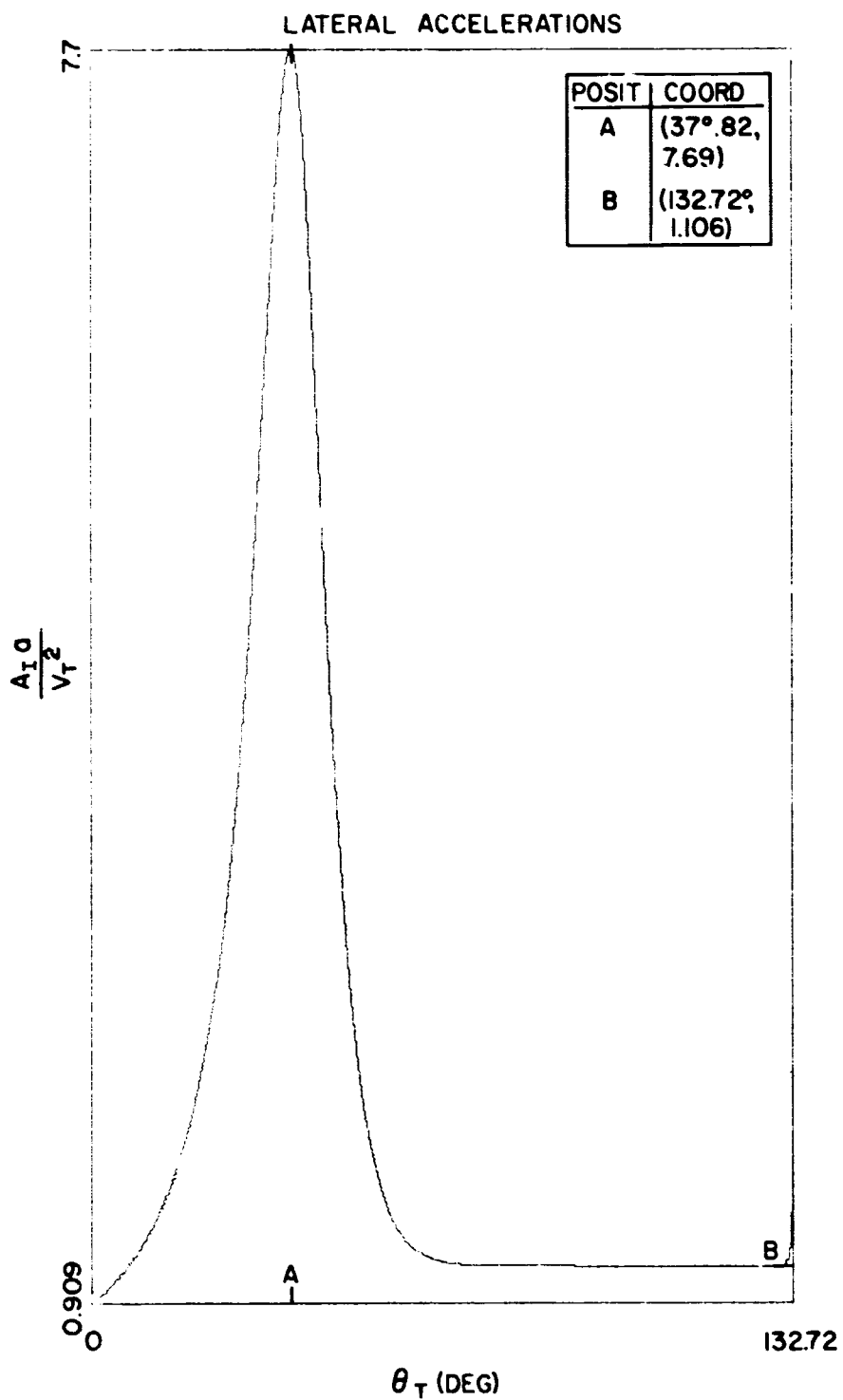
Fig. V.20(b). Dimensionless Lateral Acceleration experienced by the Interceptor during the Circular Pursuit Maneuver (for $k = 1.05$, $\varphi_0 = 330°$, $\rho_0 = a$) as a function of θ_T.

177

RANGE RATE

$\dot{\rho}/V_T$

θ_T (DEG)

-0.05

-1.556

0

132.72

POSIT	COORD
A	$(0°,0, -1.55)$
B	$(5°.15, -1.56)$
C	$(66°.5, -0.05)$
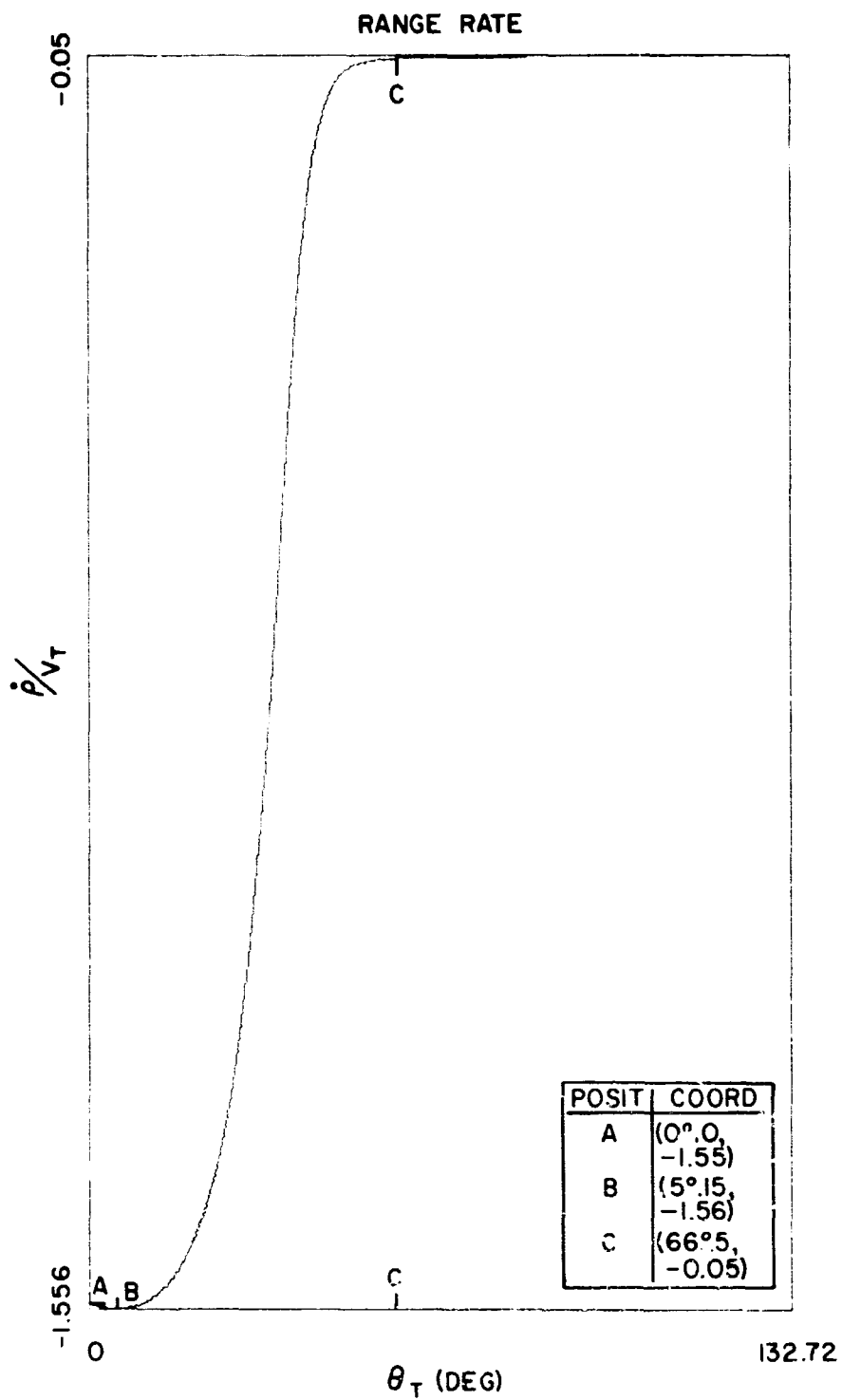
Fig. V.20(c). Dimensionless Range-Rate for the Circular Pursuit Maneuver as a function of θ_T ($k= 1.05$, $\varphi_0 = 330°$, $\rho_0 = a$).

178
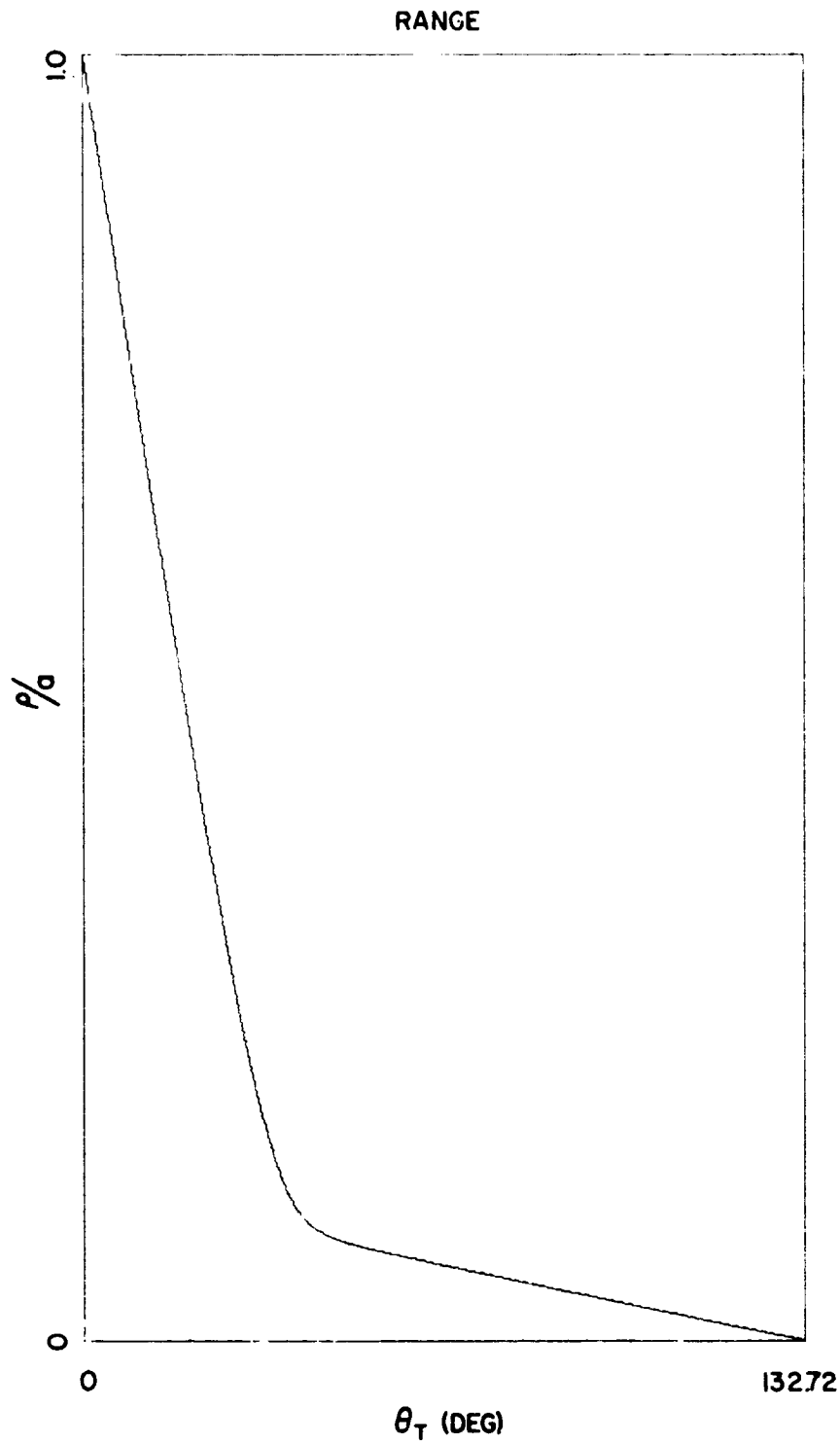
RANGE

Fig. V.20(d). Dimensionless Range for the Circular Pursuit Maneuver as a function of θ_T ($k = 1.05$, $\varphi_0 = 330°$, $\rho_0 = a$).

179

VI. SYMBOLS

A   intermediate position on the Intercept Path (Intercept Problem).

a   position coordinate for T_0 (Pursuit Problem).

$\bar{A}$, (A)   Acceleration Vector, (Acceleration Scalar).

B   "Lead" Intercept Collision Position.

b   position coordinate for T_0 (Pursuit Problem).

C   collision position (Intercept Problem).

$\mathcal{C}$ integration constant.

$\bar{e}_j$ unit vectors ($j = r, \theta, z; x, y, z; r, \alpha, z; \rho, \omega, z$).

I   position of the Intercept Vehicle.

k ratio of speeds ($\overset{\triangle}{=} V_I/V_T$).

LOS; $\angle$ (LOS)   Line-of-sight; angle for line-of-sight.

M   figure of merit (see Eq. '.35)).

O   inertial origin.

p   slope of the pursuit curve wrt the x-axis.

P   position designation (Circular Pursuit Problem).

Q   position designation (Circular Pursuit Problem).

$\bar{r}_j$, r_j position vector, (radius); j = condition or vehicle considered.

R_0 radius of the geometric intercept figure (See Eq. (III.18)).

s   designates the path of the Intercept Vehicle; s = s (x, y).

T   position of the Target Vehicle.

t   time.

$\overline{V}_j$, (V_j)	Velocity Vector, (speed); j = condition or vehicle considered.
x, y	cartesian position coordinates.
z	coordinate; transformation variable (Section IV).

Greek Letters

α	inclination of $\overline{V}_I$ wrt x-axis (Pursuit Problem); angular displacement of $\overline{r}_Q$ wrt $\overline{r}_{IQ}$ (Circular Pursuit Problem).
Δ, δ	increment quantities.
φ	Angular position of $\overline{\sigma}$ wrt $\overline{r}_T$ (Circular Pursuit Problem).
Φ_j	Angular position of velocity vectors wrt $\overline{r}_r$ (Intercept Problem).
ξ_j, η_j	dimensionless coordinates (Circular Pursuit Problem).
ξ_c, η_c	coordinates locating the center of the geometric figure for the Intercept Problem.
$\overline{\rho}$, (ρ)	vector displacement (scalar) of T wrt I (Circular Pursuit Problem).
θ_j	inclination of the velocity vector (Intercept Problem); position angle in the circular pursuit problem, (j = T, I).
θ_{T_i}	Intercept angle position, referred to target angle (Circular Pursuit Problem).
σ; $\overline{\sigma}$	path of the Target Vehicle; vector locating P wrt T (Circular Pursuit Problem).
$\overline{\omega}$; ω	rotation vector (Intercept Problem); angular position for $\overline{\rho}$ wrt the x-axis (Circular Pursuit)
χ	dimensionless quantity, ρ / a
$\overline{\Omega}$	rotation vector for the (ρ, ω, z) triad; ($|\overline{\Omega}|$ ≡ $\dot{\omega}$).

Subscripts

c	designating collision.
f	a final value (Circular Pursuit Problem).
I	intercept, interceptor.
i	intercept value.
lim	a limit value.
m	time for intercept (or collision), for Pursuit Problem.
O	initial value ($t = 0$).
r	a relative value; a range quantity.
T	target.
α	component in the α direction (parallel to $\overline{e}_\alpha$).

Superscripts

$(\dot{\ })$	differentiation wrt time.
$\overset{\frown}{(\ )}$	denotes path arc.
$\overline{(\ )}$	a vector quantity.

VII. BIBLIOGRAPHY

Davis, H. T., "Introduction to Nonlinear Differential and Integral Equations;"
    U. S. Atomic Energy Commission, 1961.

Locke, A. S., "Guidance (Principles of Guided Missile Design)," Van Nostrand,
    1955.